ZooKeys 1127: 1–60 (2022)
doi: 10.3897/zookeys.1127.85737
https://zookeys.pensoft.net

RESEARCH ARTICLE

A peer-reviewed open-access journal
ZooKeys
Launched to accelerate biodiversity research

The aquatic Adephaga of the Makay, central-western Madagascar, with description of two new diving beetle species (Coleoptera, Gyrinidae, Haliplidae, Noteridae, Dytiscidae)

Andriamirado Tahina Ramahandrison[1,2], Bakolimalala Rakouth[1], Michaël Manuel[2]

1 *Département de Biologie et Ecologie Végétales, Faculté des Sciences, BP906, Université d'Antananarivo, Antananarivo, Madagascar* **2** *Sorbonne Université, Institut de Systématique, Evolution, Biodiversité (UMR 7205), MNHN SU CNRS EPHE UA, Case 05, 7 quai St Bernard, Paris, France*

Corresponding author: Michaël Manuel (michael.manuel@upmc.fr)

Academic editor: Mariano Michat | Received 23 April 2022 | Accepted 13 July 2022 | Published 2 November 2022

https://zoobank.org/4759AFC3-2EFD-47A7-853F-645FB32829BA

Citation: Ramahandrison AT, Rakouth B, Manuel M (2022) The aquatic Adephaga of the Makay, central-western Madagascar, with description of two new diving beetle species (Coleoptera, Gyrinidae, Haliplidae, Noteridae, Dytiscidae). ZooKeys 1127: 1–60. https://doi.org/10.3897/zookeys.1127.85737

Abstract

Water beetles of the families Gyrinidae, Haliplidae, Noteridae, and Dytiscidae (aquatic Adephaga) of the Makay in central-western Madagascar were surveyed in three campaigns during the years 2016–2018. A total of 74 species was collected from 62 sampling sites, all except one being newly recorded from the Makay. *Copelatus malavergnorum* **sp. nov.** (*irinus* group) and *C. zanabato* **sp. nov.** (*erichsonii* group) (Dytiscidae, Copelatinae) are described and their habitus and male genitalia are illustrated. A systematic account is given, including description of habitat preferences for each species. Analyses of species composition and dominance, species diversity and endemism highlighted the strong singularity of the aquatic Adephaga fauna inhabiting the sandstone massif of inner Makay (notably with several local endemic dytiscids) with respect to its peripheral lowlands. These comparisons were also performed between groups of sites categorised according to vegetation context (forested, semi-forested, non-forested). Rather unexpectedly, inner Makay although well-preserved and little deforested has relatively low endemism level and low species diversity (H_1 Hill number twice lower than in the geographically close and geologically similar massif of Isalo). Species diversity was higher in the deforested and man-impacted peripheral sites, which yielded a rich contingent of western Madagascar lowland species including a few undescribed or rarely observed dytiscids.

Keywords

Conservation, *Copelatus*, distribution, diving beetles, endemism, faunistics, forest, freshwater, new species, species diversity

Introduction

The Makay massif, located in the central-western part of Madagascar (Fig. 1), is one of the most important biodiversity areas of the Island (Carret et al. 2014) and has long remained unexplored. To protect this sanctuary of biodiversity, the status of protected area was granted to the Makay in 2017 (Roubaud et al. 2018). The protected area is bounded to the north by the Malaimbandy municipality and to the south by the Beroroha municipality. With an area of 4000 km^2, the massif spans 150 km from north to south and 50 km from west to east at its widest. From a cultural point of view, the area encompasses from west to east part of the *Sakalava* country (Menabe region) and of the *Bara* country (Atsimo-Andrefana region). The morphology of the Makay massif is the result of the erosion of the crystalline bedrock (yellow Jurassic sandstone) (Prié 2011), which led to the formation of beautiful and impressive canyons. The regional climate in this part of Madagascar is arid with an average annual rainfall of less than 700 mm (Cornet and Guillaumet 1976), but each canyon presents a number of singularities with respect to microclimatic and pedological conditions, and therefore houses a multitude of micro-habitats. These canyons vary from wide and very sunny to narrow canyons permanently shaded and humid and even to crevices just wide enough to allow water to pass through.

The vegetation is adapted to these contrasting life conditions. At places a typical dense rainforest flourishes, highly similar to that usually found in the eastern part of Madagascar, with the presence of remarkable species such as *Cannarium* trees and arborescent ferns such as *Cyathea*. More open areas are colonised by riparian gallery forest and dense dry forests typical of the western Madagascar ecoregion, dominated by the Fabaceae family (Prié 2011). Microclimate largely depends on the topography of the canyons. Where the slope is very steep and never exposed to direct sunlight, canyon walls can be so damp as to keep a moss carpet and green ferns in all seasons; on the contrary other slopes are so dry that they exhibit a typical saxicolous vegetation dominated by *Pachypodium* and *Uapaca* species. Concerning hydrography, the properties of underground rocks allow them to store water, making the Makay massif the largest freshwater reservoir in western Madagascar. Four large rivers originate from the massif: the Mangoky River to the south, the Maharivo and the Morondava rivers to the west and the Tsiribihina River to the north. As a consequence of these features and of its geographical isolation (the Isalo massif, another Jurassic sandstone massif, is situated at ~ 90 km south of the Makay and separated from it by the large Mangoky River plain), the Makay massif houses a very rich biodiversity and high rates of local endemism, for plants as well as for animals (Wendenbaum 2011; Roubaud et al. 2018).

It was not until 2010 that scientific missions to explore and describe the biodiversity of the Makay started (Wendenbaum 2011; Roubaud et al. 2018). Since then, several multidisciplinary expeditions were organised (Roubaud et al. 2018). Despite some visible signs of habitat degradation resulting from local land use, there is still an exceptional level of ecosystem preservation, and the flora and fauna are highly rich and original. The massif is home to 10 species of lemurs (Dolch et al. 2011; Roubaud

et al. 2018). Among the very few other taxa for which more or less systematic species inventories have been conducted in the Makay so far are bats (Prié 2011), scorpions (Lourenço and Wilmé 2015, with description of *Grosphus makay*), and leafhoppers (Gnezdilov 2021, with description of four new species endemic to the Makay). Additional species recently described from the Makay include an Apocynaceae plant (Allorge et al. 2015), a flea species living on bat (Laudisoit et al. 2012), a fly (Feijen et al. 2021), two millipedes (Wesener 2020) and an ant (Csösz et al. 2021). To our knowledge, there are no published data concerning either Coleoptera or aquatic insects of the Makay apart from the recent description of the endemic diving beetle *Laccophilus makay* Manuel & Ramahandrison, 2020.

Currently four families and 231 species of aquatic Adephaga (predaceous water beetles) are recorded from Madagascar. The Dytiscidae (in Malagasy, "tsikovoka") comprise 182 species of which 72% are endemic to Madagascar (however 78% are endemic to the Malagasy region, including Madagascar and the archipelagos of Comoros, Mascarenes, and Seychelles) (Bergsten et al., in press). This family represents the largest portion of the aquatic Adephaga diversity in Madagascar as in the rest of the World. Second in species number is the family Gyrinidae (sister-group to all other Adephaga, Beutel et al. 2020). The Gyrinidae (in Malagasy, "fandiorano") are represented by 25 recorded species in Madagascar (96% endemic) (Gustafson et al. in press). The family Noteridae comprises 19 species in Madagascar of which 63% are endemic to the country and 68% to the Malagasy region (Bergsten and Manuel, in press). Finally, only six species of Haliplidae are known from Madagascar, all but one endemic to Madagascar and all to the Malagasy region (Bergsten, in press). Members of these last two families are not differentiated by Malagasy people and are often called "tsingala" as for many other aquatic insects (even though this Malagasy word in the strict sense refers to water bugs).

We present here the results of three sampling campaigns targeting aquatic Adephaga, conducted in the Makay area by the authors in June 2016, July-August 2017 and April 2018. A total of 87 samplings was conducted in 62 sampling sites (21 sites in northern Makay and 41 in central-southern Makay, Fig. 1). Of these sites, 50 are located in the massif itself (inner Makay: sandstone and canyons area) and 12 are located in the peripheral plain. The examined material comprises 4151 specimens and 74 species (Gyrinidae: 3; Haliplidae: 1; Noteridae: 8; Dytiscidae: 62), all except *Laccophilus makay* being newly recorded for the Makay. We consider useful to describe two new species of the genus *Copelatus*, apparently endemic to the massif, because given difficulty of access, new material of these species is not expected to become available soon, and because these species are easily diagnosed thanks to recent revision of the *Copelatus* species of Madagascar (Ranarilalatiana et al. 2019; Ranarilalatiana and Bergsten 2019; Ranarilalatiana et al. in preparation). Distribution and habitat preferences of all species of aquatic Adephaga recorded from the Makay are commented. Special emphasis is put on differences in species composition, species diversity and endemism between the massif and the surrounding plain, and on how the aquatic Adephaga fauna varies in the study area depending on surrounding vegetation (i.e., water bodies located in forested vs. semi-forested or non-forested environment).

Materials and methods

Abbreviations

a.s.l. Above sea level
E endemic to Madagascar
E* endemic to the Malagasy region (Madagascar, Seychelles, Comoros, and Mascarene islands)
F Forested
H_0 Hill number of order q = 0
H_1 Hill number of order q = 1
H_2 Hill number of order q = 2
MW Maximum width
N Non forested
pr. Printed
RFO Relative frequency of occurrence
sF Semi-forested
TL Total length
CMM Collection of Michaël Manuel, Paris, France
MNHN Muséum National d'Histoire Naturelle, Paris, France
W "widespread", distribution extending beyond the Malagasy region.

Depositories

The study specimens are deposited in the last author's research collection (CMM) and the holotypes of the new species in the MNHN collection.

Sampling

Sampling sites are numbered in chronological order of (first) visit from MAK-1 to MAK-62. They are mapped on Fig. 1 and listed below (Sampling data). When several samplings were conducted in the same site (at different sampling dates or in different ecological situations), they are distinguished by adding a letter at the end of the site code (e.g., MAK-1A, MAK-1B: two different samplings performed at site MAK-1). The maps of Fig. 1 were made with QGis 3.22. (https://www.qgis.org) using the 2018 database of the FTM (Foiben-Taosarintanin'i Madagasikara, Institut Géographique et Hygrogaphique National, Antananarivo, Madagascar). The background map was "Google Map Layer", available in the "XY Layer" menu of QGis.

Three field campaigns were conducted. The first two campaigns (2.–9.VI.2016 and 26.VII.–28.VIII.2017) were conducted in the south-central part of the Makay. In 2016, the area around the Menapanda and the Andranomanintsy rivers was explored (sites MAK-3 to MAK-17, Fig. 1D). In 2017, additional sampling was performed in the same area; furthermore, the canyon of the Makaikely River was

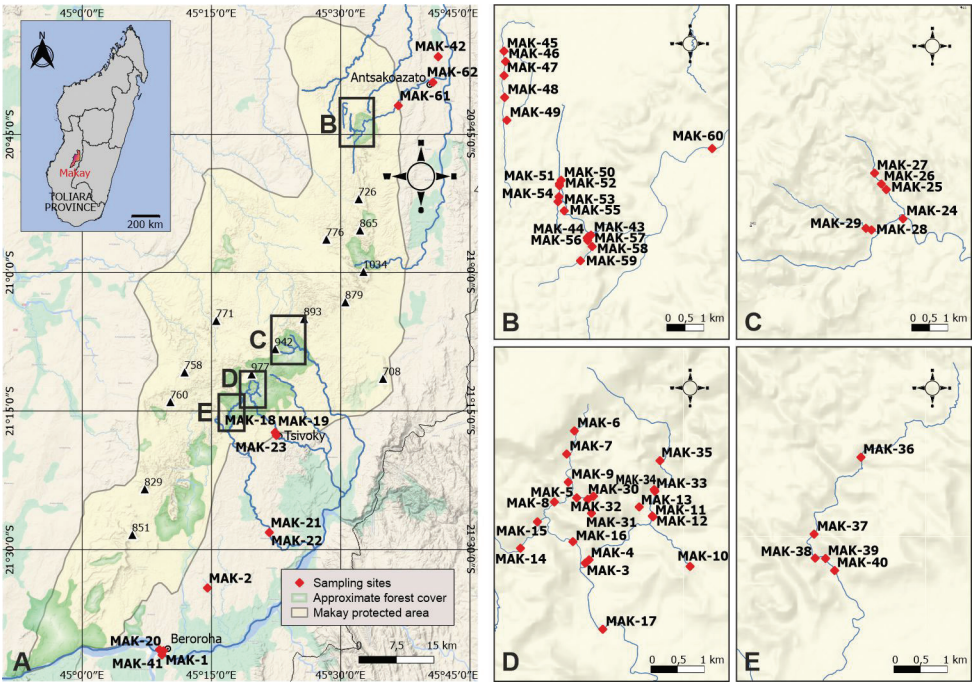

Figure 1. Distribution of sampling sites in the study area **A** map of the Makay protected area, with marked locations of the peripheral sites, and boxes indicating explored areas for inner Makay (top left inset: location of the study area on a map of Madagascar) **B, C, D, E** detailed maps corresponding to the boxes in **A** showing marked locations of the inner Makay sampling sites.

visited and more central areas of the massif along the rivers Mahasoa and Behora were targeted (sites MAK-24 to MAK-40, Fig. 1C, D, E). Sampling sites located in the peripheral plain to the south and south-east of the massif were also visited (areas around Beroroha, Tsivoky, and Makaikely), on the way to and from inner Makay, during both campaigns (sites MAK-1, MAK-2, MAK-18 to MAK23, and MAK-41; Fig. 1A). The third field campaign (10.–18.IV.2018) was carried out in the northern part of the Makay along the Sakamaly River and allowed exploration of the Andranomanga and the Ampasimaiky rivers and their surroundings (sites MAK-43 to MAK-60, Fig. 1B). It was noted that the canyons in this northern part of the Makay were drier and wider than in the south-central part. Three sites located in periphery of the massif to the north-east (MAK-42, MAK-61, MAK-62; Fig. 1A), in the areas of Antsakoazato and Tsimazava, were also visited during the 2018 campaign. Collectors were ATR and MM for the 2016 campaign and ATR for the 2017 and 2018 campaigns.

All samplings were performed in situ by hand netting using a GB-net professional hand net (NHBS, Totnes, Devon, UK) (25 cm frame; depth of net bag 50 cm; mesh 1 mm), except at site MAK-22 (light trap).

Categories of sampling sites

All sites located in the boxes within the map of Fig. 1A, and whose position is detailed in Fig. 1B–E, were categorised as "inner Makay" (i.e., the Makay massif itself, which we shall refer to also as inner area or canyon area). All sites whose position is detailed in Fig. 1A (thus located outside the boxes) were categorised as "peripheral Makay" (i.e., belonging to the Makay Protected Area but geomorphologically not located in the massif; we shall refer to the corresponding zone as the peripheral area or peripheral plain).

Sites were furthermore categorised according to their vegetation context as determined from field observation completed by inspection of satellite images (Google Earth Pro 7.3.) as "forested", "semi-forested" or "non-forested". The context was considered "semi-forested" when a sampling site was located in open or semi-open situation but close to forest edge, or at the bottom of narrow canyons without a proper gallery forest but with a certain density of trees nevertheless present.

Sampling data

In the sampling data given below, the letter between parentheses after the sampling code indicates the vegetation context: **F**, forested; **sF**, semi-forested; **N**: non-forested.

MAK-1A (N): Beroroha municipality, ca. 2 km W of Beroroa township; ca. 157 m a.s.l.; ca. 21°41'S, 45°09'E; 02.VI.2016; shallow puddles (diameter 1 to 2 meters), with sparse vegetation, along the sandy banks of the Mangoky River.

MAK-1B (N): Same as MAK-1A except 09.VI.2016; long and narrow puddle (1 m × 10 m), without vegetation.

MAK-1C (N): Same as MAK-1B except large shallow puddle (ca. 6 m × 20 m) (Fig. 2A).

MAK-2 (N): Beroroha municipality, ca. 15 km SW of Makaikely; ca. 245 m a.s.l.; 21°34'08"S, 45°14'32"E; 03.VI.2016; shallow, slowly flowing stream, sandy bottom, with high density of green algae (Fig. 2B, C).

MAK-3 (sF): Beroroha municipality, ca. 10 km NNW of Tsivoky; ca. 487 m a.s.l.; 21°13'21"S, 45°19'32"E; 04.VI.2016; puddle on the bank of the Andranomanintsy River, sandy bottom; Makay massif (Fig. 2D).

MAK-4 (sF): Beroroha municipality, ca. 10 km NNW of Tsivoky; ca. 490 m a.s.l.; 21°13'19"S, 45°19'34"E; 04.VI.2016; spring nearby Andranomanintsy River; Makay massif (Fig. 2E).

MAK-5A (sF): Beroroha municipality, ca. 10 km NW of Tsivoky; ca. 650 m a.s.l.; 21°12'42"S, 45°19'27"E; 05.VI.2016; deep pond above natural dam in a canyon; Makay massif (Fig. 2F).

MAK-5B (sF): same as MAK-5A except slow stream flowing out from the pond, with deep accumulation of organic matter on the bottom.

MAK-5C (sF): same as MAK-5A except 17.VIII.2017.

MAK-5D (sF): same as MAK-5C except under mass of *Cyathea* roots.

MAK-6 (N): Beroroha municipality, ca. 10 km NW of Tsivoky; ca. 670 m a.s.l.; 21°12'01"S, 45°19'25"E; 05.VI.2016; quiet corner on the edge of a small stream, in the bottom of a deep strongly embanked canyon, with orange masses of iron bacteria; Makay massif (Fig. 2G).

MAK-7 (sF): Beroroha municipality, ca. 10 km NW of Tsivoky; ca. 620 m a.s.l.; 21°12'15"S, 45°19'20"E; 05.VI.2016; puddle with orange masses of iron bacteria, in stream bed, in the bottom of a deep strongly embanked canyon; Makay massif (Fig. 2J, K).

MAK-8 (F): Beroroha municipality, ca. 11 km NNW of Tsivoky; ca. 551 m a.s.l.; 21°12'44"S, 45°19'12"E; 05.VI.2016; large quiet and shaded pool, along streamlet, with masses of tree roots, bottom of sand, gravel and stones; Makay massif (Fig. 2I).

MAK-9 (N): Beroroha municipality, ca. 11 km NW of Tsivoky; ca. 656 m a.s.l.; 21°12'32"S, 45°19'21"E; 05.VI.2016; vertical rock walls with water film and crust of bryophytes and algae, in the bottom of a deep canyon; Makay massif (Fig. 2H).

MAK-10 (F): Beroroha municipality, ca. 9 km NNW of Tsivoky; ca. 602 m a.s.l.; 21°13'23"S, 45°20'40"E; 06.VI.2016; small pools with clay-sandy bottom and vegetal debris, in a small canyon; Makay massif (Fig. 2L, M).

MAK-11A (N): Beroroha municipality, ca. 10 km NNW of Tsivoky; ca. 514 m a.s.l.; 21°12'53"S, 45°20'16"E; 06.VI.2016; small muddy ponds on sandy bank of the Menapanda River, with sparse vegetation, in open area; Makay massif (Fig. 2O).

MAK-11B (N): same as MAK-11A except puddle with turbid water and without vegetation (Fig. 2P).

MAK-12A (sF): Beroroha municipality, ca. 10 km NNW of Tsivoky; ca. 516 m a.s.l.; 21°12'53"S, 45°20'16"E; 06.VI.2016; shaded spring on the bank of the Menapanda River, bottom of sand, sandstone mass and decaying vegetal matter, with vegetation and with orange iron bacteria deposit; Makay massif.

MAK-12B (sF): same as MAK-12A except 19.VIII.2017.

MAK-12C (sF): same as MAK-12A except small pond next to and fed by the spring.

MAK-13 (F): Beroroha municipality, ca. 10 km NNW of Tsivoky; ca. 527 m a.s.l.; 21°12'47"S, 45°20'07"E; 06.VI.2016; streamlet with vegetation in gallery forest; Makay massif.

MAK-14A (F): Beroroha municipality, ca. 10.7 km NW of Tsivoky; ca. 537 m a.s.l.; 21°13'12"S, 45°18'50"E; 07.VI.2016; small shaded pools, with orange masses of iron bacteria, against the walls of a canyon; Makay massif (Fig. 2N).

MAK-14B (F): same as MAK-14A, except stream in the bottom of a canyon, bottom of sand and gravel, clear water.

MAK-15 (F): Beroroha municipality, ca. 10.8 km NW of Tsivoky; ca. 570 m a.s.l.; 21°12'56"S, 45°19'01"E; 07.VI.2016; shallow, shaded stream, clear water, with tree roots; Makay massif.

MAK-16 (F): Beroroha municipality, ca. 10 km NW of Tsivoky; ca. 506 m a.s.l.; 21°13'08"S, 45°19'24"E; 07.VI.2016; small pond with vegetation, on the bank of the Andranomanintsy River; Makay massif.

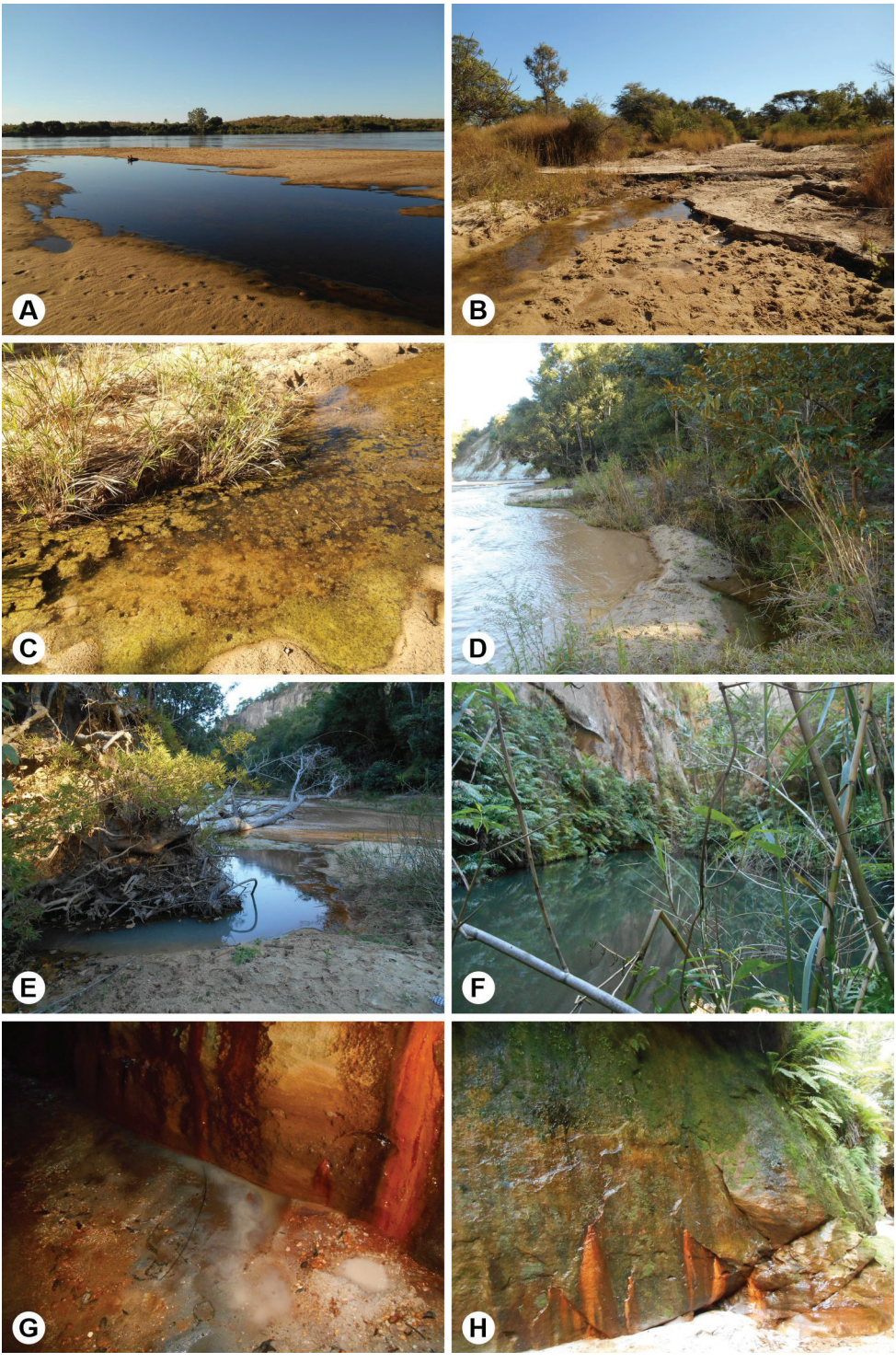
A
B
C
D
E
F
G
H

MAK-17 (sF): Beroroha municipality, ca. 8.5 km NW of Tsivoky; ca. 474 m a.s.l.; 21°14'01"S, 45°19'43"E; 08.VI.2016; small isolated puddle, on rock mass, on the bank of the Menapanda River; Makay massif.

MAK-18 (N): Beroroha municipality, ca. 1 km NW of Tsivoky; ca. 372 m a.s.l.; 21°17'13"S, 45°22'20"E; 08.VI.2016; small and shaded muddy ditch, water rather turbid, no vegetation.

MAK-19 (N): Beroroha municipality, ca. 800 m NW of Tsivoky; ca. 363 m a.s.l.; 21°17'20"S, 45°22'23"E; 08.VI.2016; large puddle with water slowly flowing, on dirty road between two rice fields, full of rice straw.

MAK-20 (N): Beroroha municipality, ca. 1,5 km W of Beroroa; ca. 157 m a.s.l.; 21°40'58"S, 45°08'57"E; 09.VI.2016; rice fields near the Mangoky River.

MAK-21 (N): Beroroha municipality, Makaikely; ca. 243 m a.s.l.; 21°28'8"S, 45°21'41"E; 26.VII.2017; puddle with sandy bottom under *Phragmites*, west bank of the Makaikely River.

MAK-22 (N): Beroroha municipality, Makaikely; ca. 243 m a.s.l.; 21°28'8"S, 45°21'43"E; 26.VII.2017; light trap.

MAK-23 (N): Beroroha municipality, Tsivoky; ca. 359 m a.s.l.; 21°17'38"S, 45°22'32"E; 27.VII.2017; Menapanda River near the village of Tsivoky, sandy bottom, with *Cyperus* and *Marsilea*.

MAK-24 (sF): Beroroha municipality, ca. 18 km NNE of Tsivoky; ca. 484 m a.s.l.; 21°08'2"S, 45°25'4"E; 29.VII.2017; Mahasoa River, sandy bottom; Makay massif.

MAK-25A (sF): Beroroha municipality, ca. 19 km NNE of Tsivoky; ca. 501 m a.s.l.; 21°07'36"S, 45°24'48"E; 30.VII.2017; puddle on the sandy banks of the Mahasoa River, with orange deposit of iron bacteria; Makay massif.

Figure 2. Representative habitats of aquatic Adephaga in Makay. **Sites located in the peripheral area: A** large shallow puddle on the sandy bank of the Mangoky River in Beroroa (MAK-1C), habitat of *Pachynectes costulifer, Yola costipennis* **B, C** shallow, slowly flowing stream in semi-open area, with sandy bottom and high density of green algae (MAK-2), habitat of *Bidessus longistriga, B. perexiguus, Canthydrus concolor, C. flavosignatus, C. guttula, Clypeodytes concivis, C.* sp. Ma3, *Cybister cinctus, Hydaticus servillianus, Hydroglyphus geminodes, Hydrovatus acuminatus, H. capnius, H. cruentatus, H. dentatus, H. otiosus, H. parvulus, H. pictulus, H. testudinarius, H.* sp. Ma7, *Laccophilus addendus, L. flaveolus, L. pallescens, L. posticus, L. rivulosus, L. seyrigi, Methles* sp. Ma5, *Neohydrocoptus seriatus, Pachynectes* sp. Ma1, *Philaccolus elongatus, Pseuduvarus* sp. Ma1, *Rhantaticus congestus, Uvarus rivulorum*. **Sites located in inner Makay: D** puddle (on the right) on the sandy bank of the Andranomanintsy River (left half of the picture) (MAK-3), habitat of *Copelatus ruficapillus, Hydrovatus acuminatus, Hyphydrus separandus, Laccophilus makay, L. posticus, Madaglymbus fairmairei, Pachynectes* sp. Ma1 **E** spring on the bank of the Andranomanintsy River (MAK-4), habitat of *Copelatus ruficapillus, Hydroglyphus capitatus, H. geminodes, Hyphydrus separandus, Laccophilus makay, L. posticus, Pachynectes* sp. Ma1 **F** deep pond above natural dam in the bottom of a canyon (MAK-5A), habitat of *Africophilus nesiotes, Hyphydrus separandus, L. addendus, Laccophilus insularum, L. makay, Neptosternus oblongus, Pachynectes* sp. Ma1, *P.* sp. Ma4 **G** edge of small shallow stream, in the bottom of a deep strongly embanked canyon, with orange deposit of iron bacteria (MAK-6), habitat of *Copelatus acamas* and *Laccophilus makay* **H** vertical rock wall with water film and crust of bryophytes and algae, in the bottom of a deep canyon (MAK-9), habitat of *Africophilus bartolozzii*

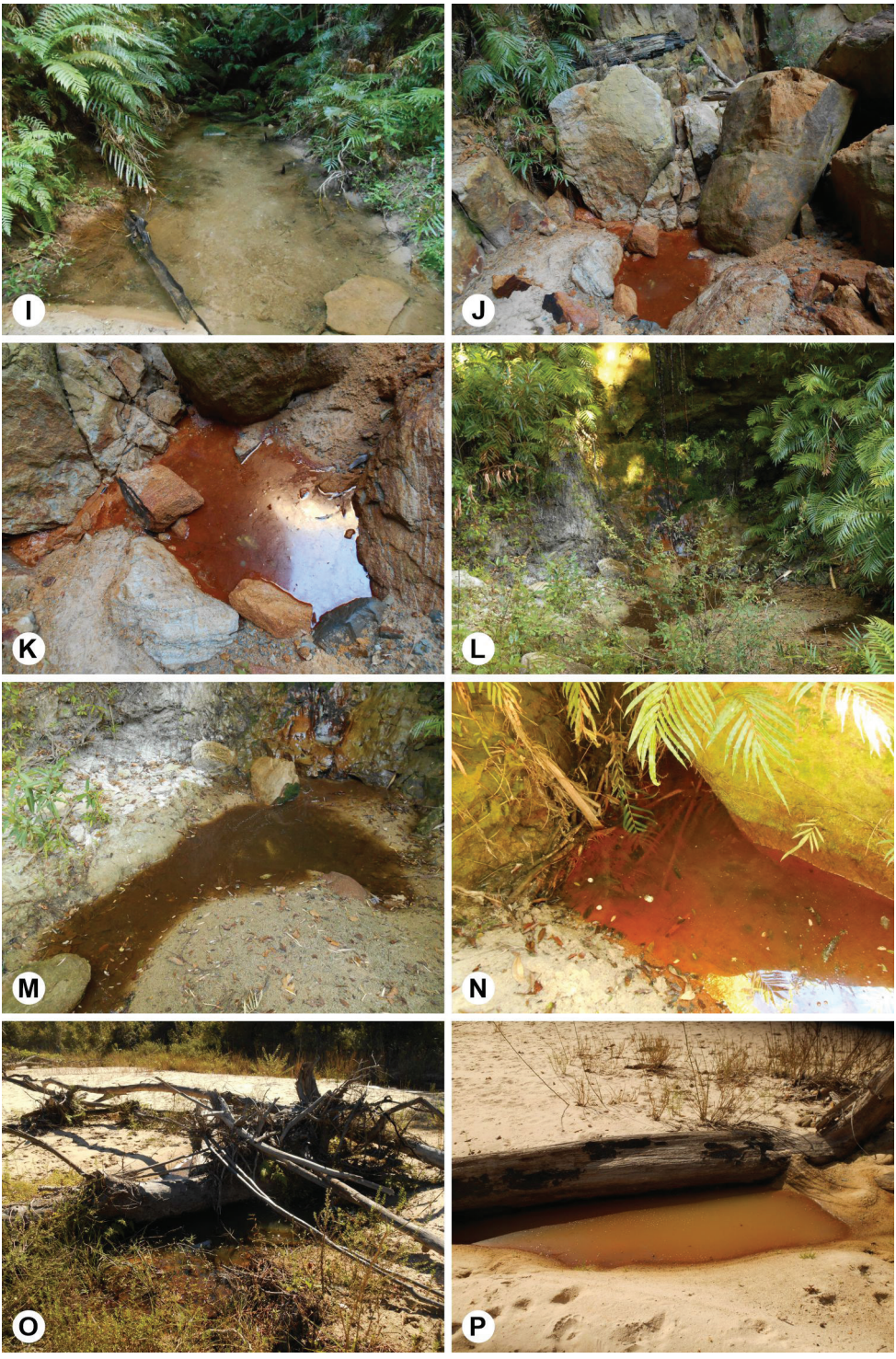
I
J
K
L
M
N
O
P

MAK-25B (sF): same as MAK-25A except small and calm pool under rock along the edge of the river, with tree roots.

MAK-26 (F): Beroroha municipality, ca. 19 km NNE of Tsivoky; ca. 514 m a.s.l.; 21°07'31"S, 45°24'44"E; 30.VII.2017; quiet part of a stream, bottom of sand and organic matter; Makay massif.

MAK-27 (F): Beroroha municipality, ca. 19 km NNE of Tsivoky; ca. 526 m a.s.l.; 21°07'22"S, 45°24'37"E; 30.VII.2017; Mahasoa River; Makay massif.

MAK-28 (sF): Beroroha municipality, ca. 18 km NNE of Tsivoky; ca. 504 m a.s.l.; 21°08'12"S, 45°24'34"E; 01.VIII.2017; small quiet pool in sandy stream bed, water turbid, with accumulation of dead tree leaves; Makay massif.

MAK-29 (sF): Beroroha municipality, ca. 18 km NNE of Tsivoky; ca. 507 m a.s.l.; 21°08'11"S, 45°24'29"E; 01.VIII.2017; small pool among rocks at the edge of a stream; Makay massif.

MAK-30 (F): Beroroha municipality, ca. 11 km NNW of Tsivoky; ca. 675 m a.s.l.; 21°12'40"S, 45°19'37"E; 17.VIII.2017; small pool in the bottom of a deep canyon; Makay massif.

MAK-31A (sF): Beroroha municipality, ca. 11 km NNW of Tsivoky; ca. 693 m a.s.l.; 21°12'51"S, 45°19'36"E; 17.VIII.2017; small pool among rocks in stream bed; Makay massif.

MAK-31B (sF): same as MAK-31A except small deep-water pool in a small cave.

MAK-31C (sF): same as MAK-31A except small shaded pool at the entrance of small cave.

MAK-32 (sF): Beroroha municipality, ca. 11 km NNW of Tsivoky; ca. 650 m a.s.l.; 21°12'42"S, 45°19'34"E; 17.VIII.2017; small pool in the bottom of a canyon, under *Cyathea* tree ferns; Makay massif.

MAK-33 (F): Beroroha municipality, ca. 10 km NNW of Tsivoky; ca. 525 m a.s.l.; 21°12'37"S, 45°20'17"E; 19.VIII.2017; small puddle with sandy bottom; Makay massif.

Figure 21. (Continued) **I** large quiet and shaded pool in forest, along streamlet, with masses of tree roots and bottom of sand, gravel and stones (MAK-8), habitat of *Africophilus bartolozzii, A. nesiotes, Copelatus ruficapillus, Hydaticus sobrinus, Hyphydrus separandus, Laccophilus makay, Pachynectes* sp. Ma1 **J** (context) **K** (close-up) Puddle with orange masses of iron bacteria, in stream bed, in the bottom of a deep strongly embanked canyon (MAK-7), habitat of *Copelatus acamas, C. ruficapillus, Laccophilus makay* **L** (context) **M** (close-up) Small pool with clay-sandy bottom and plant debris, in a small canyon, in gallery forest (MAK-10), habitat of *Copelatus ruficapillus, Hyphydrus separandus, Laccophilus makay, Madaglymbus fairmairei* **N** small shaded pool, with orange masses of iron bacteria, in gallery forest against the wall of a canyon (MAK-14A), habitat of *Africophilus nesiotes, Copelatus acamas, Hydaticus dorsiger, Hyphydrus separandus, Laccophilus makay, Pachynectes* sp. Ma1, *P.* sp. Ma4 **O** small muddy pond, with sparse vegetation, in open area on the sandy banks of the Menapanda River (MAK-11A), habitat of *Canthydrus guttula, Copelatus polystrigus, Hydaticus dorsiger, Laccophilus addendus, L. posticus, Neohydrocoptus seriatus* **P** puddle with turbid water and without vegetation, in open area on the sandy banks of the Menapanda River (MAK-11-B), habitat of *Copelatus polystrigus, C. ruficapillus, Eretes griseus, Hydaticus dorsiger, H. exclamationis, Hyphydrus separandus, Laccophilus addendus, L. posticus, Madaglymbus fairmairei*.

MAK-34A (F): Beroroha municipality, ca. 10 km NNW of Tsivoky; ca. 538 m a.s.l.; 21°12'36"S, 45°20'16"E; 19.VIII.2017; puddle and spring at the foot of a cliff; Makay massif.

MAK-34B (F): same as MAK-34A except: puddle situated more downstream than MAK-34A.

MAK-35A (F): Beroroha municipality, ca. 10.5 km NNW of Tsivoky; ca. 536 m a.s.l.; 21°12'20"S, 45°20'21"E; 19.VIII.2017; Small pool among trees, near Menapanda River; Makay massif.

MAK-35B (F): same as MAK-35A except puddle in a rock cavity.

MAK-35C (F): same as MAK-35A except small stream between MAK-35A and MAK-35B.

MAK-36A (F): Beroroha municipality, ca. 10,5 km NW of Tsivoky; ca. 561 m a.s.l.; 21°14'32"S, 45°17'32"E; 21.VIII.2017; streamlet near Andranomanintsy River; Makay massif.

MAK-36B (F): same as MAK-36A except small puddle on rock under *Pandanus* tree.

MAK-37A (F): Beroroha municipality, ca. 11 km WNW of Tsivoky; ca. 453 m a.s.l.; 21°15'19"S, 45°17'02"E; 24.VIII.2017; water hole in rock mass; Makay massif.

MAK-37B (F): same as MAK-37A except very slowly flowing river, bottom of sand and mud, no vegetation.

MAK-38A (F): Beroroha municipality, ca. 10.5 km WNW of Tsivoky; ca. 450 m a.s.l.; 21°15'32"S, 45°17'01"E; 25.VIII.2017; small stinky puddle with decaying leaves near Makaikely campment; Makay massif.

MAK-38B (F): same as MAK-38A except small pond along river, sandy bottom, water rather turbid, no vegetation.

MAK-39A (F): Beroroha municipality, ca. 10.5 km WNW of Tsivoky; ca. 448 m a.s.l.; 21°15'33"S, 45°17'09"E; 25.VIII.2017; small puddle under a *Pandanus* tree, with dead tree leaves; Makay massif.

MAK-39B (F): same as MAK-39A except small puddle among rocks along river.

MAK-40A (F): Beroroha municipality, ca. 10 km WNW of Tsivoky; ca. 442 m a.s.l.; 21°15'41"S, 45°17'15"E; 25.VIII.2017; small quiet section of a river, sandy bottom, without vegetation; Makay massif.

MAK-40B (F): same as MAK-40A except confluence of a small wet zone (located in a depression) with a river.

MAK-41 (N): Beroroha municipality; ca. 160 m a.s.l.; 21°41'18"S, 45°09'07"E; 28.VIII.2017; small puddle on sandy west bank of River Mangoky.

MAK-42 (N): Malaimbandy municipality, ca. 5 km NNE of Antsakoazato; ca. 227 m a.s.l.; 20°36'34"S, 45°41'19"E; 10.IV.2018; open marsh, with vegetation of Poaceae, *Cyperus*, *Polygonum* and *Nymphaea*, with water rather turbid and moderate density of filamentous green algae.

MAK-43 (sF): Malaimbandy municipality, ca. 20 km WSW of Tsimazava; ca. 360 m a.s.l.; 20°44'42"S, 45°31'38"E; 11.IV.2018; shallow margin of the Sakapaly River, water slowly flowing, sandy bottom, with helophytes (Poaceae); Makay massif.

MAK-44A (F): Malaimbandy municipality, ca. 20 km WSW of Tsimazava; ca. 364 m a.s.l.; 20°44'42"S, 45°31'35"E; 11.IV.2018; puddle on the east bank of the Sakapaly River, sandy bottom, without organic matter, water red-brown, containing cyanobacteria; Makay massif.

MAK-44B (F): same as MAK-44A except bottom with decaying vegetal debris.

MAK-44C (F): same as MAK-44A except blind channel connected with the Sakapaly River, with orange masses of iron bacteria on the bottom.

MAK-45 (sF): Malaimbandy municipality, ca. 21 km W of Tsimazava; ca. 419 m a.s.l.; 20°42'01"S, 45°30'17"E; 12.IV.2018; small pool in a canyon towards Andranomanga; Makay massif.

MAK-46 (sF): Malaimbandy municipality, ca. 21 km W of Tsimazava; ca. 433 m a.s.l.; 20°42'10"S, 45°30'18"E; 12.IV.2018; pool in a very narrow and dark canyon; Makay massif.

MAK-47 (sF): Malaimbandy municipality, ca. 21 km W of Tsimazava; ca. 429 m a.s.l.; 20°42'22"S, 45°30'17"E; 12.IV.2018; small pool in a canyon near the Andranomanga River; Makay massif.

MAK-48 (sF): Malaimbandy municipality, ca. 21 km W of Tsimazava; ca. 451 m a.s.l.; 20°42'41"S, 45°30'18"E; 12.IV.2018; Andranomanga River, water slowly flowing, sandy bottom, no vegetation; Makay massif.

MAK-49 (sF): Malaimbandy municipality, ca. 21 km W of Tsimazava; ca. 488 m a.s.l.; 20°43'01"S, 45°30'20"E; 12.IV.2018; small pool, bottom of gravel and stones, near the Andranomanga River; Makay massif.

MAK-50 (sF): Malaimbandy municipality, ca. 20 km WSW of Tsimazava; ca. 437 m a.s.l.; 20°43'54"S, 45°31'10"E; 14.IV.2018; small pond in a canyon at Ampasimaiky; Makay massif.

MAK-51 (sF): Malaimbandy municipality, ca. 20 km WSW of Tsimazava; ca. 429 m a.s.l.; 20°43'57"S, 45°31'8"E; 14.IV.2018; small pool on dried-out river bed; Makay massif.

MAK-52 (sF): Malaimbandy municipality, ca. 20 km WSW of Tsimazava; ca. 425 m a.s.l.; 20°43'58"S, 45°31'9"E; 14.IV.2018; sandy pool in canyon along the Ampasimaiky River; Makay massif.

MAK-53 (sF): Malaimbandy municipality, ca. 20 km WSW of Tsimazava; ca. 423 m a.s.l.; 20°44'8"S, 45°31'8"E; 14.IV.2018; small pool under trees, filled in with tree roots at Ampasimaiky; Makay massif.

MAK-54A (sF): Malaimbandy municipality, ca. 20 km WSW of Tsimazava; ca. 418 m a.s.l.; 20°44'12"S, 45°31'7"E; 14.IV.2018; small stream coming out from a canyon at Ampasimaiky; Makay massif.

MAK-54B (sF): same as MAK-54A except ca. 416 m a.s.l.; small and slowly flowing derivation of the Ampasimaiky River.

MAK-55 (sF): Malaimbandy municipality, ca. 20 km WSW of Tsimazava; ca. 409 m a.s.l.; 20°44'20"S, 45°31'13"E; 14.IV.2018; Ampasimaiky River, flowing at the bottom of a canyon; Makay massif.

MAK-56 (F): Malaimbandy municipality, ca. 20 km WSW of Tsimazava; ca. 366 m a.s.l.; 20°44'44"S, 45°31'34"E; 16.IV.2018; small stream near the Sakapaly River; Makay massif.

MAK-57 (F): Malaimbandy municipality, ca. 20 km WSW of Tsimazava; ca. 369 m a.s.l.; 20°44'46"S, 45°31'35"E; 16.IV.2018; small water hole filled in with *Pandanus* leaves, near the Sakapaly River; Makay massif.

MAK-58 (F): Malaimbandy municipality, ca. 20 km WSW of Tsimazava; ca. 377 m a.s.l.; 20°44'51"S, 45°31'39"E; 16.IV.2018; small blind channel on the bank of the Sakapaly River; Makay massif.

MAK-59A (F): Malaimbandy municipality, ca. 20 km WSW of Tsimazava; ca. 435 m a.s.l.; 20°45'4"S, 45°31'28"E; 17.IV.2018; quiet part of a stream in Ambilando Canyon, sandy bottom, no vegetation; Makay massif.

MAK-59B (F): same as MAK-59A except small pool under a rock mass along the Ambilando stream.

MAK-59C (F): same as MAK-59A except Ambilando stream, slow-flowing, sandy bottom with vegetal debris, no vegetation.

MAK-60 (sF): Malaimbandy municipality, ca. 16 km WSW of Tsimazava; ca. 324 m a.s.l.; 20°43'26"S, 45°33'31"E; 18.IV.2018; open marsh with vegetated margins (Cyperaceae and Polygonaceae), muddy bottom, near the Sakapaly River; Makay massif.

MAK-61 (N): Malaimbandy municipality, ca. 10 km W of Tsimazava; ca. 286 m a.s.l.; 20°41'53"S, 45°36'41"E; 18.IV.2018; pond along the east bank of the Sakapaly River, muddy bottom, with helophytes (Cyperaceae and Polygonaceae).

MAK-62 (N): Malaimbandy municipality, Antsakoazato; ca. 235 m a.s.l.; 20°39'21"S, 45°40'42"E; 18.IV.2018; canal at the edge of rice fields, slowly flowing, with muddy bottom, water rather turbid, without vegetation.

Morphology and taxonomy

Specimens were morphologically identified to species level by MM (when necessary, with study of dissected genitalia) using the relevant taxonomic literature (reviewed in Bergsten et al. in press) and comparisons with reference specimens in CMM. In difficult cases, type material in the MNHN collection was examined. The nomenclature for Dytiscidae follows the last version of the World Catalogue of Dytiscidae (Nilsson and Hájek 2022). Species which could not be reliably named (i.e., either undescribed species, or species belonging to difficult genera in need of revision, such as *Methles* and *Pseuduvarus*) were assigned a species code (in the form "sp. Ma1", "sp. Ma2", etc.).

For illustration of newly described species, photographs of habitus were made with an Olympus SZX12 trinocular stereomicroscope (Tokyo, Japan) using a Spot FLEX Color Pixel Shift 64 Mp camera (Diagnostic Instruments Inc., Sterling Heights, MI, USA) with SPOT BASIC software (http://www.spotimaging.com/software/spot-basic/). For each habitus picture, a Z-series of ~ 30 photos was produced and stacked

using HELICON FOCUS Software (Helicon Soft Ltd., Kharkiv, Ukraine), then the surrounding was removed in PHOTOSHOP (Adobe, San Jose, CA, USA) and the image was filtered (Higauss filter, pass 2, strength 1) using the IMAGE PRO PLUS software (Media Cybernetics, Bethesda, MD, USA, http://www.mediacy.com/imageproplus/). Male genitalia were studied and figured in wet condition. Photographs of the genitalia were taken with an Olympus BX61 microscope using a Q imaging camera (15.2 64 Mp Shifting Pixel, Diagnostic Instruments Inc.) with IMAGE PRO PLUS. They were stacked and processed as explained above. The terminology used for genitalia orientation follows Miller and Nilsson (2003). Measurements were made using the "Measure" tool in SPOT BASIC.

Label data of type material are given as written in quotation marks, with separate label lines indicated by a slash (/) and separate labels by a double slash (//). Authors' additional remarks are provided in square brackets.

Analyses of species representativeness and diversity

Relative frequency of occurrence (RFO) of a species for a given set of samplings was calculated by dividing the number of samplings with the species present by the total number of samplings, for the set under consideration.

Interpolation-extrapolation sampling curves (Chao and Jost 2012; Colwell et al. 2012; Chao et al. 2014) were built using iNEXT Online (https://chao.shinyapps.io/iNEXTOnline/) (with default endpoint, 40 nodes and 50 replicates of bootstrap) to quantify and compare species diversity, through estimates of Hill numbers of orders q = 0, q = 1, and q = 2 (respectively noted H_0, H_1, and H_2) across categories of samplings (all; peripheral Makay sites; inner Makay sites; forested sites; semi-forested sites; non-forested sites). For these analyses, numbers of specimens sampled for each species were summed up across samplings associated with each category (see Suppl. material 1: Table S1). For a general explanation about Hill numbers, see Gotelli and Ellison (2013). H_0 is equivalent to species richness; starting from q=1, the Hill number expresses in "species equivalents" a compromise between species richness and evenness (evenness is maximal if all species present have the same abundances); the higher the order, the higher the weight of evenness with respect to species richness. H_1 corresponds to the exponential of the classical Shannon index; and H_2 corresponds to the inverse of the Simpson index.

In order to compare the groups of observations with each other and to quantify similarity/dissimilarity in species composition, Jaccard (based on occurrence data) and Bray-Curtis (based on abundance data) dissimilarity indices were calculated (with the R software). The data were standardised prior to computation of Bray-Curtis indices. The Jaccard dissimilarity index between two sets of objects A and B is equal to 1 - J(A,B) where $J(A,B) = |A \cap B| / |A \cup B|$. For the formula of the Bray-Curtis dissimilarity index see Gotelli and Ellison (2013).

Results

Systematic account

Family Gyrinidae

***Dineutus proximus* Aubé, 1838**

Type locality. Madagascar.

Material examined. 1 ♂, 2 ♀♀: MAK-5B; 1 ♂, 1 ♀: MAK-5D; 2 ♂♂: MAK-13; 2 ♂♂, 3 ♀♀: MAK-14B; 2 ♂♂, 1 ♀: MAK _24; 3 ♂♂, 8 ♀ ♀: MAK-27; 1 ♀: MAK-30; 1 ♀: MAK-35C; 2 ♂♂, 2 ♀♀: MAK-37B; 2 ♀♀: MAK-40A; 2 ♂♂, 3 ♀♀: MAK-40B; 3 ♂♂, 3 ♀♀: MAK-48; 1 ♂, 2 ♀♀: MAK-55; 1 ♂, 1 ♀: MAK-59A; ; 1 ♂, 3 ♀♀: MAK-59C.

Distribution. Madagascar, widespread (Legros 1951; Brinck 1955; Bameul 1984).

Habitat in study area. Collected only in inner Makay, in permanent lotic habitats (rivers and streams) with sandy bottom (in a few sites substrate was more rocky) and with clear water, in forested or semi-forested environmental context, with little or no anthropogenic disturbance.

***Dineutus sinuosipennis sinuosipennis* Castelnau, 1840**

= *D. bidens* Vollenhoven, 1869; *D. denticulatus* Régimbart, 1882.

Type locality. Tibet (erroneous locality?).

Material examined. 1 ♂, 4 ♀♀: MAK-27; 3 ♂♂, 4 ♀♀: MAK-37B; 1 ♂, 1 ♀: MAK-40A; 1 ♂: MAK-40B; 1 ♀: MAK-48; 1 ♂, 5 ♀♀: MAK-52; 5 ♂♂, 9 ♀♀: MAK-55; 1 ♀: MAK-58.

Distribution. Madagascar, widespread (Legros 1951; Brinck 1955; Bameul 1984). Another subspecies, *D. sinuosipennis comorensis* Régimbart, 1892, is present in the Comoro archipelago (Brinck 1955; Wewalka 1980).

Habitat in study area. Same as *D. proximus* (both species often syntopic). This species is less abundant than *D. proximus* in the Makay massif.

***Orectogyrus vicinus* Régimbart, 1892**

Type locality. Madagascar, Diego Suarez (Antsiranana), Isokitra.

Material examined. 1 ♂: MAK-15; 2 ♂♂, 3 ♀♀: MAK-36A; 7 ♂♂, 6 ♀♀: MAK-37B; 1 ♀: MAK-40B; 1 ♂, 3 ♀♀: MAK-48.

Distribution. Madagascar. Previously recorded only from the northern part of the island (Legros 1951; Brinck 1956; Gustafson et al. in press).

Habitat in study area. Same as the two preceding species, with a stronger preference for forested and undisturbed habitats.

Family Haliplidae

***Peltodytes quadratus* Régimbart, 1895**

Type locality. Madagascar, Antananarivo, Ambodinandohalo Lake.

Material examined. 1 ♀: MAK-19; 1 ♂: MAK-41.

Distribution. Madagascar, widespread (Guignot 1959–1961; Bertrand and Legros 1971; Bameul 1984; Rocchi 1991; van Vondel and Bergsten 2012).

Habitat in study area. This species was only found at two sampling sites, both peripheral. One was a large puddle partially sheltered by trees, with water slowly flowing and with abundant rice straw debris, on a dirty road between two rice fields, and the other was a small puddle in open situation on the sandy bank of a river, with *Azolla* aquatic ferns (eutrophication indicator).

Family Noteridae

***Canthydrus concolor* Sharp, 1882**

Type locality. Madagascar.

Material examined. 1 ♂: MAK-2.

Distribution. Madagascar, widespread (Guignot 1959–1961; Bertrand and Legros 1971; Rocchi 1991; Nilsson 2011).

Habitat in study area (Fig. 2B, C). This species is widespread and generally common in Madagascar, in well-vegetated lentic or calm lotic environments. It is seemingly absent from inner Makay, and was sampled only once in a peripheral site. The habitat was a shallow insolated stream characterised by very weak water flow, sandy bottom, marked by anthropic disturbance (cattle trampling), sparse tufts of small Cyperaceae and strong presence of filamentous green algae.

***Canthydrus flavosignatus* Régimbart, 1903**

Type locality. Madagascar, Fort-Dauphin, Ankara.

Material examined. 2 ♂♂: MAK-2; 1 ♀: MAK-19.

Distribution. Zaire (Democratic Republic of the Congo), Madagascar (Guignot 1959–1961; Nilsson 2011).

Habitat in study area (Fig. 2B, C). This species was harvested at two sites in the Makay periphery, both in deforested areas. One was the site described for *C. concolor* and the other one was a large puddle, with water slowly flowing and with abundant rice straw debris, on a dirty road between two rice fields.

Canthydrus guttula (Aubé, 1838)

Type locality. La Réunion; Madagascar.

Material examined. 3 ♀: MAK-1A; 1 ♀: MAK-2; 1 ♀: MAK-11A; 52 ♂♂, 39 ♀♀: MAK-19; 1 ♂: MAK-20; 1 ♂, 2 ♀♀: MAK-38B; 1 ♂, 3 ♀♀: MAK-40A; 2 ♂♂, 4 ♀♀: MAK-41; 4♂♂, 8 ♀♀: MAK-42; 17 ♂♂, 11 ♀♀: MAK-60; ; 1 ♂: MAK-61.

Distribution. Madagascar and Mascarene Islands; widespread and common in Madagascar (Guignot 19591961; Betrand and Legros 1971; Bameul 1984; Rocchi 1991; Nilsson 2011).

Habitat in study area (Fig. 2B, C, O). Collected mainly in peripheral but also in a few inner massif sites. This species is found in permanent or temporary lentic habitats as well as in the calm margins of slowly flowing water bodies, with at least some amount of clay or mud at the bottom. Although a few individuals were taken at some sites without any vegetation or significant accumulation of organic debris, the species is most abundant in well-vegetated habitats and/or with bottom heavily loaded with dead vegetal material. This species has a preference for open environments and is highly tolerant to anthropogenic perturbation (e.g., present in rice fields).

Canthydrus sp. Ma5

Material examined. 1 ♀: MAK-20; 1 ♂, 3 ♀♀: MAK-60; 3 ♀♀: MAK-61.

Note. This species is very similar to *C. flavosignatus* but smaller and with a slightly different shape of the apex of the median lobe of aedeagus in lateral view. The Malagasy species of Noteridae are in great need of revision, and in the current state of knowledge we cannot assign a name to this species.

Distribution. Madagascar. In addition to the specimens from the Makay, we also have specimens from Namoroka (north-eastern part of the island).

Habitat in study area. Species collected in permanent lentic environments in open peripheral sites, with clay bottom, clear water and presence of vegetation. One of the collecting sites was a rice field.

Neohydrocoptus seriatus (Sharp, 1882)

Type locality. Madagascar.

Material examined. 2 ♂♂: MAK-2; 1 ♀: MAK-11A; 8 ♂♂, 16 ♀♀: MAK-19; 1 ♂, 2 ♀♀: MAK-21; 20 exs.: MAK-23; 1 ♂: MAK-38B; 2 ♂♂, 1 ♀: MAK-42; 8 ♂♂, 10 ♀♀: MAK-43; 1 ♂, 4 ♀♀: MAK-44A; 1 ♀: MAK-44C; 9 ♂♂, 17 ♀♀: MAK-60; 2 exs.: MAK-61.

Distribution. Africa (Angola, Guinea, Guinea-Bissau, Mali), Madagascar, and Mascarene Islands (Guignot 1959–1961; Bertrand and Legros 1971; Rocchi 1991; Nilsson 2011). In Madagascar, widespread and common.

Habitat in study area (Fig. 2B, C, O). This species is present in lentic and in slowly flowing lotic habitats. It was collected both at peripheral and inner Makay sites. The bottom varied from clay to sandy, with clear, red-brown or turbid water and with more or less abundant plant debris. This species has a clear preference for open environments and habitats with at least some vegetation, and is highly tolerant to anthropogenic disturbance.

Neohydrocoptus sp. Ma3

Material examined. 3 ♂♂, 2 ♀♀: MAK-43; 2 ♀♀: MAK-44C; 4 ♂♂, 1 ♀: MAK-56.

Note. This species is smaller than *N. seriatus* and the elytra do not bear additional serial groups of punctures beyond discal and lateral puncture rows. External features and the shape of the aedeagus evoke *N. aethiopicus* (J. Balfour-Browne, 1961), a widespread sub-Saharan species, but examination of type material in the context of a revision will be necessary to confirm the identity of this species.

Distribution. Madagascar, widespread but not very common.

Habitat in study area. This species was sampled at three sites in inner Makay, in slowly flowing lotic habitats and a dead river arm, in forested or semi-forested contexts without anthropogenic disturbance. These biotopes had sandy bottoms with moderate abundance of plant debris. Two of the sites were surrounded by a well-developed hygrophilous vegetation and contained cyanobacteria.

Sternocanthus fabiennae (Bameul, 1994)

Type locality. Madagascar, Mahajanga, Ambohimanatrika.

Material examined. 3 ♂♂, 2 ♀♀: MAK-19; 1 ♂, 1 ♀: MAK-41.

Distribution. Madagascar (Bameul 1994; Nilsson 2011); distribution within the island poorly known.

Habitat in study area. This species was collected at two peripheral sites in lentic habitats in areas with intense anthropogenic pressure: large puddle, with water slowly flowing and with abundant rice straw debris, on a dirty road between two rice fields; and puddle on the sandy banks of the Mangoky River.

Synchortus asperatus (Fairmaire, 1869)

= *S. duplicatus* Sharp, 1882.

Type locality. Madagascar.

Material examined. 1 ♀: MAK-21; 1 ♂: MAK-42.

Distribution. Madagascar; widespread and common in lowlands (Guignot 1959–1961; Bertrand and Legros 1971; Nilsson 2011).

Habitat in study area. This species was collected at two peripheral sites located in open areas, in temporary lentic habitats without water renewal, and with vegetation.

Family Dytiscidae
Subfamily Copelatinae, tribe Copelatini

***Copelatus acamas* Guignot, 1955**

Type locality. Madagascar, Isalo National Parc.

Material examined. 1 ♂, 1 ♀: MAK-6; 3 ♂♂: MAK-7; 1 ♀: MAK-14A; 7 ♂♂, 13 ♀♀: MAK-30; 18 ♂♂, 17 ♀♀: MAK-32; 2 ♂♂, 3 ♀♀: MAK-34A; 2 ♂♂, 1 ♀: MAK-34B; 3 ♀♀: MAK-35A; 1 ♂: MAK-39A; 42 ♂♂, 25 ♀♀: MAK-45; 10 ♂♂, 7 ♀♀: MAK-46; 1 ♀: MAK-47; 26 ♂♂, 44 ♀♀: MAK-49; 10 ♂♂, 3 ♀♀: MAK-50; 1 ♀: MAK-52; 11 ♂♂, 5 ♀♀: MAK-53; 1 ♂, 2 ♀♀: MAK-54A; 4 ♂♂, 5 ♀♀: MAK-54B; 48 ♂♂, 57 ♀♀: MAK-59B; 5 ♂♂, 2 ♀♀: MAK-59C.

Distribution. Madagascar; previously known only from the sandstone massif of Isalo (Guignot 1955a).

Habitat in study area (Fig. 2G, J, K, N). This species is very common in inner Makay and absent from peripheral sites. It was most often found in puddles and pools located in stream and river beds, as well as small water holes and springs; shaded or sun-exposed, with bottom of sand and/or sandstone, with or without vegetal debris. These water bodies were most often devoid of vegetation. The water was clear but often more or less heavily loaded with orange masses of iron bacteria. Almost all collection points where this species could be observed were in forested or semi-forested areas and all sites were relatively undisturbed.

***Copelatus andobonicus* Guignot, 1960**

Type locality. Madagascar, Andobo, Antsingy forest.

Material examined. 4 ♀: MAK-12A; 2 ♀♀: MAK-33; 1 ♂: MAK-57.

Distribution. Madagascar (Guignot 1960); species characteristic of dry deciduous forests in the western part of the island.

Habitat in study area. This species was collected in lentic habitats (springs and small puddles), with clay or sandy-clay bottom and a lot of plant debris, located in forested or semi-forested areas and relatively unaffected by human disturbances.

***Copelatus polystrigus* Sharp, 1882**

= *C. marginalis* Gschwendtner, 1932

Type locality. Madagascar, Senegal.

Material examined. 1 ♂: MAK-11A; 1 ♂: MAK-11B; 30 ♂♂, 41 ♀♀: MAK-12A; 1 ♂: MAK-12B; 5 ♂♂, 1 ♀: MAK-12C; 2 ♂♂, 2 ♀♀: MAK-33; 2 ♂♂, 4 ♀♀:

MAK-44A; 8 ♂♂, 22 ♀♀: MAK-44B; 23 ♂♂, 22 ♀♀: MAK-44C; 3 ♂♂, 8 ♀♀: MAK-56; 21 ♂♂, 16 ♀♀: MAK-57; 1 ♂: MAK-58.

Distribution. Continental Africa south from Egypt and Sahara, Madagascar (Guignot 1959–1961; Bertrand and Legros 1971). In Madagascar, widespread and common.

Habitat in study area (Fig. 2O, P). This species was found in inner Makay, in pools and puddles, mainly in forest. These water bodies were shallow and did not exceed 1 m in depth. The mineral substratum was either clay or sand (or a mixture of both) and there was always a substantial quantity of plant debris.

Copelatus ruficapillus Régimbart, 1895

Type locality. Madagascar, Antsiranana, Montagne d'Ambre, Ambohitra National Park.

Material examined. 6 ♂♂, 3 ♀♀: MAK-3; 4 ♂♂, 7 ♀♀: MAK-4; 1 ♂: MAK-7; 1 ♀: MAK-8; 6 ♂♂, 10 ♀♀: MAK-10; 1 ♀: MAK-11B; 2 ♂♂, 6 ♀♀: MAK-12A; 2 ♀♀: MAK-12B; 2 ♀♀: MAK-16; 1 ♀: MAK-25A; 1 ♂: MAK-25B; 3 ♂♂, 5 ♀♀: MAK-28; 1 ♂: MAK-29; 1 ♂, 1 ♀: MAK-33; 1 ♀: MAK-34B; 2 ♂♂, 2 ♀♀: MAK-35A; 4 ♂♂: MAK-38A; 1 ♂, 5 ♀♀: MAK-39A; 6 ♂♂, 5 ♀♀: MAK-39B; 1 ♀: MAK-45; 2 ♂♂: MAK-50.

Distribution. Madagascar, widespread (Guignot 1959–1961; Bertrand and Legros 1971).

Habitat in study area (Fig. 2D, E, I–M, P). Similar to *C. acamas* (see above).

Copelatus vigintistriatus Fairmaire, 1869

Type locality. Mayotte.

Material examined. 1 ♀: MAK-44B; 2 ♂♂, 2 ♀♀: MAK-44C; 1 ♀: MAK-56; 2 ♀♀: MAK-60.

Distribution. Madagascar (widespread), Mayotte (Guignot 1959–1961; Bertrand and Legros 1971).

Habitat in study area. This species has been captured in a few inner massif sites all situated in northern Makay: a puddle, a blind channel, a small stream (these sites in forest) and an open marsh. These habitats had slightly turbid water and a mineral bottom ranging from clay to sand with moderate quantity of plant debris, and no vegetation.

Copelatus malavergnorum Manuel & Ramahandrison, sp. nov.

https://zoobank.org/C80CC169-845D-438C-A8D4-17939302C057
Figs 3A, 4A–D

Type locality. Madagascar, Toliara province, Malaimbandy municipality, Makay massif (northern part), ca. 20 km WSW Tsimazava, ca. 20°45'S, 45°31'E, altitude ca. 360 m a.s.l.

Type material. ***Holotype*** ♂: "Madagascar. Ex-prov. Toliara / Makay massif, ca. 20 km / WSW Tsimazava / 20°44'42"S, 45°31'35"E / 11.IV.2018. Ramahandrison leg. [pr.] // Alt. 364 m. Blind channel / connected with the Sakapaly / River, with orange masses of / iron bacteria on the bottom. [pr.] // Holotype / Copelatus malavergnorum sp. nov. / Manuel & Ramahandrison, 2022 [red, pr.]" (MNHN).

Diagnosis. This species belongs to the *Copelatus irinus*-group and the *C. insuetus*-complex (revised in Ranarilalatiana et al. 2019). It differs from *C. insuetus* Guignot, 1941 by: smaller size; narrower and more parallel habitus, dorsally flatter; broader pronotum with lateral margins posteriorly more parallel; colour of dorsal and ventral surfaces paler; testaceous basal band of elytron broader; discal stria I on elytron more weakly impressed; strioles on postero-lateral region of pronotum and on metacoxal plate sparser; metacoxal lines shorter; medial lobe of aedeagus in lateral view with apical half of more even width and with apex less narrowly acute, in ventral view distinctly more evenly narrowed from base to apex. This species is externally similar to *C. vokoka* Ranarilalatiana & Bergsten, 2019, but differs by: habitus narrower and more parallel, dorsally flatter; pronotum broader and with lateral margins posteriorly more parallel; discal stria I on elytron more weakly impressed and anteriorly more strongly abbreviated; strioles on pronotum and metacoxal plates much sparser; metacoxal lines shorter; median lobe of aedeagus in lateral view with apical half broader and less strongly arcuate, in ventral view with apex twisted to the left (straight in *C. vokoka*). Finally, it differs from *C. kely* Ranarilalatiana & Bergsten, 2019 notably by the lateral margins of pronotum anteriorly more strongly convergent, the lateral margins of elytra posteriorly more strongly attenuated, the median lobe in lateral view with the distal half much thicker and the dorsal outline less strongly curved, and in ventro-apical view much more gradually narrowed (in *C. kely* abruptly narrowed at ca. midlength from base to apex), subapically thicker and less strongly bent to the left.

Description of holotype. Body elongated and parallel-sided (Fig. 3A), weakly convex dorsally. Pronotum broad (ratio between maximum width of pronotum and maximum body width ~ 0.97), with sides posteriorly subparallel. Head rufo-testaceous with only very faint infuscation between eyes. Ratio between interocular distance and maximum width of head ~ 0.66. Pronotum rufo-testaceous as head, with weak medial infuscation. Elytra brown with broad testaceous basal band; testaceous band very diffusely transitioning into darker colour posteriorly (Fig. 3A).

Elytra with six discal and one submarginal striae. Stria I very weakly impressed. Striae I, V, and VI abbreviated anteriorly. Submarginal stria very weakly impressed, starting slightly before elytron midlength. Head, pronotum and elytra with fine reticulation and fine punctation. Posterolateral region of pronotum with few short and weakly impressed strioles.

Ventral side rufo-testaceous, slightly darker laterally on metacoxal plate and on abdominal ventrites. Metacoxal plates with sparse and very fine short strioles; visible abdominal ventrites I-III with denser and longer very fine strioles. Prosternal process rather short and broad, with blunt apex. Metacoxal lines rather long, ending anteriorly at quite small distance from posterior margin of metaventrite, diverging anteriorly.

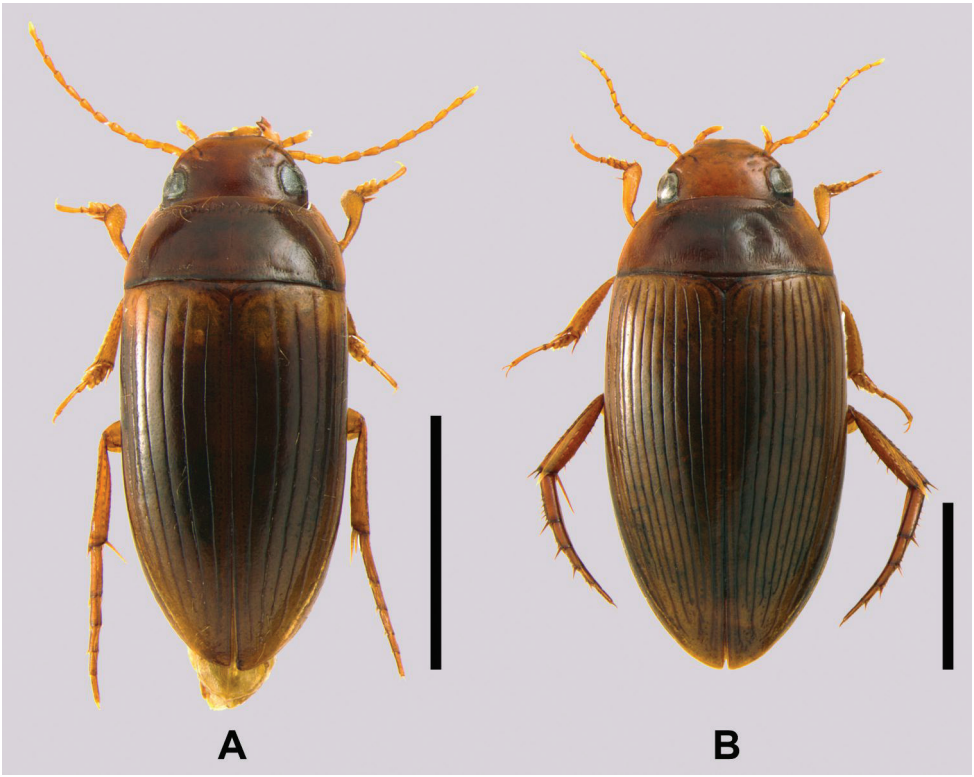

Figure 3. Habitus in dorsal view. Scale bars: 2 mm **A** *Copelatus malavergnorum* sp. nov. (holotype) **B** *Copelatus zanabato* sp. nov. (holotype).

Appendages: Antennae, palps and legs testaceous. Antennae particularly long (Fig. 3A). First three pro- and mesotarsomeres widened and ventrally equipped with suction cups; number of suction cups per articles (I-III) 7:4:4 on both pro- and mesotarsus. Protibia at base narrow, with bisinuate ventral margin, distally strongly broadened. Pro- and mesotarsal claws unmodified.

Median lobe and parameres as in Fig. 4A–D.

Female. Unknown.

Measurements. TL 4.2 mm, TL without head 3.7 mm, MW 1.8 mm, ratio TL/MW 2.34.

Etymology. This species is dedicated to the Malavergne family (Dominique, Catherine, Clémence, Jacques, and Laurence, Marie-José) in recognition of their constant help and support to the first author during his PhD thesis. The species epithet is a name in the genitive plural.

Distribution. So far known only from northern Makay in Madagascar.

Habitat. The external morphology of this species (very narrow and parallel habitus, broad pronotum, pale colour, long antennae) suggests that it might be a semi-subterranean species. The habitat where the single specimen was found (MAK-44C)

was a blind channel connected to River Sakapaly, in northern inner Makay. There was no apparent water flow but the bottom was covered with conspicuous orange masses of iron bacteria, which might be an indication of slow water seepage from underground. The substratum was sandy with moderate amount of decaying vegetal material and the water was red-brown coloured. This water body was fully shaded under trees in forest. There was no vegetation in the water but the surrounding forest floor displayed a typical hygrophilic vegetation of Poaceae, *Cyperus* and *Pandanus*. Other species of aquatic Adephaga (all Dytiscidae) sampled at the same site: *Copelatus polystrigus*, *C. vigintistriatus*, *Hydrovatus acuminatus* Motschulsky, 1860, *Laccophilus makay*, *Methles* sp. Ma1, *M.* sp. Ma5, *Neohydrocoptus* sp. Ma3, and *Pachynectes* sp. Ma1.

Copelatus zanabato Manuel & Ramahandrison, sp. nov.

https://zoobank.org/7D683E52-D50E-485A-B2CA-5E44D3F4CC5C
Figs 3B, 4E–H

Type locality. Madagascar, Toliara province, Malaimbandy municipality, Makay massif (northern part), ca. 21 km W of Tsimazava, ca. 20°42'S, 45°30'E, altitude ca. 430 m a.s.l.

Type material. ***Holotype*** ♂: "Madagascar. Ex-prov. Toliara / Makay massif, ca. 21 km / W Tsimazava / 20°42'10"S, 45°30'18"E [pr.] // 12.IV.2018. Ramahandrison leg. / Alt. 433 m. Pool in a / very narrow and dark / canyon. [pr.] // Holotype / Copelatus zanabato sp. nov. / Manuel & Ramahandrison, 2022 [red, pr.]" (MNHN). Paratypes: 1 ♀: same as holotype. 1 ♂: "Madagascar. Ex-prov. Toliara / Makay massif, ca. 20 km / WSW Tsimazava / 20°43'54"S, 45°31'10"E / 14.IV.2018. Ramahandrison leg. [pr.] // Alt. 437 m. Small / pond in a canyon at / Ampasimaiky [pr.]" (CMM). Both paratypes with respective red label.

Diagnosis. This species belongs to the *Copelatus erichsonii*-group. It is externally rather similar to *C. acamas*, from which it differs by distinctly smaller size; habitus narrower with sides more parallel, dorsally much flatter; discal stria IX on elytron more strongly abbreviated anteriorly; strioles on pronotum surface sparser and much more weakly impressed; shape of median lobe of aedeagus very different. Among *Copelatus* species known from Madagascar, the aedeagus of *C. zanabato* sp. nov. is most similar to that of *C. andobonicus*. From the latter, the new species differs by: habitus narrower with sides more parallel, dorsally much flatter; pronotum paler and elytra with darker linear colouration following the striae much less contrasted with respect to paler background; strioles on pronotum surface denser, present on whole surface (in *C. andobonicus* almost without striae in anterior disk region); median lobe of aedeagus in lateral view with broad flat protuberance on ventral side ca. halfway between base and apex (in *C. andobonicus* with much smaller protuberance at ca. basal third) and apical third much broader, in ventral view with apical region much broader and evenly narrowed, twisted on the left farther from apex.

Figure 4. Male genitalia. Scale bars: 200 μm **A–D** *Copelatus malavergnorum* sp. nov. (holotype) **E–H** *Copelatus zanabato* sp. nov. (holotype) **A, E** Median lobe of aedeagus in right lateral view **B, F** Median lobe of aedeagus in ventral view **C, G** Median lobe of aedeagus in left lateral view **D, H** Left paramere.

Description of holotype. Body shape elongate oval, with sides subparallel (Fig. 3B), dorsally weakly convex. Pronotum sides evenly curved and converging from posterior angle. Ratio between maximum width of pronotum and maximum body width ~ 0.90. Head uniformly light rufo-testaceous. Ratio between interocular distance and maximum width of head ~ 0.68. Pronotum medially rufous, laterally colour becoming gradually rufo-testaceous. Elytra light chestnut brown, with darker linear colouration along striae (Fig. 3B).

Elytra with ten well-impressed discal and one submarginal striae. Stria IX abbreviated anteriorly. Striae I and II diverging anteriorly. Submarginal stria starting slightly before elytron midlength, fragmented anteriorly. Head, pronotum and elytra with fine reticulation and fine punctation. Whole surface of pronotum with rather dense, short and fine strioles, in medial disk region strioles even finer.

Ventral side uniformly rufo-testaceous. Metacoxal plates with moderately impressed short strioles; visible abdominal ventrites I-III with denser and longer very fine

strioles. Prosternal process short and broad, with rounded apex. Metacoxal lines short, ending anteriorly at large distance from posterior margin of metaventrite, moderately diverging anteriorly.

Appendages: Antennae, palps, forelegs and midlegs testaceous, hindlegs rufo-testaceous. First three pro- and mesotarsomeres widened and ventrally equipped with suction cups; number of suction cups per article (I-III) 7:4:4 on both pro- and mesotarsus. Protibia at base shortly narrow, with shallow protuberance along ventral margin, distally broadened. Pro- and mesotarsal claws unmodified.

Median lobe and parameres as in Fig. 4E–H.

Female. Strioles on pronotum surface denser. Pro- and mesotarsomeres and protibia unmodified.

Measurements. Holotype: TL 6.35 mm, TL without head 5.7 mm, MW 2.9 mm, ratio TL/MW 2.20. Paratypes: TL 6.55–6.8 mm, TL without head 5.9–6.1 mm, MW 3.0–3.1 mm, ratio TL/MW 2.17.

Variation. In the male paratype, strioles on pronotum are longer and more deeply impressed than in the holotype, and the metacoxal lines are slightly longer. In the female paratype, the elytral stria V is slightly abbreviated anteriorly.

Etymology. The species name literally means "son of the rock" in Malagasy. It is an invariable name standing in apposition.

Distribution. So far known only from northern Makay in Madagascar.

Habitat. This species was collected at two sites located in two nearby canyons in northern inner Makay. Two specimens were sampled at site MAK-46, an isolated pool (~ 1 m × 3 m) on the bottom of a narrow and dark canyon, and one specimen at site MAK-50, a stagnant temporary pond (~ 3 m × 7 m) situated in a wider canyon and in a more open environment. Both habitats were characterised by sandy bottom with some plant debris, absence of visible inflow / outflow, somewhat turbid water and no vegetation. Other species of aquatic Adephaga (all Dytiscidae) sampled at the same sites: *Copelatus acamas*, *C. ruficapillus*, *Cybister operosus* Sharp, 1882, *Hydaticus sobrinus* Aubé, 1838, *Hyphydrus separandus* Régimbart, 1895, *Laccophilus makay*, *Pachynectes* sp. Ma1, and *P.* sp. Ma4.

Madaglymbus fairmairei (Zimmermann, 1919)

= *Madaglymbus regimbartii* Fairmaire, 1898.

Type locality. Madagascar, Maevatanana.

Material examined. 1 ♂, 2 ♀: MAK-3; 2 ♂♂, 8 ♀♀: MAK-10; 1 ♂, 1 ♀: MAK-11B; 2 ♂♂, 2 ♀♀: MAK-12A; 1 ♂: MAK-15; 1 ♂, 1 ♀: MAK-16; 9 ♂♂, 1 ♀: MAK-25A; 3 ♂♂, 1 ♀: MAK-29; 1 ♂: MAK-35A; 1 ♀: MAK-37A; 4 ♂♂, 2 ♀♀: MAK-39A; 1 ♂: MAK-40B.

Distribution. Madagascar (distribution within the island poorly known) (Guignot 1959–1961).

Habitat in study area (Fig. 2D, L, M, P). We met this species only in the central part of inner Makay, mainly in puddles and pools with or without water circulation and in small streams, with clear or turbid water, sandy bottom (at some sites with gravel and stones) and moderate to abundant plant debris or tree roots, in forested or semi-forested environments untouched by anthropogenic disturbance.

Subfamily Cybistrinae, tribe Cybistrini

***Cybister cinctus* Sharp, 1882**

Type locality. Madagascar.

Material examined. 1 ex.: MAK-1A; 1 ♂, 1 ♂: MAK-2; 1 ♂, 3 ♀♀: MAK-19; 4 ♂♂, 1 ex.: MAK-20; 1 ♀: MAK-23; 1 ♀: MAK-41.

Distribution. Madagascar (widespread and common) (Guignot 1959–1961; Bertrand and Legros 1971; Bameul 1984; Rocchi 1991; Bukontaite et al. 2015).

Habitat in study area (Fig. 2B, C). This species was collected only at peripheral sites, in various kinds of water bodies (lentic or slowly flowing) in open areas. It prefers habitats with at least some vegetation and is tolerant to anthropogenic pressure.

***Cybister operosus* Sharp, 1882**

Type locality. Madagascar.

Material examined. 1 ♀: MAK-50.

Distribution. Madagascar (widespread but localised) (Guignot 1959–1961; Bukontaite et al. 2015).

Habitat in study area. This species was captured only once, in northern inner Makay, in a large temporary pond located in a shallow open area on sand. This single capture does not reflect the usual habitat preferences of this species. According to our observations in Isalo and Ankarafantsika, this is a lotic species (an exceptional ecology for the genus) inhabiting the margins of streams and rivers with some vegetation and / or tree roots and / or plant debris, in well-preserved forested or semi-forested environments.

Subfamily Dytiscinae, tribe Aciliini

***Rhantaticus congestus* (Klug, 1833)**

= *R. rochasi* (Perroud & Montrouzier, 1864); *R. signatipennis* (Laporte, 1835).

Type locality. Madagascar.

Material examined. 1 ♂: MAK-2; 2 ♀♀: MAK-19; 1 ♂: MAK-41.

Distribution. From sub-Saharan Africa to Australia through tropical Asia and the Oriental region (Guignot 1959–1961; Bertrand and Legros 1971; Watts 1978; Bameul 1984; Hendrich et al. 2010). In Madagascar, widespread.

Habitat in study area (Fig. 2B, C). This species was found at three sampling sites in the periphery of the Makay massif: a large puddle partially sheltered by trees, with water slowly flowing and with abundant rice straw debris, on a dirty road between two rice fields; a small puddle in open situation on the sandy bank of a river, with *Azolla* aquatic ferns (eutrophication indicator); and a shallow isolated stream characterised by very weak water flow, sandy bottom, sparse tufts of small Cyperaceae and strong presence of filamentous green algae. These habitats were all situated in open environments and more or less affected by anthropogenic disturbance.

Tribe Eretini

***Eretes griseus* (Fabricius, 1781)**

= *E. plicipennis* (Motschulsky, 1845); *E. succinctus* (Klug, 1834).

Type locality. India.

Material examined. 1 ♂, 1 ♀: MAK-11B.

Distribution. Southern half of the Palearctic region, Africa, Oriental region (Guignot 1959–1961; Miller 2002). In Madagascar, widespread.

Habitat in study area (Fig. 2P). This species was collected at a single site in central inner Makay, in an isolated shallow temporary puddle located in the middle of a large flat accumulation of sand in the outer part of river meander. The environment was totally open with no trees, the water was turbid and there was no vegetation. These habitat characteristics are very representative of the ecology of members of the genus *Eretes* everywhere in the world (Miller 2002).

Tribe Hydaticini

***Hydaticus dorsiger* Aubé, 1838**

Type locality. Madagascar.

Material examined. 1 ♂: MAK-11A; 1 ♀: MAK-11B; 1 ♂, 1 ♀: MAK-12A; 1 ♂: MAK-14A; 1 ♂: MAK-18; 8 ♂♂, 6 ♀♀: MAK-19; 1 ♂: MAK-23.

Distribution. Whole tropical Africa to Arabia, Madagascar (where it is widespread and common) (Guignot 1959–1961; Bertrand and Legros 1971; Bameul 1984; Rocchi 1991; Hájek and Reiter 2014; Bukontaite et al. 2015).

Habitat in study area (Fig. 2N–P). This species has been observed mainly at peripheral sites and in open areas, in lentic environments that were permanent or temporary, with or without slow water flow, with bottom often muddy, and with or without marginal vegetation. This species is tolerant to anthropogenic disturbance.

Hydaticus exclamationis Aubé, 1838

Type locality. Madagascar.

Material examined. 1 ♂: MAK-11B.

Distribution. Sub-Saharan Africa, Mauritius, Madagascar (Guignot 1959–1961; Bameul 1984; Bukontaite et al. 2015). In Madagascar, widespread and common, especially in lowlands.

Habitat in study area (Fig. 2P). This species was collected at a single site in south-central inner Makay (see description of the habitat above under *Eretes griseus*). It usually prefers lentic or slowly flowing habitats with at least some vegetation.

Hydaticus petitii Aubé, 1838

Type locality. Madagascar.

Material examined. 1 ♂: MAK-52.

Distribution. Madagascar, widespread (Guignot 1959–1961; Bukontaite et al. 2015).

Habitat in study area. This species was collected once, in northern inner Makay, in a calm pool (~ 3 m × 7 m) on the bottom of a canyon, with inflow and outflow from the nearby Ampasimaiky River. This pool was rather deep (> 1 m), with bottom of sand covered with a thin layer of clay, almost without vegetal detritus, with moderately turbid water and no vegetation. The environment was semi-forested and the pond was surrounded by *Ravenea* palm trees. As a rule this Malagasy endemic species is encountered in forest massifs in more or less undisturbed habitats.

Hydaticus servillianus Aubé, 1838

= *H. discoidalis* Hope, 1843; *H. flavomarginatus* Zimmermann, 1920).

Type locality. South Africa, Western Cape, Cape of Good Hope.

Material examined. 1 ♀: MAK-1A; 1 ♂: MAK-2; 13 ♂♂, 7 ♀♀: MAK-19; 1 ♂, 3 ♀♀: MAK-23; 2 ♂♂: MAK-40A; 1 ♂, 6 ♀♀: MAK-61; 1 ♂: MAK-62.

Distribution. Sub-Saharan Africa, Madagascar (Guignot 1959–1961; Bameul 1984; Hájek and Reiter 2014; Bukontaite et al. 2015).

Habitat in study area (Fig. 2B, C). This species has been found in peripheral sites and at one inner massif site, in lentic and slowly flowing lotic habitats, mainly in open areas. The bottom comprised various amounts of sand and clay/mud and moderate to abundant plant debris. The water was clear to moderately turbid. The vegetation was variously developed. This eurytopic species is tolerant to anthropogenic perturbation.

***Hydaticus sobrinus* Aubé, 1838**

= *Hydaticus matruelis* var. *obliquevittatus* Régimbart, 1895).

Type locality. Madagascar, Mascarene Islands (Guignot 1959–1961; Bertrand and Legros 1971; Bameul 1984; Bukontaite et al. 2015).

Material examined. 1 ♀: MAK- 8; 2 ♀: MAK-50; 2 ♀♀: MAK-53; 1 ♂: MAK-54A; 2 ♀♀: MAK-59C.

Distribution. Mauritius, La Réunion, Madagascar. In Madagascar, widespread.

Habitat in study area. This species was collected only in inner Makay, in well-preserved forested or semi-forested areas. The habitats were isolated pools and very slowly flowing streams, with clear or slightly turbid water, sandy bottom (sometimes with stones), with moderate amount of plant debris and no vegetation.

Subfamily Hydroporinae, tribe Bidessini

***Bidessus longistriga* Régimbart, 1895**

Type locality. Madagascar, Antsiranana,

Material examined. 1 ♀: MAK-1A; 1 ♂: MAK-2; 2 ♀♀: MAK-19; 17 exs.: MAK-42; 1 ex.: MAK-60; 1 ex.: MAK-61.

Distribution. Madagascar, widespread (Guignot 1959–1961; Bertrand and Legros 1971; Bameul 1984; Biström 1985; Rocchi 1991; Bergsten et al. 2020).

Habitat in study area (Fig. 2B, C). *Bidessus longistriga* was sampled at peripheral sites and at one inner massif site, in open areas, in permanent or temporary lentic environments, with water stagnant or slowly flowing, clear or turbid, with sand and/or clay bottom. It prefers habitats with at least some marginal vegetation, and is tolerant to anthropogenic disturbance.

***Bidessus perexiguus* H. J. Kolbe, 1883**

Type locality. Madagascar, South inner part.

Material examined. 1 ex.: MAK-1A; 4 ♂♂, 1 ex.: MAK-2; 1 ♂: MAK-17; 82 exs.: MAK-18; 4 ♂♂, 25 exs.: MAK-19; 3 exs.: MAK-60; 1 ex.: MAK-61.

Distribution. Madagascar, widespread (Guignot 1959–1961; Biström 1985; Bergsten et al. 2020).

Habitat in study area (Fig. 2B, C). This species was collected mainly at peripheral sites. Its ecology is similar to that of *B. longistriga*, and both species were several times sampled in the same habitats, but *B. perexiguus* has a marked preference for small and very shallow water bodies without vegetation. Notably, this species was particularly

abundant in a small muddy ditch only 5 cm deep, shaded under trees, without water flow and with turbid water, trampled by cattle and with no vegetation (MAK-18).

Clypeodytes concivis Guignot, 1955

Type locality. Madagascar, Iharanandriana mountain.

Material examined. 3 ♂♂, 3 ♀♀: MAK-2; 1 ♂: MAK-61.

Distribution. Madagascar, widespread (Guignot 1955b; Biström 1988a).

Habitat in study area (Fig. 2B, C). This species was collected at two peripheral sites, a very slowly flowing and shallow stream, and a shallow stagnant pond, both in open environments. The mineral substratum was a mixture of sand and clay in the first case, and of clay and mud in the second case, with moderate amount of plant debris. The water was clear and there was a marginal vegetation of helophytes; at site MAK-2 with abundant filamentous green algae. At both sites, the biotope was trampled and enriched in nutrients by cattle.

Clypeodytes insularis Guignot, 1956

Type locality. Madagascar, Bas Mangoky agricultural station.

Material examined. 1 ♂: MAK-20.

Distribution. Madagascar, widespread but not common (Guignot 1956; Biström 1988a)

Habitat in study area. A single specimen of this species was taken in a rice field on the banks of the Mangoky River (a peripheral site), at shallow depth. The bottom was composed of sand and clay with some plant debris; there was no visible inlet or outlet, the water was clear and there was a moderate presence of green algae. The environment was open with no trees in the surroundings.

Clypeodytes sp. Ma3

Material examined. 1 ♂: MAK-2.

Distribution. Madagascar (known to us only from site MAK-2).

Note. This is an undescribed species, close to *C. spangleri* Biström, 1988 and *C. pseudolentus* Biström, 1988 from continental Africa.

Habitat in study area (Fig. 2B, C). This species was sampled only once in a peripheral site. The habitat was a shallow isolated stream characterised by very weak water flow, sandy bottom, marked anthropic disturbance (cattle trampling), sparse tufts of small Cyperaceae and strong presence of filamentous green algae.

***Hydroglyphus capitatus* (Régimbart, 1895)**

= *H. longivittis* Régimbart, 1903.

Type locality. Madagascar, Antsiranana.

Material examined. 13 ♂♂, 20 ♀: MAK-1A; 1 ♂, 1 ♀: MAK-4; 5 ♂♂: MAK-61.

Distribution. Seychelles, Madagascar (Guignot 1959–1961; Biström 1986; Rocchi 1991). In Madagascar, widespread and common particularly in lowlands.

Habitat in study area (Fig. 2E). This species was captured at two peripheral and at one inner massif sites, in highly contrasted habitats, including shallow puddles on the sandy banks of the Mangoky River, a shallow pond with clay-mud bottom and marginal helophytes, and (for the inner Makay site) a marginal spring on the bank of a river, full of orange masses of iron bacteria. The environment was open and strongly impacted by human activities in the two peripheral sites (where the species was more abundant); semi-forested and rather well preserved in the inner massif site.

***Hydroglyphus geminodes* (Régimbart, 1895)**

= *H. africanus* Régimbart, 1895.

Type locality. Madagascar, Antsiranana.

Material examined. 6 ♂♂, 3 ♀: MAK-1A; 1 ♂, 2 ♀: MAK-2; 6 ♂♂, 3 ♀♀: MAK-4; 2 ♂♂, 10 ♀♀: MAK-17; 1 ♂: MAK-18; 4 ♂♂, 3 ♀♀: MAK-19; 4 ♂♂, 1 ♀: MAK-61.

Distribution. Sub-Saharan Africa, Mauritius, La Réunion, Madagascar (Guignot 1959–1961; Bertrand and Legros 1971; Bameul 1984; Biström 1986; Rocchi 1991). In Madagascar, widespread and common.

Habitat in study area (Fig. 2B, C, E). This species has been found mainly at peripheral sites in open areas, at shallow depth in various kinds of water bodies (temporary or permanent lentic habitats with water stagnant or very slowly flowing). The water was generally clear and the bottom consisted of sand and/or clay, with some plant debris. There was either no vegetation or sparse helophytes and at some sites presence of filamentous green algae. This species is tolerant to anthropogenic disturbance.

***Hydroglyphus plagiatus* (H.J. Kolbe, 1883)**

Type locality. Eastern part of Madagascar.

Material examined. 1 ♂: MAK-17.

Distribution. Madagascar, common in the Central Highlands (Guignot 1959–1961; Bertrand and Legros 1971; Bameul 1984, Biström 1986; Rocchi 1991).

Habitat in study area. This species seems very rare in the Makay since only one specimen was found, in an inner massif site located in a semi-forested environment. The habitat was a small, isolated, sun-exposed puddle on rock mass, on the bank of

a river. The bottom consisted of sandstone, sand and clay without organic debris, the water was clear and there was no vegetation.

Liodessus luteopictus (Régimbart, 1897)

= *L. poecilopterus* Régimbart, 1900.

Type locality. Mascarene Islands, Mauritius, Curepipe.

Material examined. 1 ♂: MAK-16.

Distribution. Mauritius, La Réunion, Comoros, Madagascar (Guignot 1959–1961; Bameul 1984; Biström 1988b). In Madagascar, widespread.

Habitat in study area. This species was sampled at a single inner massif site, a small pond, partly shaded, at the edge of a gallery forest close to River Andranomanintsy. The water was slowly renewed from the nearby river, the bottom was sandy with moderate plant debris and the water was clear. This small water body was filled in with subaquatic Poaceae including a *Panicum* species.

Pachynectes costulifer (Régimbart, 1903)

Type locality. Madagascar, Imanombo.

Material examined. 4 ♂♂, 2 ♀♀: MAK-1A; 3 ♂♂, 11 ♀♀: MAK-1B; 12 ♂♂, 26 ♀♀: MAK-1C; 2 ♂♂: MAK-20; 2 ♂♂: MAK-22.

Distribution. Madagascar, western and southern parts of the island (Guignot 1959–1961; Bertrand and Legros 1971; Biström 1987; Rocchi 1991).

Habitat in study area (Fig. 2A). This species was found only at peripheral sites located on the large sandy banks of the Mangoky River close to Beroroha, in small to large shallow isolated puddles, with sand or sand-clay bottom and clear water, without vegetation or with sparse vegetation, with or without presence of filamentous green algae.

Pachynectes sp. Ma1

Material examined. 5 ♂♂, 2 ♀♀: MAK-2; 25 ♂♂, 22 ♀♀: MAK-3; 8 ♂♂, 4 ♀♀: MAK-4; 3 ♂♂, 1 ♀: MAK-5A; ; 8 exs.: MAK-5D; 2 ♀♀: MAK-8; 29 ♂♂, 14 ♀♀: MAK-14A; 5 ♂♂, 5 ♀♀: MAK-16; 24 exs.: MAK-28; 24 exs.: MAK-29; 3 exs.: MAK-36B; 91 exs.: MAK-37A; 3 exs: MAK-38B; 53 exs.: MAK-40A; 1 ex.: MAK-43; 1 ex.: MAK-44C; 2 exs.: MAK-45; 28 exs.: MAK-47; 5 exs.: MAK-49; 31 exs.: MAK-50; 15 exs.: MAK-51; 37 exs.: MAK-52; 10 exs.: MAK-53; 2 exs.: MAK-54B; 6 exs.: MAK-58; 39 exs.: MAK-59A; 25 exs.: MAK-59C.

Note. This is a probably undescribed species close to *P. hygrotoides* (Régimbart, 1895). The Malagasy endemic genus *Pachynectes* is currently being revised (J. Bergsten, pers. comm.) and many species are awaiting description.

Distribution. Madagascar. The exact distribution of this species within the island remains to be established in the context of the upcoming revision, but it is not endemic to the Makay (sampled by us notably in the Isalo Massif).

Habitat in study area (Fig. 2B–F, I, N). This is one of the most abundant species of aquatic Adephaga in inner Makay, and it was also collected at one peripheral site (MAK-2). It was sampled in all kinds of lentic or very slowly flowing lotic habitats (puddles, pools, ponds, small streams, blind channels of rivers, etc.), with substrate sandy or stony, water generally clear, and in most cases without vegetation. This species has a preference for exposed or semi-shaded situations (majority of observations in semi-forested environments).

Pachynectes sp. Ma4

Material examined. 1 ♂: MAK-5A; 2 ♂♂: MAK-5D; 1 ♂, 1 ♂: MAK-14A; 1 ♂, 1 ♀: MAK-29; 1 ♀: MAK-45; 8 ♂♂, 4 ♀♀: MAK-50; 1 ♂, 4 ♀♀: MAK-51; 57 ♂♂, 37 ♀♀: MAK-52; 1 ♀: MAK-59C.

Distribution. Madagascar. So far endemic to the Makay massif.

Note. This is an undescribed species, rather large for the genus, and very close to another undescribed species which lives in the Isalo massif.

Habitat in study area (Fig. 2F, N). Similar to *Pachynectes* sp. Ma1 (with which it was syntopic at all sites), but this species is rarer.

Pseuduvarus sp. Ma1

Material examined. 1 ♀: MAK-2; 1 ♂: MAK-61.

Distribution. Madagascar (widespread).

Note. This species corresponds to *P. ornatipennis* (Régimbart, 1900), currently wrongly considered a junior synonym of *P. vitticollis* (Boheman, 1848). A revision of the species of *Hydroglyphus* / *Pseuduvarus* is currently in preparation (J. Bergsten, pers. comm.).

Habitat in study area. Same as *Clypeodytes concivis* (see above).

Uvarus betsimisarakus (Guignot, 1939)

Type locality. Madagascar, Maroantsetra.

Material examined. 1 ♂, 1 ♀: MAK-19.

Distribution. Madagascar (Guignot 1959–1961; Biström 1988c). Common in the Central Highlands.

Habitat in study area. This species was collected only once, in a peripheral site located in a semi-open area impacted by human activities. The habitat was a large puddle partially sheltered by trees, with water slowly flowing and with abundant rice straw debris, on a dirty road between two rice fields.

***Uvarus rivulorum* (Régimbart, 1895)**

= *U. cilunculus* Guignot, 1950.

Type locality. Madagascar, Antsiranana.

Material examined. 1 ♀: MAK-1A; 2 ♀♀: MAK-2; 1 ♀: MAK-18; 4 ♂♂, 2 ♀♀: MAK-19; 4 exs.: MAK-60.

Distribution. Madagascar, widespread in lowlands (Guignot 1959–1961; Rocchi 1991; Biström 1988c).

Habitat in study area (Fig. 2B, C). This species was collected mainly at peripheral sites, in shallow lentic or slowly flowing lotic habitats, with or without marginal vegetation. The environment was open (non-forested), at some sites partly sheltered by sparse trees, and at most sites impacted by anthropogenic pressures (notably cattle trampling). The bottom varied from clay to sand and more or less abundant plant debris; the water was clear to turbid.

***Yola costipennis* (Fairmaire, 1869)**

Type locality. Madagascar, Sainte Marie Island.

Material examined. 5 exs.: MAK-1A; 2 exs.: MAK-1C; 4 exs.: MAK-19; 6 exs.: MAK-20; 4 exs.: MAK-41; 1 ex.: MAK-42; 1 ex.: MAK-60; 3 exs.: MAK-62.

Distribution. Madagascar, widespread and common (Guignot 1959–1961; Bertrand and Legros 1971; Biström 1983; Bameul 1984; Rocchi 1991).

Habitat in study area (Fig. 2A). This species was collected mainly at peripheral sites and always in open areas, often impacted by human activities. The habitats were various kinds of shallow lentic water bodies, most without but some with water circulation. They were sun-exposed (at one site partly sheltered by trees), with bottom of sand, clay, or a mix of sand and clay, with organic debris varying from absent to forming a thick layer above the mineral substratum, with water clear to moderately turbid; vegetation was absent or sparse, and filamentous green algae were either undetectable or variously developed.

Tribe Hydrovatini

***Hydrovatus acuminatus* Motschulsky, 1860**

= *H. affinis* Régimbart, 1895; *H. badius* (Clark, 1863); *H. consanguineus* Régimbart, 1880; *H. ferrugineus* Zimmermann, 1919; *H. humilis* Sharp, 1882; *H. malaccae* (Clark, 1863); *H. obscurus* Motschulsky, 1860; *H. obscurus* Régimbart, 1895; *H. sordidus* Sharp, 1882.

Type locality. South-East Asia (Indian continent).

Material examined. 1 ♂, 1 ♀: MAK-1A; 6 ♂♂, 6 ♀♀: MAK-2; 1 ♀: MAK-3; 2 ♂♂, 1 ♀: MAK-19; 1 ♂, 2 ♀♀: MAK-21; 1 ♂: MAK-23; 1 ♀: MAK-44C; 1 ♂, 2 ♀♀: MAK-60; 1 ♂, 1 ♀: MAK-61; 1 ♂: MAK-62.

Distribution. Sub-Saharan Africa, Madagascar, Seychelles, Turkey, Egypt, Arabian Peninsula, south-eastern Palearctic region from India to south Japan, Oriental region (Biström 1996; Hájek and Reiter 2014). In Madagascar, widespread and common in lowlands (absent from the Central Highlands).

Habitat in study area (Fig. 2B–D). This species is present in lentic and in slowly flowing lotic habitats. It was collected both at peripheral and inner massif sites. The bottom varied from clayey to sandy, with clear, red-brown or turbid water and with more or less abundant plant debris. This species has a clear preference for open environments and habitats with at least some vegetation and is highly tolerant to anthropogenic disturbance.

Hydrovatus capnius Guignot, 1950

Type locality. Zambia (Congo Belge), Musosa.

Material examined. 1 ♂: MAK-2; 1 ♂, 1 ♀: MAK-42.

Distribution. Sudan, Democratic Republic of the Congo, Madagascar (Guignot 1959–1961; Biström 1996). Distribution within Madagascar poorly known, but probably restricted to lowlands.

Habitat in study area (Fig. 2B, C). This species was found at only two peripheral sites, in open and non-forested environments, both markedly eutrophic. The first site was a shallow isolated stream characterised by very weak water flow, sandy bottom, marked anthropic disturbance (cattle trampling), sparse tufts of small Cyperaceae and strong presence of filamentous green algae. The second site was an open marsh, relatively preserved from anthropogenic pressure, without water flow, with sandy bottom and moderate quantity of plant debris, moderately turbid water, sparse helophytes (*Cyperus*) and aquatic plants (*Nymphaea* and *Polygonum*), floating ferns (*Azolla*, an indicator of eutrophication) and moderate abundance of filamentous green algae.

Hydrovatus crassicornis (H.J. Kolbe, 1883)

Type locality. Eastern part of Madagascar

Material examined. 1 ♂, 1 ♀: MAK-42; 1 ♂: MAK-60; 1 ♂, 1 ♀: MAK-61.

Distribution. Madagascar, widespread (Guignot 1959–1961; Bertrand and Legros 1971; Biström 1996).

Habitat in study area. This species was collected at two peripheral and one inner massif sites. The habitats were located in open areas and were lentic water bodies (with or without slow water circulation) with sand-clay bottom and with plant debris, with water clear to moderately turbid, with discontinuous marginal belts of helophytes and at one site with filamentous green algae.

Hydrovatus cruentatus H.J. Kolbe, 1883

Type locality. Eastern part of Madagascar.

Material examined. 1 ♂: MAK-2; 1 ♀: MAK-42.

Distribution. Madagascar, widespread (Guignot 1959–1961; Biström 1996).

Habitat in study area. Same as *Hydrovatus capnius* (see above).

Hydrovatus dentatus Bilardo & Rocchi, 1990

Type locality. Zambia, Luangwa valley, Chibembe.

Material examined. 1 ♂: MAK-2.

Distribution. Zambia, South Africa (Biström 1996), Madagascar. For Madagascar, the first record is recent (Ranarilalatiana 2019) and was from Anjozorobe-Angavo in the Central Highlands.

Habitat in study area (Fig. 2B, C). This species was sampled only once in a peripheral site. The habitat was a shallow insolated stream characterised by very weak water flow, sandy bottom, marked anthropic disturbance (cattle trampling), sparse tufts of small Cyperaceae and strong presence of filamentous green algae.

Hydrovatus otiosus Guignot, 1945

Type locality. Madagascar, Antananarivo, Ikopa River.

Material examined. 3 ♂♂, 2 ♀♀: MAK-2; 3 ♂♂, 1 ♀: MAK-62.

Distribution. Madagascar, widespread (Guignot 1959–1961; Bertrand and Legros 1971; Biström 1996); common in the Central Highlands.

Habitat in study area (Fig. 2B, C). This species was collected at only two peripheral sampling sites. The first site was the one described above for *H. dentatus*. The second one was a canal at the edge of rice fields, with water slowly flowing, muddy bottom, water rather turbid, and without vegetation. Both sites were significantly impacted by anthropogenic disturbance.

Hydrovatus parvulus Régimbart, 1900

= *H. noctivagus* Guignot, 1953; *H. ocnerus* Guignot, 1958; *H. socors* Guignot, 1954.

Type locality. Madagascar, Antongil Bay.

Material examined. 2 ♂♂: MAK-2; 2 exs.: MAK-43; 3 exs.: MAK-61.

Distribution. Sub-Saharan Africa, Madagascar (Guignot 1959–1961; Biström 1996). In Madagascar, widespread and common.

Habitat in study area (Fig. 2B, C). This species was collected at three peripheral sampling sites, in open, non-forested environments. Two of the sites were lotic habitats

(a shallow stream and the calm margin of a river) and one was lentic (a shallow pond ~ 25 m in diameter). In all cases, the bottom consisted of sand and clay, the water was clear, and the marginal zone where the beetles were collected was vegetated.

Hydrovatus pictulus Sharp, 1882

H. dilutus H.J. Kolbe, 1883; *H. scymnoides* Régimbart, 1895.

Type locality. Madagascar.

Material examined. 5 ♂♂, 1 ♀: MAK-2; 1 ♂: MAK-62.

Distribution. Sub-Saharan Africa, Madagascar (Guignot 1959–1961; Biström 1996). In Madagascar, widespread.

Habitat in study area. Same as *Hydrovatus otiosus* (see above). Throughout Madagascar, this species has an ecological optimum in the calm parts of rivers and streams or their satellite puddles and pools, with sandy or muddy bottom and few or no vegetation and is quite tolerant to anthropogenic disturbance.

Hydrovatus testudinarius Régimbart, 1895

Type locality. Madagascar, Antananarivo, Ambodinandohalo Lake.

Material examined. 7 ♂♂, 3 ♀♀: MAK-2.

Distribution. Madagascar, widespread but not common (Guignot 1959–1961; Rocchi 1991; Biström 1996).

Habitat in study area. Same as *Hydrovatus dentatus* (see above).

Hydrovatus sp. Ma7

Material examined. 1 ♂, 1 ♀: MAK-2.

Note. This large species may be *H. confusus* Régimbart, 1903, a species endemic to Madagascar, or *H. badeni* Sharp, 1882, also present in continental Sub-Saharan Africa (Biström 1996).

Distribution. Unknown.

Habitat in study area. Same as *Hydrovatus dentatus* (see above)

Tribe Hyphydrini

Hyphydrus separandus Régimbart, 1895

= *H. oncodes* Guignot, 1955.

Type locality. Madagascar, Montagne d'Ambre, Ambohitra National Park.

Material examined. 2 ♂♂, 8 ♀♀: MAK-3; 2 ♀♀: MAK-4; 30 exs.: MAK-5A; 8 exs.: MAK-5B; 15 exs.: MAK-5C; 85 exs.: MAK-5D; 5 ♂♂, 6 ♀♀: MAK-8; 1 ♀: MAK-10; 1 ♀: MAK-11B; 3 ♂♂, 5 ♀♀: MAK-14A; 1 ♀: MAK-16; 1 ♂, 1 ♀: MAK-25B; 4 exs.: MAK-28; 14 exs.: MAK-29; 1 ♂: MAK-35B; 1 ♂, 1 ♀: MAK-37A; 5 ♂♂: MAK-40A; 1 ex.: MAK-40B; 1 ♂: MAK-50; 2 ♂♂, 1 ♀: MAK-52; 1 ♂: MAK-59C.

Distribution. Comoro Islands, Madagascar (Guignot 1959–1961; Wewalka 1980; Biström 1982). In Madagascar, widespread.

Habitat in study area (Fig. 2D–F, I, L–N, P). This species was collected only in inner Makay where it is one of the most common species of aquatic Adephaga. It was found in puddles, pools, ponds and slowly flowing streams, from a few centimetres to 150 cm in depth, with sandy or rocky bottom, clear water and more or less abundant plant debris, often without vegetation. Almost all collecting sites were located in forested or semi-forested environment.

Hyphydrus stipes Sharp, 1882

= *H. soarezicus* Alluaud, 1897.

Type locality. Madagascar.

Material examined. 1 ♂: MAK-29.

Distribution. Madagascar, widespread (Biström 1982; Rocchi 1991).

Habitat in study area. This species was collected at a single site located in inner Makay, in a semi-forested small valley. The habitat was a sun-exposed isolated pool on sandstone rock, rather deep (70 cm), with bottom made up of sand and stones with a moderate quantity of plant debris, with clear water and no vegetation. This site was well preserved from anthropogenic disturbance.

Tribe Methlini

Methles sp. Ma1

Material examined. 4 ♂♂, 3 ♀♀: MAK-44C; 1 ♂, 2 ♀♀: MAK-60.

Note. The Malagasy species of the genus *Methles* are in great need of revision, and in the current state of knowledge we cannot assign a name to this species.

Distribution. Unknown (but not confined to the Makay area).

Habitat in study area. This species was collected at two inner massif sites in northern Makay, with very different habitat characteristics. One was a blind channel in forest connected to River Sakapaly; this site is the locus typicus of *Copelatus malavergnorum* sp. nov. (see "Habitat" under description of this species). The other site was an open marsh with vegetated margins (Cyperaceae and Polygonaceae), with muddy bottom and water rather turbid, in semi-forested context near the Sakapaly River. Both sites were preserved from anthropogenic disturbance.

Methles sp. Ma5

Material examined. 1 ♀: MAK-2; 3 ♂♂, 3 ♀♀: MAK-42; 1 ♀: MAK-43; 1 ♂: MAK-44C; 1 ♂, 3 ♀♀: MAK-60; 19 ♂♂, 24 ♀♀: MAK-61; 3 ♂♂, 1 ♀: MAK-62.

Note. The Malagasy species of the genus *Methles* are in great need of revision, and in the current state of knowledge we cannot assign a name to this species.

Distribution. Unknown (but not confined to the Makay area).

Habitat in study area (Fig. 2B, C). This species is present in lentic and in slowly flowing lotic habitats. It was collected both at peripheral and inner massif sites. The bottom varied from clay to sandy, with more or less abundant plant debris. The water was either clear, red-brown or turbid. This species has a clear preference for open environments and habitats with at least some vegetation and is tolerant to anthropogenic disturbance.

Subfamily Laccophilinae, tribe Laccophilini

Africophilus bartolozzii Rocchi, 1991

Type locality. Madagascar, Isalo National Park, Canyon des Singes.

Material examined. 1 ♀: MAK-8; 8 ♂♂, 8 ♀♀: MAK-9; 1 ♀: MAK-36B; 1 ♀: MAK-39B.

Distribution. Madagascar; previously known only from the sandstone massif of Isalo (Rocchi 1991).

Habitat in study area (Fig. 2H, I). This hygropetric species was collected only in inner Makay. Three of the sampling sites were situated in forested contexts and one site in a non-forested context. In the latter (MAK-9), the habitat was vertical rock walls with water film and crust of bryophytes and algae, at the bottom of a narrow and deep canyon. The other habitats were puddles and pools with sandy – stony bottom along small streams. Like other members of the genus, this species lives at the edge of small water bodies in the water film retained by capillarity on the substratum surface above water line, or on rock surface covered with a thin and slowly seeping water film, often close to cascades.

Africophilus nesiotes Guignot, 1951

Type locality. Madagascar, Ambalavao region.

Material examined. 5 ♂♂, 8 ♀♀: MAK-5A; 1 ♀: MAK-5B; 1 ♀: MAK-8; 2 ♀♀: MAK-13; 3 ♂♂, 4 ♀♀: MAK-14A; 1 ♀: MAK-26; 1 ♀: MAK-39A; 2 ♂♂: MAK-40A

Distribution. Sub-Saharan Africa, Madagascar (Guignot 1959–1961; Bertrand and Legros 1971; Franciscolo 1994; Bilardo et al. 2020). In Madagascar, widespread.

Habitat in study area (Fig. 2F, I, N). Similar to *A. bartolozzii* (see above) but more common.

Laccophilus addendus Sharp, 1882

Type locality. Madagascar.

Material examined. 1 ♀: MAK-2; 1 ♀: MAK-5A; 28 ♂♂, 19 ♀♀: MAK-11A; 1 ♀: MAK-11B; 2 ♂♂, 1 ♀: MAK-19; 2 ♂♂, 1 ♀: MAK-25A; 1 ♂: MAK-26; 1 ♂: MAK-38A; 1 ♂, 1 ♀: MAK-62.

Distribution. Madagascar, widespread (Guignot 1959–1961; Bameul 1984; Rocchi 1991; Biström et al. 2015). Previous records from outside Madagascar are considered uncertain by Biström et al. (2015).

Habitat in study area (Fig. 2B, C, F, O, P). This species was collected at peripheral and inner massif sites, mainly in non-forested areas, in lentic or very slow flowing lotic habitats, most often sun-exposed but at a few sites partly shaded by trees. The bottom consisted of various amounts of sand, clay and mud, with moderate to abundant plant debris, and marginal vegetation was absent to well developed. The water was clear to rather turbid. This species occurs both in strongly anthropised contexts and in habitats preserved from anthropogenic pressure.

Laccophilus flaveolus Régimbart, 1906

= *L. pampinatus* Guignot, 1941.

Type locality. Kenya, Winam, Kavirondo Bay.

Material examined. 1 ♂: MAK-2.

Distribution. Eastern Sub-Saharan Africa, Madagascar (Guignot 1959–1961; Bameul 1984; Biström et al. 2015).

Habitat in study area (Fig. 2B, C). This species was sampled only once at a peripheral site. The habitat was a shallow insolated stream characterised by very weak water flow, sandy bottom, marked anthropic disturbance (cattle trampling), sparse tufts of small Cyperaceae and strong presence of filamentous green algae.

Laccophilus insularum Biström, Nilsson & Bergsten, 2015

Type locality. Madagascar, Ankarafantsika National Park, Mahajanga, Boeny.

Material examined. 2 ♂♂, 2 ♀♀: MAK-5A.

Distribution. Madagascar, widespread (Biström et al. 2015).

Habitat in study area (Fig. 2F). This species was encountered only once, in south-central inner Makay. The habitat was a deep pond (dimensions about 30 m × 15 m) at the bottom of a small canyon along the course of a stream. This water body was formed as a result of the collapse of downstream canyon walls (natural dam). It was shaded by the canyon walls and surrounded by trees (notably *Cyathea* tree ferns) and hygrophilous vegetation. The habitat was furthermore characterised by clay bottom,

with moderate amount of plant debris, clear water, and absence of marginal vegetation. This site was unaffected by anthropic disturbance.

Laccophilus luctuosus Sharp, 1882

Type locality. Madagascar.

Material examined. 1 ♂, 1 ♀: MAK-21.

Distribution. Madagascar (widespread in lowlands) (Guignot 1959–1961; Bertrand and Legros 1971; Rocchi 1991; Biström et al. 2015).

Habitat in study area. This species was encountered only once in a peripheral site located in an open area. The habitat was a small isolated temporary puddle with sandy bottom and clear water under *Phragmites*, on the west bank of the Makaikely River. There was a moderate amount of plant debris, and no vegetation.

Laccophilus makay Manuel & Ramahandrison, 2020

Type locality. Madagascar, Toliara, Makay massif, 10.7 km NW of Tsivoky.

Material examined. 8 ♂♂, 7 ♀♀: MAK-3; 2 ♂♂, 1 ♀: MAK-4; 4 ♂♂, 1 ♀: MAK-5A; 3 ♂♂: MAK-5B; 2 ♂♂: MAK-5C; 7 ♂♂, 5 ♀♀: MAK-5D; 1 ♂, 2 ♀♀: MAK-6; 1 ♂, 1 ♀: MAK-7; 11 ♂♂, 9 ♀♀: MAK-8; 2 ♂♂, 4 ♀♀: MAK-10; 13 ♂♂, 6 ♀♀: MAK-14A; 3 ♂♂, 2 ♀♀: MAK-15; 1 ♂, 1 ♀: MAK-16; 1 ♂, 1 ♀: MAK-25A; 9 ♂♂, 22 ♀♀: MAK-25B; 1 ♂, 1 ♀: MAK-26; 4 ♂♂, 4 ♀♀: MAK-28; 1 ♀: MAK-29; 5 ♂♂, 2 ♀♀: MAK-30; 3 ♂♂, 5 ♀♀: MAK-31A; 5 ♂♂, 2 ♀♀: MAK-31B; 4 ♂♂, 1 ♀: MAK-31C; 12 ♂♂, 20 ♀♀: MAK-32; 1 ♂, 4 ♀♀: MAK-33; 1 ♂: MAK-34A; 2 ♂♂, 3 ♀♀: MAK-34B; 11 ♂♂, 3 ♀♀: MAK-35A; 4 ♂♂: MAK-35B; 5 ♂♂: MAK-35C; 6 ♂♂, 5 ♀♀: MAK-36B; 8 ♂♂, 11 ♀♀: MAK-38A; 1 ♂, 1 ♀: MAK-39A; 3 ♂♂, 1 ♀: MAK-39B; 1 ♂: MAK-44C; 68 exs.: MAK-45; 2 ♂♂, 5 ♀♀: MAK-46; 4 ♂♂, 6 ♀♀: MAK-47; 21 exs.: MAK-49; 130 exs.: MAK-50; 26 exs.: MAK-51; 111 exs.: MAK-52; 108 exs.: MAK-53; 16 ♂♂, 19 ♀♀: MAK-54A; 64 exs: MAK-54B; 8 ♂♂, 1 ♀: MAK-58; 37 exs.: MAK-59A; 5 ♂♂, 2 ♀♀: MAK-59B; 62 exs: MAK-59C.

Distribution. So far endemic to the Makay massif, Madagascar (Manuel and Ramahandrison 2020).

Habitat in study area (Fig. 2D–G, I–N). This species was collected only at inner massif sites, in both south-central and northern Makay, where it is by far the most common and abundant species of aquatic Adephaga. It was found in a wide diversity of lentic water bodies (puddles, pools, ponds, a blind river channel, etc.), isolated or with slow water renewal, as well as in very slowly flowing streams. The surrounding environment was forested or semi-forested and free from anthropisation. These habitats were further characterised by sandy bottom (sometimes with stones), various amounts of plant debris, clear water (but often with orange masses of iron bacteria), and marginal vegetation absent or poorly developed.

Laccophilus pallescens Régimbart, 1903

Type locality. Southern Madagascar, Pays Androy.

Material examined. 1 ♀: MAK-1A; 8 ♂♂, 5 ♀♀: MAK-2; 1 ♂: MAK-18; 1 ♂: MAK-19.

Distribution. Sub Saharan-Africa, Arabian Peninsula, Madagascar (Guignot 1959–1961; Bertrand and Legros 1971; Hájek and Reiter 2014; Biström et al. 2015).

Habitat in study area (Fig. 2B, C). This species was collected only at peripheral sites, in shallow lentic or slowly flowing lotic habitats, with or without marginal vegetation. The environment was open (non-forested), at some sites partly sheltered by sparse trees, and at most sites impacted by anthropogenic pressures (notably cattle trampling). The bottom varied from clay to sand and more or less abundant plant debris, and the water was clear to turbid.

Laccophilus posticus Aubé, 1838

Type locality. Mascarene Islands, Mauritius.

Material examined. 5 ♂♂: MAK-1A; 1 ♂: MAK-2; 1 ♀: MAK-3; 3 ♀♀: MAK-4; 4 ♂♂, 3 ♀♀: MAK-11A; 1 ♂: MAK-11B; 1 ♂: MAK-17; 1 ♂: MAK-18; 243 exs.: MAK-19; 1 ♀: MAK-21; 3 ♂♂, 9 ♀♀: MAK-23; 1 ♀: MAK-28; 1 ♂, 2 ♀♀: MAK-40A; 11 ♂♂, 14 ♀♀: MAK-41; 37 exs.: MAK-42; 1 ♂: MAK-44A; 1 ♂: MAK-59C; 4 ♂♂, 6 ♀♀: MAK-60; 6 ♂♂, 1 ♀: MAK-62.

Distribution. Mauritius, Aldabra, Madagascar (Guignot 1959–1961; Bertrand and Legros 1971; Bameul 1984; Rocchi 1991; Biström et al. 2015). In Madagascar, widespread and common in lowlands.

Habitat in study area (Fig. 2B–E, O, P). This species was captured both at peripheral and inner massif sites, in various kinds of lentic habitats (puddles, pools, ponds, ditches) and in very slowly flowing streams. These habitats were most often located in open areas. The bottom variously consisted of sand, clay or stones, generally with plant debris. The water was clear to turbid and marginal vegetation was absent or variously developed. This species is highly tolerant to anthropogenic pressure.

Laccophilus rivulosus Klug, 1833

Type locality. Madagascar.

Material examined. 1 ♀: MAK-2; 2 ♂♂, 7 ♀♀: MAK-19.

Distribution. Madagascar, widespread but not very common (Guignot 1959–1961; Bertrand and Legros 1971; Biström et al. 2015).

Habitat in study area (Fig. 2B, C). This species was found at two sampling sites located in the periphery of the Makay massif: a shallow isolated stream characterised by very weak water flow, sandy bottom, sparse tufts of small Cyperaceae and strong presence of filamentous green algae, and a large puddle partially sheltered by trees, with water slowly flowing and with abundant rice straw debris, on a dirty road between two rice fields. These habitats were situated in open environments and were impacted by anthropogenic disturbance (notably cattle trampling).

Laccophilus seyrigi Guignot, 1937

Type locality. Southern Madagascar, near Bekily.

Material examined. 1 ♀: MAK-2.

Distribution. South and south-western Madagascar (very rare); the present record is the first since the original description of the species (Guignot 1959–1961; Biström et al. 2015).

Habitat in study area. Same as *Laccophilus flaveolus* (see above).

Laccophilus transversovittatus Biström, Nilsson & Bergsten, 2015

Type locality. Madagascar, Isalo, Menamaty River.

Material examined. 1 ♂, 1 ♀: MAK-12C; 1 ♀: MAK-26; 1 ♀: MAK-52.

Distribution. Madagascar, widespread outside from the Central Highlands (Biström et al. 2015). The record from Ankaratra in Biström et al. (2015) is probably attributable to *L. rakouthae* Manuel & Ramahandrison, 2020.

Habitat in study area. This species was found at three inner massif sites, two in south-central and one in northern Makay. The surrounding was forested or semi-forested and without visible anthropogenic disturbance. The habitats were: a small pond with water slowly renewed, just downstream from a spring, partly sheltered by trees, with clay bottom, with plant debris and clear water, with sparse helophytes (*Cyperus*); a slowly flowing stream, partly shaded, with sandy bottom, important accumulation of plant debris, clear water and sparse helophytes; and a small, isolated pool, partly shaded, with sandy bottom, no plant debris, tinted water, and no marginal vegetation.

Laccophilus sp. Ma19

Material examined. 1 ♂: MAK-21.

Note. This is an undescribed species close to *L. lateralis* Sharp, 1882.

Distribution. Madagascar (widespread in lowlands).

Habitat in study area. Same as *Laccophilus luctuosus* (see above).

Neptosternus oblongus Régimbart, 1895

Type locality. Madagascar, Annanarivo (= Antananarivo?).

Material examined. 35 ♂♂, 50 ♀♀: MAK-5A; 3 ♂♂: MAK-5B.

Distribution. Central and southern Madagascar (Guignot 1959–1961; Bilardo and Rocchi 2012). Distribution within the island poorly known.

Habitat in study area. Same as *Laccophilus insularum* (see above).

Philaccolus elongatus (Régimbart, 1903)

Type locality. Madagascar, Sainte Marie Island.

Material examined. 1 ♂: MAK-2.

Note. There is a complex of very similar species around *P. elongatus*, and future studies may show that the specimen recorded here belong to a different species.

Distribution. Madagascar (Guignot 1959–1961; Bertrand and Legros 1971). Distribution within the island poorly known.

Habitat in study area. Same as *Laccophilus flaveolus* (see above).

Comparisons of species frequency, diversity, and endemism in different areas and vegetation contexts

Relative frequencies of occurrence of species across samplings for different sets of sampling sites (all, inner Makay, peripheral Makay, forested sites, semi-forested sites, non-forested sites) are given in Table 1. With samplings performed in the peripheral plain surrounding the Makay massif, the most dominant species (RFO > 20%; following species list ranked according to RFO value) were *Laccophilus posticus* (RFO 64.4%; all following species with RFO ≤ 50%), *Canthydrus guttula*, *Hydrovatus acuminatus*, *Yola costipennis*, *Neohydrocoptus seriatus*, *Hydaticus servillianus*, *Cybister cinctus*, *Bidessus perexiguus*, *Hydroglyphus geminodes*, *Bidessus longistriga*, *Pachynectes costulifer*, *Methles* sp. Ma5, *Uvarus rivulorum*, *Laccophilus pallescens*, *L. addendus*, *Hydaticus dorsiger*, and *Rhantaticus congestus*. For samplings in inner Makay, the most dominant species (same criteron and listing order) were *Laccophilus makay* (RFO 65.6%; all following species with RFO < 36%), *Pachynectes* sp. Ma1, *Copelatus ruficapillus*, *Hyphydrus separandus*, *Copelatus acamas*, and *Dineutus proximus*. Hence, with a RFO threshold of 20%, there is not a single species in common among dominant species of inner vs. peripheral Makay. When the threshold is lowered to a RFO of 10%, only *Laccophilus posticus* (RFO peripheral: 64.4%; inner: 13.7%) shows up among dominant species in both areas. The species community of aquatic Adephaga populating the freshwater biota associated with the sandstone canyons of inner Makay is therefore highly original with respect to the community associated with the surrounding plain, the latter reflecting what can be found virtually anywhere in the western lowlands of Madagascar, in water bodies located in more or less deforested and man-impacted environments.

Table 1. List of the species sampled, with indication of status and values of relative frequencies of occurrence (RFO). E: endemic of Madagascar; E*: endemic of the Malagasy region; W (widespread): distribution extending outside the Malagasy region. NbOc (third column): total number of occurrences, i.e., number of samplings in which the species was present out of the 87 samplings performed. For RFO calculated by categories of sites, total number of samplings for each category indicated between parentheses in column headings.

Species	Status	NbOc (RFO %) all samplings (n = 87)	RFO % inner Makay (n = 73)	RFO % peripheral Makay (n = 14)	RFO % forested sites (n = 35)	RFO % semi-forested sites (n = 34)	RFO % non-forested sites (n = 18)
Gyrinidae							
Dineutus proximus	E	15 (17.2)	20.6	0	28.6	14.7	0
D. s. sinuosipennis	E	8 (9.2)	11.0	0	14.3	8.8	0
Orectogyrus vicinus	E	5 (5.7)	6.9	0	11.4	2.9	0
Haliplidae							
Peltodytes quadratus	E	2 (2.3)	0	14.3	0	0	11.1
Noteridae							
Canthydrus concolor	E	1 (1.1)	0	7.1	0	0	5.6
C. flavosignatus	W	2 (2.3)	0	14.3	0	0	11.1
C. guttula	E*	11 (12.6)	5.5	50.0	5.7	2.9	44.4
C. sp. Ma5	?	3 (3.4)	1.4	14.3	0	2.9	11.1
Neohydrocoptus seriatus	W	12 (13.8)	8.2	42.9	8.6	5.9	38.9
N. sp. Ma3	?	3 (3.4)	4.1	0	5.7	2.9	0
Sternocanthus fabiennae	E	2 (2.3)	0	14.3	0	0	11.1
Synchortus asperatus	E	2 (2.3)	0	14.3	0	0	11.1
Dytiscidae							
Copelatinae							
Copelatus acamas	E	20 (23.0)	27.4	0	25.7	29.4	5.6
C. andobonicus	E	3 (3.4)	4.1	0	5.7	2.9	0
C. polystrigus	W	12 (13.8)	16.4	0	20.0	8.8	11.1
C. ruficapillus	E	21 (24.1)	28.8	0	25.7	32.3	5.6
C. vigintistriatus	E*	4 (4.6)	5.5	0	8.6	2.9	0
C. malavergnorum sp. nov.	E	1 (1.1)	1.4	0	2.9	0	0
C. zanabato sp. nov.	E	2 (2.3)	2.7	0	0	5.9	0
Madaglymbus fairmairei	E	12 (13.8)	16.4	0	20.0	11.8	5.6
Cybistrinae							
Cybister cinctus	E	6 (6.9)	0	42.9	0	0	33.3
C. operosus	E	1 (1.1)	1.4	0	0	2.9	0
Dytiscinae, Aciliini							
Rhantaticus congestus	W	3 (3.4)	0	21.4	0	0	16.7
Dytiscinae, Eretini							
Eretes griseus	W	1 (1.1)	1.4	0	0	0	5.6
Dytiscinae, Hydaticini							
Hydaticus dorsiger	W	7 (8.0)	5.5	21.4	2.9	2.9	27.8
H. exclamationis	W	1 (1.1)	1.4	0	0	0	5.6
H. petitii	E	1 (1.1)	1.4	0	0	2.9	0
H. servillianus	W	7 (8.0)	1.4	42.9	2.9	0	33.3
H. sobrinus	E*	5 (5.7)	6.8	0	5.7	8.8	0
Hydroporinae, Bidessini							
Bidessus longistriga	E	6 (6.9)	1.4	35.7	0	2.9	27.8
B. perexiguus	E	7 (8.0)	2.7	35.7	0	5.9	27.8
Clypeodytes concivis	E	2 (2.3)	0	14.3	0	0	11.1
C. insularis	E	1 (1.1)	0	7.1	0	0	5.6
C. sp. Ma3	?	1 (1.1)	0	7.1	0	0	5.6
Hydroglyphus capitatus	E*	3 (3.4)	1.4	7.1	0	2.9	5.6
H. geminodes	W	7 (8.0)	2.7	35.7	0	5.9	27.8

Species	Status	NbOc (RFO %) all samplings (n = 87)	RFO % inner Makay (n = 73)	RFO % peripheral Makay (n = 14)	RFO % forested sites (n = 35)	RFO % semi-forested sites (n = 34)	RFO % non-forested sites (n = 18)
H. plagiatus	E	1 (1.1)	1.4	0	0	2.9	0
Liodessus luteopictus	E*	1 (1.1)	1.4	0	2.9	0	0
Pachynectes costulifer	E	5 (5.7)	0	35.7	0	0	27.8
P. sp. Ma1	E	27 (31.0)	35.6	7.1	31.4	44.1	5.6
P. sp. Ma4	E	9 (10.3)	12.3	0	5.7	20.6	0
Pseuduvarus sp. Ma1	?	2 (2.3)	0	14.3	0	0	11.1
Uvarus betsimisarakus	E	1 (1.1)	0	7.1	0	0	5.6
U. rivulorum	E	5 (5.7)	1.4	28.6	0	2.9	22.2
Yola costipennis	E	8 (9.2)	1.4	50.0	0	2.9	38.9
Hydroporinae, Hydrovatini							
Hydrovatus acuminatus	W	10 (11.5)	4.1	50.0	2.9	5.9	38.9
H. capnius	W	2 (2.3)	0	14.3	0	0	11.1
H. crassicornis	E	3 (3.4)	1.4	7.1	0	2.9	5.6
H. cruentatus	E	2 (2.3)	0	14.3	0	0	11.1
H. dentatus	W	1 (1.1)	0	7.1	0	0	5.6
H. otiosus	E	2 (2.3)	0	14.3	0	0	11.1
H. parvulus	W	3 (3.4)	1.4	7.1	0	2.9	5.6
H. pictulus	W	2 (2.3)	0	14.3	0	0	11.1
H. testudinarius	E	1 (1.1)	0	7.1	0	0	5.6
H. sp. Ma7	?	1 (1.1)	0	7.1	0	0	5.6
Hydroporinae, Hyphydrini							
Hyphydrus separandus	E*	21 (24.1)	28.8	0	25.7	32.4	5.6
H. stipes	E	1 (1.1)	1.4	0	0	2.9	0
Hydroporinae, Methlini							
Methles sp. Ma1	?	2 (2.3)	2.7	0	2.9	2.9	0
M. sp. Ma5	?	7 (8.0)	4.1	28.6	2.9	5.9	22.2
Laccophilinae							
Africophilus bartolozzii	E	4 (4.6)	5.5	0	8.6	0	5.6
A. nesiotes	W	8 (9.2)	11.0	0	17.1	5.9	0
Laccophilus addendus	E	9 (10.3)	8.2	21.4	5.7	5.9	27.8
L. flaveolus	W	1 (1.1)	0	7.1	0	0	5.6
L. insularum	E	1 (1.1)	1.4	0	0	2.9	0
L. luctuosus	E	1 (1.1)	0	7.1	0	0	5.6
L. makay	E	48 (55.2)	65.6	0	62.9	73.5	5.6
L. pallescens	W	4 (4.6)	0	28.6	0	0	22.2
L. posticus	E*	19 (21.8)	13.7	64.3	8.6	14.7	61.1
L. rivulosus	E	2 (2.3)	0	14.3	0	0	11.1
L. seyrigi	E	1 (1.1)	0	7.1	0	0	5.6
L. transversovittatus	E	3 (3.4)	4.1	0	2.9	5.9	0
L. sp. Ma19	E	1 (1.1)	0	7.1	0	0	5.6
Neptosternus oblongus	E	2 (2.3)	2.7	0	0	5.9	0
Philaccolus elongatus	E	1 (1.1)	0	7.1	0	0	5.6

According to vegetation contexts, dominant species (RFO > 20%) in forested areas were *Laccophilus makay* (RFO 62.9%, all following species with RFO < 32%), *Pachynectes* sp. Ma1, *Dineutus proximus*, *Copelatus ruficapillus*, *Hyphydrus separandus*, *Copelatus acamas*, *C. polystrigus*, and *Madaglymbus fairmairei*. For semi-forested sites (for how "forested" vs. "semi-forested" environments were defined in this study, see Material and methods, Categories of sampling sites), species with RFO > 20% were *Laccophilus makay* (RFO 73.5%; all following species with RFO < 45%), *Pachynectes*

sp. Ma1, *Hyphydrus separandus*, *Copelatus ruficapillus*, *C. acamas*, and *Pachynectes* sp. Ma4. Thus, dominant species of aquatic Adephaga are largely the same in forested and semi-forested areas of inner Makay (these two environment categories not comprising any peripheral site), but with some differences. Some species seem to prefer water bodies located in forest (RFO "forested" vs. "semi-forested"; *Dineutus proximus*: 28.6% vs. 14.7%; *Madaglymbus fairmairei*: 20% vs. 11.8%). Another example of a species found predominantly in forested contexts (but with RFO < 20% in both) is *Orectogyrus vicinus* with 11.4% vs. 2.9%. In constrast, species of the genus *Pachynectes* seem to prefer semi-open contexts (*Pachynectes* sp. Ma1: 31.4% vs. 44.1%; *Pachynectes* sp. Ma4: 5.7% vs. 20.6%). The remaining dominant species in inner Makay sites have similar RFO values in forested vs. semi-forested contexts (e.g., *Laccophilus makay*, *Copelatus ruficapillus*, *C. acamas*, *Hyphydrus separandus*; Table 1). Dominant species for non-forested sites are largely the same as those listed above for peripheral sites (most non-forested sites being located in the peripheral area), and therefore are completely different from the dominant species in forested and semi-forested sites.

We also computed dissimilarity indices based on all species to see how the whole community varies across categories of sites (Jaccard dissimilarity index, calculated from occurrence data; Bray-Curtis dissimilarity index, taking into account numbers of individuals captured for each species; Fig. 5D). This approach confirms that sites located in the peripheral plain vs. in inner Makay have very different species composition (Jaccard index:

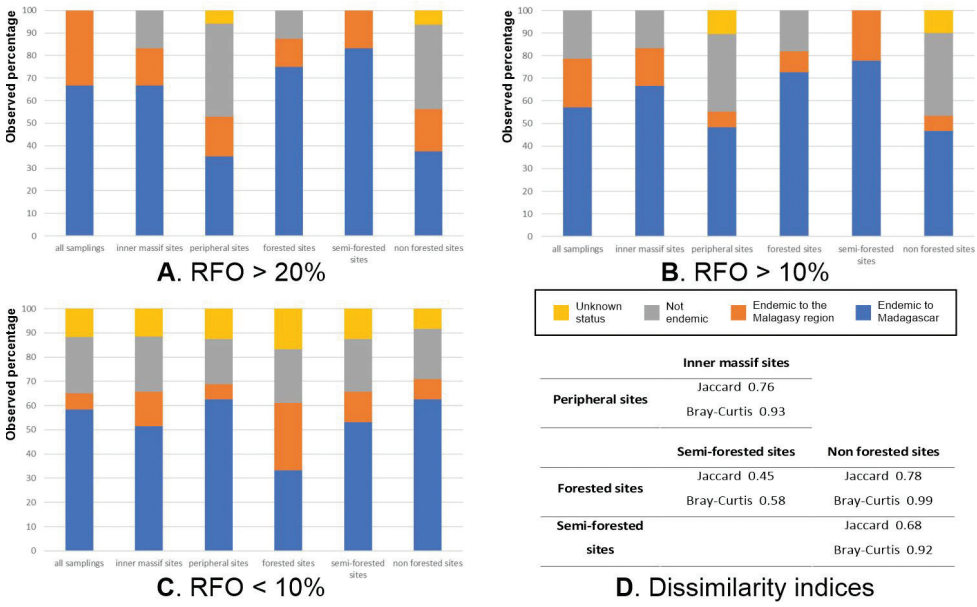

Figure 5. Comparison across site categories of percentages of endemics for dominant or rare species, and calculated dissimilarity indices for species composition **A–C** percentages of endemics among species whose relative frequency of occurrence (RFO), for the corresponding category of sites, is above or below a certain threshold **D** calculated values of Jaccard and Bray-Curtis dissimilarity indices between pairs of site categories.

0.76; Bray-Curtis index: 0.93; Fig. 5D). Sites in forested vs. semi-forested context support more similar communities (Jaccard index: 0.45; Bray-Curtis index: 0.58), whereas sites in non-forested environment harbour communities that are highly different both to those in forested environment (Jaccard index: 0.78; Bray-Curtis index: 0.99) and to a lesser extent in semi-forested environment (Jaccard index: 0.68; Bray-Curtis index: 0.92; Fig. 5D).

Observed percentages of species endemic to Madagascar are 58.1% for all samplings, 55.3% for inner Makay, 53.3% for peripheral Makay, 48.3% for forested sites, 58.5% for semi-forested sites and 53.7% for non-forested sites. Thus, when all sampled species are considered, rather surprisingly, endemicity is very similar in inner Makay vs. in the (deforested) peripheral plain and is also similar across categories of environment with the lowest value for forested areas, the highest for semi-forested areas, and non-forested areas standing in-between. When looking at percentages of endemic species among dominant species (RFO > 20% or RFO > 10%), a different picture emerges (Fig. 5A–C). Among species with RFO > 20% (Fig. 5A), the percentage of endemics is 83.3% for samplings in inner Makay and only 41.2% for samplings in the peripheral area. With a 10% cut-off (Fig. 5B), the pattern is similar although the magnitude of the difference is smaller. For vegetation contexts, endemicity for dominant species (RFO > 20%) is 75% in forested environment, 83.3% in semi-forested environment, and only 43.8% in non-forested environment (Fig. 5A); here again, lowering the cut-off to RFO 10% yields a similar pattern (Fig. 5B). When considering now only rare species (RFO < 10%) (Fig. 5C), for sites located in forest, the percentage of endemics is only 33.3%, whereas for non-forested sites, it is 62.5%. This opposite pattern of contrasted endemism levels for dominant vs. rare species is also apparent when comparing inner Makay sites (high endemism for dominant species, low endemism for rare species) and peripheral sites (vice-versa) (Fig. 5A–C). Indeed, a large fraction of the species that are found only occasionally in inner Makay are species that are extremely common in the peripheral area, and more generally in western Madagascar lowlands, most being non endemic (e.g., *Laccophilus posticus*, *Hydrovatus acuminatus*, *Hydroglyphus geminodes*, *Hydaticus dorsiger*, *H. servillianus*, etc.).

Observed species richness (number of species counted in the samplings) was 74 for all samplings, 45 for peripheral Makay, 47 for inner Makay, 29 for forested sites, 41 for semi-forested sites and 54 for deforested sites. Because observed species richness is a very poor proxy for species diversity, we ran interpolation-extrapolation analyses to obtain estimates of the H_0, H_1 and H_2 metrics (see Material and methods) for the various categories of sites (Fig. 6). For all of these categories, sample coverage plotted against number of individuals attained a plateau well before reaching the extrapolated part of the curve, and was > 0.99 with the observed number of individuals (Fig. 6A). This means that the samples sufficiently cover the original communities for estimates of species diversity to be accurate. For species richness (H_0), interpolation suggests that the number of species is higher in peripheral than in inner Makay. Indeed, a random sampling of 1000 individuals (this number being just below the minimal number of specimens sampled for any category) statistically gives ~ 44 species in peripheral Makay and ~ 36 species in inner Makay, without overlap between the 95% confidence intervals (Fig. 6B). The analysis also suggests more species in non-forested areas than

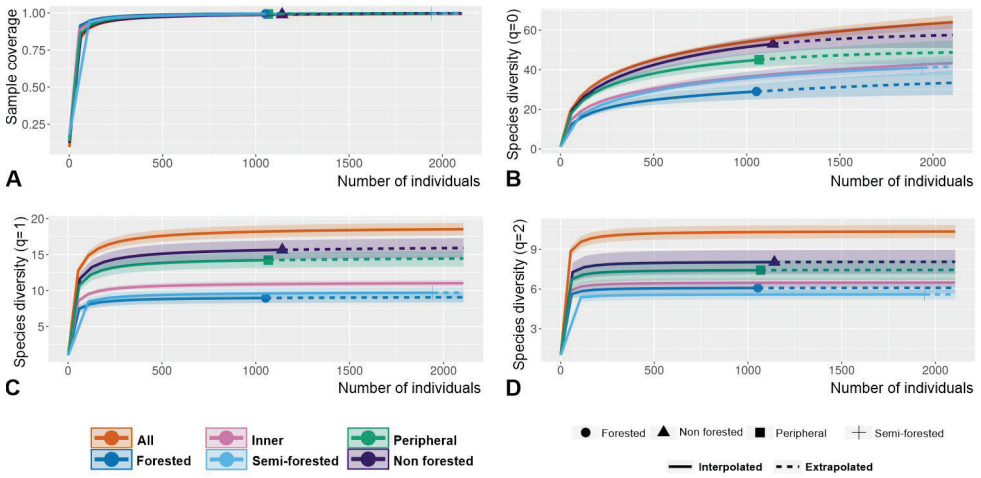

Figure 6. Interpolation-extrapolation graphs for the whole Makay dataset (All), for samplings in inner and in peripheral Makay, and for samplings in different vegetation contexts. Coloured lines represent the interpolated (solid line) or extrapolated (dashed line) estimate of the metric against number of individuals; the surface of lighter colour surrounding each curve materialises the 95% confidence interval **A** sample coverage **B** Hill number of order q=0 (H_0 or species richness) **C** Hill number of order q = 1 (H_1) **D** Hill number of order q = 2 (H_2).

in forested or semi-forested ones (for a random sampling of 1000 individuals: forested, 28 species; semi-forested, 36 species; non-forested, 51 species; confidence intervals not overlapping between "non-forested" and the other two categories) (Fig. 6B). However, extrapolation for higher numbers of individuals (Fig. 6B) as well as the asymptotic analysis yielded overlapping 95% confidence intervals for H_0 estimates between all pairs of compared categories, so that in fact these categories cannot be ranked with certainty for species richness. Estimates of H_1 (which takes into account both species richness and abundance evenness) were more straightforward (Fig. 6C), indicating higher species diversity for peripheral sites than for inner Makay sites, and higher species diversity for sites located in non-forested environments than for sites located in arbored environments (for both comparisons, with no overlap of confidence intervals in the asymptotic analysis), but no difference between forested and semi-forested sites. Estimates using H_2 (which put more weight on evenness than H_1) led to the same conclusions for vegetation contexts, but no significant difference between the peripheral and inner massif areas (overlapping confidence intervals; Fig. 6D).

Discussion

This faunistic study represents the first survey of predaceous water beetles (aquatic Adephaga) in freshwater habitats of the Makay massif and its immediate surroundings. All of the 74 sampled species except *Laccophilus makay* are newly recorded for the study area. In line with previous studies on terrestrial taxa (see Introduction), the

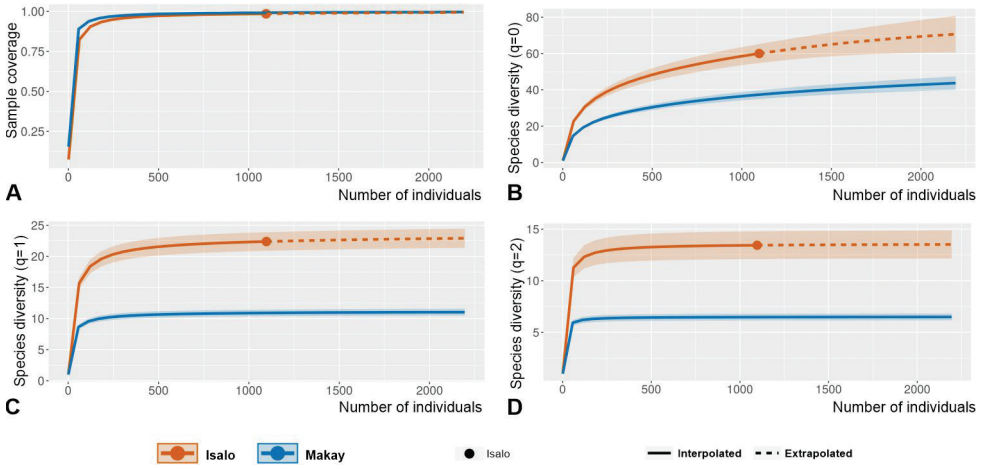

Figure 7. Interpolation-extrapolation graphs for inner Makay and inner Isalo. Coloured lines represent the interpolated (solid line) or extrapolated (dashed line) estimate of the metric against number of individuals; the surface of lighter colour surrounding each curve materialises the 95% confidence interval **A** sample coverage **B** Hill number of order q=0 (H_0 or species richness) **C** Hill number of order q = 1 (H_1) **D** Hill number of order q = 2 (H_2).

results highlight the considerable interest and originality of the Makay as a biodiversity sanctuary. At the same time, as we will see, the results reveal that for aquatic Adephaga, levels of species diversity and endemicity in inner Makay are comparatively and rather curiously low. Both areas of the Makay massif explored in this study (northern and central-southern sites) appear to be highly homogeneous in terms of species contingent. Notably, for inner massif sites the dominant species were the same in both areas. A few remarkable species (*Cybister operosus*, *Hydaticus petitii*, and the two newly described *Copelatus*) were found in the northern area only, but we cannot exclude their presence in the central-southern area as well.

In the current state of knowledge, five species of aquatic Adephaga (all belonging to family Dytiscidae) are endemic to the Makay: *Clypeodytes* sp. Ma3 (undescribed), *Copelatus malavergnorum* sp. nov., *Copelatus zanabato* sp. nov., *Laccophilus makay*, and *Pachynectes* sp. Ma4 (undescribed). Although *Clypeodyes* sp. Ma3 was collected at a site located in the peripheral plain and probably exists elsewhere in western Madagascar, the four other species are more likely to be true Makay endemics as they were exclusively sampled among the canyons of inner Makay. With a relative frequency of occurrence of 65.6% and high density of individuals at many sites, *Laccophilus makay* is by far the most abundant species of aquatic Adephaga in inner Makay, where this species can be found in virtually any kind of calm water habitat. *Pachynectes* sp. Ma4 is rarer but widespread in the massif and occasionally abundant. In contrast, the two newly described species of *Copelatus* are known from few specimens and localities, so far only in the northern part of the massif, and they seem to have more specialised ecologies (presumably semi-subterranean for *C. malavergnorum*). Other species that can be considered local endemics are those known only from the massifs of Makay and

Isalo: *Africophilus bartolozzii* (described from the Isalo massif; this species appears to be abundant in some hygropetric habitats of the Makay canyons) and *Copelatus acamas* (also described and to date recorded only from the Isalo massif; one of the dominant species of Dytiscidae in the Makay canyons).

Notwithstanding this singularity and an undeniable patrimonial value, the aquatic Adephaga fauna of inner Makay is in fact rather poor. Our impression in the field when conducting samplings was that we were finding relatively few species, and almost always the same, again and again. Our data analyses showed that species diversity in inner Makay for aquatic Adephaga is lower than in the peripheral deforested lowlands, furthermore with an endemism level of only 55.3% (53.3% for the peripheral lowlands), to be compared with the global percentage of endemic species for aquatic Adephaga in Madagascar, ~ 74% (value compiled from data in Bergsten in press, Bergsten and Manuel in press; Bergsten et al. in press; Gustafson et al. in press). This relatively low relative endemism level for inner Makay is at least in part due to the presence in low numbers of many of the non-endemic species that are common in the surrounding peripheral area. The degree of this effect might constitute a difference between the drier forests of western Madagascar and the more closed-canopy humid forests of the northern and eastern parts of the country. From a more qualitative point of view, the relative poorness of the inner Makay aquatic Adephaga fauna is also exemplified by the absence (or low species number) in inner Makay for some particular taxa, known throughout Madagascar to be good indicators for well-preserved wooded habitats (discussed in Bergsten et al. in press). The Gyrinidae of inner Makay are poorly diversified with only three species in our samplings, including a single species for the genus *Orectogyrus* and noticeably no species of *Aulonogyrus*. Among Dytiscidae, three genera (*Madaglymbus*, *Hovahydrus*, and *Uvarus* – the first two being Malagasy endemic genera) are usually rich in local endemics in well-preserved forested environments in Madagascar. In Makay, we found only one widespread *Madaglymbus* species (*M. fairmairei*), no *Hovahydrus*, and no locally endemic *Uvarus* species.

There is a critical lack of published studies with comparable datasets on which to confront quantitatively species diversity and endemism level of inner Makay with those of other Malagasy massifs, in order to substantiate the conclusion that species diversity and endemism level of aquatic Adephaga in the Makay massif are relatively poor. In the Central Highlands, Ranarilalatiana (2019) sampled 46, 47, and 48 species, respectively, in the relict forest massifs of Manjakatompo-Ankaratra, Ambohitantely, and Anjozorobe-Angavo. These numbers are very close to our observed species richness for inner Makay (47); however, observed species richness depends strongly on sampling strategy and sample coverage so that these quantities are in fact not directly comparable. Interestingly, for Ambohitantely, observed species richness was higher outside the protected area boundaries than inside, which is reminiscent of the results we obtained for the Makay from interpolation-extrapolation analyses, whereas for the other two Central Highland massifs, the pattern was the opposite (Ranarilalatiana 2019).

The Makay massif bears strong similarities and a geographical proximity with the massif of Isalo, making comparison of the aquatic Adephaga fauna between these two

massifs particularly appealing. The massifs of Makay and Isalo, isolated from each other by the large Mangoky River plain, are at first approximation rather similar in terms of geology (sandstone substratum) and geomorphology (deep canyons). For aquatic Adephaga, they also have strong faunistic affinities. Of the six species for which we obtained RFO>20% in inner Makay, five are also present and common in Isalo (*Copelatus acamas*, *C. ruficapillus*, *Dineutus proximus*, *Hyphydrus separandus* and *Pachynectes* sp. Ma1). In addition to the two local endemics known only from Isalo and Makay mentioned above, a few endemics with more widespread but more or less localised distributions in Madagascar are also present in both massifs: *Cybister operosus*, *Laccophilus transversovittatus*, and *Neptosternus oblongus.* Furthermore, we can mention two interesting cases of local endemic vicariance between Isalo and Makay. *Laccophilus makay* is replaced in the Isalo massif by another species of the *alluaudi*-group, *L. pseustes* Guignot, 1955, which is very abundant in habitats similar to those occupied by *L. makay* in the Makay. In Isalo, there is an undescribed species of *Pachynectes* which is morphologically very close to *P.* sp. Ma4 and has the same habitat preferences.

We are able to provide comparative estimates of species diversity, based on our own unpublished sampling data in southern Isalo (obtained in May 2016, using similar collecting techniques to those deployed in the Makay; with satisfying sample coverage as shown in Fig. 7A). The following comparisons are based on samplings performed in the massif themselves (i.e., inner areas), for both Makay and Isalo (see Suppl. material 2: Table S2). The percentage of endemics among the 60 species in our sampling in inner Isalo was 60%, thus slightly higher than in inner Makay. Species richness (H_0) appears to be higher in Isalo than in Makay according to the interpolation analysis: a random sampling of 1000 individuals statistically gives ~ 58 species in Isalo, vs. ~ 37 species in Makay, without overlap between the confidence intervals (Fig. 7B). Using the H_1 metric, species diversity is twice higher in Isalo than in Makay (Fig. 7C); the H_1 asymptotic analysis gives 21.61–25.05 species equivalents for Isalo, vs. 10.70–11.66 for Makay. Using the H_2 metric, species diversity is also significantly higher in Isalo than in Makay (Fig. 7D).

Why is species diversity of aquatic Adephaga so much lower in Makay than in Isalo? Makay is much dryer than Isalo (average annual rainfall for 2009–2020 according to https://www.historique-meteo.net/: in Isalo 1485 mm, in Morombe close to the Makay 877 mm; an older reference gives 700 mm for Makay, Cornet and Guillaumet 1976), and this might be part of the explanation, but our field observations suggest additional hypotheses. The mineral substratum of inner Makay streams and rivers is almost invariably fine sand (with few or no stones, pebbles and gravel), which is not the case in Isalo. This might be due to some erosion properties of the Makay sandstone. As a consequence, in association with the strongly constraining geomorphology, the habitats available to aquatic Adephaga beetles in Makay might be characterised by a relatively high level of homogeneity and thereby low diversity of ecological niches. Another possible cause of low species diversity (but with high abundance of a few well adapted specialists) may relate to geochemistry. Slow streams and their satellite pools in Makay are very often conspicuously filled in by orange masses of iron bacte-

ria, which may reflect peculiar geochemical characteristics of the mineral substratum. Furthermore, during field work in central-southern Makay, we were often struck by the strange smell (evoking sulphur) at places emanating from the rivers water. Studies focused on the physical characteristics of freshwater habitats and water chemistry in the Makay massif may help to assess these hypotheses. To improve knowledge on freshwater ecology of the inner Makay, it will of course also be necessary to obtain data on the diversity of other aquatic animal taxa, particularly among freshwater invertebrates. This would notably help to determine whether or not our conclusions from the study of aquatic Adephaga reflect a general trend for aquatic taxa in this area.

Finally, we would like to point out a few remarkable findings from our samplings in the peripheral plain surrounding the Makay massif. At ~ 15 km south-west of Makaikely, a small and shallow stream (MAK-2) with sandy bottom and very slowly flowing water, strongly impacted by cattle trampling and highly eutrophicated, provided an impressive sampling with 32 species of aquatic Adephaga (listed in the legend of Fig. 2B), collected in just a few square meters in ca. one hour. This included several remarkable species, such as *Laccophilus seyrigi* (first observation to our knowledge since its original description in 1937), *L. rivulosus* (a large, beautiful and rather uncommon *Laccophilus* species), *Hydrovatus dentatus* (second record for Madagascar), *H. testudinarius*, *Philaccolus elongatus*, and an undescribed species of *Clypeodytes*. Another noticeable finding, at two other peripheral sites, was *Peltodytes quadratus*, which despite being the less rare of the Malagasy Haliplidae (Van Vondel and Bergsten 2012), is nevertheless an uncommon and rather localised species. Altogether, the 12 sites located in the surroundings of the massif yielded a highly diversified and interesting set of species, showing that this largely deforested area, impacted notably by wood gathering, fires, and cattle trampling, still comprises some rich and singular elements of freshwater biodiversity.

Acknowledgements

We warmly acknowledge for their decisive contribution to our field work our colleague Catherine Reeb and our guide and driver Parsson. We are very grateful to Bernard Forgeau for sharing with us his deep knowledge of the Makay and its people, for guidance in the field and assistance in field work, and for ensuring good interface with the local population of the Makay. Local guides are also thanked for their help. Jean-François Cart is warmly acknowledged for help in field work during one of the campaigns and for constant material support to ATR during his PhD thesis. ATR addresses a special acknowledgement to Clémence, his parents and other members of the Malavergne family, for their constant help and support, and notably financial support to help his sister when she needed health care as well as their decisive material help toward the completion of his PhD thesis, notably through financing his last stay in France, and much more. The association Nature Evolution partly organised the field trips of 2017 and 2018 in which ATR participated. We thank Muriel Jager for technical help and Antoine Mantilleri for access to material of the MNHN collection. We are grateful to Johannes Bergsten and Tolotra Ranarilalatiana

for sending us an unpublished draft of their revision of the *erichsonii*-group species of Malagasy *Copelatus*. MM acknowledges his former lab supervisors Dominique Higuet and Hervé Le Guyader for personal and financial support. We are grateful to Amélie Faramalala, Harison Rabarison, and Roger Edmond from the "Département de Biologie et d'Ecologie Végétale" of the Antananarivo University for providing logistic help to some of the missions and supporting this work. The association Tsimbina provided financial support to ATR during his PhD thesis. The field work was funded by IFS grant # I-2-A-6098-1 to ATR. This study also benefited from Synthesys grant CZ-TAF-6684 and Agence Nationale de la Recherche grant AAPG-2019 Evo-AquaSense to MM and from French Government scholarships to ATR (BFG program 2018 and 2019). The field work was conducted under research permits No 79/16/MEEMF/SG/DGF/DAPT/SCBT.Re and 73/18/MEEF/SG/DGF/DSAP/SCB.Re, and specimens were exported under permit 203N-EA06/MG16 and 172N-EA06/MG18, issued by the "Ministère de l'Environnement et du Développement Durable" of the Republic of Madagascar.

References

Allorge L, Phillipson PB, Razakamalala R (2015) *Catharanthus makayensis* L. Allorge, Phillipson and Razakamal. (Apocynaceae) a new species from Madagascar. Candollea 70(1): 61–66. https://doi.org/10.15553/c2015v701a7

Bameul F (1984) Haliplidae, Noteridae, Dytiscidae et Gyrinidae capturés dans les îles Mascareignes et à Madagascar par Yves Gomy (Coleoptera, Hydradephaga). Nouvelle Revue d'Entomologie 1(1): 87–103. [Nouvelle Série]

Bameul F (1994) Un nouvel *Hydrocanthus* Say de Madagascar (Coleoptera Noteridae). Bulletin Mensuel de la Societe Linneenne de Lyon 63(10): 356–365. https://doi.org/10.3406/linly.1994.11051

Bergsten J (In press) Haliplidae, crawling water beetles. In: Goodman SM (Ed.) The new natural history of Madagascar. Vol. 1. Princeton University Press, Princeton, 2296 pp.

Bergsten J, Manuel M (In press) Noteridae, burrowing water beetles. In: Goodman SM (Ed.) The new natural history of Madagascar. Vol. 1. Princeton University Press, Princeton, 2296 pp.

Bergsten J, Ranarilalatiana T, Biström O (2020) A new species of *Bidessus* from Anjozorobe-Angavo and a review of Malagasy *Bidessus* (Coleoptera, Dytiscidae). European Journal of Taxonomy 717: 1–18. https://doi.org/10.5852/ejt.2020.720.1109

Bergsten J, Manuel M, Ranarilalatiana T, Ramahandrison AT, Hájek J (In press) Coleoptera: Dytiscidae, diving beetles, tsikovoka, [1024–1034]. In: Goodman SM (Ed.) The new natural history of Madagascar. Vol. 1. Princeton University Press, Princeton, 2296 pp.

Bertrand H, Legros C (1971) Hydrocanthares (excl. Gyrinidae) recueillis à Madagascar (mission Bertrand, 1960). Cahiers ORSTOM, série hydrobiologie 5(3–4): 241–249.

Beutel RG, Ribera I, Fikáček M, Vasilikopoulos A, Misof B, Balke M (2020) The morphological evolution of the Adephaga (Coleoptera). Systematic Entomology 45(2): 378–395. https://doi.org/10.1111/syen.12403

Bilardo A, Rocchi S (2012) A revision of the African species of the genus *Neptosternus* Sharp, 1882 (Coleoptera Dytiscidae). Memorie della Società Italiana di Scienze Naturali e del Museo Civico di Storia Naturale di Milano 37(3): 1–48.

Bilardo A, Rocchi S, Jäch MA (2020) First record of the genus *Africophilus* Guignot, 1948 from Central Africa, with description of a new species from Gabon (Coleoptera: Dytiscidae: Laccophilinae). Koleopterologische Rundschau 90: 17–24.

Biström O (1982) A revision of the genus *Hyphydrus* Illiger (Coleoptera, Dytiscidae). Acta Zoologica Fennica 165: 1–121.

Biström O (1983) Revision of the genera *Yola* Des Gozis and *Yolina* Guignot (Coleoptera, Dytiscidae). Acta Zoologica Fennica 176: 1–67.

Biström O (1985) A revision of the species group *B. sharpi* in the genus *Bidessus* (Coleoptera, Dytiscidae). Acta Zoologica Fennica 178: 1–40.

Biström O (1986) Review of the genus *Hydroglyphus* Motschulsky (= *Guignotus* Houlbert) in Africa (Coleoptera, Dytiscidae). Acta Zoologica Fennica 182: 1–56.

Biström O (1987) Revision of the genus Pachynectes Régimbart (Coleoptera, Dytiscidae). Annales Entomologici Fennici 53: 48–52.

Biström O (1988a) Revision of the genus *Clypeodytes* Régimbart in Africa (Coleoptera: Dytiscidae). Entomologica Scandinavica 19(2): 199–238. https://doi.org/10.1163/187631289X00159

Biström O (1988b) Review of the genus *Liodessus* in Africa (Coleoptera, Dytiscidae). Annales Entomologici Fennici 54: 21–28.

Biström O (1988c) Review of the genus *Uvarus* Guignot in Africa (Coleoptera, Dytiscidae). Acta Entomologica Fennica 51: 1–38.

Biström O (1996) Taxonomic revision of the genus *Hydrovatus* Motschulsky (Coleoptera, Dytiscidae). Entomologica Basiliensia 19: 57–584.

Biström O, Nilsson AN, Bergsten J (2015) Taxonomic revision of Afrotropical *Laccophilus* Leach, 1815 (Coleoptera, Dytiscidae). ZooKeys 542: 1–379. https://doi.org/10.3897/zookeys.542.5975

Brinck P (1955) A revision of the Gyrinidae (Coleoptera) of the Ethiopian region. I. Acta Universitatis Lundensis. Nova Series 51 (16): 1–141.

Brinck P (1956) A revision of the Gyrinidae (Coleoptera) of the Ethiopian region. II. Acta Universitatis Lundensis. Nova Series 52 (14): 1–190.

Bukontaite R, Ranarilalatiana T, Randriamihaja JH, Bergsten J (2015) In or out-of- Madagascar? Colonization patterns for large-bodied diving beetles (Coleoptera: Dytiscidae). PLoS ONE 10(3): e0120777. https://doi.org/10.1371/journal.pone.0120777

Carret P, Rabarison H, Rabibisoa N, Andriamanaitra S, Andriamboavonjy E, Ramarojaona P, Ramahefamanana NM, Andriamaro L, Andrianarisata M, Randrianasolo H, Rabearisoa A, Rasolohery A, Randrianarisoa J, Labedan A, Rafamatanantsoa G, Souquet M, Giloux Y, Florens FBV, Ibrahim Y, Rocamora G (2014) Profil d'écosystème. Hotspot de Madagascar et des îles de l'Ocean Indien. Critical Ecosystem Partnership Fund, 1–314. https://www.cepf.net/sites/default/files/ecosystemprofile_madagascar_fr.pdf

Chao A, Jost L (2012) Coverage-based rarefaction and extrapolation: Standardizing samples by completeness rather than size. Ecology 93(12): 2533–2547. https://doi.org/10.1890/11-1952.1

Chao A, Gotelli NJ, Hsieh TC, Sander EL, Colwell RK (2014) Rarefaction and Extrapolation with Hill Numbers: A Framework for Sampling and Estimation in Species Diversity Studies. Ecological Monographs 84(1): 45–67. https://doi.org/10.1890/13-0133.1

Colwell RK, Chao A, Gotelli NJ, Lin SY, Mao CX, Chazdon RL, Longino JT (2012) Models and estimators linking individual-based and sample-based rarefaction, extrapolation and comparison of assemblages. Journal of Plant Ecology 5(1): 3–21. https://doi.org/10.1093/jpe/rtr044

Cornet A, Guillaumet JL (1976) Divisions floristiques et étages de végétation à Madagascar. ORSTOM, Paris 6(1): 35–40.

Csösz S, Loss AC, Fisher BL (2021) Taxonomic revision of the Malagasy *Aphaenogaster swammerdami* group (Hymenoptera: Formicidae). PeerJ 9: e10900. https://doi.org/10.7717/peerj.10900

Dolch R, Ratsisetraina R, Markolf M, Ratolojanahary T, Rakotonirina H, Louis Jr E, Wendenbaum E (2011) Assessment of lemur diversity in the Makay massif. Lemur News 16(1): 48–53.

Feijen HR, Feijen FAA, Feijen C, Gilles B (2021) A review of *Madagopsina* Feijen, Feijen & Feijen (Diptera, Diopsidae) with description of a new species, key to the species, and discussion of intrageneric relationships. ZooKeys 1057: 1–21. https://doi.org/10.3897/zookeys.1057.67433

Franciscolo ME (1994) Three new *Africophilus* Guignot and new records of Gyrinidae and Dytiscidae from Sierra Leone (Coleoptera). Accademia Nazionale dei Lincei. Quaderno 267: 267–298.

Gnezdilov VM (2021) New species of the genera *Limentinus* Distant, 1917 and *Calodia* Nielson, 1982 (Hemiptera, Auchenorrhyncha, Cicadellidae, Coelidiinae) from the Makay Massif of Madagascar, with a key to Malagasy species. Zoosystema 43(16): 297–310. https://doi.org/10.5252/zoosystema2021v43a16

Gotelli NJ, Ellison AM (2013) A primer of ecological statistics. 2nd Edn. Sinauer, Sunderland, MA, 1–9.

Guignot F (1955a) Dytiscides et gyrinides nouveaux de Madagascar (coléoptères). Le Naturaliste Malgache 7(1): 63–70.

Guignot F (1955b) Nouveaux dytiscides de Madagascar. Le Naturaliste Malgache 7(2): 139–144. https://doi.org/10.3406/linly.1956.7820

Guignot F (1956) Contribution à la connaissance de la faune dystiscidienne malgache. Le Naturaliste Malgache 8(1): 75–80.

Guignot F (1960) Haliplides et dytiscides nouveaux ou intéressants de Madagascar. Le Naturaliste Malgache 11 (1959): 95–101.

Guignot F (1959–1961) Révision des Hydrocanthares d'Afrique (Coleoptera Dytiscoidea), parts 1-3. Annales du Musée Royal du Congo Belge Tervuren (8) Sciences Zoologiques 70, 78, 90: 1–995.

Gustafson GT, Ranarilalatiana T, Bergsten J (In press) Gyrinidae, whirligig beetles, fandiorano. In: Goodman SM (Ed.) The new natural history of Madagascar. Vol. 1. Princeton University Press, Princeton, 2296 pp.

Hájek J, Reiter A (2014) Adephagous water beetles (Coleoptera: Gyrinidae, Haliplidae, Noteridae, Dytiscidae) of Yemen and Dhofar region (Oman) with description of a new *Hyphydrus* from Socotra Island. Acta Entomologica Musei Nationalis Pragae 54(Supplementum): 63–99.

Hendrich L, Balke M, Wewalka G (2010) Dytiscidae: Annotated checklist of Bidessini, Hydrovatini, Hyphydrini, Laccophilinae and Dytiscinae (Coleoptera), [171–194]. In: Jäch MA, Balke M (Eds) Water beetles of New Caledonia (part 1). Monographs on Coleoptera 3.

Laudisoit A, Prié V, Beaucournu JC (2012) Une nouvelle espèce de *Lagaropsylla* Jordan & Rothschild, 1921 de Madagascar (Insecta, Siphonaptera, Ischnopsyllidae). Zoosystema 34(4): 737–744. https://doi.org/10.5252/z2012n4a5

Legros C (1951) Les gyrins de Madagascar (Coléoptères). Le Naturaliste Malgache 3: 117–123.

Lourenço W, Wilmé L (2015) Scorpions collected in the Makay Mountain Range, Madagascar (Scorpiones: Hormuridae, Buthidae) with description of a new species. Revista Iberica de Aracnologia 26: 55–61.

Manuel M, Ramahandrison AT (2020) Four new species of the diving beetle genus *Laccophilus* Leach, 1815 from Madagascar (Coleoptera, Dytiscidae, Laccophilini). Zootaxa 4822(4): 485–502. https://doi.org/10.11646/zootaxa.4822.4.2

Miller KB (2002) Revision of the genus *Eretes* Laporte, 1833 (Coleoptera: Dytiscidae). Aquatic Insects 24(4): 247–272. https://doi.org/10.1076/aqin.24.4.247.8238

Miller KB, Nilsson AN (2003) Homology and terminology: Communicating information about rotated structures in water beetles. Latissimus 17: 1–4.

Nilsson AN (2011) A world catalogue of the Family Noteridae, or the burrowing water beetles (Coleoptera, Adephaga). Version 16. VIII. 2011. http://www.waterbeetles.eu [accessed 10 March 2022]

Nilsson AN, Hájek J (2022) A world catalogue of the family Dytiscidae, or the diving beetles (Coleoptera, Adephaga). Version 1. I. 2022. http://www.waterbeetles.eu [accessed 10 March 2022]

Prié V (2011) Les chauves-souris du massif du Makay (Madagascar): Premier inventaire chiroptérologique dans le cadre du projet Makay Nature. Le Vespère 2: 107–123.

Ranarilalatiana T (2019) Diversité de *Copelatus* Erichson, 1832 (Coleoptera, Dytiscidae) de Madagascar et des Coléoptères Adephaga aquatiques dans les vestiges forestiers du Haut Plateau Central particulièrement sur les aires protégées de Manjakatompo Ankaratra, d'Ambohitantely et d'Anjozorobe-Angavo. PhD Thesis, Université d'Antananarivo, Antananarivo, Madagascar.

Ranarilalatiana T, Bergsten J (2019) Discovery of a specialist Copelatinae fauna on Madagascar: Highly ephemeral tropical forest floor depressions as an overlooked habitat for diving beetles (Coleoptera, Dytiscidae). ZooKeys 871: 89–118. https://doi.org/10.3897/zookeys.871.36337

Ranarilalatiana T, Ravaomanarivo LHR, Bergsten J (2019) Taxonomic revision of the genus *Copelatus* of Madagascar (Coleoptera, Dytiscidae, Copelatinae): The non-*erichsonii* group species. ZooKeys 869: 19–90. https://doi.org/10.3897/zookeys.869.33997

Rocchi S (1991) Contributo alla conoscenza degli Haliplidae e dei Dytiscidae del Madagascar con descrizione di due nuove specie (Coleoptera). Frustula Entomologica 14(27): 71–89. [Nuova Serie]

Roubaud F, Razafindrakoto M, Carrière SM, Culas C, Pannier E (2018) Mise en place d'un dispositif de connaissance, suivi et évaluation socio-économique et environnemental de la Nouvelle Aire Protégée (NAP) du Makay, Madagascar. Document de travail UMR DIAL, 1–32. https://horizon.documentation.ird.fr/exl-doc/pleins_textes/divers19-03/010074728.pdf

van Vondel B, Bergsten J (2012) Review of the Haliplidae of Madagascar, with description of two new species (Coleoptera). Tijdschrift voor Entomologie 155(1): 57–66. https://doi.org/10.1163/221194312X651382

Watts CHS (1978) A revision of the Australian Dytiscidae (Coleoptera). Australian Journal of Zoology, Supplementary Series 57: 1–166. https://doi.org/10.1071/AJZS057

Wendenbaum E (2011) Makay. A la découverte du dernier éden. Editions de La Martinière, Paris, 176 pp.

Wesener T (2020) Ecotone shifts in southern Madagascar: First barcoding data and six new species of the endemic millipede genus *Riotintobolus* (Spirobolida, Pachybolidae). ZooKeys 953: 1–29. https://doi.org/10.3897/zookeys.953.53977

Wewalka G (1980) Results of the Austrian Hydrobiological Mission, 1974, to the Seychelles-, Comores- and Mascarene Archipelagos. Part VII: Dytiscidae, Gyrinidae (Coleoptera). Annalen des Naturhistorischen Museums in Wien 83: 723–732.

Supplementary material 1

Table S1

Authors: Andriamirado T. Ramahandrison, Bakolimalala Rakouth, Michaël Manuel

Data type: Cumulated abundances of species per categories of sampling sites in Makay

Explanation note: This table gives for each category of sites and for each species the total number of specimens sampled. The second column indicates the status of the species with respect to endemism. These data were used to build the graphs of Figs 5, 6. The table is in Excel format (.xls).

Link: https://doi.org/10.3897/zookeys.1127.85737.suppl1

Supplementary material 2

Table S2

Authors: Andriamirado T. Ramahandrison, Bakolimalala Rakouth, Michaël Manuel

Data type: Cumulated abundances of species sampled in inner Makay vs. in inner Isalo.

Explanation note: This table gives for each species the total number of specimens sampled in inner Makay and in inner Isalo. These data were used to build the graphs of Fig. 7. The table is in Excel format (.xls).

Link: https://doi.org/10.3897/zookeys.1127.85737.suppl2

ZooKeys 1127: 61–77 (2022)
doi: 10.3897/zookeys.1127.91310
https://zookeys.pensoft.net

DATA PAPER

A peer-reviewed open-access journal
ZooKeys
Launched to accelerate biodiversity research

Complete distribution of the genus *Laevilitorina* (Littorinimorpha, Littorinidae) in the Southern Hemisphere: remarks and natural history

Sebastián Rosenfeld[1,2,3,4], Claudia S. Maturana[2,3,5], Hamish G. Spencer[6], Peter Convey[2,3,7,8], Thomas Saucède[9], Paul Brickle[10,11], Francisco Bahamonde[1,3], Quentin Jossart[9,12], Elie Poulin[2,5], Claudio Gonzalez-Wevar[2,13]

1 *Laboratorio de Ecosistemas Marinos Antárticos y Subantárticos, Universidad de Magallanes, Punta Arenas, Chile* **2** *Millennium Institute Biodiversity of Antarctic and Subantarctic Ecosystems (BASE), Las Palmeras 3425, Santiago, Chile* **3** *Cape Horn International Center (CHIC), Puerto Williams, Chile* **4** *Centro de Investigación Gaia-Antártica, Universidad de Magallanes, Avenida Bulnes 01855, Punta Arenas, Chile* **5** *Institute of Ecology and Biodiversity (IEB), Las Palmeras 3425, Santiago, Chile* **6** *Department of Zoology, University of Otago, Dunedin, New Zealand* **7** *British Antarctic Survey (BAS), Cambridge, UK* **8** *Department of Zoology, University of Johannesburg, Johannesburg, South Africa* **9** *Biogéosciences, UMR 6282 CNRS, Université Bourgogne Franche-Comté, 6, boulevard Gabriel, 21000, Dijon, France* **10** *South Atlantic Environmental Research Institute, Ross Road, Stanley, Falkland Islands, UK* **11** *School of Biological Sciences (Zoology), University of Aberdeen, Aberdeen, UK* **12** *Marine Biology, Université Libre de Bruxelles (ULB), Brussels, Belgium* **13** *Centro FONDAP IDEAL, Instituto de Ciencias Marinas y Limnológicas (ICML) Facultad de Ciencias, Universidad Austral de Chile, Casilla 567, Valdivia, Chile*

Corresponding author: Sebastián Rosenfeld (sebastian.rosenfeld@umag.c)

Academic editor: Frank Köhler | Received 5 August 2022 | Accepted 3 October 2022 | Published 2 November 2022

https://zoobank.org/44F6411B-41E1-4C99-86F0-62519C8CBA0F

Citation: Rosenfeld S, Maturana CS, Spencer HG, Convey P, Saucède T, Brickle P, Bahamonde F, Jossart Q, Poulin E, Gonzalez-Wevar C (2022) Complete distribution of the genus *Laevilitorina* (Littorinimorpha, Littorinidae) in the Southern Hemisphere: remarks and natural history. ZooKeys 1127: 61–77. https://doi.org/10.3897/zookeys.1127.91310

Abstract

Littorinid snails are present in most coastal areas globally, playing a significant role in the ecology of intertidal communities. *Laevilitorina* is a marine gastropod genus distributed exclusively in the Southern Hemisphere, with 21 species reported from South America, the sub-Antarctic islands, Antarctica, New Zealand, Australia and Tasmania. Here, an updated database of 21 species generated from a combination of sources is presented: 1) new field sampling data; 2) published records; 3) the Global Biodiversity Information Facility (GBIF) and The Atlas of Living Australia (ALA), to provide a comprehensive description of the known geographic distribution of the genus and detailed occurrences for each of the 21 species. The database includes 813 records (occurrences), 53 from field sampling, 174 from the literature, 128

from GBIF, and 458 from ALA. West Antarctica had the highest species richness (8 species), followed by sub-Antarctic islands of New Zealand (4 species) and the south-east shelf of Australia (4 species). The provinces of Magellan, New Zealand South Island, and sub-Antarctic Islands of the Indian Ocean include two species each. This study specifically highlights reports of *L. pygmaea* and *L. venusta*, species that have been almost unrecorded since their description. Recent advances in molecular studies of *L. caliginosa* showed that this species does not correspond to a widely distributed taxon, but to multiple divergent lineages distributed throughout the Southern Ocean. Ongoing molecular and taxonomic studies are necessary for a better understanding of the diversity and biogeography of this genus.

Keywords
Antarctic, endemism, Laevilitorininae, sub-Antarctic

Introduction

One of the most common challenges facing studies or the construction of inventories of biodiversity is the absence of detailed information on the distribution of taxa throughout the different geographical regions of the planet. Furthermore, species distribution data are usually scattered across different sources of information such as taxonomic reviews, species lists, reports and natural history collections (Beck et al. 2013). Therefore, it is important to merge these different sources into robust and freely accessible biodiversity databases. The Global Biodiversity Information Facility (GBIF) project has enabled the creation of a platform where museums, herbaria and researchers can publish their databases and make them freely available for use (Flemons et al. 2007). However, despite increasing the international effort devoted to the digitisation of specimen catalogues in museums and other repositories, even today only a small proportion of global records are estimated to have been made available online through the efforts of the GBIF and other platforms like the Ocean Biodiversity Information System (OBIS) (Ariño 2010; Maturana et al. 2019; OBIS 2022).

The family Littorinidae represents one of the most conspicuous and abundant components of intertidal communities that inhabit rocky shores across the world's coasts (Reid 1989). Being such a widespread and accessible group, they have been amongst the most intensively studied marine molluscs (Reid 2007; Reid and Williams 2012; González-Wevar et al. 2022). They play a significant role in the ecology of intertidal communities and have been widely used as models in microevolutionary studies of natural selection and genetic differentiation (Williams et al. 2003; Kess et al. 2018; Estevez et al. 2021; Bosso et al. 2022). In addition, with the advance of molecular tools, the systematics and taxonomy of the family have been updated (Reid and Williams 2004) to give a more accurate classification of species and description of their distributions. Members of the group are present in both hemispheres (Reid 1989; Williams et al. 2003). In the Southern Hemisphere, tropical and temperate species have received most research attention (e.g., Williams et al. 2003; Reid and Williams 2004). As a consequence, while some littorinids are known from southern South America and the Southern Ocean (SO), no recent taxonomic examinations are available and occurrence information remains scarce as and dispersed (Reid 1989).

Laevilitorina Pfeffer, 1886 is the most widely distributed genus of marine gastropods present at high latitudes in the Southern Hemisphere (Reid 1989). Its known distribution range includes South America, New Zealand, Australia, Tasmania, and Antarctic (West and East parts), and many peri-(sub)Antarctic islands (South Shetland Islands, South Orkney Islands, Falkland/Malvinas Islands, South Georgia, Crozet, Kerguelen, Heard, Macquarie, Campbell, Auckland, and Antipodes Island). The genus *Laevilitorina* Pfeffer, 1886 is characterised by a thick, generally smooth shell, a non-planktotrophic protoconch and a generally paucispiral operculum (Reid 1989; Warén and Hain 1996). At present, 21 species of *Laevilitorina* are taxonomically accepted (MolluscaBase 2022).

The present study documents the state of knowledge of the genus and provides an updated database, using a combination of recent sampling data, published records available in the literature, and available information from GBIF and other repositories. The objectives of the study are: i) to report new records of *Laevilitorina* species present in Antarctic and sub-Antarctic environments and ii) to evaluate the distribution and richness of *Laevilitorina* species throughout the Southern Hemisphere, using an updated database. The updated database will serve as a basis for future comprehensive systematic research on the genus, including the application of molecular phylogenetic approaches to help infer its regional evolutionary history.

Materials and methods

Construction of the database

Laevilitorina records across the Southern Hemisphere were compiled from four main sources: 1) field sampling data; 2) published literature; 3) data already present in GBIF and 4) the data present in the repository of the Atlas of Living Australia (ALA) (Belbin 2011). Duplicate records were removed to construct a unified database. In addition, the records available in GBIF and ALA were used to describe the distribution range of each species. To ensure the quality of the occurrence data, dubious records were excluded from the geospatial analysis. The criterion used to determine dubious records was records of species in geographic areas outside the distribution range described in the original descriptions and taxonomic revisions.

Twelve marine biogeographical provinces in the Southern Hemisphere were considered for the purpose of our geospatial analyses, including the Magellan province (southern South America and Falkland / Malvinas Islands), West Antarctic, East Antarctica, Indian Ocean sub-Antarctic islands (Prince Edward Islands, Crozet Island, Kerguelen and Heard Islands), Macquarie Island, New Zealand sub-Antarctic islands, Southern New Zealand, Northern New Zealand, South-east Australian Shelf, South-west Australian Shelf, West Central Australian Shelf and East Central Australian Shelf, as defined in Spalding et al. (2007) and Koubbi et al. (2014). All spatial analyses were carried out on the unified database.

Recent sampling data

New material was collected from multiple locations in southern South America between the Strait of Magellan (53°36'S, 70°55'W) and the Diego Ramirez archipelago (56°31.345'S, 68°43.622'W). In the Falkland/Malvinas Islands, specimens were collected from the intertidal zone of Hooker Point (51°42'S, 57°46'W). New Antarctic material was collected from the South Shetland Islands, Doumer Island, Palmer Land, and Avian Island under the framework of Antarctic Scientific Expeditions (**ECA**) 49, 53, 54 and 58 of the Chilean Antarctic Institute (**INACH**). Samples from the South Orkney Islands and South Georgia were obtained during British Antarctic Survey (**BAS**) and SAERI expeditions (2016–2017, 2017–2018 and 2021). Samples from Kerguelen and Crozet archipelagos were obtained through the PROTEKER project under the framework of the French Polar Institute Paul Emile Victor (**IPEV**) summer campaign 2017.

Sample collection

Samples were collected using two methods: 1) manual collection in the intertidal zone, with littorinids being sampled individually, and 2) SCUBA diving between 1 and 15 m depth, where substrates (e.g. sediments, macroalgae) were collected. Rock substrates were subsequently scraped to ensure that all species and specimens were collected. Each macroalga sample was placed in a plastic bag. After collection, specimens were kept alive and transported onboard or to the research station. Each sample was then gently agitated to detach the associated fauna. All *Laevilitorina* samples were immediately preserved in ethanol (95%) to be transported to the laboratory. Geographic coordinates were recorded using GPS for each sample location.

Taxonomic identification

Morphological observations were performed under an OLYMPUS stereomicroscope CX31. The following morphological measurements were taken, following Reid (2007): shell height (H), the maximum dimension parallel to the axis of coiling; shell breadth (B), the maximum dimension perpendicular to H; length of the aperture (LA), the greatest length from the junction of the outer lip with the penultimate whorl to the anterior lip. For determination to species level, each individual was identified following the taxonomic studies of Martens and Pfeffer (1886), Suter (1913), Powell (1951, 1955), Dell (1964), Arnaud and Bandel (1976), Waren and Hain (1996) and Zelaya (2005).

Published literature

To ensure maximum coverage of the generated dataset, information was gathered from all available scientific publications that have sampled or reviewed *Laevilitorina* species throughout the genus' distribution, from the description of the first species (Gould 1849) to the present. These records and their respective geographical positions were

entered into a spreadsheet following the Darwin Core Standard structured procedure (Wieczorek et al. 2012). Taxonomy used in these publications was updated following the most recent systematic revision (Reid 1989; Waren and Hain 1996; Engl 2012; Bouchet et al. 2017; MolluscaBase 2022). We did not follow González-Wevar et al. (2022) for species names and databases, mainly because the lineages that would correspond to new species have not yet been formally described. However, the implications of these results for the taxonomy and biogeography of *Laevilitorina* are discussed (González-Wevar et al. 2022).

Digital database GBIF and ALA

All georeferenced records of the genus *Laevilitorina* were retrieved from the GBIF and ALA database on 12 September 2022 (Rosenfeld et al. 2022). The point-radius method was used for georeferencing records lacking precise geographic location (coordinates), by identifying locality description included in the relevant metadata of the reported collection. This method considers the precision, datum and specificity of the locality description to determine the coordinates (Wieczorek et al. 2004; Wieczorek and Wieczorek 2021). The species list was updated to exclude erroneous or suspect records, rule out possible synonymy and follow current taxonomy.

Results

Database summary

The complete database (https://www.gbif.org/dataset/cd023c5e-8729-41b2-b9df-1419289c0e40) includes 813 records. Most records (458) were obtained from the ALA repository, followed by literature (174) obtained from 63 reviewed articles, GBIF (128), and new sampling records (53).

Dubious records

Laevilitorina antarctica (Smith, 1902), originally described from Cape Adare in the Ross Sea, is also reported in GBIF from Macquarie Island (https://www.gbif.org/es/occurrence/search?taxon_key=9810991). However, this species has historically been reported primarily from the biogeographic provinces of East Antarctica and West Antarctica (Arnaud and Bandel 1976; Dell 1990). Therefore, the presence of *L. antarctica* on Macquarie Island requires confirmation and was not included in our database.

New record

This study includes the first record of the species *Laevilitorina delli* Powell, 1955, in GBIF database, previously described by Powell (1955) from the South Island of New Zealand and Antipodes Island.

Morphological identification

All newly collected *Laevilitorina* specimens identified in this study showed morphological characteristics corresponding to those described in the literature (Fig. 1a–f). The specimens of *L. pygmaea* Pfeffer, 1886 and *L. venusta* Pfeffer, 1886 identified from South Georgia are consistent with the morphological characteristics described by Martens and Pfeffer (1886) for these species (Fig. 1b, c). Individuals of *L. pygmaea* had a high spire, reddish-brown periostracum, with five convex whorls. The last whorl was 50% of the total height of the spire and the aperture was ~ 59% of the length of the last whorl (Fig. 1b). *L. venusta* individuals were between 3.7 and 5.6 mm in height, with a short spire, and 4.5 convex whorls. The aperture was wide, occupying a little more than half of the total height of the shell (54%); the columellar callus was sharp, white and expanded towards the umbilicus, all characteristics again consistent with Martens and Pfeffer (1886) (Fig. 1c).

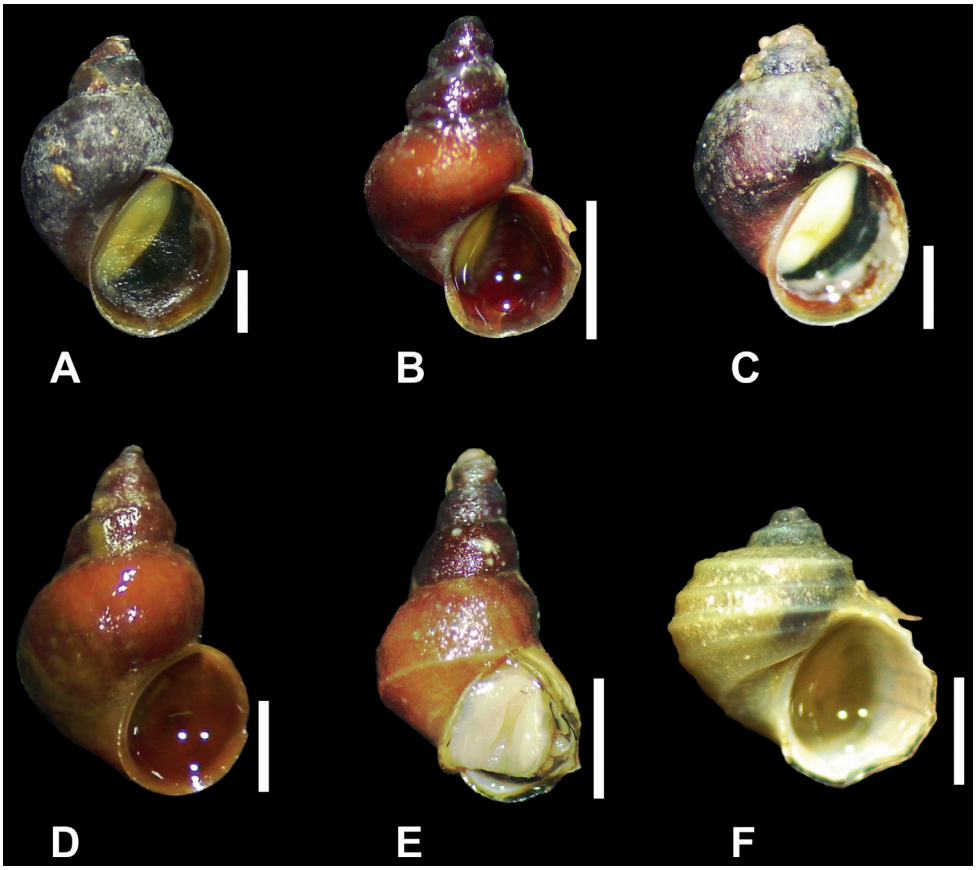

Figure 1. A *Laevilitorina caliginosa* (4.8 mm) **B** *Laevilitorina pygmaea* (2.5 mm) **C** *Laevilitorina venusta* (3.7 mm) **D** *Laevilitorina claviformis* (3.9 mm) **E** *Laevilitorina umbilicata* (2.8 mm) **F** *Laevilitorina wandelensis* (2.7 mm). Scale bars: 1 mm. Photographs by Sebastián Rosenfeld.

Species richness

A total of 21 species of *Laevilitorina* were recorded in the Southern Hemisphere; West Antarctica was the province with the highest species richness (S = 8, Fig. 2a, b), followed by the New Zealand sub-Antarctic islands, the south-east shelf of Australia (S = 4, Fig. 2a, b) and the south-west Australian Shelf (S = 3, Fig. 2a, b). The provinces of Magellan, south New Zealand, and Indian Ocean sub-Antarctic islands had two species each (Fig. 2 a, b) and the remaining provinces had only one species each (Fig. 2 a, b). However, based on the latest molecular study of González-Wevar et al. (2022), there are four new species-level lineages of *Laevilitorina* in the Magellan province where species richness would increase to six taxa (Fig. 2 a, b). The species with the highest number of records was *L. caliginosa* (Gould, 1849) (158). Most of these records came from the Magellan province (79), of which nine were from the Falkland/Malvinas Islands.

Within the West Antarctic province eight species were reported, of which *L. venusta* and *Laevilitorina granum* Pfeffer, 1886 were recorded exclusively from South Georgia (Fig. 3), while *L. wandelensis* (Lamy, 1906) and *L. antarctica* were recorded exclusively from Antarctic provinces, without no records from South Georgia (Fig. 3).

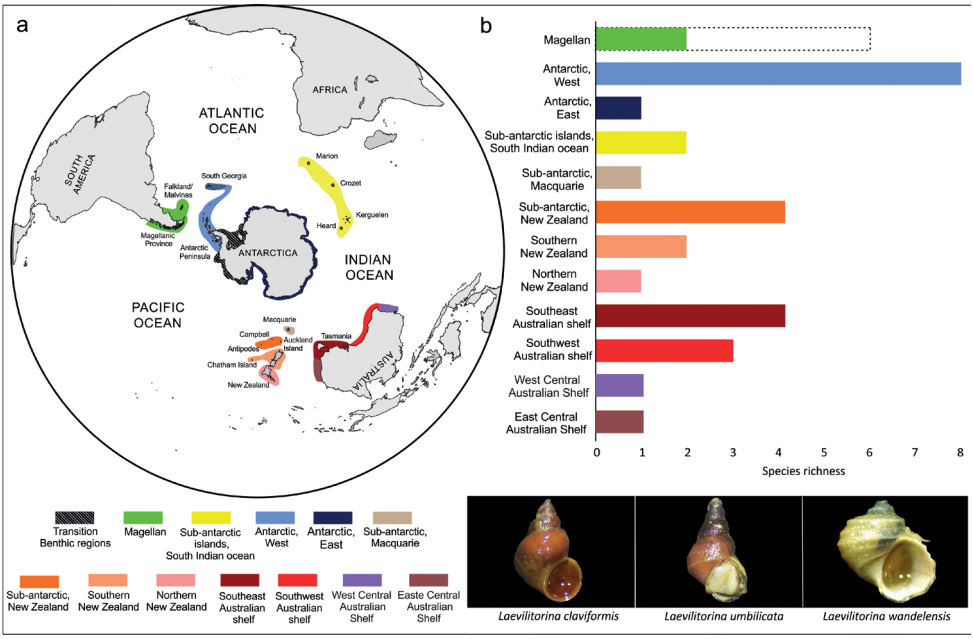

Figure 2. a Delimitation of Antarctic and Southern Ocean marine biogeographic provinces according to Spalding et al. (2007) and Koubbi et al. (2014) **b** Species richness of *Laevilitorina* in each of the biogeographical provinces. The dotted lines in the Magellan Province show the new richness value based on the revision of González-Wevar et al. (2022).

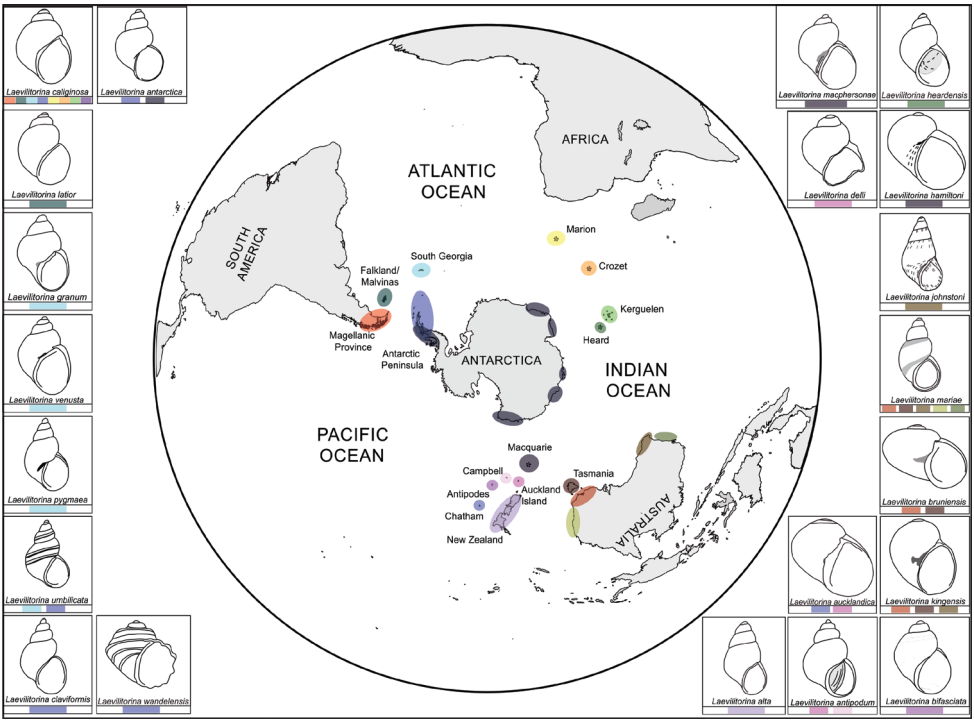

Figure 3. The distributions of the 21 different *Laevilitorina* species in the Southern Hemisphere. The colours below each panel indicate the geographic distribution of each species. Drawings of each species were made from holotypes or from illustrations made in published revisions (Gould 1849; Martens and Pfeffer 1886; Smith 1902; Lamy 1906; Suter 1913; Preston 1916; May 1924; Powell 1933; Powell 1940; Cotton 1945; Powell 1955; Dell 1964).

Only two species were recorded from the main New Zealand islands, *L. alta* (Powell, 1940) from North Island and *L. delli* from South Island. Three species were reported from Campbell, Antipodes and Auckland Islands, *L. aucklandica* (Powell, 1930), *L. bifasciata* Suter, 1913 and *L. antipodum* (Filhol 1880), none of which were shared with the North and South Islands of New Zealand (Fig. 3). In Australia, four species, *L. johnstoni* (Cotton, 1945), *L. mariae* (Tenison Woods, 1876), *L. bruniensis* (Beddome, 1883), and *L. kingensis* (May, 1924), were recorded from mainland Australia. *L. johnstoni* would be the only species restricted to mainland Australia, while *L. kingensis*, *L. mariae*, and *L. bruniensis* are also present in Tasmania (Fig. 3).

Based on our new sampling data only, we identified and reported seven *Laevilitorina* species in the Magellanic Province (*L. caliginosa*), Falkland/Malvinas Islands (*L. caliginosa*, *L. latior*), South Georgia (*L. caliginosa*, *L. pygmaea*, *L. venusta*; Fig. 1b, c), Kerguelen and Crozet Islands (*L. caliginosa*), South Orkney Islands (Signy Island) (*L. caliginosa*), and Antarctic Peninsula (*L. caliginosa*, *L. claviformis*, *L. umbilicata*, *L. wandelensis*; Fig. 1d–f), adding 43 new records to the previously available data. These new records are generally consistent with the existing literature and GBIF data,

with the exceptions of (i) new records of *L. caliginosa* on Horn and Diego Ramirez Islands, (ii) *L. umbilicata* on Avian Island, and (iii) *L. caliginosa* on Lagotellerie Island, the latter two being the southernmost records of both species.

Discussion

The increasing application of integrated taxonomy coupled with new modelling approaches, requires data to be Findable, Accessible, Interoperable, and Reusable in the long term (Wilkinson et al. 2016). There is a need to revise the geographic distribution and taxonomic description of many taxa, as it can provide information about changes in the composition of communities in different environments, particularly in sensitive ecosystems (Maturana et al. 2019). A number of studies have already discussed the importance of making an updated revision of the taxonomic status of several *Laevilitorina* species throughout their distribution (Powell 1960; Reid 1989; Engl 2012).

The compilation and unification of records of *Laevilitorina* in the Southern Hemisphere presented here contributes to improve our knowledge of the diversity and biogeography of the members of the genus in twelve biogeographic provinces of the Southern Hemisphere. However, it is also important to note that, despite the unification and update of records of *Laevilitorina*, this study does not reflect the full systematic and biogeographic complexity of this genus. Distribution data are not currently available for many members of the genus, which have not been reported since their description. For example, among the five species of *Laevilitorina* described from South Georgia, three of them (*L. pygmaea*, *L. venusta*, and *L. granum*) have not been reported since their original description (Castellanos 1989), leaving doubts about the taxonomic validity of these species (Castellanos 1989; Reid 1989; Engl 2012).

In this study, the report of *L. pygmaea* is only the third record of the species, in addition to being the first record from shallow depths thereby extending our knowledge of its bathymetric range. Previously, *L. pygmaea* had been reported between 252 and 310 m depth (Castellanos 1989). Similarly, the record of *L. venusta* is the first report of this species since its description by Martens and Pfeffer (1886). In general, the morphology of new *L. pygmaea* and *L. venusta* specimens corresponded well with the original descriptions. However, in our individuals of *L. pygmaea* the aperture was slightly higher than that described by Martens and Pfeffer (1886). This difference could be due to morphological plasticity within *L. pygmaea*, as it has been reported for other species of the genus (Reid 1989; Engl 2012). In the case of *L. venusta*, our specimens presented characteristics and measurements similar to those described by Martens and Pfeffer (1886), where the length of the opening of our specimens represented ~ 54% of the total height of the shell, the same as the measurements of the holotype of Martens and Pfeffer (1886). The morphology of *L. venusta* is quite similar to that of the widely distributed *L. caliginosa*, a species characterised by wide morphological plasticity throughout its distribution (see Engl 2012; González-Wevar et al. 2022). However, measurements of specimens of *L. caliginosa* from the Falkland/Malvinas Islands and

South Georgia show a longer and more expanded aperture than *L. venusta*, occupying between 58 and 67% of the total height of the shell (Castellanos 1989; Zelaya 2005). In this sense, it would be interesting in the future to carry out molecular studies with the species of South Georgia to corroborate the validity of the species described in that site. The recent study by González-Wevar et al. (2022) was able to detect only two lineages of *Laevilitorina* there: i) one that would correspond to *L. caliginosa* and ii) a second lineage that is also distributed in the Antarctic Peninsula and expands its distribution towards sub-Antarctic islands of the Indian Ocean like Marion, Crozet, and Kerguelen. The latter does not resemble any known South Georgian species and probably represents a new species (González-Wevar et al. 2022).

Taxonomic uncertainties within the genus *Laevilitorina* are related both to the morphological plasticity that exists in at least some species (Reid 1989; Engl 2012) and also to practical logistical challenges in accessing species' type localities and the level of geographical accuracy relating to some records. For example, the type locality of *L. caliginosa* (Gould (1849) is described as "Terra del Fuego", which covers a large and diverse area and could generate many ambiguities for researchers attempting to collect correctly identified individuals from this locality. Tierra del Fuego is one of the largest islands in southern South America and extends south and east of the Strait of Magellan between the Atlantic and Pacific Oceans. Gould's description was made using material collected during the "United States Exploring Expedition" carried out between 1838 and 1842 (Gould 1849). Fortunately, in the narrative of this expedition (Wilkes 1845; chapter VI, "Terra del Fuego") it is specified that the ship was in Orange Bay located in Hoste Island (see Wilkes 1845: 123) when this material was collected. Consequently, the type locality of *L. caliginosa* can be defined as Orange Bay in Hoste Island, and not the coastal area of Tierra del Fuego.

Historically, because of the complexity of obtaining material due to the wide distribution of *Laevilitorina*, taxonomic revisions have been restricted to certain geographic areas (e.g., Powell 1951, 1957; Dell 1964; Arnaud and Bandel 1976; Zelaya 2005; Engl 2012). The most complete review published to date was by Reid (1989), where he analysed material from Antarctica (*L. antarctica*), sub-Antarctic Islands (*L. caliginosa* and *L. hamiltoni*), New Zealand (*L. alta*), and Australia (*L. bruniensis* and *L. mariae*). This represents a very low percentage of the diversity of the entire genus. In addition, some of the described species present morphological similarities, which makes identification more complex (Reid 1989) and therefore caution must be exercised with some historical records. Fortunately, several of the described species have material deposited in museums (e.g., ALA 2022), which would allow a more extensive revision of the group. Therefore, a systematic revision of *Laevilitorina* is currently very relevant to understand better the current status of this genus, its richness and distribution in the Southern Hemisphere.

Laevilitorina is one of the most widely distributed genera of marine gastropods at high latitudes in the Southern Hemisphere (Reid 1989; this study). The 21 species of *Laevilitorina* have different distribution patterns (Fig. 3). For example, seven of the 21 *Laevilitorina* species reported in this study have different distribution ranges (*L. caliginosa*, *L. latior*, *L. pygmaea*, *L. venusta*, *L. claviformis*, *L. umbilicata*,

L. wandelensis) (Fig. 4b). *Laevilitorina latior* has been reported exclusively from the Falkland/Malvinas Islands (Preston 1912), *L. claviformis* and *L. wandelensis* exclusively from Antarctic Peninsula (Reid 1989; Engl 2012), and *L. venusta* only from South Georgia (Castellanos 1989; Zelaya 2005). *Laevilitorina umbilicata* and *L. pygmaea* have wider distribution ranges, including both South Georgia and the Antarctic Peninsula (Zelaya 2005; Engl 2012). *Laevilitorina caliginosa* has by far the widest distribution, being recorded in four Southern Ocean biogeographic provinces (i.e., Magellan, West Antarctica, Indian Ocean sub-Antarctic, and Macquarie Island). Nevertheless, as previously stated, the taxonomy within this taxon is much more complex than previously thought (González-Wevar et al. 2022).

The majority of *Laevilitorina* species inhabit shallow rocky coasts and may be associated with different species of macroalgae (Simpson 1972; Reid 1989; Amsler et al. 2015; Rosenfeld et al. 2017). Another important characteristic of this genus is the absence of pelagic larva: the female deposits egg masses on rocks or macroalgae from which the juvenile subsequently hatches (Picken 1979; Simpson and Harrington 1985) (Fig. 4a). In the literature, this type of benthic protected development is often assumed to be associated with restricted dispersal capability and hence narrow geographic range (Simpson and Harrington 1985; Barroso et al. 2022), a feature of the majority of *Laevilitorina* species (Fig. 4b). On the basis of reproductive strategy, the wide distribution of *L. caliginosa* is paradoxical and exceptional within the genus (Reid 1989; Griffiths and Waller 2016) (Fig. 4b). Some authors (Griffiths and Waller 2016; González-Wevar et al. 2022) have suggested that dispersal associated with dislodged rafts of the seaweed *Durvillaea antarctica* Hariot, 1882 may have facilitated the species' wider establishment, since both species co-occur across most of their distribution ranges. However, a recent phylogenetic study of *L. caliginosa* evidenced that this taxon does not correspond to a widely distributed species, but rather to multiple divergent lineages distributed along the SO (González-Wevar et al. 2022). In fact, phylogenetic reconstructions recognised the presence of at least seven *Laevilitorina* lineages within the nominal taxon *L. caliginosa*. Of these, six species are endemic to the Magellan Province and most of them are new to science (González-Wevar et al. 2022). Just one "caliginosa" lineage has a broad distribution that includes the Antarctic Peninsula, South Georgia and sub-Antarctic islands of the Indian Ocean (Marion, Crozet, and Kerguelen islands) (González-Wevar et al. 2022). Hence, the taxonomy of *Laevilitorina* is still unsettled and requires a detailed revision. Previously the Magellan province was considered as a species-poor area for *Laevilitorina*, in fact it represents an area where the genus diversified over the last 30 million years (González-Wevar et al. 2022).

This study shows a detailed review of the records, distribution and richness patterns of the genus *Laevilitorina* throughout its range. However, more research and sampling effort is still needed to "recover" and confirm many of the *Laevilitorina* species that are present throughout the sub-Antarctic Islands. In addition, based on the results of González-Wevar et al. (2022) and this work, we conclude that it is important to continue investigating this genus because: i) the recent discovery of new lineages in the Magellan province highlights the need for a thorough taxonomic

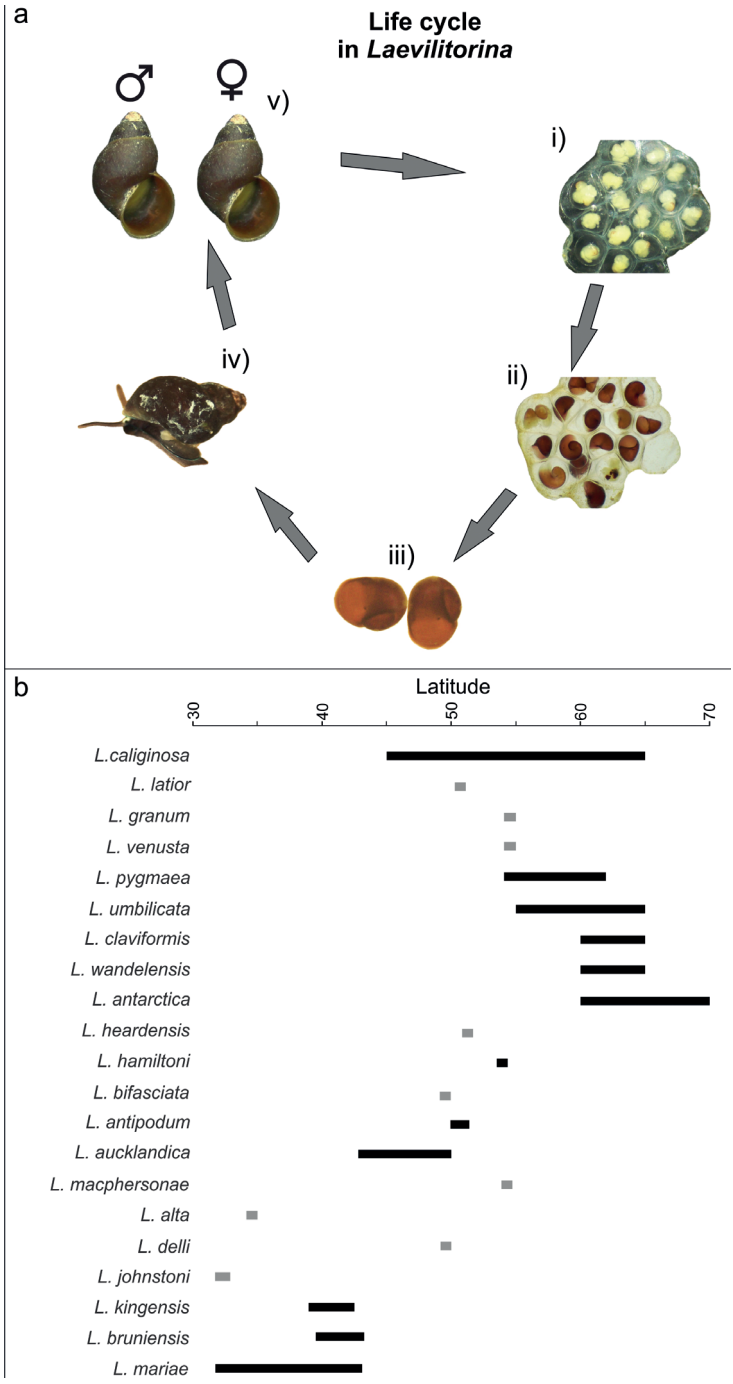

Figure 4. a Life cycle of members of the genus *Laevilitorina* without a planktotrophic larval stage, i) general view of the egg mass with early-stage embryos, ii) late-stage embryos, iii) recently hatched juveniles, iv) developing adult, and v) male and female of the genus (photographs S. Rosenfeld) **b** Latitudinal distribution of *Laevilitorina* species in the Southern Hemisphere, grey bars indicate presence in a single geographic area or island.

revision of *Laevilitorina* species and improved estimate of the genus diversity, and ii) the marked endemism of some species along with differences in species richness across the Southern Hemisphere marine provinces suggest contrasting biogeographical patterns of importance for conservation issues and evolutionary studies. Finally, these differences raise further questions about the underlying processes and mechanisms associated with the evolution of this genus in the Southern Hemisphere.

Acknowledgements

This work was funded by, ANID-Millennium Science Initiative Program ICN2021_002 to SR, CM, PC, EP, and CGW, Fondecyt Regular Project 1210787 to CGW and SR, and ANID/BASAL FB210018 to SR and CM. We also appreciate the support of the following projects: Fondecyt Postdoctoral 3210063 to CM, IPEV program PROTEKER (#1044). We are grateful to the Government of South Georgia & South Sandwich Islands (GSGSSI), South Atlantic Environmental Research Institute (SAERI), Natural History Museum (NHM) London, the Shallow Marine Surveys Group (SMSG) for organising the research cruise (Operation *Himantothallus* – Darwin Plus Marine Biodiversity Research Cruise, *Pharos SG*-11-2021), and Tritonia Scientific Ltd for diving operations and dive safety. The research cruise was funded by GSGSSI and a Darwin Plus Grant (DPLUS122) to the NHM. We also are grateful to the officers and crew of the *Pharos SG* for their professionalism and support. S.R. gives particular thanks to the Chilean Navy, the Commander in Chief of the III Naval Zone, Rear Admiral Ivo Brito, the Chief of General Staff, Vice Admiral José Miguel Rivera, the National Oceanographic Committee, and the Naval Beagle Command, as well as the crew of the ship OPV 83 Marinero Fuentealba, and the helicopter and institutional logistics personnel. We also thank Roy Mackenzie and the staff of the lighthouse of Gonzalo Island for their invaluable support for the development of field research at the permanent ecological studies site implemented in the Diego Ramírez archipelago and Hornos Island. We especially thank Lafayette Eaton for English revision and editing and to the Subject editor Frank Köhler and two anonymous reviewers for their helpful comments.

References

Amsler MO, Huang I, Engl W, McClintock JB, Amsler CD (2015) Abundance and diversity of gastropods associated with dominant subtidal macroalgae from the western Antarctic Peninsula. Polar Biology 38(8): 1171–1181. https://doi.org/10.1007/s00300-015-1681-4

Ariño AH (2010) Approaches to estimating the universe of natural history collections data. Biodiversity Informatics 7(2): 81–92. https://doi.org/10.17161/bi.v7i2.3991

Arnaud P, Bandel K (1976) Comments on six species of marine Antarctic Littorinacea (Mollusca, Gastropoda). THETYS 8(3): 213–230.

ALA (2022) Atlas of Living Australia. https://bie.ala.org.au/search?q=Laevilitorina [Acceded 12 September 2022]

Barroso C, Lotufo T, Matos A, Carneiro P, Matthews-Cascon H (2022) The distribution of marine gastropods is more influenced by larval development than by adult characteristics. Marine Biology 169(6): e83. https://doi.org/10.1007/s00227-022-04069-0

Beck J, Ballesteros-Mejia L, Nagel P, Kitching I (2013) Online solutions and the 'Wallacean shortfall': What does GBIF contribute to our knowledge of species' ranges? Diversity & Distributions 19(8): 1043–1050. https://doi.org/10.1111/ddi.12083

Belbin L (2011) The Atlas of Livings Australia's Spatial Portal. In: Jones M, Gries C (Eds) Proceedings of the Environmental Information Management Conference, Santa Barbara, 39–43.

Bosso L, Smeraldo S, Russo D, Chiusano ML, Bertorelle G, Johannesson K, Butlin RK, Danovaro R, Raffini F (2022) The rise and fall of an alien: Why the successful colonizer Littorina saxatilis failed to invade the Mediterranean Sea. Biological Invasions 24(10): 3169–3187. https://doi.org/10.1007/s10530-022-02838-y

Bouchet P, Rocroi J, Hausdorf B, Kaim A, Kano Y, Nützel A, Parkhaev P, Schrödl M, Strong E (2017) Revised classification, nomenclator and typification of gastropod and monoplacophoran families. Malacologia 61(1–2): 1–526. https://doi.org/10.4002/040.061.0201

Castellanos ZA (1989) Catálogo descriptivo de la malacofauna marina Magallánica 4. Mesogastropoda. Comisión de Investigaciones Científicas, Provincia de Buenos Aires, 44 pp.

Cotton BC (1945) Southern Australian Gastropoda. Part 1. Streptoneura. Transactions of the Royal Society of South Australia 69(1): 150–171.

Dell RK (1964) Marine Mollusca from Macquarie and Heard Islands. Record of the Dominion Museum Wellington 267–301.

Dell RK (1990) Antarctic Mollusca with special reference to the fauna of the Ross Sea. Bulletin - Royal Society of New Zealand 27: 1–311.

Engl W (2012) Shells of Antarctica. ConchBooks, Hackenheim, 402 pp.

Estevez D, Galindo J, Rolan-Alvarez E (2021) Negative frequency-dependent selection maintains shell banding polymorphisms in two marine snails (*Littorina fabalis* and *Littorina saxatilis*). Ecology and Evolution 11(11): 6381–6390. https://doi.org/10.1002/ece3.7489

Flemons P, Guralnick R, Krieger J, Ranipeta A, Neufeld D (2007) A web-based GIS tool for exploring the world's biodiversity: The Global Biodiversity Information Facility Mapping and Analysis Portal Application (GBIF-MAPA). Ecological Informatics 2(1): 49–60. https://doi.org/10.1016/j.ecoinf.2007.03.004

González-Wevar CA, Segovia NI, Rosenfeld S, Maturana CS, Jeldres V, Pinochet R, Saucède T, Morley SA, Brickle P, Wilson NG, Spencer HG, Poulin E (2022) Seven snail species hidden in one: Biogeographic diversity in an apparently widespread periwinkle in the Southern Ocean. Journal of Biogeography 49(8): 1521–1534. https://doi.org/10.1111/jbi.14453

Gould AA (1849) Descriptions of new species of shells, brought home by the U. S. Exploring Expedition. Proceedings of the Boston Society of Natural History 3: 83–85.

Griffiths HJ, Waller C (2016) The first comprehensive description of the biodiversity and biogeography of Antarctic and sub-Antarctic intertidal communities. Journal of Biogeography 43(6): 1143–1155. https://doi.org/10.1111/jbi.12708

Kess T, Galindo J, Boulding EG (2018) Genomic divergence between Spanish *Littorina saxatilis* ecotypes unravels limited admixture and extensive parallelism associated with population history. Ecology and Evolution 8(16): 8311–8327. https://doi.org/10.1002/ece3.4304

Koubbi P, De Broyer C, Griffiths HJ, Raymond B, d'Udekem d'Acoz C, Van de Putte AP, Danis B, David B, Grant S, Gutt J, Held C, Hosie G, Huettmann F, Post A, Ropert-Coudert Y, Stoddart M, Swadling KM, Wadley V (2014) Conclusions: present and future of Southern Ocean biogeography. In: De Broyer C, Koubbi P, Griffiths HJ, Raymond B, Udekem d'Acoz C, Van de Putte AP, Danis B, David B, Grant S, Gutt J, Held C, Hosie G, Huettmann F, Post A, Ropert-Coudert Y (Eds) Biogeographic atlas of the Southern Ocean. Sicentific Committee on Antarctic Research, Cambridge, 470–475.

Lamy E (1906) Gastropodes Prosobranches et Pélécypodes. Expédition Antarctique Française (1903–05), Sciences Naturelles, Paris, 20 pp.

Martens E, Pfeffer G (1886) Die Mollusken von Süd–Georgien nach der Ausbeute der Deutschen Station 1882–83. Jahrbuch der Hamburgischen Wissenschaftlichen Anstalten 3: 65–135. https://doi.org/10.5962/bhl.title.12280

Maturana C, Rosenfeld S, Naretto J, Convey P, Poulin E (2019) Distribution of the genus *Boeckella* (Crustacea, Copepoda, Calanoida, Centropagidae) at high latitudes in South America and the main Antarctic biogeographic regions. ZooKeys 854: 1–15. https://doi.org/10.3897/zooke ys.854.29614

May WL (1924) Mollusca of King Island With description of five new species. Papers and Proceedings of the Royal Society of Tasmania 1923: 47–55.

MolluscaBase [Eds] (2022) MolluscaBase. *Laevilitorina* Pfeffer, 1886. World Register of Marine Species. https://www.marinespecies.org/aphia.php?p=taxdetails&id=196959 [on 2022-06-22]

OBIS (2022) Ocean Biogeographic Information System. Census of Marine Life. http://iobis.org/

Picken GB (1979) Non-pelagic reproduction of some Antarctic prosobranch gastropods from Signy Island, South Orkney Islands. Malacologia 19(1): 109–128.

Powell AWB (1933) New species of marine Mollusca from the subantarctic islands of New Zealand. Proceedings of the Malacological Society of London 20(5): 232–236. https://doi.org/10.1093/oxfordjournals.mollus.a064194

Powell AWB (1940) The marine Mollusca of the Auporian Province, New Zeland. Transactions of the Royal Society of New Zealand 70: 205–248.

Powell AWB (1951) Antarctic and Subantarctic Mollusca: Pelecypoda and Gastropoda. Discovery Reports 26: 47–196. https://doi.org/10.5962/bhl.part.16335

Powell AWB (1955) Mollusca of the southern islands of New Zealand. Department of Scientific and Industrial Research Cape Expedition Series Bulletin 15: 1–151. [5 pl]

Powell AWB (1957) Mollusca of Kerguelen and Macquarie Islands. B. A. N. Z. Antarctic Research Expedition, 1929–1931. Report B 6: 107–149.

Powell AWB (1960) Antarctic and Subantarctic Mollusca (catalogue). Records of the Auckland Institute and Museum 5(3–4): 117–193.

Preston HB (1912) Characters of six new pelecypods and two new gastropods from the Falkland Islands. Annals and Magazine of Natural History 9(8): 636–640 https://doi.org/10.1080/00222931208693180

Preston HB (1916) Descriptions of eight new species of marine Mollusca from the South Shetland Islands. Annals and Magazine of Natural History 18(8): 269–272. https://doi.org/10.1080/00222931608693847

Reid DG (1989) The comparative morphology, phylogeny, and evolution of the gastropod family Littorinidae. Littorinidae Philosophical Transactions of the Royal Society of London B 324: 1–110. https://doi.org/10.1098/rstb.1989.0040

Reid DG (2007) The genus *Echinolittorina* Habe, 1956 (Gastropoda: Littorinidae) in the Indo-West Pacific Ocean. Zootaxa 1420(1): 1–161. https://doi.org/10.11646/zootaxa.1420.1.1

Reid DG, Williams ST (2004) The subfamily Littorininae (Gastropoda: Littorinidae) in the temperate Southern Hemisphere: the genera *Nodilittorina*, *Austrolittorina* and *Afrolittorina*. Records of the Australian Museum 56(1): 75–122. https://doi.org/10.3853/j.0067-1975.56.2004.1393

Reid DG, Williams ST (2012) A global molecular phylogeny of 147 periwinkle species (Gastropoda, Littorininae). Zoologica Scripta 41(2): 125–136. https://doi.org/10.1111/j.1463-6409.2011.00505.x

Rosenfeld S, Aldea C, Ojeda J, Marambio J, Hüne M, Troncoso J, Mansilla A (2017) Molluscan assemblages associated with *Gigartina* beds in the Strait of Magellan and the South Shetland Islands (Antarctica): A comparison of composition and abundance. Polar Research 36(1): 1–10. https://doi.org/10.1080/17518369.2017.1297915

Rosenfeld S, Maturana C, González Wevar C, Poulin E, Gérard K, Naretto J, Ojeda J, Lopez Z, Brickle P, Saucède T, Kraft S, Aldea C (2022) Distribution and Occurrences of Laevilitorina across the Southern Hemisphere. Instituto de Biodiversidad de Ecosistemas Antárticos y Subantárticos (BASE). Occurrence dataset. https://doi.org/10.15468/dsacsj [accessed via GBIF.org on 2022-10-11]

Simpson R (1972) The ecology and biology of molluscs in the littoral and sublittoral zones at Macquarie Island, with special reference to Patinigera macquariensis (Finlay, 1927). Thesis presented for the Degree of Doctor of Philosophy. University of Adelaide.

Simpson RD, Harrington SA (1985) Egg masses of three gastropods, *Kerguelenella lateralis* (Siphonariidae), *Laevilitorina caliginosa* and *Macquariella hamiltoni* (Littorinidae), from Macquarie Island (sub- Antarctic). Journal of the Malacological Society of Australia 7(1–2): 17–28. https://doi.org/10.1080/00852988.1985.10673973

Smith EA (1902) Mollusca. In: Lankester ER, Bell J (Eds) Report on the collections of natural history made in Antarctic regions during the voyage of the Southern Cross. British Museum (Natural History), London, 201–213.

Spalding MD, Fox HE, Allen GR, Davidson N, Ferdaña ZA, Finlayson M, Halpern BS, Jorge MA, Lombana A, Lourie SA, Martin KD, Mcmanus E, Molnar J, Recchia CA, Robertson J (2007) Marine ecoregions of the world: A bioregionalization of coastal and shelf areas. Bioscience 57(7): 573–583. https://doi.org/10.1641/B570707

Suter H (1913) Manual of the New Zealand Mollusca with an atlas of quarto plates. Wellington, [xxiii +] 1120 pp. [(1913) and Atlas pls 1–72 (1915)] https://doi.org/10.5962/bhl.title.1716

Warén A, Hain S (1996) Description of Zerotulidae fam. Nov. (Littorinoidea), with comments on an Antarctic Littorinid Gastropod. The Veliger 39(4): 277–334.

Wieczorek J, Guo Q, Hijmans R (2004) The point-radius method for georeferencing locality descriptions and calculating associated uncertainty. International Journal of Geographical Information Science 18(8): 745–767. https://doi.org/10.1080/13658810412331280211

Wieczorek C, Wieczorek J (2021) Georeferencing Calculator. http://georeferencing.org/georef-calculator/gc.html [Accessed 10 March 2022]

Wieczorek J, Bloom D, Guralnick R, Blum S, Döring M, Giovanni R, Robertson T, Vieglais D (2012) Darwin Core: An evolving community-developed biodiversity data standard. PLoS ONE 7(1): e29715. https://doi.org/10.1371/journal.pone.0029715

Wilkes C (1845) Narrative of the United States Exploring Expedition. During the years 1838, 1839, 1840, 1841, 1842. Lea and Blanchard, Philadelphia, 1845. https://doi.org/10.5962/bhl.title.61621

Wilkinson M, Dumontier M, Aalbersberg IJ, Appleton G, Axton M, Baak A, Blomberg N, Boiten J, da Silva Santos LB, Bourne P, Bouwman J, Brookes A, Clark T, Crosas M, Dillo I, Dumon O, Edmunds S, Evelo C, Finkers R, Gonzalez-Beltran A, Gray AG, Groth P, Goble C, Grethe J, Heringa J, 't Hoen PC, Hooft R, Kuhn T, Kok R, Kok J, Lusher S, Martone M, Mons A, Packer A, Persson B, Rocca-Serra P, Roos M, van Schaik R, Sansone S, Schultes E, Sengstag T, Slater T, Strawn G, Swertz M, Thompson M, van der Lei J, van Mulligen E, Velterop J, Waagmeester A, Wittenburg P, Wolstencroft K, Zhao J, Mons B (2016) The FAIR Guiding Principles for scientific data management and stewardship. Scientific Data 3(1): e160018. https://doi.org/10.1038/sdata.2016.18

Williams ST, Reid DG, Littlewood DTJ (2003) A molecular phylogeny of the Littorininae (Gastropoda: Littorinidae): unequal evolutionary rates, morphological parallelism, and biogeography of the Southern Ocean. Molecular Phylogenetics and Evolution 28(1): 60–86. https://doi.org/10.1016/S1055-7903(03)00038-1

Zelaya DG (2005) Systematics and biogeography of marine gastropods molluscs from South Georgia. Spixiana 28(2): 109–139.

ZooKeys 1127: 79–90 (2022)
doi: 10.3897/zookeys.1127.83240
https://zookeys.pensoft.net

RESEARCH ARTICLE

A peer-reviewed open-access journal
ZooKeys
Launched to accelerate biodiversity research

Taxonomic note on the species status of *Epiophlebia diana* (Insecta, Odonata, Epiophlebiidae), including remarks on biogeography and possible species distribution

Sebastian Büsse[1], Jessica L. Ware[2]

1 *Functional Morphology and Biomechanics, Institute of Zoology, Kiel University, Am Botanischen Garten 9, 24118 Kiel, Germany* **2** *Division of Invertebrate Zoology, American Museum of Natural History, 200 Central Park West, New York, NY 10024, USA*

Corresponding author: Sebastian Büsse (sbuesse@zoologie.uni-kiel.de)

Academic editor: Jan van Tol | Received 7 March 2022 | Accepted 24 August 2022 | Published 2 November 2022

https://zoobank.org/7B4F73BA-EDC7-4CC0-9D91-4C236678AED8

Citation: Büsse S, Ware JL (2022) Taxonomic note on the species status of *Epiophlebia diana* (Insecta, Odonata, Epiophlebiidae), including remarks on biogeography and possible species distribution. ZooKeys 1127: 79–90. https://doi.org/10.3897/zookeys.1127.83240

Abstract

The species included in the genus *Epiophlebia* Calvert, 1903 represent an exception within Recent lineages – they do not belong to either dragonflies (Anisoptera) nor damselflies (Zygoptera). Nowadays, the genus is solely known from the Asian continent. Due to their stenoecious lifestyle, representatives of *Epiophlebia* are found in often very small relict populations in Nepal, Bhutan, India, Vietnam, China, North Korea, and Japan. We here present a taxonomic re-evaluation on the species status of *Epiophlebia diana* Carle, 2012, known from the Sichuan province in China, supplemented with a morphological character mapping on a genetic tree to highlight synapomorphies of *E. diana* and *E. laidlawi* Tillyard, 1921. We conclude that *E. diana* is a junior synonym of *E. laidlawi*. Furthermore, we discuss the Recent distribution of the group, allowing for predictions of new habitats of representatives of this group.

Keywords

Anisozygoptera, *Epiophlebia laidlawi*, *E. sinensis*, *E. superstes*, genetic sequences, relict dragonfly, synonymy

Introduction

Odonata Fabricius, 1793 are classified into the suborders Anisoptera Sélys, 1854 (dragonflies), Zygoptera Sélys, 1854 (damselflies), and the enigmatic taxon, *Epiophlebia* Calvert, 1903. Presently, the genus *Epiophlebia* is considered to be the sister-group of the Anisoptera [Anisoptera + *Epiophlebia* = Epiprocta Lohmann, 1996], with several extinct lineages nested in between (cf. Bechly 1996; Lohmann 1996; Rehn 2003; Fleck et al. 2003; Grimaldi and Engel 2005); the validity of Epiprocta is supported by numerous phylogenetic studies (cf. Hovmöller et al. 2002; Fleck et al. 2008; Bybee et al. 2008, 2021; Blanke et al. 2012, 2013; Misof et al. 2014; Letsch et al. 2016; Büsse et al. 2018; Kohli et al. 2021; Suarov et al. 2021). These taxa were considered to form a suborder, called "Anisozygoptera", which comprise mainly Jurassic fossils (Nel 1993) and the recent species of the genus *Epiophlebia*, until it was shown that "Anisozygoptera" are polyphyletic (Nel 1993; Lohmann 1996; Rehn 2003). Because the species of the genus *Epiophlebia* show some distinct characters of Zygoptera as well as Anisoptera (Asahina 1954; Büsse 2016), they are often considered as relict species (Asahina 1954; Davies 1992; Mahato 1993). From a morphological point of view, the genus *Epiophlebia* seems to represent the most ancestral character distribution of Recent Odonata (Blanke et al. 2012, 2015; Büsse et al. 2015; Büsse 2016).

Adult *Epiophlebia* are very conspicuous (Fig. 1), and in the field they can easily be identified by the black-yellow striped coloration (Asahina 1954) and their characteristic slow and rather uncoordinated appearing undulating flight (Rüppell and Hilfert 1993). Morphologically, the anisopterous body shape, the zygopterous shape of the wings, and the convex frons are some of the main distinguishing characteristics (Asahina 1954; Büsse 2016). The larvae of *Epiophlebia* also resemble dragonflies, as they use a rectal chamber for respiration, but jet propulsion, which is typical for Anisoptera (Corbet 1999), has never been observed (Tabaru 1984). Their morphological distinction is rather subtle, so they are easily mixed up with, for example, gomphids or petalurids (Asahina 1954) – as happened to *Epiophlebia diana* Carle, 2012. The type specimens of *E. diana* were collected by "Dr. David C. Graham in the mountainous regions of western Szechuan" (Needham 1930). Needham however, misidentified the larvae of *Epiophlebia* as Gomphidae (Carle 2012).

While the ancestors of present *Epiophlebia* species were at their peak in the Mesozoic era and were possibly distributed over large areas on the pre-Asian continent (Carpenter 1992; Nel et al.1993), recent species have restricted ranges, often confined to small areas in Asia: *Epiophlebia superstes* Selys, 1889 in Japan; *Epiophlebia laidlawi* Tillyard, 1921 in Nepal, India, Bhutan, and Vietnam; *Epiophlebia sinensis* Li & Nel, 2012 in North Korea and China, and *Epiophlebia diana* also in China (Asahina 1954; 1963; Tani and Miyatake 1979; Büsse et al. 2012; Carle 2012; Li et al. 2012; Fleck et al. 2013; Büsse 2016) showing a characteristic disjunct distribution (Büsse et al. 2012).

Since the habitat requirements of the genus *Epiophlebia* seem to be very specific, the range of Recent habitats is extremely restricted. *Epiophlebia* species prefer cold mountain streams with temperatures of about 4 to 5 °C in winter and about 16–17 °C in summer (data published for *E. superstes* by Tabaru (1984)) and altitudes between 1,300 to approximately 3,000 m (data published for *E. laidlawi* by Brockhaus and

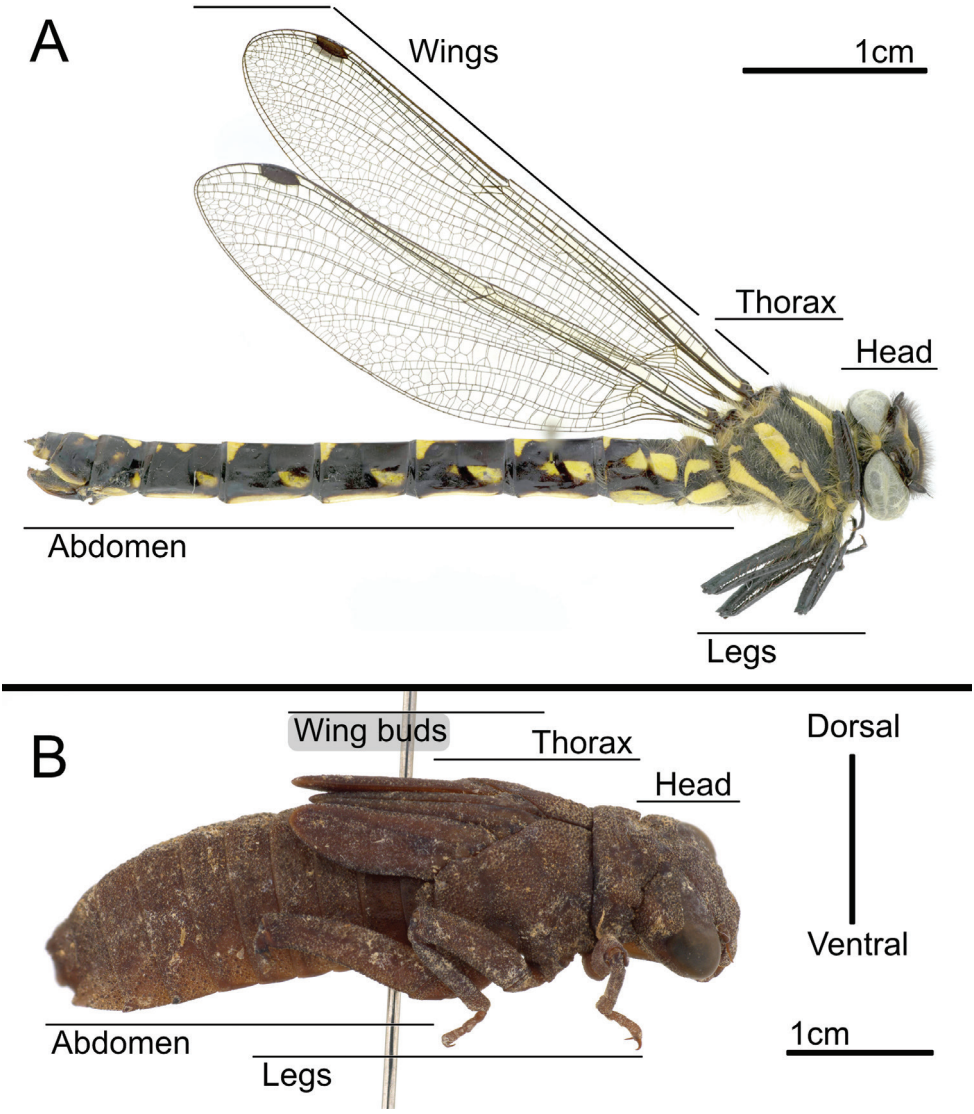

Figure 1. *Epiophlebia superstes* from Japan, lateral view **A** adult **B** larva.

Hartmann (2009)). This stenoecious lifestyle has restricted the genus *Epiophlebia* to cold habitats, like glacial refuges (De Lattin 1967; Büsse et al. 2012).

For recently diverged species, or for taxa that are described under the assumption of incipient speciation, it can be challenging to develop a morphological character set that reveals the true pattern of evolutionary history for a taxon. Further complicating matters is that there are often separate, not cross-referenced, descriptions of adults and larvae for Odonata. In the case of the genus *Epiophlebia*, adults and larvae are described for *E. superstes* and *E. laidlawi*, while for *E. sinensis* only the adults and for *E. diana* only the larva is known. The species status of *E. diana* has already been critically discussed and

is doubtful (cf. Dijkstra et al. 2013; Büsse 2016). We, therefore, present a taxonomic re-evaluation of the species status of *E. diana*. Unfortunately, the type specimen is untraceable and seems lost (F.L. Carle, author of *E. diana* as well as J.J. Dombroskie of the Cornell University Insect Collection, New York, USA: personal communication, see Büsse 2016). However, a combination of morphology, phylogeny, and biogeography, described here, lays a solid basis for the designation of *E. diana* as junior synonym of *E. laidlawi*.

Materials and methods

Here, we examined morphological data from Büsse (2016) and several other publications (i.e., Asahina 1954, 1961; Büsse et al. 2012; Carle 2012; Li et al. 2012; Dorji 2015). A matrix composed of all characters used in the past to evaluate *Epiophlebia* larval and adult characters is shown in Table 1; briefly this includes larval traits and adult characters related to size and colouration, features of the head, abdomen, genitalia, and appendages. The phylogeny that was used here was based on Büsse et al. (2012; fig. 2). The main justification for using Büsse's and colleagues (2012) phylogeny is that presently there are few overlapping sequence fragments across the species of *Epiophlebia*. Here, we examined all available mitochondrial and nuclear gene fragments for the genus *Epiophlebia* from GenBank to evaluate what available data was present for the genus (Table 2). Unfortunately, to date *E. superstes* is the only species for which sequence data are available for a broad sampling of genes. No genetic data is available for *E. diana*, presumably because the describing author has misplaced the existing specimens (F.L. Carle personal communication). With such a dataset, we decided to use the phylogeny provided by Büsse et al. (2012) which is the most comprehensively sampled phylogeny for the genus currently available. In terms of character mapping, briefly, characters were traced in Mesquite (Maddison and Maddison 2016) using both the ancestral state reconstruction parsimony and likelihood functions. Consistency index values for a matrix including all traits in Table 1 were evaluated in Mesquite against a tree assuming (*E. sinensis* (*E. superstes* (*E. diana*, *E. laidlawi*))) and found to be 1.0.

For photography, we used specimens of *E. superstes* (because of availability) to depict the general habitus of the very similar *Epiophlebia* species. For stacked photography, a custom-made 3D-printed illumination dome system (Bäumler et al. 2020) and an Olympus OMD 10mkII digital camera (Olympus K.K., Tokyo, Japan), equipped with a Leica 45 mm macro lens (Leica Camera AG, Wetzlar, Germany) was used. All images were subsequently processed in Affinity Photo and Affinity Designer (Serif Ltd, Nottingham, United Kingdom).

Results and discussion

Taxonomy

A comparison of the morphological characters used in past studies to the currently accepted phylogeny of the genus *Epiophlebia* suggests that several characters are not

Table 1. Morphological matrix for larvae and adults for key differences between *Epiophlebia* species (character states).

	Character	*E. superstes*	*E. laidlawi*	*E. diana*	*E. sinensis*
Larvae					
1	General colouration: 0 = darker, 1 = lighter (Büsse 2016), (Carle 2012), (Dorji 2015)	0	1	1	?
2	Scape and pedicle: 0 = scape and pedicle same length as flagellomere or shorter 1 = scape and pedicle always longer than first flagellomere (Büsse 2016), Carle 2012	0	{01}	1	?
3	Flagellomere: 0 = maximally as long as the 2nd and 3rd together or shorter, 1 = first longer than the 2nd and 3rd together (Büsse 2016), Carle 2012	0	1	1	?
4	Premental cleft: 0 = not distinctly developed, 1 = distinctly developed (Büsse 2016), Carle 2012	0	1	1	?
5	Spearhead-like processes on notum: 0 = not so, 1 = depressed posterolaterally (Büsse 2016)	0	1	?	?
6	Anterior ridge of the metathoracic post sternum: 0 = shallow, 1 = deep, cone like (Büsse 2016)	1	0	?	?
7	Abdominal stridulatory file of segment 7: 0 = well developed, 1 = vestigial on segment 3 (Büsse 2016), Carle 2012	0	[01}	1	?
8	Dorso-lateral edges abdominal segments 7–9: 0 = protruding and pointed, 1 = rounded (Büsse 2016), Carle 2012	0	1	1	?
9	Lateral abdominal lobes on segment 9: 0 = not very sinuous margins, not much protruding by lobes on segment 9, 1 = sinuous margins, lobes protrude on segment 9 (Büsse 2016), Carle 2012	0	1	1	?
10	Apices of the epiproct: 0 = divided distinctly, 1 = divided slightly (Büsse 2016)	1	0	?	?
Adult					
11	Adult abdomen colour: 0 = blackish with more yellow markings; 1 = brownish with less yellow markings (Asahina 1954; 1961) (Büsse 2016), (Dorji 2015) (Li et al., 2012)	0	1	?	0
12	Adult abdomen segments 2–7with yellow spot on posterior margins: 0 = no, 1 = yes (Asahina 1954; 1961) (Li et al., 2012)	0	1	?	0
13	Adult thorax with 2 narrow yellow lateral stripes: 0 = no, 1 = yes (Asahina 1954; 1961) (Li et al., 2012)	0	1	?	0
14	Forewing and Hindwing light yellow brownish: 0 = hyaline, 1 = light yellow brownish wings (Asahina 1954; 1961) (Li et al., 2012)	0	1	?	0
15	Abdomen with dorsal stripes: 0 = no, 1 = yes, (Asahina 1954; 1961) (Li et al., 2012)	1	0	?	1
16	Abdomen segment 10: 0 = mainly black with yellow lateral spots, 1 = not so (Asahina 1954; 1961) (Li et al., 2012)	1	0	?	1

Table 2. Available mitochondrial and nuclear gene fragments for *Epiophlebia* species in GenBank.

	COI	**COII**	**12S & 16S**	**Complete mitochondrial genome**	**18S & 28S**	**Elongation Factor alpha**	**Opsin fragments**	**Histone 3**	**ITS1 & ITS2**
Epiophlebia diana	–	–	–	–	–	–	–	–	
Epiophlebia laidlawi	–	2 sequences	–	–	6 sequences	–	–	–	3 sequences
Epiophlebia sinensis	–	–	–	–	–	–	–	–	2 sequences
Epiophlebia superstes	19 sequences	1 sequence	23 sequences	2 sequences	24 sequences	1 sequence	24 sequences	1 sequence	2 sequences

useful for reconstruction of the evolutionary history, as they are only known for adults of all species except *E. diana*, or only known for larvae of all species except *E. sinensis*. Using parsimony, we found 10 characters supporting a clade comprising *E. laidlawi* and *E. diana* (Fig. 2), but as five of those characters are based on adult traits, there are missing data for *E. diana*. Furthermore, for several distinguishing characters employed by Carle

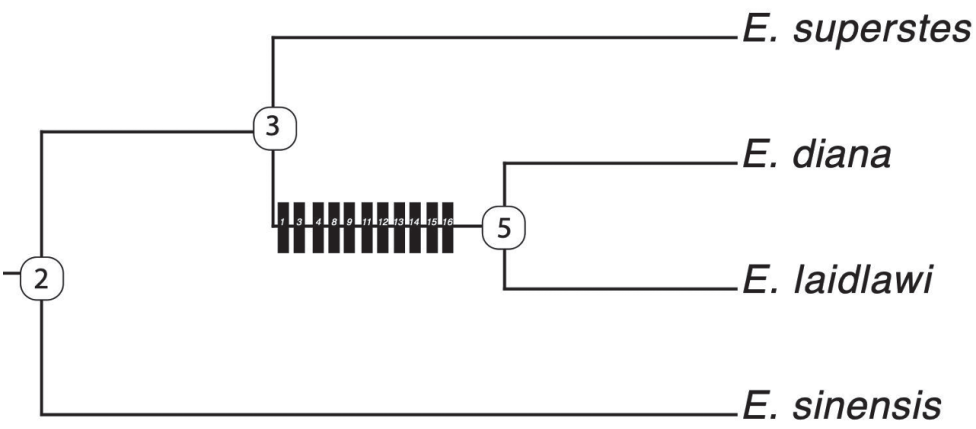

Figure 2. Character mapping on a strict consensus tree based on Büsse et al. (2012). Synapomorphies are shown as black boxes, numbers indicate which of the characters shown in Table 1 serves as the synapomorphy.

(2012), the reported characters of *E. diana* fall within the trait range reported for *E. laidlawi*, while some characters even seemed to be poorly scored by Carle (2012). For example, he described the abdominal stridulatory files (ASF) in the genus *Epiophlebia*. He mentioned for *E. superstes* that the ASF of segment 3 is well developed, and the ASF segment 4 is about as high as long, and the ASF segment 7 is vestigial. In the data of Büsse (2016), specimens of *E. superstes* can be found with almost no stridulatory file on segment 3, and the ASF of segment 4 all can be seen higher as long, shorter as long, and as long as high. Furthermore, Carle (2012) suggested for the distinction of *E. diana* differences in the ASF (for *E. diana* he listed ASF of segment 7 c. 3/4 length of segment and for *E. laidlawi* the ASF of segment 7 c. 1/2 length of segment), but these are not valid as there are *E. laidlawi* in the data showing c. 3/4 as well (Büsse 2016). Next, Carle (2012) listed distinctions between the two species based on the degree of sinuity in the premental margins (in *E. laidlawi*, prementum with lateral margins slightly sinuous, but in *E. diana*, prementum with lateral margins strongly sinuous). It is difficult to estimate what slightly and strongly means, as such wording is subjective in nature; other points of view may consider the lateral margins of the prementum in *E. laidlawi* to be not just slightly sinuous, and without a figure showing data from Carle, it is impossible to say whether the sinuous nature of the prementum in *E. diana* is more pronounced; this character is not diagnostic. Similarly, Carle (2012) listed the fore-femur as being c. 3.0× as long as wide in *E. laidlawi* and for *E. diana* 2.5× as long as wide; this character is not valid for distinction between these species as there is variation in this trait and *E. laidlawi* have been documented with fore-femur that are only 2× as long as wide and there are *E. superstes* in the data showing a fore-femur c. 3× as long as wide (Büsse 2016). In fact, Asahina (1961) noted as the distinguishing character of *E. laidlawi* and *E. superstes* that the fore-femur of *E. laidlawi* was longer. It seems this character is very variable and impractical for taxonomic use. Indeed, fore-femur length has been shown to be influenced by ontogeny, and it is rarely used to infer evolutionary history.

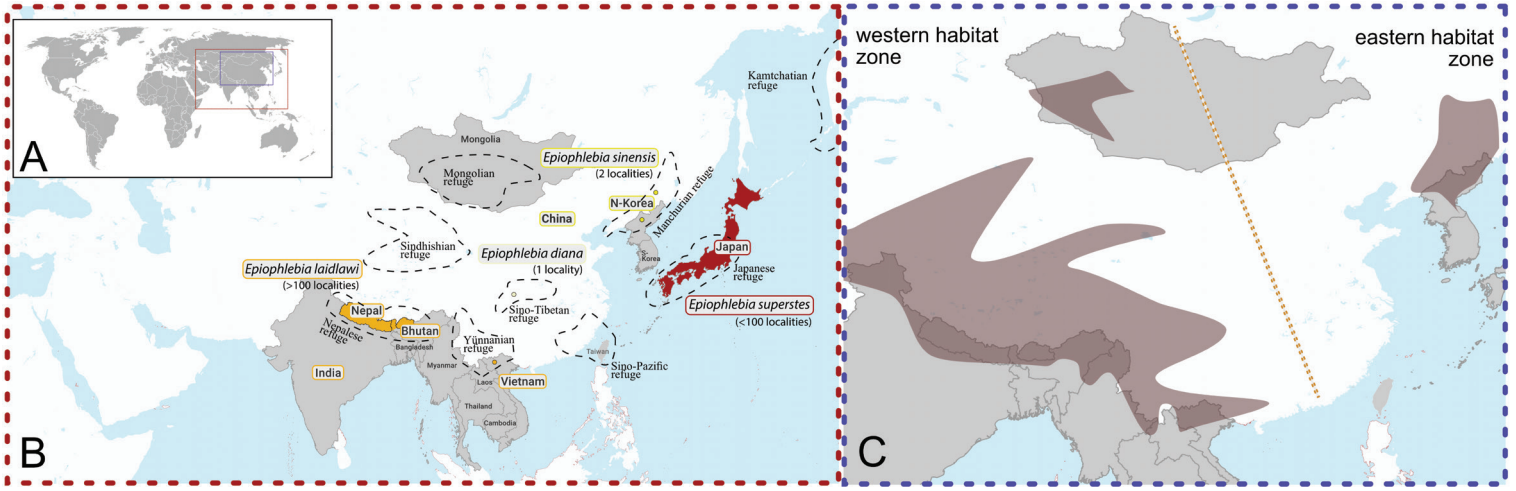

Figure 3. Maps of Asia (excerpt) **A** overview map, indicating map excerption of **B** red square and **C** blue square **B** known distribution of *Epiophlebia* species in: Bhutan, China, India, Japan, Nepal, North Korea, and Vietnam, and including glacial refuges after De Lattin (1967) **C** simplified mountain regions (brownish shadings) of the Asian mainland. Illustrating the large portions of temperate Chinese lowlands separating the western and eastern *Epiophlebia* habitat zones, clearly showing the affiliation of *E. diana* to the western (*E. laidlawi*) habitat zone.

Lastly, Carle (2012) listed *E. laidlawi* with lateral abdominal lobes slightly protruding on segment 9 and *E. diana* with lateral abdominal lobes protruding on segment 9. Again, these are subjective descriptions, and Büsse's (2016) data show abdominal lobes slightly protruding on segment 9 in *E. superstes* and distinctively produdent, forming a distinctive overhanging protrusion at the end of the segment 9 compared to the preceding segments, in *E. laidlawi*, comparable to Carle's (2012) fig. 3D. Only younger larvae of *E. laidlawi* seem to have only slight protudents on segment 9; here the abdominal segments resemble each other comparable to Carle's (2012) fig. 2D. In short, although no specimens of *E. diana* are available to examine, the characters used by Carle (2012) to describe the species do not seem to show a bimodal distribution of character values between *E. diana* and *E. laidlawi*, and given known and documented phenotypic variation in these traits for *E. laidlawi*, we consider *E. diana* a synonym of *E. laidlawi*.

Biogeography

The described stenoecious lifestyle has restricted the genus of *Epiophlebia* to cold habitats, indicated by the recent distribution in glacial refuges (Fig. 3B; De Lattin 1967; Büsse et al. 2012) – *E. superstes* from the Japanese refuge, *E. laidlawi* from the Nepalese and the Yunnanian refuges, *E. sinensis* from the Manchurian refuge (more precisely Ussurian secondary centre), and '*E. diana*' from the Sino-Tibetan refuge – thus, clearly showing a separation in a western and eastern habitat zone (Fig. 3C). Due to the distribution in the mentioned glacial refuges, we predict that other *Epiophlebia* habitats may exist in the Sino-Pacific refuge, the Sindhisian refuge, the Mongolian refuge, and further populations in the Manchurian refuge because it is divided into secondary refuges, as well as the Kamtchatian refuge. Whether one can expect new species of *Epiophlebia* or new populations of a known species in these possible habitats is to be answered.

Indeed, the connection between Japan and the Asian mainland, as well as regions of the Himalayas and other parts of Asia, has been well documented by Ikeda and Ohba (1998) and is known as the Sino-Japanese floristic region during the last ice ages (Ikeda and Ohba 1998; Büsse et al. 2012). The question remains as to when the extant *Epiophlebia* species diverged, as two contradicting hypotheses are plausible: i) *Epiophlebia* dates back to the Jurassic when Pangaea broke apart (Brockhaus and Hartmann 2009), or ii) *Epiophlebia* diverged during to the last or second last ice age period (Büsse et al. 2012; Büsse 2016). To substantiate one of these biogeographic scenarios, a re-analysis is absolutely necessary.

Nowadays, the habitats of *Epiophlebia* species are widely separated. Japan is separated from the mainland by sea-straits with depths of approximately 55 m north of Hokkaido and 130 m between the southern island of Kyushu and Korea (Millien-Parra and Jaeger 1999). In addition to the ocean, there are approximately 3000 km (respectively more than 3600 km) of temperate lowlands separating Japan, inhabited by *E. superstes* and the known ranges of *E. laidlawi* and '*E. diana*'. The same is true for the habitat of *E. sinensis* in Heilongjiang province, China (Li et al. 2012), as it is more than 3000 km away from the cold mountain habitat of *E. laidlawi* in the Himalayas and separated by temperate lowlands. The eastern and western habitat zones are, thus, separated by unsuitable, temperate lowlands (Fig. 3C). The location where the synonymized '*Epiophlebia diana*' was

found in Sichuan province, China (Carle 2012), is also part of the western habitat zone, as the known range of *E. laidlawi*. The known distributions of '*E. diana*' and *E. laidlawi* are around 1000 km apart but are connected by the mountain range of the Himalayas, which contains ample suitable habitats for an *Epiophlebia* species.

Acknowledgements

We are grateful to SM Bybee and D Paulson for pushing us to write this manuscript. SB is grateful for the constant support of SN Gorb and was directly supported through the DFG grants BU3169/1-1 and 1–2. Furthermore, SB wants to thank H Lohmann for many elucidating discussions on the biogeography of *Epiophlebia* species. JLW is grateful for many thoughtful discussions about odonate morphology with ML May.

References

Asahina S (1954) A Morphological Study of a Relic Dragonfly *Epiophlebia superstes* Selys (Odonata, Anisozygoptera). The Japan Society for the Promotion of Science, Tokyo, 153 pp.

Asahina A (1961) Is *Epiophlebia laidlawi* Tillyard (Odonata, Anisozygoptera) a good species? Internationale Revue der Gesamten Hydrobiologie und Hydrographie 46(3): 441–446. https://doi.org/10.1002/iroh.19610460310

Asahina A (1963) Description of the possible adult dragonfly of *Epiophlebia laidlawi* from the Himalayas. Tombo 6: 18–20.

Bäumler F, Koehnsen A, Tramsen HT, Gorb SN, Büsse S (2020) Illuminating nature's beauty: Modular, scalable and low-cost LED dome illumination system using 3D-printing technology. Scientific Reports 10(1): e12172. https://doi.org/10.1038/s41598-020-69075-y

Bechly G (1996) Morphologische Untersuchungen am Flügelgeäder der rezenten Libellen und deren Stammgruppenvertreter (Insecta; Pterygota; Odonata) unter besonderer Berücksichtigung der Phylogenetischen Systematik und des Grundplanes der Odonata. Petalura 2: 1–402.

Blanke A, Beckmann F, Misof B (2012) The head anatomy of *Epiophlebia superstes* (Odonata: Epiophlebiidae). Organisms, Diversity & Evolution 13(1): 55–66. https://doi.org/10.1007/s13127-012-0097-z

Blanke A, Greve C, Mokso R, Beckmann F, Misof B (2013) An updated phylogeny of Anisoptera including formal convergence analysis of morphological characters. Systematic Entomology 38(3): 474–490. https://doi.org/10.1111/syen.12012

Blanke A, Büsse S, Machida R (2015) Coding characters from different life stages for phylogenetic reconstruction: a case study on dragonfly adults and larvae, including a description of the larval head anatomy of *Epiophlebia superstes* (Odonata: Epiophlebiidae). Zoological Journal of the Linnean Society 174(4): 718–732. https://doi.org/10.1111/zoj.12258

Brockhaus T, Hartmann A (2009) New records of *Epiophlebia laidlawi* Tillyard in Bhutan, with notes on its biology, ecology, distribution, biogeography and threat status (Anisozy-

goptera: Epiophlebiidae). Odonatologica 38: 203–215. http://natuurtijdschriften.nl/record/592664

Büsse S (2016) Morphological re-examination of *Epiophlebia laidlawi* (Insecta: Odonata) including remarks on taxonomy. International Journal of Odonatology 19(4): 221–238. https://doi.org/10.1080/13887890.2016.1257442

Büsse S, Grumbkow P, Hummel S, Shah DN, Tachamo Shah RD, Li J, Zhang X, Yoshizawa K, Wedmann S, Hörnschemeyer T (2012) Phylogeographic analysis elucidates the influence of the ice ages on the disjunct distribution of relict dragonflies in Asia. PLoS ONE 7(5): e38132. https://doi.org/10.1371/journal.pone.0038132

Büsse S, Helmker B, Hörnschemeyer T (2015) The thorax morphology of *Epiophlebia* (Insecta: Odonata) nymphs – including remarks on ontogenesis and evolution. Scientific Reports 5(1): e12835. https://doi.org/10.1038/srep12835

Büsse S, Heckmann S, Hörnschemeyer T, Bybee SM (2018) The phylogenetic relevance of thoracic musculature: a case study including a description of the thorax anatomy of Zygoptera (Insecta: Odonata) larvae. Systematic Entomology 43(1): 31–42. https://doi.org/10.1111/syen.12246

Bybee SM, Ogden TH, Branham MA, Whiting MF (2008) Molecules, morphology and fossils: A comprehensive approach to odonate phylogeny and the evolution of the odonate wing. Cladistics 23(4): 1–38. https://doi.org/10.1111/j.1096-0031.2007.00191.x

Bybee SM, Kalkman VJ, Erickson RJ, Frandsen PB, Breinholt JW, Suvorov A, Dijkstra K-D, Cordero-Rivera A, Skevington JH, Abbott JC, Sanchez Herrera M, Lemmon AR, Lemmon EM, Ware JL (2021) Phylogeny and classification of Odonata using targeted genomics. Molecular Phylogenetics and Evolution 160: e107115. https://doi.org/10.1016/j.ympev.2021.107115

Carle FL (2012) A new Epiophlebia (Odonata: Epiophlebioidea) from China with a review of epiophlebian taxonomy, life history, and biogeography. Arthropod Systematics & Phylogeny 70(2): 75–83.

Carpenter FM (1992) Superclass Hexapoda. In: Moore RC, Kaesler RL (Eds) Treatise on Invertebrate Paleontology: Part R, Arthropoda 4, Vol. 4. The Geological Society of America, Boulder, 59–89.

Corbet PS (1999) Dragonflies: Behavior and Ecology of Odonata. Cornell University Press, NewYork, 864 pp.

Davies A (1992) *Epiophlebia laidlawi* – Flying! Kimminsia 3: 10–11.

De Lattin G (1967) Grundriss der Zoogeographie. Gustav Fischer Verlag, Jena.

Dijkstra K-D, Bechly G, Bybee SM, Dow R, Dumont H, Fleck G, Garrison RW, Hämäläinen M, Kalkman VJ, Karube H, May ML, Orr AG, Paulson DR, Rehn AC, Theischinger G, Trueman JWH, van Tol J, von Ellenrieder N, Ware J (2013) The classification and diversity of dragonflies and damselflies (Odonata). In: Zhang Z-Q (Ed.) Animal Biodiversity: An Outline of Higher-level Classification and Survey of Taxonomic Richness (Addenda 2013). Zootaxa 3703: 36–45. https://doi.org/10.11646/zootaxa.3703.1.9

Dorji T (2015) New distribution records of *Epiophlebia laidlawi* Tillyard, 1921 (Insecta: Odonata) in Bhutan. Journal of Threatened Taxa 7(10): 7668–7675. https://doi.org/10.11609/JoTT.o4092.7668-75

Fleck G, Bechly G, Martínez-Delclós X, Jarzembowski E, Coram R, Nel A (2003) Phylogeny and classification of the Stenophlebioptera (Odonata: Epiproctophora). Annales de la So-

ciété Entomologique de France (N.S.) 39: 55–93. https://doi.org/10.1080/00379271.2003.10697363

Fleck G, Brenk M, Misof B (2008) Larval and molecular characters help to solve phylogenetic puzzles in the highly diverse dragonfly family Libellulidae (Insecta: Odonata: Anisoptera): the Tetrathemistinae are a polyphyletic group. Organisms, Diversity & Evolution 8(1): 1–16. https://doi.org/10.1016/j.ode.2006.08.003

Fleck G, Li J, Schorr M, Nel A, Lin L, Gao M (2013) *Epiophlebia sinensis* Li and Nel 2011 in Li et al. (2012) (Odonatan) newly recorded in North Korea. International Dragonfly Fund-Report 61: 1–4.

Grimaldi D, Engel MS (2005) Evolution of the Insects. Cambridge University Press, Cambridge.

Hovmöller R, Pape T, Källersjö M (2002) The Palaeoptera problem: Basal pterygote phylogeny inferred from 18 S and 28 S rDNA sequences. Cladistics 18(3): 313–323. https://doi.org/10.1111/j.1096-0031.2002.tb00153.x

Ikeda H, Ohba H (1998) Himalayan Potentilla and its Relation to the Sino- Japanese Floristic Region. In: Boufford E, Ohba H (Eds) Sino-Japanese flora its characteristics and diversification Bulletin No. 37. The University Museum The University of Tokyo, Tokyo.

Kohli M, Djernæs M, Sanchez Herrera M, Sahlen G, Pilgrim E, Simonsen TJ, Olsen K, Ware J (2021) Comparative phylogeography uncovers evolutionary past of Holarctic dragonflies. PeerJ 9: e11338. https://doi.org/10.7717/peerj.11338

Letsch H, Gottsberger B, Ware JL (2016) Not going with the flow: a comprehensive time-calibrated phylogeny of dragonflies (Anisoptera: Odonata: Insecta) provides evidence for the role of lentic habitats on diversification. Molecular Ecology 25(6): 1340–1353. https://doi.org/10.1111/mec.13562

Li J-K, Nel A, Zhang X-P, Fleck G, Gao M-X, Lin L, Zhou J (2012) A third species of the relict family Epiophlebiidae discovered in China (Odonata: Epiproctophora). Systematic Entomology 37(2): 408–412. https://doi.org/10.1111/j.1365-3113.2011.00610.x

Lohmann H (1996) Das phylogenetische System der Anisoptera (Odonata). Entomologische Zeitschrift 106: 209–266.

Maddison WP, Maddison DR (2016) Mesquite: a Modular System for Evolutionary Analysis. Version 3.10. http://mesquiteproject.org [Accessed on: 2022-9-9]

Mahato M (1993) *Epiophlebia laidlawi* – A living ghost. Selysia 22: 2.

Millien-Parra V, Jaeger J-J (1999) Island biogeography ofthe Japanese terrestrial mammal assemblages: an example of a relict fauna. Journal of Biogeography 26: 959–972. https://doi.org/10.1046/j.1365-2699.1999.00346.x

Misof B, Liu S, Meusemann K, Peters RS, Donath A, Mayer C, Frandsen PB, Ware J, Flouri T, Beutel RG, Niehuis O, Petersen M, Izquierdo-Carrasco F, Wappler T, Rust J, Aberer AJ, Aspöck U, Aspöck H, Bartel D, Blanke A, Berger S, Böhm A, Buckley TR, Calcott B, Chen J, Friedrich F, Fukui M, Fujita M, Greve C, Grobe P, Gu S, Huang Y, Jermiin LS, Kawahara AY, Krogmann L, Kubiak M, Lanfear R, Letsch H, Li Y, Li Z, Li J, Lu H, Machida R, Mashimo Y, Kapli P, McKenna DD, Meng G, Nakagaki Y, Navarrete-Heredia JL, Ott M, Ou Y, Pass G, Podsiadlowski L, Pohl H, von Reumont BM, Schütte K, Sekiya K, Shimizu S, Slipinski A, Stamatakis A, Song W, Su X, Szucsich NU, Tan M, Tan X, Tang M, Tang J, Timelthaler G, Tomizuka S, Trautwein M, Tong X, Uchifune T, Walzl MG,

Wiegmann BM, Wilbrandt J, Wipfler B, Wong TKF, Wu Q, Wu G, Xie Y, Yang S, Yang Q, Yeates DK, Yoshizawa K, Zhang Q, Zhang R, Zhang W, Zhang Y, Zhao J, Zhou C, Zhou L, Ziesmann T, Zou S, Li Y, Xu X, Zhang Y, Yang H, Wang J, Wang J, Kjer KM, Zhou X (2014) Phylogenomics resolves the timing and pattern of insect evolution. Science 346(6210): 763–767. https://doi.org/10.1126/science.1257570

Needham JG (1930) A manual of the dragonflies of China: a monographic study of Chinese Odonata. Zoologica Sinica (Series A. Invertebrates of China Volume II, Fascicle 1). Fan Memorial Institute of Biology, Peking, 399 pp.

Nel A (1993) Les "Anisozygoptera" fossiles-phylogénie et classification. Martinia, hors série 3: 1–311.

Rehn AC (2003) Phylogenetic analysis of higher-level relationships of Odonata. Systematic Entomology 28(2): 181–239. https://doi.org/10.1046/j.1365-3113.2003.00210.x

Rüppell G, Hilfert D (1993) The flight of the relict dragonfly *Epiophlebia superstes* (Selys) in comparison with that of the modern Odonata (Anisozygoptera: Epiophlebiidae). Odonatologica 22: 295–309.

Suvorov A, Scornavacca C, Fujimoto MS, Bodily P, Clement M, Crandall KA, Whiting MF, Schrider DR, Bybee SM (2021) Deep ancestral introgression shapes evolutionary history of dragonflies and damselflies. bioRxiv, 1–37. https://doi.org/10.1101/2020.06.25.172619

Tabaru N (1984) Larval development of *Epiophlebia superstes* in Kyushu. Tombo 27: 27–31.

Tani K, Miyatake Y (1979) The discovery of *Epiophlebia laidlawi* Tillyard, 1921 in the Kathmandu Valley, Nepal (Anisozygoptera: Epiophlebiidae). Odonatologica 8: 329–332.

ZooKeys 1127: 91–116 (2022)
doi: 10.3897/zookeys.1127.84942
https://zookeys.pensoft.net

RESEARCH ARTICLE

A peer-reviewed open-access journal
ZooKeys
Launched to accelerate biodiversity research

A new species of feather-tailed leaf-toed gecko, *Kolekanos* Heinicke, Daza, Greenbaum, Jackman, Bauer, 2014 (Squamata, Gekkonidae) from the poorly explored savannah of western Angola

Javier Lobón-Rovira[1,2,3], Werner Conradie[4,5], Ninda L. Baptista[1,2,3,6], Pedro Vaz Pinto[1,3,7,8]

1 *CIBIO, Centro de Investigação em Biodiversidade e Recursos Genéticos, InBIO Laboratório Associado, Campus de Vairão, Universidade do Porto, 4485-661 Vairão, Portugal* **2** *Departamento de Biologia, Faculdade de Ciências, Universidade do Porto, 4099-002 Porto, Portugal* **3** *BIOPOLIS Program in Genomics, Biodiversity and Land Planning, CIBIO, Campus de Vairão, 4485-661 Vairão, Portugal* **4** *Port Elizabeth Museum, P.O. Box 13147, Humewood 6013, South Africa* **5** *Department of Nature Conservation Management, Natural Resource Science and Management Cluster, Faculty of Science, George Campus, Nelson Mandela University, George, South Africa* **6** *Instituto Superior de Ciências da Educação da Huíla (ISCED-Huíla), Rua Sarmento Rodrigues, Lubango, Angola* **7** *Fundação Kissama, Rua 60 Casa 560, Lar do Patriota, Luanda, Angola* **8** *TwinLab CIBIO/ISCED, Instituto Superior de Ciências da Educação da Huíla, Lubango, Angola*

Corresponding author: Javier Lobón-Rovira (j.lobon.rovira@cibio.up.pt)

Academic editor: Johannes Penner | Received 6 April 2022 | Accepted 4 October 2022 | Published 2 November 2022

https://zoobank.org/1FA39C0E-21C3-4137-A0B3-CB08300CF6AC

Citation: Lobón-Rovira J, Conradie W, Baptista NL, Vaz Pinto P (2022) A new species of feather-tailed leaf-toed gecko, *Kolekanos* Heinicke, Daza, Greenbaum, Jackman, Bauer, 2014 (Squamata, Gekkonidae) from the poorly explored savannah of western Angola. ZooKeys 1127: 91–116. https://doi.org/10.3897/zookeys.1127.84942

Abstract

We here describe a new species of feather-tailed leaf-toed gecko, *Kolekanos*, from southern Benguela Province, Angola, based on morphological and osteological evidence, supported by phylogenetic analysis of mitochondrial data. The new species adds to the rapidly growing and newly-recognised endemic biodiversity of Angola, doubling the number of *Kolekanos* species, breaking the pattern observed within other closely-related African members of a clade of circum-Indian Ocean leaf-toed geckos – *Ramigekko*, *Cryptactites* and *Afrogecko* – all of which are presently monotypic. The new species is easily distinguished from *K. plumicaudus*, based on spine-like (as opposed to feather-like) scales on the margins of the original tail. Phylogenetic analyses also recovered the new taxon as monophyletic, with a well-supported sister relationship to *K. plumicaudus*, from which it differs by a substantial 24.1% NADH-dehydrogenase subunit 2 mitochondrial gene uncorrected p-distance.

Keywords
Biodiversity, ct-scan, herpetology, osteology, Reptilia, taxonomy

Introduction

African leaf-toed geckos are among the most ancient and taxonomically problematic Gekkonidae groups in Africa (Lobón-Rovira et al. 2022a). Not surprisingly, these geckos have been the focus of several studies (Underwood 1954; Kluge 1983; Bauer et al. 1997; Bauer and Menegon 2006; Rocha et al. 2011; Gamble et al. 2012; Heinicke et al. 2014; Lobón-Rovira et al. 2022a), being partially resolved into three main groups: a circum-Indian Ocean group, an Afro-Malagasy group, and *Urocotyledon* spp. (see Heinicke et al. 2014; Lobón-Rovira et al. 2022a). However, the relationship within each of these groups still remains unresolved in most cases, with poorly-supported deep phylogenetic nodes and several species still excluded from phylogenetic analysis, due to the lack of fresh genetic material or access to new technologies to obtain DNA from formalin-fixed specimens (Lobón-Rovira et al. 2022a, b).

Circum-Indian Ocean leaf-toed geckos, understood as a monophyletic group that attained their current geographic distributions to reflect the landmasses distributed around the Indian Ocean during the Eocene (~40 mya) (Heinicke et al. 2014), have until recently been considered as a group that includes four genera from mainland Africa (*Afrogecko* [2 spp.], *Ramigekko* [1 sp.], *Cryptactites* [1 sp.] and *Kolekanos* [1 sp.]), *Christinus* from Australia and *Matoatoa* from Madagascar (Heinicke et al. 2014). However, a recent phylogenetic analysis that includes, for the first time, material of *Afrogecko ansorgii*, has demonstrated a paraphyletic status of this species, being consequently described as a new genus (*Bauerius*) as separate clade to the circum-Indian Ocean leaf-toed geckos and rendering the four mainland Africa circum-Indian Ocean leaf-toed geckos as monotypic genera (Lobón-Rovira et al. 2022a). Nevertheless, phylogenetic analysis (Heinicke et al. 2014) also suggested cryptic diversification within *Afrogecko porphyreus* that requires further investigation.

This new paradigm for circum-Indian leaf-toed geckos has only been addressed thanks to the rapid growth of new molecular techniques in the last two decades and the intensive surveys in previously poorly or unexplored regions in Africa, like Angola (Vaz Pinto et al. 2019, 2021; Lobón-Rovira et al. 2022a).

Access to newly-collected material from these regions has brought new opportunities to understand the evolutionary patterns of African herpetofauna, especially African gekkonids. This is particularly noteworthy in terms of the remarkable increase in knowledge of Angolan herpetofauna, with the description of 34 new species (Conradie et al. 2012a, b, 2013, 2020a, 2022a; Stanley et al. 2016; Ceríaco et al. 2018a, 2020a, b, c, 2021; Branch et al. 2019a, 2021; Marques et al. 2019a, b, 2020, 2022a, b; Hallermann et al. 2020; Nielsen et al. 2020; Baptista et al. 2021; Lobón-Rovira et al. 2021; Parrinha et al. 2021; Wagner et al. 2021) and several new country records (Branch and

Conradie 2013; Conradie and Bourquin 2013; Ernst et al. 2014, 2015; Branch et al. 2019b; Conradie et al. 2020b, 2021; Lobón-Rovira et al. 2022c) in the last decade. This increase has been especially evident within gekkonids, where the number of taxa has risen to over 45 recognised species for the country (Marques et al. 2020; Ceríaco et al. 2020a, b; Branch et al. 2021; Lobón-Rovira et al. 2021, 2022c; Conradie et al. 2022b) including two endemic leaf-toed gecko genera, *Kolekanos* (Heinicke et al. 2004) and *Bauerius* (Lobón-Rovira et al. 2022a).

Angolan leaf-toed geckos had previously been considered as members of *Afrogecko* Bauer, Good & Branch, 1997, represented by two species, *A. plumicaudus* Haacke, 2008 and *A. ansorgii* (Boulenger 1902). Until recent studies, both species were poorly known and with very restricted geographical distribution in south-western Angola (Haacke 2008; Agarwal et al. 2017; Marques et al. 2018; Vaz Pinto et al. 2019, 2021). With the availability of new material, both species were subsequently assigned to separate monotypic genera. Heinicke et al. (2014) erected *Kolekanos* to accommodate *A. plumicaudus*, while Lobón-Rovira et al. (2022a) created *Bauerius* to accommodate *A. ansorgii*. Furthermore, the known distribution of these two species have been extended over 200 km north- and southwards (Vaz Pinto et al. 2021) and 300 km northwards (Lobón-Rovira et al. 2022a), respectively. The range extension was especially remarkable for *K. plumicaudus*, which is now known to be present from sea level to over 2000 m a.s.l. and covering different ecological zones in south-western Angola (Vaz Pinto et al. 2021).

Scientific studies have been increasing in Angola in recent years, following a long civil war that prevented fieldwork in this region of Africa for several decades until the early 2000s (Huntley and Ferrand 2019). The improved political stability and strengthening of local institutions have motivated further surveys in the coastal regions of Angola, amongst others, with the aim of assessing the distribution of these poorly-known and emblematic taxa. New material of *Kolekanos*, collected well outside its known distributional range (~180 km north from the northernmost record of *K. plumicaudus*), prompted the current study aiming to investigate the potential diversification within this poorly-known genus. Due to the relevance of this group to understand the evolutionary history of African leaf-toed geckos, we herein also provide an updated phylogenetic hypothesis of the circum-Indian Ocean leaf-toed geckos with newly-collected material of *Kolekanos* from Angola to shed light into the taxonomic, distribution and conservation status of this taxon.

Materials and methods

Sampling

Kolekanos specimens and tissue samples have been collected from Namibe Province, Angola, since 2009 (Vaz Pinto et al. 2021). In August 2021, a new population was detected in southern Benguela Province (~180 km north from the northernmost record

of *K. plumicaudus*) and, subsequently, nine specimens were collected from two different sites (Table 1). Specimens collected as vouchers were euthanised with injection of tricaine methanesulphonate (MS222) (Conroy et al. 2009). After euthanasia, specimens were fixed in 10% formalin, after which they were transferred to 70% ethanol for long-term storage in the Museo Nacional de Ciencias Naturales (**MNCN**), Spain and Fundação Kissama (**FKH**), Angola. For molecular analyses, liver samples were collected prior to formalin fixing and stored in 95–99% ethanol. For each specimen/sample collected, its location was recorded using a handheld GPS, in the WGS84 coordinate system.

Molecular data

A mitochondrial gene NADH-dehydrogenase subunit 2 (ND2, 1041 bp) was used, comprising information from nine individuals of *Kolekanos* from the new northern records, to generate data for phylogenetic analysis to explore phylogenetic relationships amongst *Kolekanos* (Table 1). DNA was extracted using EasySpin Genomic DNA Tissue Kit (Citomed, Portugal), following the manufacturer's protocols. PCR amplifications were performed using the following primers (L4437 and H5540; Macey et al. 1997) and concentrations (5 µl QIAGEN PCR MasterMix, 0.4 µl each primer, 3.2 µl H_2O and 2 µl DNA (DNA elution were adjusted to extraction results). PCR reactions were adjusted following: initial denaturing step at 95 °C for 15 min, followed by 5 cycles of 95 °C for 30 s, 64 °C for 20 s and 72 °C for 60 s (decreasing annealing temperature by -0.5 °C/cycle), followed by 35 cycles of 95 °C for 30 s, 64 °C for 20 s and 72 °C for 60 s, with a final extension at 60 °C for 10 min. For phylogenetic comparisons, we combined the newly-generated ND2 sequences with previously published sequences from Lobón-Rovira et al. (2022a) and Heinicke et al. (2014), deposited in GenBank (http://www.ncbi.nlm.nih.gov/genbank/). The final dataset consisted of our newly-sequenced material and 204 additional sequences, representing a total of 45 different Gekkonidae genera. As outgroup, we used four members of the genus *Phyllodactylus* (family Phyllodactylidae), representatives of the sister family to the family Gekkonidae (Pyron et al. 2013). All sequences were checked and edited using GENEIOUS Prime v.2021.1.1 (http://www.geneious.com/) and aligned using the MUSCLE plugin for GENEIOUS.

Phylogenetic analysis and p-distance analysis

To determine the correct placement of the species and explore diversification within *Kolekanos plumicaudus*, Bayesian Inference (**BI**) and Maximum Likelihood (**ML**) analyses were performed using the ND2 sequence alignment. The best partition scheme and best-fitting models of molecular evolution were selected using PartitionFinder v.1.1.1 (Lanfear et al. 2012). The best-fitting model scheme selected was as follows: TVM+I+G, TVM+G and TrN+I+G, by codon position. Bayesian Inference (BI) (MrBayes v.3.2.7a; Ronquist et al. 2012) was implemented on the CIPRES Science Gateway XSEDE online resource (http://www.phylo.org; Miller et al. 2010; Tamura et al. 2013). Maximum Likelihood (ML) analysis was conducted using IQ-TREE

Table 1. Detailed collection and observational records of *Kolekanos* spp., including information on species, catalogue numbers, field numbers, localities, geographical coordinates and source of records. Abbreviations: California Academy of Science (CAS), Florida Museum of Natural History (UF), Kissama Foundation (FKH), National Museum of Namibia, Windhoek (NMNW), Ditsong National Museum of Natural History (formerly the Transvaal Museum; TM) and Port Elizabeth Museum (PEM). Where material was not collected, references are stated as Not Available (NA).

Species	Catalog Number	Field Number	Locality	GPS Coordinates	Source
Kolekanos plumicaudus	TM 40521–31	–	Tambor	-16.1355, 12.4297	Haacke (2008)
Kolekanos plumicaudus	TM 40553–55	–	Curoca River Crossing	-16.3027, 12.4165	Haacke (2008)
Kolekanos plumicaudus	TM 40755–61	–	11 km NE from Iona	-16.8606, 12.6106	Haacke (2008)
Kolekanos plumicaudus	PEM R18047; PEM R18010–5; CAS 248782	–	7 km NE from Iona	-16.8583, 12.6127	Vaz Pinto et al. (2021)
Kolekanos plumicaudus	FKH 0235	P9.254	Camp Baptista Cunene	-17.1603, 12.0182	Vaz Pinto et al. (2021)
Kolekanos plumicaudus	FKH 0236	P9.255	Camp Baptista Cunene	-17.1603, 12.0182	Vaz Pinto et al. (2021)
Kolekanos plumicaudus	UF 187219–22; CAS 262389–91	–	Omauha	-16.1996, 12.3987	Agarwal et al. (2017)
Kolekanos plumicaudus	FKH-0782	JLRZC0109	Omauha	-16.1987, 12,401258	Vaz Pinto et al. (2021)
Kolekanos plumicaudus	FKH-0343	P9.286	Omauha	-16.1996, 12.3987	Vaz Pinto et al. (2021)
Kolekanos plumicaudus	FKH-0344	P9.287	Omauha	-16.1996, 12.3987	Vaz Pinto et al. (2021)
Kolekanos plumicaudus	FKH-0345	P9.288	Omauha	-16.1996, 12.3987	Vaz Pinto et al. (2021)
Kolekanos plumicaudus	FKH-0346	P9.289	Omauha	-16.1996, 12.3987	Vaz Pinto et al. (2021)
Kolekanos plumicaudus	NA	NA	Mutuovano	-15.9153, 12.3848	Vaz Pinto et al. (2021)
Kolekanos plumicaudus	NA	NA	Muende-Curoca	-16.2892, 12.3180	Vaz Pinto et al. (2021)
Kolekanos plumicaudus	NA	NA	Tchitchaki	-16.2877, 12.2753	Vaz Pinto et al. (2021)
Kolekanos plumicaudus	NA	NA	Humbi	-16.9858, 12.5415	Vaz Pinto et al. (2021)
Kolekanos plumicaudus	NA	NA	Congundo	-17.0396, 12.6013	Vaz Pinto et al. (2021)
Kolekanos plumicaudus	NA	NA	Conguiungulo	-16.8437, 12.6141	Vaz Pinto et al. (2021)
Kolekanos plumicaudus	FKH-0534	P1.021	Maongo-Giraul	-15.0326, 12.4146	Vaz Pinto et al. (2021)
Kolekanos plumicaudus	FKH-0535	P1.022	Maongo-Giraul	-15.0326, 12.4146	Vaz Pinto et al. (2021)
Kolekanos plumicaudus	–	P1.075	Chamaleva	-15.6863, 12.6124	Vaz Pinto et al. (2021)
Kolekanos plumicaudus	NMNW R11011	–	Tchamalindi	-16.9752, 12.8833	Vaz Pinto et al. (2021)
Kolekanos plumicaudus	NMNW R11012	–	Tchamalindi	-16.9752, 12.8833	Vaz Pinto et al. (2021)
Kolekanos plumicaudus	–	P1.126	Cafema	-17.1289, 12.5138	Vaz Pinto et al. (2021)
Kolekanos plumicaudus	–	P1.127	Cafema	-17.1306, 12.5067	Vaz Pinto et al. (2021)
Kolekanos plumicaudus	FKH-0574	P1.115	Tchamalinde	-16.9752, 12.8833	This work
Kolekanos plumicaudus	FKH-0661	P1.246	Maongo	-15.0461, 12.4310	This work
Kolekanos plumicaudus	FKH-0662	P1.247	Maongo	-15.0461, 12.4310	This work
Kolekanos plumicaudus	FKH-0663	P1.248	Maongo	-15.0461, 12.4310	This work
Kolekanos spinicaudus sp. nov.	FKH-0645	P1.227	Carivo	-13.1923, 13.4211	This work
Kolekanos spinicaudus sp. nov.	MNCN 50768	P1.228	Carivo	-13.1923, 13.4211	This work
Kolekanos spinicaudus sp. nov.	FKH-0647	P1.229	Carivo	-13.1923, 13.4211	This work
Kolekanos spinicaudus sp. nov.	FKH-0648	P1.230	Carivo	-13.1923, 13.4211	This work
Kolekanos spinicaudus sp. nov.	FKH-0649	P1.231	Carivo	-13.1923, 13.4211	This work
Kolekanos spinicaudus sp. nov.	FKH-0650	P1.232	Carivo	-13.1923, 13.4211	This work
Kolekanos spinicaudus sp. nov.	MNCN 50766	JLRZC0212	Ekongo	-13.2494, 13.2065	This work
Kolekanos spinicaudus sp. nov.	FKH-0845	JLRZC0213	Ekongo	-13.2494, 13.2065	This work
Kolekanos spinicaudus sp. nov.	MNCN 50767	JLRZC0214	Ekongo	-13.2494, 13.2065	This work

v.2.1.2 (Nguyen et al. 2015), using a random starting tree and the ultrafast bootstrap approximation (UFBoot) method (Hoang et al. 2018) with 1000 bootstrap replicates, using the gene-partitioned scheme mentioned above.

Finally, uncorrected pairwise sequence divergences (p-distance) were calculated for the ND2 sequences, in MEGA v.10.1.7 (Kumar et al. 2018) to explore intra- and interspecific variation. Standard errors (s.e.) were also calculated in MEGA v.10.1.7.

Morphology

For this study, we examined 19 adult specimens of *Kolekanos*, collected during different expeditions and deposited in the National Museum of Natural Science (**MNCN**), Spain, Fundação Kissama (**FKH**), Angola and Port Elizabeth Museum (**PEM**), South Africa. Additionally, we reviewed the descriptions of external morphologies of *K. plumicaudus* (Haacke 2008) and other circum-Indian Ocean leaf-toed geckos (Heinicke et al. 2014), as well as osteological features provided by Heinicke et al. (2014) for all representative species within this group. The morphometric and meristic details collected were as follows: snout-vent length (**SVL**, from tip of snout to anteriorly cloacal opening), tail length (**TL**, from posteriorly cloacal opening to tip of tail), trunk length (**TRL**, from posterior insertion of the forelimb to anterior insertion of the hindlimb), head length (**HL**, from snout to the posterior section of the ear aperture), head width (**HW**, measured at the widest portion of the head), head height (**HH**, measured at the highest portion of the head), maximum horizontal orbital diameter (**OD**), maximum ear diameter (**EarL**), crus length (**CL**, from base of heel to knee), forearm length (**FL**, from insertion to the palm), nares to eye distance (**NE**, distance between anteriormost point of eye and nostril), snout to eye distance (**SE**, distance between anteriormost point of eye and tip of snout), eye to ear distance (**EE**, distance from anterior edge of ear opening to posterior corner of eye), internarial distance (**IN**, shortest distance between nares), interorbital distance (**IO**, shortest distance between left and right supraciliary scale rows). All measurements were taken in millimetres (mm) with a digital caliper (accuracy of 0.01 mm). The meristic data collected were: number of supralabials, number of infralabials, subdigital lamellae from the base of the digits to the leaf-toed lamellae on the first and fourth finger and toe, respectively, number of scales from the anterior part of ear opening to the posterior part of the eye, number of scales from anterior eye to nostril, number of scales between the eyes and tail ornamentation. Meristic data were collected with the help of a Leica LD2500 or Nikon SMZ1270 dissecting microscope. In order to undertake a preliminary examination of the overall morphometric variation, we performed a Principal Component Analysis (PCA), using only continuous variables, which we first log transformed and then corrected for size (by dividing the transformed data by the SVL) before the PCA analysis. We also tested the existence of variation between the two-representative taxa and between sexes of each separate taxon, using permutational ANOVAs (in the case of SVL) and ANCOVAs (in the case of the other variables, using SVL as a covariate). Both statistical analyses were performed in R v.3.6.2.

For osteological comparisons, we performed High Resolution X-ray Computed Tomography (HRCT) scans of one adult female (MNCN 50770) from the southern range and two adult males (MNCN 50769 and MNCN 50766) from the northern range of *Kolekanos*, at Centro de Instrumentación Científica of Granada (CIC), Spain, using a Zeiss Xradia 510 Versa, under the following settings: voltage = 80 kV,

current = 60 μA, exposure time = 3 sec and computed voxel size (volumetric pixel) of 12.67 μm. Additionally, we examined in detail the HRCT of an adult male of *K. plumicaudus* (CAS 248782; ark:/87602/m4/M101108) provided by Heinicke et al. (2014). HRCT scans have been deposited in Morphosource (Project ID 000433817; MNCN 50766; MNCN 50769; MNCN 50770). 3D segmentation models were generated for the articulated skulls in Avizo Lite 2020.2 (Thermo Fisher Scientific 2020). To facilitate visualisation, individual bone units for skulls and jaws were coloured following the same colour pallet as Lobón-Rovira and Bauer (2021). Annotations were made in Adobe Illustrator CC 22.0.1 (Adobe Systems Incorporated 2017) following the anatomical terminology of Daza et al. (2008), Evans (2008) and Heinicke et al. (2014).

Results

While the two phylogenetic analyses (BI and ML) did not retrieve the same topology with regard to the deeper-level topological structuring, both were largely concordant in recovering the monophyletic circum-Indian Ocean group and recognising two clearly distinct sister taxa within *Kolekanos* (Fig. 1). The two lineages here recognised are molecularly well-differentiated, with 24.1% ND2 uncorrected p-distance from each other and regarded as separate species (Table 2). Both species presented a large disparity in the intraspecific variation. While *K. plumicaudus* showed lower intraspecific variation (3.8% ± 0.4 s.e.), with the maximum p-distance (5.2%) found between two isolated highlands in Iona National Park (Tchamalindi and Cafema), the new undescribed species presented high intraspecific diversity (7.3% ± 0.6 s.e.) between the two populations found in relatively close proximity in Benguela Province (Table 2).

Morphological analysis revealed morphological differences between the two main clades within *Kolekanos*. PCA analysis explained a considerable part of the variation within these clades, with PC1 (46.9% of variation) and PC2 (15.6% of variation) showing two well-separated groups (Fig. 2A). These results are supported by the univariate morphometric analysis (ANOVA), which detected significant differences between clades (Fig. 2B), in head width (HW, $F_{1,14} = 59.451$, $p = 0.000$), forearm length (FL, $F_{1,14} = 7.764$, $p = 0.015$), snout to eye distance (SE, $F_{1,14} = 5.905$, $p = 0.030$) and interorbital distance (IO, $F_{1,14} = 25.834$, $p = 0.000$) (Suppl. material 2). Additionally, visual comparison suggested that both species could be separated also based on the robustness stage, relative to body and hindlimbs. However, we failed to retrieve any statistically significant differences from the morphometric traits analysed to confirm this visual difference (Suppl. material 2).

Although the osteological reconstruction demonstrated the skulls of *Kolekanos* to be very conserved, we did find differences, mostly in overall shape of the head, supporting the above morphological findings (Fig. 3). While *K. plumicaudus* presented

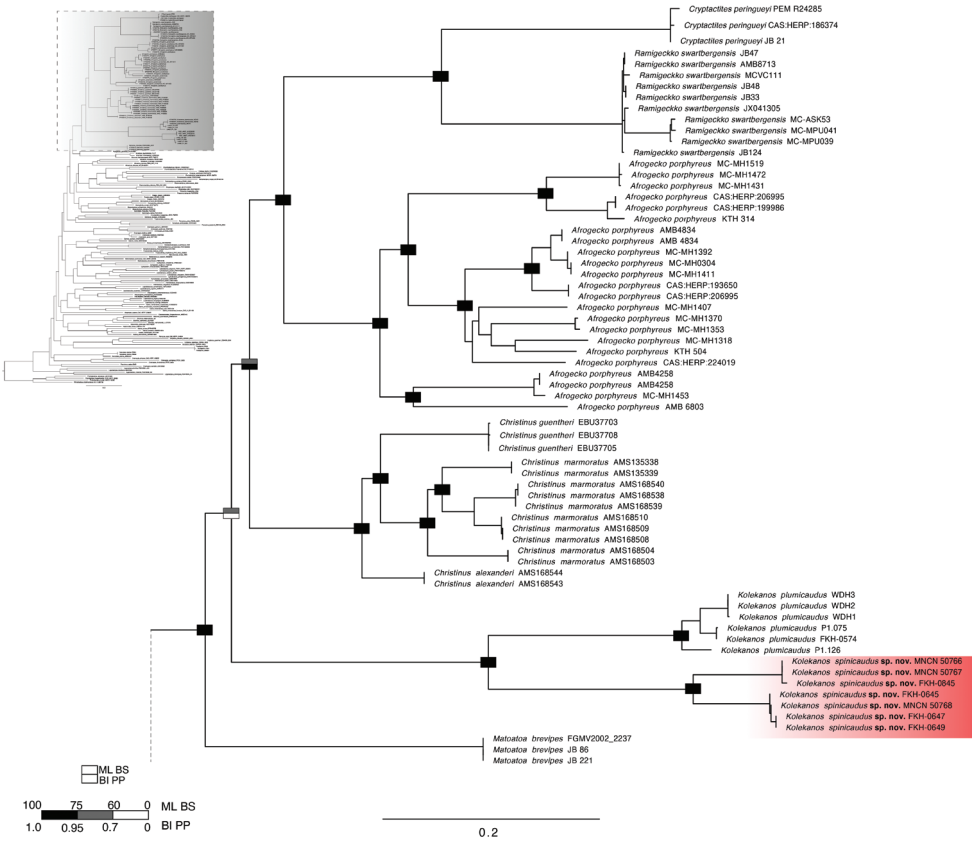

Figure 1. Maximum Likelihood phylogeny, with Bayesian Inference support overlaid. Support values (ML BS = Maximum Likelihood bootstrap values; BI PP = Bayesian Inference posterior probabilities) are shown graphically at the nodes according to the colours shown in the inset key. *Kolekanos spinicaudus* sp. nov. is highlighted in red.

Table 2. ND2 divergences (uncorrected pairwise distances) between circum-Indian leaf-toed geckos. Bold values depict intraspecific divergences.

ID	1	2	3	4	5	6	7	8	9	10
1. *Afrogecko porphyreus*	**16.28**									
2. *Ramigekko swartbergensis*	28.11	**2.55**								
3. *Kolekanos plumicaudus*	30.83	32.48	**3.79**							
4. *Kolekanos spinicaudus* sp. nov.	31.33	31.43	24.49	**7.26**						
5. *Cryptactites peringueyi*	28.27	23.06	32.83	31.51	**0.58**					
6. *Matoatoa breviceps*	26.50	28.07	29.95	30.01	28.75	**0**				
7. *Christinus alexanderi*	24.50	26.32	29.92	31.75	26.42	23.42	**0**			
8. *Christinus marmoratus*	25.32	27.08	29.40	30.80	27.20	25.31	13.52	**7.95**		
9. *Christinus guentheri*	24.29	26.47	29.06	29.13	26.84	23.49	13.52	15.03	**0.32**	
10. *Goggia lineata*	31.11	32.42	34.74	35.29	32.15	30.70	28.80	30.19	29.56	**n/c**

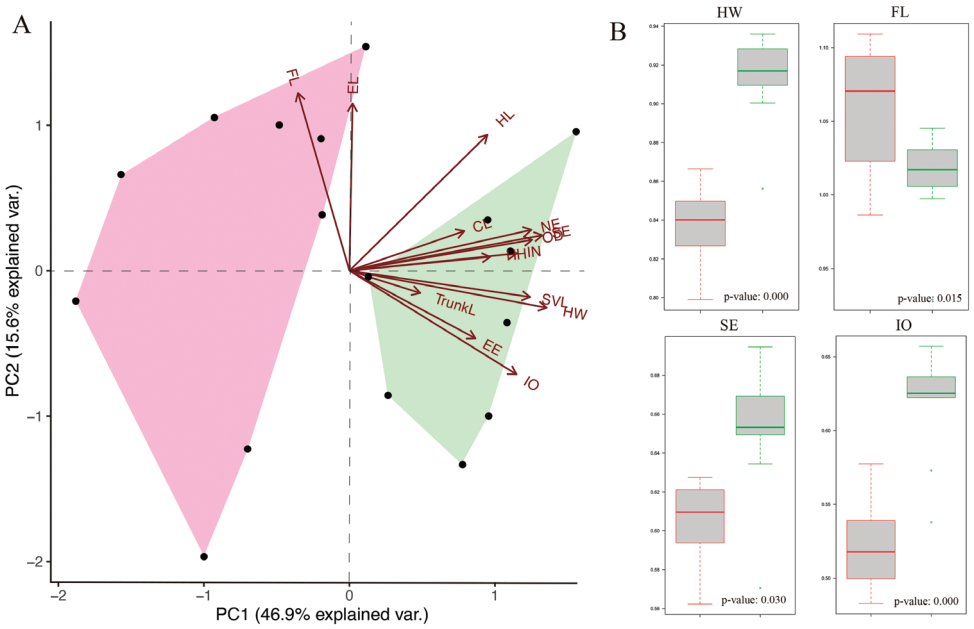

Figure 2. A PCA plots of the first principal component (PC 1) versus the second (PC 2) of morphometric analysis for the two species of *Kolekanos*. The green polygon denotes the distribution within PCAs of *K. spinicaudus* sp. nov. and the pink polygon of *K. plumicaudus*. For loadings of all axis and explained variance, see Suppl. material 3. **B** boxplots (top whisker – maximum value; lower whisker – minimum value; bold horizontal line – median; box – 1st and 3rd quartile) of morphological features where ANOVA t-values where ≤ 0.05; p-value of the one-way ANOVA test is indicated at the bottom of each boxplot. For abbreviations, see Material and methods section.

a more slender and longer-snouted head shape (Fig. 3G), the here recognised new taxon displayed a more rounded and laterally broader head shape (Fig. 3A), with a more compressed head shape in its dorsoventral profile. This modification in the head shape seems to be reflected in osteological features in the northern clade, such as larger jugal bone, more elongated lateral process of the postorbitofrontal, more compressed premaxilla and maxilla bones in its dorsoventral view and wider in the lateral profile of the bones. It is noteworthy that the specimen CAS 248782 had a pair of nasal bones, in contrast with the three specimens analysed in this study, which presented one fused nasal bone.

Therefore, the above morphological and phylogenetic differences support the recognition of two different species within *Kolekanos* and we take the opportunity to describe the second lineage recovered as a new species below. In this manuscript, we have applied the general lineage-based species concept, where we treat all independent evolving lineages represented and supported by multiple lines of evidence, as listed above, as separate species (de Queiroz 1998).

***Kolekanos spinicaudus* sp. nov.**
https://zoobank.org/80186811-4C1C-4F26-B791-0824BA79E221
Figs 3–7, Tables 3, 4, Suppl. material 2

Holotype. MNCN 50769, adult male, with regenerated tail and incision in the ventral region, collected in Carivo (-13.19225, 13.42108, 362 m a.s.l.), Benguela Province, Angola, by Pedro and Afonso Vaz Pinto on 19 August 2021.

Paratypes. MNCN 50766, adult male, collected from Ekongo (-13.24940, 13.20650, 636 m a.s.l.), Benguela Province, Angola, by Javier Lobón-Rovira and Pedro Vaz Pinto on 22 November 2021; MNCN 50767 & FKH-0845, adult females, with the same collecting data as the previous. FKH-0645 & FKH-0650, adult females, FKH-0647–8, adult males, MNCN 50768, subadult male, all with the same collecting data as the holotype.

Etymology. The name "*spinicaudus"* is derived from the combination of the Latin words "spina" and "cauda", that refers to the spiny appearance of the tail of the new species. The species epithet is used as a singular nominative adjective "*-us*".

Diagnosis. *Kolekanos* can be easily differentiated from other circum-Indian leaf-toed and African leaf-toed geckos, based on its ornamented tail (versus non-ornamented tail in the remaining genera). The new species differs from *K. plumicaudus*, based on the following characters: different ornamentation of the tail, being composed by modified scales on the margins of the original tail which resemble white lateral spines (versus feathered-like tail in *K. plumicaudus*); broader head (minimum HW = 7.95 mm versus maximum HW = 7.35 mm in *K. plumicaudus*); more robust body, with shorter forelimbs (versus thinner and more slender body in *K. plumicaudus*, Fig. 5); proportionally larger snout to eye distance (SE mean 4.48 mm ± 0.34 s.e. versus 3.99 mm ± 0.22 s.e. in *K. plumicaudus*) and interorbital distance (IO mean 4.14 mm ± 0.34 s.e. versus 3.33 mm ± 0.28 s.e. in *K. plumicaudus*); and dorsal pattern is less contrasted, based on zig-zag black patches surrounded by lighter patches (versus dark blocks well contrasted, not surrounded by lighter patches in *K. plumicaudus*). The new species can also be differentiated from *K. plumicaudus* by the following osteological characteristics: 1) larger jugal bone (versus reduced jugal); 2) more prominent lateral process of the postorbitofrontal (versus less prominent lateral process of postorbitofrontal); 3) more compressed premaxilla and maxilla bone on its dorsoventral profile and wider in the lateral profile of the bones; 4) ascending process of the premaxilla shorter (versus more elongated); 5) braincase compressed dorsoventrally (versus more rounded in *K. plumicaudus*); 6) palatine length and width equal (versus unequal); 7) postero-lateral process of parietal rounded and slightly curved (versus flat postero-lateral process of parietal broad and flat that curves downwards posteriorly); 8) anterolateral process of the coronoid markedly enlarged (versus more reduced anterolateral process). *Kolekanos spinicaudus* sp. nov. also differs from *K. plumicaudus* by circa 24% (uncorrected p-distance) ND2 mitochondrial DNA.

Holotype description. (Fig. 4). Measurements and meristic characters of the holotype are presented in Table 3. Adult male with a SVL of 44.59 mm and partially (2/3) regenerated tail, tail length (TL) 36.77 mm. Body moderately slender, nape distinct.

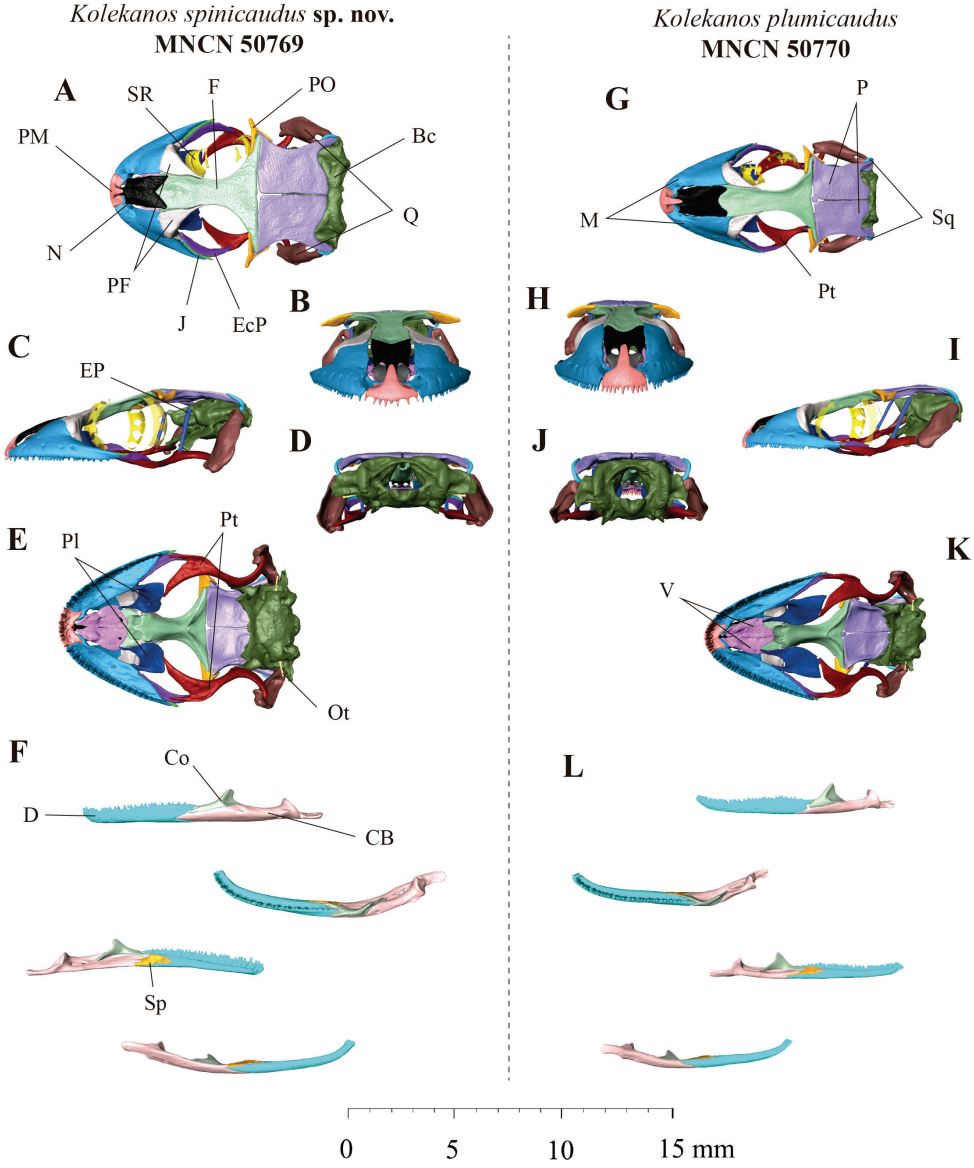

Figure 3. Detailed views in **A** dorsal **B** frontal **C** lateral **D** posterior and **E** ventral of skull and **F** lateral, dorsal, medial and ventral of left jaw (from top to bottom) of *K. spinicaudus* sp. nov. (MNCN50769). Detailed views in **G** dorsal **H** frontal **I** lateral **G** posterior and **K** ventral view of skull and **L** lateral, dorsal, medial and ventral of left jaw (from top to bottom) of *Kolekanos plumicaudus* (MNCN50770). Abbreviations: Bc, braincase; Co, coronoid; CB, compound bone; D, dentary; EcP, ectopterygoid; EP, epipterygoid; F, frontal; J, jugal; M, maxilla; N, nasal; Ot, otostapes; P, parietal; PF, prefrontal; Pl, palatine; PM, premaxilla; PO, postorbitofrontal; Pt, pterygoid; Q, quadrate; Sp, splenial; SR, sclerotic ring; V, vomer.

Head slightly broader than the body and markedly compressed dorsoventrally (HH/HL = 0.27). Canthus rostralis smooth, almost absent. Eye diameter (2.35 mm), with vertical pupil and crenulated margin. Supraciliar scales small and rounded. Ear height

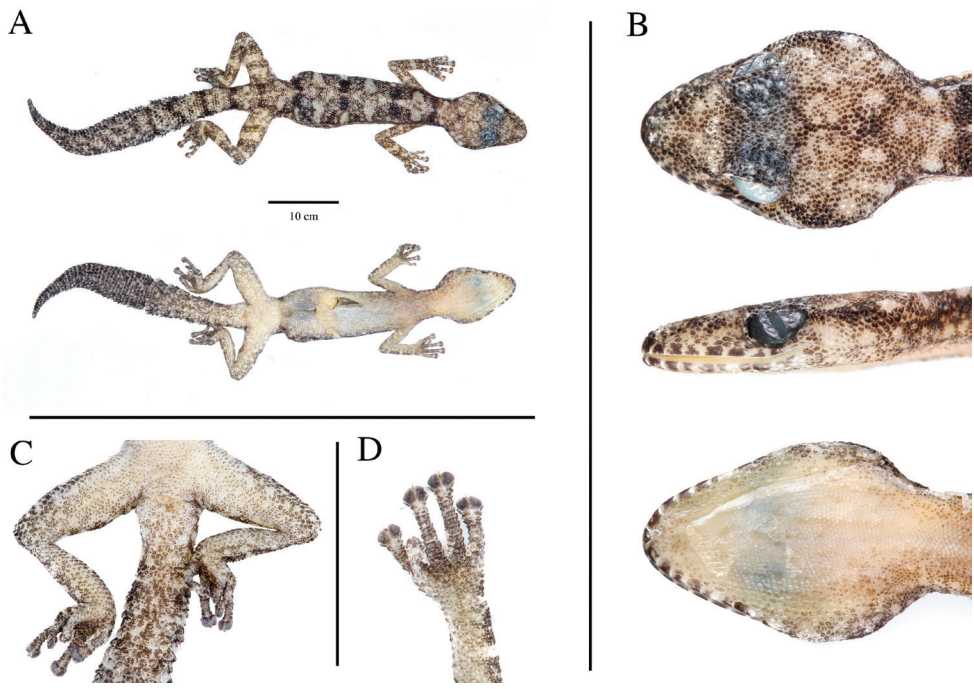

Figure 4. Holotype of *Kolekanos spinicaudus* sp. nov. (MNCN50769) from Carivo, Benguela Province, Angola **A** dorsal and ventral view of whole specimen **B** detail of head (from top to bottom) in dorsal, lateral and ventral views **C** detail of pelvic region and hind-limbs in ventral view **D** detail of left fingers. Photos by Alberto Sanchez Vialas (MNCN).

(0.47 mm). Ear to eye distance larger than eye diameter (3.72 mm). Snout rounded and slightly pointed. Body relatively slender and elongated (TrunkL/SVL = 0.44). Fore- and hindlimbs moderate and stout, forearm large (FL/SVL 0.23), tibia short (CL/SVL 0.18). Digits elongated and clawed. All digits of manus and pes indistinctly webbed. All digits with granular basal scales and more distal widened divided lamellae. One pair of leaf-like terminal scansors. Number of scansors: 7-10-10-11-10 (right manus) and 7-10-10-11-10 (left manus)/7-9-11-11–10 (right pes) and 7-9-11-11–9 (left pes). Relative length of digits manus I < II < III < IV > V and pes I < II < III > IV > V. Scalation: Frontal scales granular and larger than occipital scales. Occipital scales small and granular. Rostral in direct contact with nostrils, 1st supralabials, supranasals and one internasal scales. 8/8 supralabial and 9/9 infralabials. First supralabial in contact with the nostril. Nostril circular and surrounded by rostral, 1st supralabial, supranasal and three reduced postnasals. Lower postnasal half the size of the upper postnasal and supranasal. Two rows of scales between supralabials and the orbit. Mental triangular and rounded posteriorly, with two small rounded postmental scales. 1st infralabial rectangular and slightly larger than mental. Gular scales small and granular. Ventral scales small and granular. Precloacal pores absent. The dorsal pholidosis present homogenous granular scales from head to tail. The first third of the original

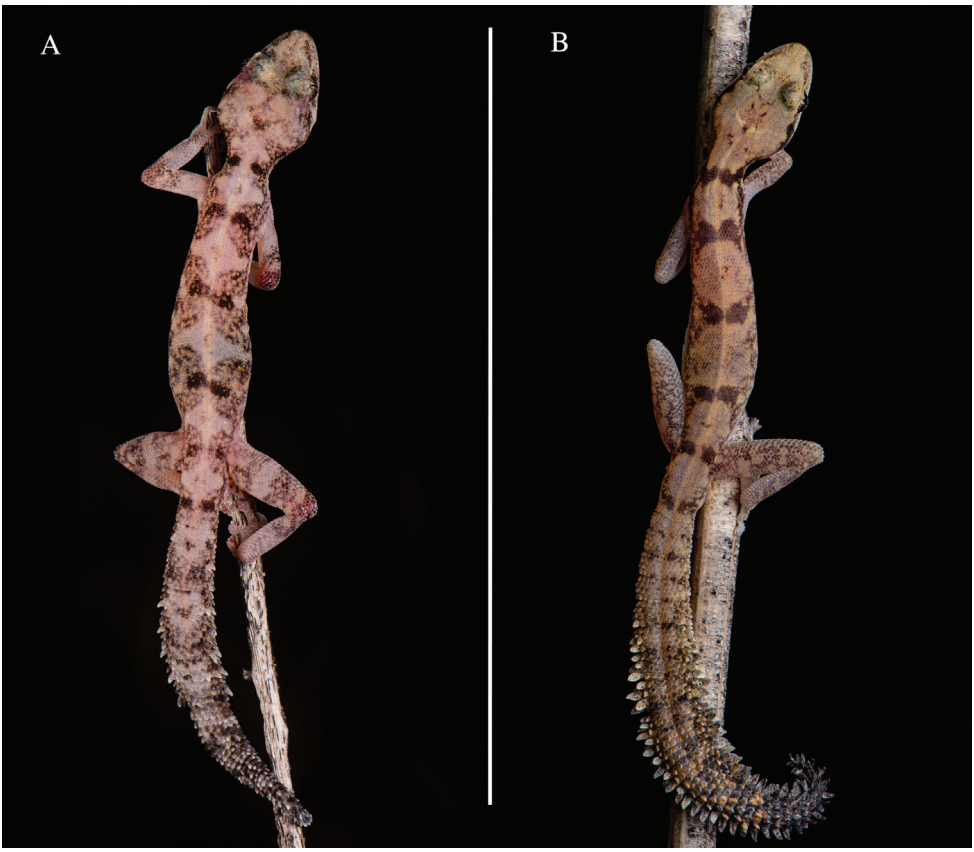

Figure 5. A dorsal view in life of *K. spinicaudus* sp. nov. from Carivo and **B** *K. plumicaudus* from Omahua. Photos Javier Lobón-Rovira.

tail presents lateral whitish "spine-like" scales, being absent in the last portion of the tail. Post-cloacal scales slightly larger and quadrangular. Osteology: the skull (Fig. 3) displays no co-ossification with the overlying skin. Nasals are fused. Single frontal. Paired parietals. Stapes imperforate. 14 scleral ossicles. 11 premaxillary tooth loci. 36–38 maxillary and 38 dentary tooth loci. Braincase elements fused. Postorbitofrontal arrow-shaped, with lateral process as long as anterior and posterior process. Parietal wider than longer. Jugal small, but visible.

Variation. Variation in scalation and body measurements of the paratypes of *K. spinicaudus* sp. nov. are reported in Table 3. All the material analysed agrees with the holotype description with the exception of the tooth loci, where the specimen MNCN 50766 presented a larger number in the tooth loci of maxilla and dentary (> 40).

Colouration. ***In life*** (Fig. 5A): dorsal colouration varies from light pinkish to light brown, with black spots surrounded by lighter brownish regions disposed in zig-zag, from nape to tail. Dorsal reticulated light brownish colouration on tail and fore- and hind-limbs. Anterior part of the tail with marked hourglass-shaped pattern. Ventrum

Table 3. Morphological (morphometric and meristic) of *Kolekanos spinicaudus* sp. nov. Measurements are represented in millimetres (mm). For abbreviations, see Material and methods section. R = regenerated tail, M = male, F = female.

Species	*K. spinicaudus* sp. nov.	*K. spinicaudus* sp. nov.	*K. spinicaudus* sp. nov.	*K. spinicaudus* sp. nov.	*K. spinicaudus* sp. nov.	*K. spinicaudus* sp. nov.	*K. spinicaudus* sp. nov.	*K. spinicaudus* sp. nov.	*K. spinicaudus* sp. nov.
Catalogue#	**MNCN 50769**	**FKH0845**	**MNCN 50767**	**MNCN 50766**	**FKH-0645**	**FKH-0648**	**FKH-0647**	**FKH-0650**	**MNCN 50768**
Status	**Holotype**	**Paratype**	**Paratype**	**Paratype**	**Paratype**	**Paratype**	**Paratype**	**Paratype**	**Paratype**
Sex	**M**	**F**	**F**	**M**	**F**	**M**	**M**	**F**	**M**
SVL	44.59	43.19	44.15	40.82	43.71	41.66	42.72	41.65	35.87
TAL	R 36.77	–	R 22.26	R 39.76	R 31.39	36.85	R 28.85	–	39.44
TrunkL (mm)	19.82	17.87	18.65	16.85	19.36	18.44	19.80	18.27	16.71
HL (mm)	10.99	11.67	11.6	11.09	11.10	10.76	11.06	10.88	9.59
HW (mm)	8.63	8.12	8.56	8.48	8.28	7.95	8.21	8.26	7.18
HH (mm)	2.95	4.20	3.80	4.00	3.52	3.77	3.86	3.60	3.17
OD	2.35	2.35	2.50	2.51	2.62	2.35	2.62	2.21	2.08
EL	0.47	0.65	0.85	0.69	0.76	0.64	0.48	0.47	0.54
CL	8.03	8.59	9.01	8.74	8.15	8.01	7.80	8.15	7.94
FL	10.39	10,.68	11.10	9.94	10.93	10.73	10.13	10.40	8.49
NE	3.30	3.40	3.75	3.44	3.61	3.35	3.55	3.43	2.99
SE	4.48	4.50	4.95	4.68	4.56	4.31	4.67	4.46	3.72
EE	3.72	3.21	3.65	3.76	3.66	3.31	3.57	3.10	3.12
IN	1.55	1.55	1.48	1.45	1.45	1.40	1.34	1.39	1.22
IO	4.29	4.33	4.22	4.54	4.33	3.45	4.19	4.21	3.74
N° lamellae 1st toe (Right/Left)	4/3	5/5	4/5	4/5	4/4	4/4	4/3	4/3	5/4
N° lamellae 4th toe (Right/Left)	5/5	7/5	6/6	6/5	6/7	5/5	6/5	6/6	6/6
N° lamellae 1st finger (Right/Left)	3/4	4/	4/4	3/3	4/4	5/4	4/3	3/4	3/3
N° lamellae 4th finger (Right/Left)	6/7	5/6	6/7	6/6	5/6	5/6	6/4	5/7	7/6
N° postmental	2	2	2	2	2	2	2	2	2
N° infralabial	9	8	8	9	9	9	9	9	9
N° supralabial	8	10	10	10	9	9	10	9	9
N° internasal	1	1	1	1	1	1	1	2	1
N° scales ear to eye	17	18	16	17	12	13	14	15	16
N° scales eye to nostril	11	13	11	12	11	10	11	10	12
N° scales eye to eye	17	20	15	16	16	15	17	18	16

uniformly light cream pink from snout to posterior region of the cloaca. Tail slightly darker than the dorsum dorsally, being even darker in the ventral section, with white lateral spine-like scales on original tail. Last fourth portion of tail black. ***In preservative*** (After 4 months in preservation; Fig. 4): dorsal pattern persistent as "*in life*" with dorsal colouration whitish-greyish. Dark section more marked.

Distribution. (Fig. 6). This species has only been found at two sites in a very restricted region, in southern Benguela Province. The area lies above the first elevational range recognised for southern Angola's orographic relief, with specimens retrieved between 400 m and 650 m a.s.l. It can be broadly characterised as a rugged and transitional semi-arid landscape, albeit more vegetated and less arid than the coastal lowlands to the west and less mountainous and forested than eastern regions neighbouring the great escarpment. Despite its unique and unmistakable features, this species had eluded previous surveys conducted in coastal Benguela Province. In the last 5 years our team visited the

Table 4. Morphological (morphometric and meristic) of *Kolekanos plumicaudus*. Measurements are represented in millimetres (mm). For abbreviations, see Material and methods section, R = regenerated, M = male, F = female.

Species	*K. plumicaudus*	*K. plumicaudus*	*K. plumicaudus*	*K. plumicaudus*	*K. plumicaudus*	*K. plumicaudus*	*K. plumicaudus*	*K. plumicaudus*	*K. plumicaudus*	*K. plumicaudus*
Catalogue#	**MNCN 50770**	**FKH-0661**	**FKH-0663**	**PEM R18010**	**PEM R18014**	**PEM R18011**	**PEM R18015**	**PEM R18012**	**PEM R18013**	**PEM R18047**
Status	–	–	–	–	–	–	–	–	–	–
Sex	**F**	**F**	**F**	**F**	**M**	**M**	**F**	**F**	**F**	**M**
SVL	41.91	38.45	40.22	42.05	42	36.57	41.84	36.97	41.84	37.38
TAL	R 34.14	R 34.38	41.91	40.34	–	R 26.35	–	33.34	–	34.68
TrunkL (mm)	19.08	17.84	19.07	18.35	18.38	16.20	18.41	16.97	19.38	20.03
HL (mm)	10.04	9.42	9.89	11.11	11.17	10.59	11.59	10.22	11.53	10.98
HW (mm)	7.03	6.91	6.81	6.71	7.07	6.29	7.13	6.92	7.35	6.70
HH (mm)	3.50	3.38	3.27	3.45	3.19	2.76	3.62	2.90	3.21	30.70
OD	2.08	2.28	2.17	2.35	2.31	2.11	2.34	2.14	2.42	2.10
EL	0.59	0.49	0.50	0.71	0.79	0.58	0.63	0.87	0.75	0.62
CL	8.15	7.39	8.11	8.90	8.34	7.33	7.45	8.05	8.41	7.85
FL	10.75	8.77	9.69	10.38	11.76	10.54	12.42	11.85	12.86	12.66
NE	2.91	2.80	2.97	3.15	3.23	3.15	3.49	2.83	3.32	3.06
SE	3.89	3.61	3.65	4.18	4.07	3.98	4.13	3.92	4.24	4.18
EE	3.71	3.00	3.49	3.47	3.45	2.91	3.49	3.19	3.25	2.96
IN	1.30	1.29	1.24	1.30	1.21	1.11	1.25	1.26	1.45	1.43
IO	3.71	3.57	3.78	3.16	3.06	3.03	3.29	3.19	3.46	3.04
N° lamellae 1st toe (Right/Left)	4/4	3/3	4/3	4/4	4/4	4/4	4/4	6/6	5/4	4/4
N° lamellae 4th toe (Right/Left)	6/5	5/6	5/6	6/6	7/7	6/6	7/4	5/6	6/7	7/8
N° lamellae 1st finger (Right/Left)	3/4	3/4	3/4	4/4	4/4	4/4	4/4	4/4	4/4	4/4
N° lamellae 4th finger (Right/Left)	d/6	6/6	6/6	6/6	8/8	7/7	8/8	7/7	7/7	7/7
N° postmental	2	1	2	3	2	2	2	3	2	2
N° infralabial	8	8	9	9	9	9	9	9	9	9
N° supralabial	10	10	10	10	9	10	9	10	9	10
N° internasal	1	1	1	0	1	0	0	1	1	1
N° scales ear to eye	13	14	15	17	17	17	18	16	15	17
N° scales eye to nostril	11	9	11	10	9	10	8	8	8	9
N° scales eye to eye	15	14	15	16	18	15	14	15	15	14

same area at least five times preceding the discovery, spending at least two days per survey. Even though we found the species to be relatively common at the two referred sites, we failed to confirm its presence in several other locations with presumably suitable habitat, suggesting that it might be highly specialised and sensitive to local environmental conditions. It is possible for the species to be more common and widely distributed in poorly-surveyed regions to the southeast or north of its known range and we recommend further surveys in the region to address the conservation status of this poorly-known species.

Habitat and natural history notes. (Fig. 7). The local habitat, at both sites where the species was discovered, seems to be a transitional zone in coastal Angola, displaying a rich vegetation mosaic of acacia and mopane savannah, including *Senegalia mellifera*, *Senegalia* spp., *Colophospermum mopane*, *Terminalia prunioides*, *Commiphora* spp. and presence of succulents, such as *Euphorbia* spp. and *Aloe littoralis*. In contrast, and despite being known from a relatively wider region and

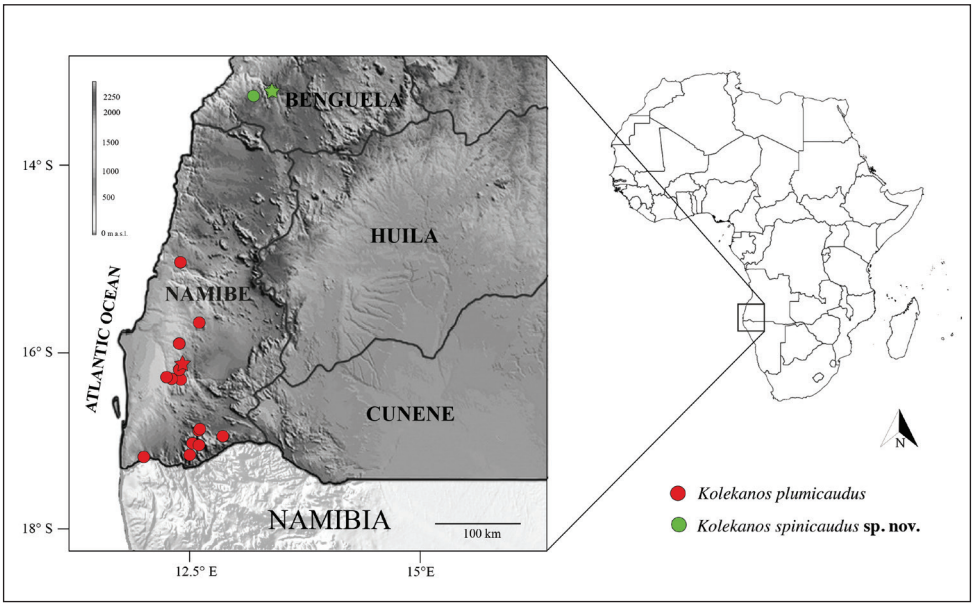

Figure 6. Geographical records of *Kolekanos* within Angolan territory. Red circles depict records of *K. plumicaudus*; green circles represent *K. spinicaudus* sp. nov. Stars represent type localities. Background grey scale represent elevation (Huntley and Ferrand 2019).

across considerable elevational ranges, *K. plumicaudus* is found in much more arid and sparsely vegetated environments. The new species was mostly found at night foraging in the ecotone between the trees/bushes and moderate to large granite boulders. One individual (not collected) was retrieved while sheltering under a rock flake during the day, behaviour which has been documented for the closely-related *K. plumicaudus* (Agarwal et al. 2017; Vaz Pinto et al. 2021). When not stretched horizontally, this species curls the tail laterally, but not upwards, while *K. plumicaudus* often erects the tail upwards and may wave the tip (Agarwal et al. 2017). The first individual observed was seen running fast on the ground between a granite boulder and a tree, but more often, they were found perched on branches and once on a grass stem. Unlike *K. plumicaudus*, which readily jumps amongst thin branches when disturbed, *K. spinicaudus* sp. nov. seems to prefer to run along thicker branches or drop to the ground and run for safety. Two individuals were observed mating at night (18 August 2021 19 h 55 m) on a thin branch of *Salvadora persica*. One female specimen (FKH-0645) collected in November 2021 contained two well-developed eggs. This species has been found in syntopy with another Angolan leaf-toed gecko, *Bauerius ansorgii*. Finally, due to the complex biogeography of Angola, an updated and stabilized biogeographic classification, especially for south-western Angola, is still lacking. Current schemes depend on the authors interpretation and underlying data used (e.g. phytocoria, centres of endemism, realms, biomes, ecoregions) resulting in different units recognised and sharp boundaries (Burgess et al. 2004; Dinerstein et al. 2017) which often do not match the situation on the ground. Thus, we cannot

Figure 7. Habitat of *Kolekanos spinicaudus* sp. nov. at **A** Carivo and **B** Ekongo. Photos Javier Lobón-Rovira.

currently assign any specific biogeographic region to any of these two taxa and are anticipating a better review of Angolan biogeographic units through Huntley (in prep.) in the near future.

Conservation status. The species seems relatively common, but highly localised. Although the general habitat does not appear to be threatened, more research is needed to confirm if the species' distribution is larger than currently known. Therefore, following the IUCN Red List guidelines (IUCN 2022), the species should be considered as Data Deficient (DD).

Discussion

Using molecular and morphological evidence, we herein described a new leaf-toed gecko, from southern Benguela Province, Angola, *Kolekanos spinicaudus* sp. nov., thereby adding another species to the growing list of gekkonids described in the last decade from this poorly-known African country (Ceríaco et al. 2020a, b; Marques et al. 2020; Branch et al.

2021; Lobón-Rovira et al. 2021; Conradie et al. 2022b). The recognition of *K. spinicaudus* sp. nov. as a sister species of *K. plumicaudus*, contradicts the previous knowledge of mainland circum-Indian Ocean leaf-toed geckos as monotypic genera (Lobón-Rovira et al. 2022a) and reinforces the need of further investigation on the potential cryptic diversification within another related species, such as *Afrogecko porphyreus* (Heinicke et al. 2014). Therefore, we provide a new perspective for future work within this group, which may improve the knowledge regarding Angolan and western African gekkonid diversity.

The molecular analysis, provided in this work, has shown a large divergence of the ND2 mitochondrial gene between *K. spinicaudus* sp. nov. and *K. plumicaudus*, being even higher than the molecular divergence found between closely-related genera, such as with *Rammigekko* and *Cryptactites*. However, the external morphological similarities between these two taxa support differentiation only at species level. This high divergence can be explained by the ancient character of this group (Heinicke et al. 2014), having persisted through extreme climatological and environmental changes and, consequently, experiencing long isolation periods in southwest Africa (Chase et al. 2009; Garzanti et al. 2018). Both species revealed notable genetic intraspecific variation between close localities, which can, in both cases, be explained by the high ecological specialisation in these geckos, promoting and maintaining isolation and by the relatively fast mtDNA evolutionary rates (Jesus et al. 2006).

Regarding interspecific variation, both species have exhibited a high degree of morphological and ecological differentiation. While *K. plumicaudus* presented a more slender head and body and seems more strongly associated with the more arid environments of the Angolan Kaokoveld Desert in Namibe Province, the sister species, *K. spinicaudus* sp. nov. presented a more robust head, body and limbs and is apparently only found in the semi-arid savannahs of Benguela Province (Lobón-Rovira et al 2021). The two species are quite agile and often found foraging in bushes. *Kolekanos plumicaudus* sometimes wag their tail semi-erected when disturbed and readily jumps amongst thin branches as a primary escape strategy (Agarwal et al. 2017; Vaz Pinto et al. 2021), while *K. spinicaudus* sp. nov., when threatened, is primarily a swift runner either along branches or on the ground. These behavioural differences may likely reflect subtle adaptations to local conditions, including vegetation cover, predation, foraging and sheltering habits. In addition, both species present a distinctive tail ornamentation that can be used as a clear morphological diagnostic feature between them. These findings seem to be consistent with the idea that habitat diversity leads to species and morphological diversification (Losos and Parent 2009; Tejero-Cicuéndez et al. 2021).

Some of the osteological features provided by Heinicke et al. (2014) seem to be non-homoplastic apomorphic characters for *Kolekanos* genus, such as ectopterygoid width more or less constant along the length of the bone, prootic contacting the epipterygoid far behind from the posterior process of the postorbitofrontal and groove associated with the surangular foramen and coronoid abutting the dentary. We failed to recover some of the proposed characters for either of the two species of *Kolekanos*, such as jugal bone being very reduced, almost vestigial (versus moderated size) and anterolateral corner of parietal not clasping the frontal (versus clasping anterolateral section). Furthermore, the *K. plumicaudus* CT-scanned in this work was not fully concordant

with the diagnosis presented in the description of this unique genus (Heinicke et al. 2014), for example, fused nasal bones and well-developed postorbitofrontal bone (versus unfused nasal bones and reduced, almost vestigial, postorbitofrontal bone, Heinicke et al. 2014). However, this difference could be associated with sexual dimorphism, since the only two specimens of *K. plumicaudus* represent one of each sex. Thus, this work underlines the importance of using larger series of material to fully infer diagnostic characters between species (Lobón-Rovira et al. 2021) and these being even more important to infer osteological variability (Bochaton et al. 2018), including sexual dimorphism. While we consider that the external diagnostic characters are sufficient to identify these species, we suggest caution while using the osteological differences to distinguish these two taxa due to the small sampling size available.

We here provide another example of diversification in south-western Angola, leading to speciation in the more arid desert ecosystems of Namibe Province and in the semi-arid coastal savannahs of Benguela Province, a pattern that has been found in other studies (e.g. *Hemidactylus benguellensis*-group, Lobón-Rovira et al. 2021). Our findings underline the remarkable herpetological value of coastal Benguela Province and particularly as a potential gekkonid hotspot. We have confirmed at Carivo that at least 14 species, representing all eight Angolan genera, are living in sympatry. This is the highest number of gekkonid species recorded in a single site in the country. In addition, we also report, for the first time, the two endemic Angolan leaf-toed gecko genera (*Bauerius* and *Kolekanos*) found in syntopy in both localities where *K. spinicaudus* sp. nov. has been found.

To conclude, we recommend additional surveys in Benguela Province to study the distribution and abundance of this new species to assess its conservation status and further research is needed in northern Namibe Province to explore potential contact zones between the two *Kolekanos* species. Due to the high genetic divergence between the two recorded populations of *K. spinicaudus* sp. nov., we also suggest caution when addressing conservation strategies in western Angola, since it may affect ongoing speciation processes within *Kolekanos* in this region.

Acknowledgements

We thank Alvarito Eugénio, the owner of Carivo Farm, where we performed frequent surveys and where topotypical material was recovered, for his very kind hospitality. We also thank Luis Pittagrós and "Bibi" for their logistical support and precious advice. In addition, the INBC – Instituto Nacional da Biodiversidade e Conservação within the Ministry of Culture, Tourism and Environment (MCTE) and especially Director of INBC, Drª Albertina Nzuzi, for issuing research and export permits (no. 01/2021). We thank Fernanda Lages and ISCED – Instituto Superior de Ciências da Educação da Huíla for logistical support. We are grateful to Vladimir Russo from Fundação Kissama for critical administrative and logistical support. We also thank to Alberto Sanchez Vialas from MNCN for providing the photos and detailed information of type material. Afonso Vaz Pinto for unconditional support and collecting in the field. Special thanks to Aaron Bauer for providing the raw files for the CT reconstruction of the CAS specimen. We also thank Centre

for Molecular Analysis (CTM) workers (especially Susana Lopes, Sofia Mourão and Patricia Ribeiro) at CIBIO for their tireless work and support in the molecular lab. To Fatima Linares from Centro de Instrumentación Científica of Granada for her incredible work on the CT scanning. JLR and NLB are currently supported by Fundação para a Ciência e Tecnologia (FCT) contracts PD/BD/140808/2018 and PD/BD/140810/2018, and BIOPOLIS 2022-18 and 2022-19. This work was supported by the European Union's Horizon 2020 Research and Innovation Programme under the Grant Agreement Number 857251 and by National Funds through FCT-Fundação para a Ciência e Tecnologia, under the scope of project UIDP/50027/2020. Finally, we thank to Stuart Nielsen and an anonymous reviewer for the comments, which certainly have improved this manuscript.

References

Agarwal I, Ceríaco LMP, Bauer AM, Bandeira SA (2017) *Kolekanos plumicaudus* (Slender Feather-tailed Gecko) Habitat use. Herpetological Review 48(3): 649–650.

Baptista NL, Vaz Pinto P, Keates C, Edwards S, Roedel MO, Conradie W (2021) A new species of red toad, *Schismaderma* Smith, 1849 (Anura: Bufonidae), from central Angola. Zootaxa 5081(3): 301–332. https://doi.org/10.11646/zootaxa.5081.3.1

Bauer AM, Menegon M (2006) A new species of prehensile-tailed gecko, *Urocotyledon* (Squamata: Gekkonidae), from the Udzungwa Mountains, Tanzania. African Journal of Herpetology 55(1): 13–22. https://doi.org/10.1080/21564574.2006.9635537

Bauer AM, Branch WR, Good DA (1997) The taxonomy of the southern African leaf-toed geckos (Squamata: Gekkonidae), with a review of old world. Proceedings of the California Academy of Sciences 49(14): 447–497.

Bochaton C, Daza JD, Lenoble A (2018) Identifying gecko species from Lesser Antillean paleontological assemblages: Intraspecific osteological variation within and interspecific osteological differences between *Thecadactylus rapicauda* (Houttuyn, 1782) (Phyllodactylidae) and *Hemidactylus mabouia* (Moreau de Jonnès, 1818)(Gekkonidae). Journal of Herpetology 52(3): 313–320. https://doi.org/10.1670/17-093

Branch WR, Conradie W (2013) *Naja annulata annulata* (Bucholtz & Peters, 1876). African Herp News 59: 50–53.

Branch WR, Conradie W, Vaz Pinto P, Tolley K (2019a) Another Angolan Namib endemic species: a new *Nucras* Gray, 1838 (Squamata: Lacertidae) from south-western Angola. Amphibian & Reptile Conservation 12(2): 85–95.

Branch WR, Baptista N, Keates C, Edwards S (2019b) Rediscovery, taxonomic status, and phylogenetic relationships of two rare and endemic snakes (Serpentes: Psammophiinae) from the southwestern Angolan plateau. Zootaxa 4590(3): 342–366. https://doi.org/10.11646/zootaxa.4590.3.2

Branch WR, Schmitz A, Lobón-Rovira J, Baptista NL, António T, Conradie W (2021) Rock island melody: A revision of the *Afroedura bogerti* Loveridge, 1944 group, with descriptions of four new endemic species from Angola. Zoosystematics and Evolution 97(1): 55–82. https://doi.org/10.3897/zse.97.57202

Burgess N, Hales JD, Underwood E, Dinerstein E, Olson D, Itoua I, Schipper J, Ricketts T, Newman K (2004) Terrestrial ecoregions of Africa and Madagascar – a conservation assessment. Island Press, Washington (DC), 501 pp.

Ceríaco LMP, Marques MP, Bandeira S, Agarwal I, Stanley EL, Bauer AM, Heinicke MP, Blackburn DC (2018a) A new earless species of *Poyntonophrynus* (Anura, Bufonidae) from the Serra da Neve Inselberg, Namibe Province, Angola. ZooKeys 780: 109–136. https://doi.org/10.3897/zookeys.780.25859

Ceríaco LMP, Agarwal I, Marques MP, Bauer AM (2020a) A review of the genus *Hemidactylus* Goldfuss, 1820 (Squamata: Gekkonidae) from Angola, with the description of two new species. Zootaxa 4746(1): 1–71. https://doi.org/10.11646/zootaxa.4746.1.1

Ceríaco LMP, Heinicke MP, Parker K, Marques MP, Bauer AM (2020b) A review of the African snake-eyed skinks (Scincidae: *Panaspis*) from Angola, with the description of a new species. Zootaxa 4747(1): 77–112. https://doi.org/10.11646/zootaxa.4747.1.3

Ceríaco LMP, Agarwal I, Marques MP, Bauer AM (2020c) A correction to a recent review of the genus *Hemidactylus* Goldfuss, 1820 (Squamata: Gekkonidae) from Angola, with the description of two additional species. Zootaxa 4861(1): 92–106. https://doi.org/10.11646/zootaxa.4861.1.6

Ceríaco LMP, Santos BS, Marques MP, Bauer AM, Tiutenko A (2021) Citizen science meets specimens in old formalin filled jars: A new species of Banded Rubber Frog, genus *Phrynomantis* (Anura: Microhylidae) from Angola. Alytes 38(1–4): 18–48.

Chase BM, Meadows ME, Scott L, Thomas DSG, Marais E, Sealy J, Reimer PJ (2009) A record of rapid Holocene climate change preserved in hyrax middens from southwestern Africa. Geology 37(8): 703–706. https://doi.org/10.1130/G30053A.1

Conradie W, Bourquin S (2013) Geographical Distributions: *Acontias kgalagadi kgalagadi* (Lamb, Biswas & Bauer, 2010). African Hep News 60: 29–30.

Conradie W, Branch WR, Measey GJ, Tolley KA (2012a) A new species of *Hyperolius* Rapp, 1842 (Anura: Hyperoliidae) from the Serra da Chela mountains, southwestern Angola. Zootaxa 3269(1): 1–17. https://doi.org/10.11646/zootaxa.3269.1.1

Conradie W, Measey GJ, Branch WR, Tolley KA (2012b) Revised phylogeny of African sand lizards (*Pedioplanis*), with the description of two new species from south-western Angola. African Journal of Herpetology 61(2): 91–112. https://doi.org/10.1080/21564574.2012.676079

Conradie W, Branch WR, Tolley KA (2013) Fifty shades of grey: giving colour to the poorly known Angolan Ashy reed frog (Hyperoliidae: *Hyperolius cinereus*), with the description of a new species. Zootaxa 3635(3): 201–223. https://doi.org/10.11646/zootaxa.3635.3.1

Conradie W, Deepak V, Keates C, Gower DJ (2020a) Kissing cousins: a review of the African genus *Limnophis* Günther, 1865 (Colubridae: Natricinae), with the description of a new species from north-eastern Angola. African Journal of Herpetology 69(1): 79–107. https://doi.org/10.1080/21564574.2020.1782483

Conradie W, Keates C, Lobón-Rovira J, Vaz Pinto P, Verburgt L, Baptista NL, Harvey J, Júlio T (2020b) New insights into the taxonomic status, distribution and natural history of De Witte's Clicking Frog (*Kassinula wittei* Laurent, 1940). African Zoology 55(4): 311–322. https://doi.org/10.1080/15627020.2020.1821771

Conradie W, Baptista NL, Verburgt L, Keates C, Harvey J, Júlio T, Neef G (2021) Contributions to the herpetofauna of the Angolan Okavango-Cuando-Zambezi river drainages.

Part 1: Serpentes (snakes). Amphibian & Reptile Conservation 15(2)[General Section]: 244–278. [e292]

Conradie W, Keates C, Baptista NL, Lobón-Rovira J (2022a) Taxonomical review of *Prosymna angolensis* Boulenger, 1915 (Elapoidea, Prosymnidae) with the description of two new species. ZooKeys 1121: 97–143. https://doi.org/10.3897/zookeys.1121.85693

Conradie W, Schmitz A, Lobón-Rovira J, Becker FS, Vaz Pinto P, Hauptfleisch ML (2022b) Rock island melody remastered: two new species in the *Afroedura bogerti* Loveridge, 1944 group from Angola and Namibia. Zoosystematics and Evolution (in press).

Conroy CJ, Papenfuss T, Parker J, Hahn NE (2009) Use of Tricaine Methanesulfonate (MS222) for Euthanasia of Reptiles. Journal of the American Association for Laboratory Animal Science [JAALAS] 48: 28–32.

Daza JD, Abdala V, Thomas R, Bauer AM (2008) Skull anatomy of the miniaturized gecko *Sphaerodactylus roosevelti* (Squamata: Gekkota). Journal of Morphology 269(11): 1340–1364. https://doi.org/10.1002/jmor.10664

De Queiroz K (1998) The general lineage concept of species, species criteria, and the process of speciation: a conceptual unification and terminological recommendations. In: Howard DJ, Berlocher SH (Eds) Endless forms: species and speciation. Oxford University Press, New York, 57–75.

Dinerstein E, Olson D, Joshi A, Vynne C, Burgess ND, Wikramanayake E, Hahn N, Palminteri S, Hedao P, Noss R, Hansen M, Locke H, Ellis EC, Jones B, Barber CV, Hayes R, Kormos C, Martin V, Crist E, Sechrest W, Price L, Baillie JEM, Weeden D, Suckling K, Davis C, Sizer N, Moore R, Thau D, Birch T, Potapov P, Turubanova S, Tyukavina A, de Souza N, Pintea L, Brito JC, Llewellyn OA, Miller AG, Patzelt A, Ghazanfar SA, Timberlake J, Klöser H, Shennan-Farpón Y, Kindt R, Barnekow Lillesø JS, van Breugel P, Graudal L, Voge M, Al-Shammari KF, Saleem M (2017) An Ecoregion-Based Approach to Protecting Half the Terrestrial Real. Bioscience 67(6): 534–545. https://doi.org/10.1093/biosci/bix014

Ernst R, Nienguesso ABT, Lautenschläger T, Barej MF, Schmitz A, Hölting M (2014) Relicts of a forested past: Southernmost distribution of the hairy frog genus *Trichobatrachus* Boulenger, 1900 (Anura: Arthroleptidae) in the Serra do Pingano region of Angola with comments on its taxonomic status. Zootaxa 3779(2): 297–300. https://doi.org/10.11646/zootaxa.3779.2.10

Ernst R, Schmitz A, Wagner P, Branquima MF, Hölting M (2015) A window to Central African forest history: Distribution of the *Xenopus fraseri* subgroup south of the Congo Basin, including arst country record of *Xenopus andrei* from Angola. Salamandra 51: 147–155.

Evans SE (2008) The skull of lizards and tuatara. In: Gans C, Gaunt S, Adler K (Eds) Biology of the Reptilia. Ithaca: Morphology H. Society for the Study of Amphibians and Reptiles 20, 1–347.

Gamble T, Greenbaum E, Jackman TR, Russell AP, Bauer AM (2012) Repeated origin and loss of adhesive toepads in geckos. PLoS ONE 7(6): e39429. https://doi.org/10.1371/journal.pone.0039429

Garzanti E, Dinis P, Vermeesch P, Andò S, Hahn A, Huvi J, Limonta M, Padoan M, Resentini A, Rittner M, Vezzoli G (2018) Dynamic uplift, recycling, and climate control on the petrology of passive-margin sand (Angola). Sedimentary Geology 375: 86–104. https://doi.org/10.1016/j.sedgeo.2017.12.009

Haacke WD (2008) A new leaf-toed gecko (Reptilia: Gekkonidae) from south-western Angola. African Journal of Herpetology 57(2): 85–92. https://doi.org/10.1080/21564574.2008.9635571

Hallermann J, Ceríaco LMP, Schmitz A, Ernst R, Conradie W, Verburgt L, Marques MP, Bauer AM (2020) A review of the Angolan House snakes, genus *Boaedon* Duméril, Bibron and Duméril (1854) (Serpentes: Lamprophiidae), with description of three new species in the *Boaedon fuliginosus* (Boie, 1827) species complex. African Journal of Herpetology 69(1): 29–78. https://doi.org/10.1080/21564574.2020.1777470

Heinicke MP, Daza JD, Greenbaum E, Jackman TR, Bauer AM (2014) Phylogeny, taxonomy and biogeography of a circum-Indian Ocean clade of leaf-toed geckos (Reptilia: Gekkota), with a description of two new genera. Systematics and Biodiversity 12(1): 23–42. https://doi.org/10.1080/14772000.2013.877999

Hoang DT, Chernomor O, Von Haeseler A, Minh BQ, Vinh LS (2018) UFBoot2: Improving the ultrafast bootstrap approximation. Molecular Biology and Evolution 35(2): 518–522. https://doi.org/10.1093/molbev/msx281

Huntley BJ, Ferrand N (2019) Angolan Biodiversity: Towards a modern Synthesis. In: Huntley BJ, Russo V, Lages F, Ferrand N (Eds) Biodiversity of Angola. Science and Conservation: A Modern Synthesis. Springer Nature, Cham, 3–14. https://doi.org/10.1007/978-3-030-03083-4_1

Jesus J, Brehm A, Harris DJ (2006) Phylogenetic relationships of *Lygodactylus* geckos from the Gulf of Guinea islands: Rapid rates of mitochondrial DNA sequence evolution? The Herpetological Journal 16(3): 291–295.

Kluge A (1983) Cladistic Relationships among Gekkonid Lizards. Copeia 1983(2): 465–475. https://doi.org/10.2307/1444392

Kumar S, Stecher G, Li M, Knyaz C, Tamura K (2018) MEGA X : Molecular Evolutionary Genetics Analysis across Computing Platforms. Molecular Biology and Evolution 35(6): 1547–1549. https://doi.org/10.1093/molbev/msy096

Lanfear R, Calcott B, Ho SY, Guindon S (2012) PartitionFinder: combined selection of partitioning schemes and substitution models for phylogenetic analyses. Molecular biology and evolution 29(6): 1695–1701.https://doi.org/10.1093/molbev/mss020

Lobón-Rovira J, Bauer AM (2021) Bone-by-bone: A detailed skull description of White-headed dwarf gecko *Lygodactylus picturatus* (Peters, 1870). African Journal of Herpetology 70(2): 1–20. https://doi.org/10.1080/21564574.2021.1980120

Lobón-Rovira J, Conradie W, Buckley Iglesias D, Ernst R, Veríssimo L, Baptista N, Vaz Pinto P (2021) Between sand, rocks and branches: An integrative taxonomic revision of Angolan *Hemidactylus* Goldfuss, 1820, with description of four new species. Vertebrate Zoology 71: 465–501. https://doi.org/10.3897/vz.71.e64781

Lobón-Rovira J, Conradie W, Vaz Pinto P, Keates C, Edwards S, Du Plessis A, Branch WR (2022a) Systematic revision of *Afrogecko ansorgii* (Boulenger, 1907) (Sauria: Gekkonidae) from western Angola. Zootaxa 5124(4): 401–430. https://doi.org/10.11646/zootaxa.5124.4.1

Lobón-Rovira J, Rocha S, Gower DJ, Perera A, Harris DJ (2022b) The unexpected gecko: A new cryptic species within *Urocotyledon inexpectata* (Stejneger, 1893) from the northern granitic Seychelles. Zootaxa 5150(4): 556–578. https://doi.org/10.11646/zootaxa.5150.4.5

Lobón-Rovira J, Vaz Pinto P, Becker FS, Tolley KA, Measey J, Bennet B, Boon B, de Sá S, Conradie W (2022c) An updated herpetofaunal species inventory of Iona National Park in southwestern Angola. Check List 18(2): 289–231. https://doi.org/10.15560/18.2.289

Losos JB, Parent CE (2009) The speciation-area relationship. In: Losos JB, Ricklefs RE (Eds) The theory of island biogeography revisited. Princeton University Press, Princeton, NJ, 415–438. https://doi.org/10.1515/9781400831920.415

Macey JR, Larson A, Ananjeva NB, Fang Z, Papenfuss TJ (1997) Two novel gene orders and the role of light-strand replication in rearrangement of the vertebrate mitochondrial genome. Molecular Biology and Evolution 14(1): 91–104. https://doi.org/10.1093/oxfordjournals.molbev.a025706

Marques MP, Ceríaco LMP, Blackburn DC, Bauer AM (2018) Diversity and distribution of the amphibians and terrestrial reptiles of Angola - Atlas of historical and bibliographic records (1840–2017). Proceedings of the California Academy of Sciences, Series 4, 65(2): 1–501.

Marques MP, Ceríaco LMP, Buehler MD, Bandeira S, Janota JM, Bauer AM (2020) A revision of the Dwarf Geckos, genus *Lygodactylus* (Squamata: Gekkonidae), from Angola, with the description of three new species. Zootaxa 4583 (3): 301–352. https://doi.org/10.11646/zootaxa.4853.3.1

Marques MP, Ceríaco LMP, Bandeira S, Pauwels OSG, Bauer AM (2019a) Description of a new long-tailed skink (Scincidae: *Trachylepis*) from Angola and the Democratic Republic of Congo. Zootaxa 4568(1): 51–68. https://doi.org/10.11646/zootaxa.4568.1.3

Marques MP, Ceríaco LM, Stanley EL, Bandeira SA, Agarwal I, Bauer AM (2019b) A new species of Girdled Lizard (Squamata: Cordylidae) from the Serra da Neve Inselberg, Namibe Province, southwestern Angola. Zootaxa 4668(4): 503–524. https://doi.org/10.11646/zootaxa.4668.4.4

Marques MP, Parrinha D, Santos BS, Bandeira S, Butler BO, Sousa ACA, Bauer AM, Wagner P (2022a) All in all it's just another branch in the tree: A new species of *Acanthocercus* Fitzinger, 1843 (Squamata: Agamidae), from Angola. Zootaxa 5099(2): 221–243. https://doi.org/10.11646/zootaxa.5099.2.4

Marques MP, Ceríaco LMP, Heinicke MP, Chehouri RM, Conradie W, Tolley KA, Bauer A (2022b) The Angolan Bushveld Lizards, genus *Heliobolus* Fitzinger, 1843 (Squamata: Lacertidae): integrative taxonomy and the description of two new species. Vertebrate Zoology 72: 745–769. https://doi.org/10.3897/vz.72.e85269

Miller MA, Pfeiffer W, Schwartz T (2010) Creating the CIPRES Science Gateway for Inference of Large Phylogenetic Trees. In: Gateway Computing Environments Workshop, 1–8. https://doi.org/10.1109/GCE.2010.5676129

Nguyen LT, Schmidt HA, Von Haeseler A, Minh BQ (2015) IQ-TREE: A fast and effective stochastic algorithm for estimating maximum-likelihood phylogenies. Molecular Biology and Evolution 32(1): 268–274. https://doi.org/10.1093/molbev/msu300

Nielsen SV, Conradie W, Ceríaco LMP, Bauer AM, Heinicke MP, Stanley EL, Blackburn DC (2020) A new species of Rain Frog (Brevicipitidae, *Breviceps*) endemic to Angola. ZooKeys 979: 133–160. https://doi.org/10.3897/zookeys.979.56863

Parrinha D, Marques MP, Heinicke MP, Khalid F, Parker KL, Tolley KA, Childers JL, Conradie W, Bauer AM, Ceríaco LM (2021) A revision of Angolan species in the genus *Pedioplanis* Fitzinger (Squamata: Lacertidae), with the description of a new species. Zootaxa 5032(1): 1–46. https://doi.org/10.11646/zootaxa.5032.1.1

Pyron RA, Burbrink FT, Wiens JJ (2013) A phylogeny and revised classification of Squamata, including 4161 species of lizards and snakes. BMC Evolutionary Biology 13(1): 1–54. https://doi.org/10.1186/1471-2148-13-93

Rocha S, Harris DJ, Posada D (2011) Cryptic diversity within the endemic prehensile-tailed gecko *Urocotyledon inexpectata* across the Seychelles Islands: Patterns of phylogeographical structure and isolation at the multilocus level. Biological Journal of the Linnean Society. Linnean Society of London 104(1): 177–191. https://doi.org/10.1111/j.1095-8312.2011.01710.x

Ronquist F, Teslenko M, Van Der Mark P, Ayres DL, Darling A, Hohna S, Larget B, Liu L, Suchard MA, Huelsenback JP (2012) MrBayes 3.2 : Efficient Bayesian Phylogenetic Inference and Model Choice Across a Large Model Space. Software for Systematic and Evolution 61(3): 539–542. https://doi.org/10.1093/sysbio/sys029

Stanley EL, Ceríaco LM, Bandeira S, Valerio H, Bates MF, Branch WR (2016) A review of *Cordylus machadoi* (Squamata: Cordylidae) in southwestern Angola, with the description of a new species from the Pro-Namib desert. Zootaxa 4061(3): 201–226. https://doi.org/10.11646/zootaxa.4061.3.1

Tamura K, Stecher G, Peterson D, Filipski A, Kumar S (2013) MEGA6 : Molecular Evolutionary Genetics Analysis V. 6.0. Molecular Biology and Evolution 30(12): 2725–2729. https://doi.org/10.1093/molbev/mst197

Tejero-Cicuéndez H, Simó-Riudalbas M, Menéndez I, Carranza S (2021) Ecological specialization, rather than the island effect, explains morphological diversification in an ancient radiation of geckos. Proceedings of the Royal Society B 288(1965): e20211821. https://doi:/10.1098/rspb.2021.1821

IUCN (2022) The IUCN Red List of Threatened Species. Version 2022-1. https://www.iucnredlist.org [accessed 10 February 2022]

Underwood G (1954) On the classification and evolution of geckos. Proceedings of the Zoological Society of London 124(3): 469–492. https://doi.org/10.1111/j.1469-7998.1954.tb07789.x

Vaz Pinto P, Luis Veríssimo L, Branch WR (2019) Hiding in the bushes for 110 years: rediscovery of an iconic Angolan gecko (*Afrogecko ansorgii* Boulenger, 1907, Sauria: Gekkonidae). Amphibian & Reptile Conservation 13(2): 29–41.

Vaz Pinto P, Conradie W, Becker F, Lobón-Rovira J (2021) Updated distribution of *Kolekanus plumicaudus* (Sauria: Gekkonidae), with some annotation on its natural history. Herpetology Notes 14: 1207–1212.

Wagner P, Butler BO, Ceríaco LM, Bauer AM (2021) A new species of the *Acanthocercus atricollis* (Smith, 1849) complex (Squamata, Agamidae). Salamandra (Frankfurt) 57: 449–463.

Supplementary material 1

Additional genetic material used for this work with their corresponding field numbers, catalog numbers and GenBank accession numbers

Authors: Javier Lobón-Rovira, Werner Conradie, Ninda L. Baptista, Pedro Vaz Pinto

Data type: Genetic material.

Explanation note: AMB – A. M. Bauer field series; AMS – Australian Museum; CAS – California Academy of Sciences; CHL – Colecção Herpetologica do Lubango, Angola; EBU – Evolutionary biology unit, Australian Museum; ERP – E.R. Pianka field series; FB – Francois Becker field series; FG/MV – F. Glaw/M. Vences field series; FKH – Fundação Kissama, Angola; FLMNH – Florida Museum of Natural History; JB – J. Boone personal collection; JVV – J.V. Vindum field series; GVH – G. Haagner field series; KTH – K. Tolley field series; MC – M. Cunningham personal collection; MCZ – Museum of Comparative Zoology, Harvard University; MNCN – Museo Nacional de Ciencias Naturales, Madrid, Spain; MVZ – Museum of Vertebrate Zoology, University of California, Berkeley; PEM – Port Elizabeth Museum (Bayworld); RAH – R.A. Hitchmough field series; ROM – Royal Ontario Museum; SAMA – South Australian Museum; TG – T. Gamble field series; WDH – W.D. Haacke personal collection; WRB – W.R. Branch field series; WC – W. Conradie field series; YPM – Yale Peabody Museum; ZSM – Zoologische Staatssammlung München. Dash (–) indicate no sequences available.

Link: https://doi.org/10.3897/zookeys.1127.84942.suppl1

Supplementary material 2

Results of the analysis of morphometric differences between *Kolekanos* spp. and sexes

Authors: Javier Lobón-Rovira, Werner Conradie, Ninda L. Baptista, Pedro Vaz Pinto

Data type: Morphological results.

Explanation note: Analyses were performed using permutational ANOVAs (for SVL, indicated as an *, and with an associated degrees of freedom of 1,14) and ANCOVAs (all the other variables, using SVL as a covariate). Significant results (p-values < 0.05) are highlighted in bold. For abbreviations see Material and methods section.

Link: https://doi.org/10.3897/zookeys.1127.84942.suppl2

Supplementary material 3

Principal Component Analysis (PCA) loadings for each morphological variable measured in of *Kolekanos* spp., including standard deviation (SD), percentage of variance (% Variance) and cumulative proportion for each component.

Authors: Javier Lobón-Rovira, Werner Conradie, Ninda L. Baptista, Pedro Vaz Pinto

Data type: Statistics.

Explanation note: For abbreviations, see Materials and Methods section.

Link: https://doi.org/10.3897/zookeys.1127.84942.suppl3

ZooKeys 1127: 119–134 (2022)
doi: 10.3897/zookeys.1127.84920
https://zookeys.pensoft.net

RESEARCH ARTICLE

A peer-reviewed open-access journal
ZooKeys
Launched to accelerate biodiversity research

Molecular and biometric data on *Carabus* (*Macrothorax*) *morbillosus* Fabricius, 1792 (Coleoptera, Carabidae) from Mid Mediterranean areas

Mariastella Colomba[1], Gabriella Lo Verde[2], Fabio Liberto[3], Armando Gregorini[1], Ignazio Sparacio[4]

1 *Department of Biomolecular Sciences, University of Urbino Carlo Bo, Via Maggetti 22, 61029 Urbino (PU), Italy* **2** *Dipartimento di Scienze Agrarie, Alimentari e Forestali (SAAF), Università degli Studi di Palermo, Viale delle Scienze edificio 5, 90128 Palermo, Italy* **3** *Via del Giubileo Magno 93, 90015 Cefalù (PA), Italy* **4** *Via Principe di Paternò 3, 90144 Palermo, Italy*

Corresponding author: Mariastella Colomba (mariastella.colomba@uniurb.it)

Academic editor: Pavel Stoev | Received 5 April 2022 | Accepted 28 September 2022 | Published 2 November 2022

https://zoobank.org/3713E09B-C25F-4DAB-B029-739318E042D4

Citation: Colomba M, Lo Verde G, Liberto F, Gregorini A, Sparacio I (2022) Molecular and biometric data on *Carabus* (*Macrothorax*) *morbillosus* Fabricius, 1792 (Coleoptera, Carabidae) from Mid Mediterranean areas. ZooKeys 1127: 119–134. https://doi.org/10.3897/zookeys.1127.84920

Abstract

The present study was carried out using molecular and biometric data of *Carabus* (*Macrothorax*) *morbillosus* from mid-Mediterranean areas to determine additional information on basal relationships among its representative subspecies. To this aim, two different kinds of approach were employed, including a morphometric analysis of four morphological parameters (i.e., elytra length, elytra width, pronotum length, pronotum width) of 128 specimens, and a Bayesian genetic analysis of 44 cytochrome oxidase subunit I (COI) partial sequences (i.e., 38 examined for the first time and six retrieved from GenBank database). Representative populations of *C.* (*M.*) *morbillosus* were sampled in four countries, namely Italy, Malta, Spain, and Tunisia. The present findings support the validity of four *C.* (*M.*) *morbillosus* subspecies, specifically *C.* (*M.*) *m. alternans*, *C.* (*M.*) *m. bruttianus*, *C.* (*M.*) *m. constantinus*, and *C.* (*M.*) *m. macilentus*, and redefine these subspecies' distributions. Notably, within the *C.* (*M.*) *m. constantinus* clade, two (i.e., Sardinia/Tuscany and Lampedusa) out of the three subgroups appear as homogeneous geographical groupings.

Keywords

Bayesian analysis, biogeography, carabids, COI, elytra, morphometric analysis, pronotum, taxonomy

Introduction

The genus *Carabus* Linnaeus, 1758 (Coleoptera, Carabidae) includes about 1000 species currently classified in over 91 subgenera. This genus is widespread in the Holarctic area but nearly all species are distributed in the Palearctic region including Japan, Iceland, Canary Islands, and North Africa, with only a few (11 species) in North America (Deuve 2004).

Carabids are mostly nocturnal predators represented by numerous brachypterous (i.e., wingless) species with low dispersal power, living in restricted areas, sometimes punctiform, and with extreme specialization towards particular environments (forests, grasslands, or agricultural landscapes) and prey (snails, earthworms, or caterpillars). Such a high degree of ecological differentiation is represented by numerous (morphological) subspecific forms (Březina 1999; Deuve 2004) but, despite the number of studies conducted so far (see Mossakowski 2003 and references therein; Osawa et al. 2004; Andújar et al. 2014), the global evolutionary history of this hyper-diverse genus still remains poorly understood.

Molecular genetic studies confirmed a substantial monophyly of the morphological subgroups of *Carabus* (Sota and Ishikawa 2004 and references therein; Deuve et al. 2012) which are subdivided into clades that diverged around 10 Mya (6.6–14.8). However, many issues on this topic remain unsolved, such as the correct dating of the speciation events using the molecular clock (Prüser and Mossakowski 1998; Andújar et al. 2012a, 2012b). In fact, following Andújar et al. (2012b), dates obtained either for the origin of the genus or for the split of different subgenera are in line with the hypothesis suggested by Deuve et al. (2012), whereas a recent study gives the origin of *Carabus* in the Eocene (Opgenoorth et al. 2021).

Within the large Carabidae family, speciation processes are probably due to geological and paleo-ecological events, and, for the Euro-Mediterranean area, they can be explained by the Eurasian forest fragmentation consequent to the Miocene climatic changes and subsequent Plio-Pleistocene climatic events (see also Prüser and Mossakowski 1998; Turin et al. 2003; Deuve et al. 2012). Particularly, during the Messinian salinity crisis (5.9−5.3 Mya), severe environmental changes occurred in the Mediterranean region leading to the reduction of tropical forests and to more xeric (hot and dry) habitats. Species which were adapted to tropical environments became extinct (Deuve 1998) and taxa (including *Carabus*) which resulted more suited to the new climatic conditions evolved and prevailed. More specifically, the colonization of mid-Mediterranean areas is testified by the dispersion of several taxa such as the subgenus *Macrothorax* Desmarest, 1850 (Prüser and Mossakowski 1998), the Corso-Sardinian *C.* (*Eurycarabus*) *genei* Gené, 1839, *C.* (*Macrothorax*) *planatus* Chaudoir, 1843 (today endemic of montane forests of northern Sicily), and a number of subspecies of *C.* (*Macrothorax*) *rugosus* Fabricius, 1792 and *C.* (*Rhabdotocarabus*) *melancholicus* Fabricius, 1798 (Turin et al. 2003).

The subgenus *Macrothorax* was described by Desmarest (1850) and includes a group of species morphologically and geographically well-isolated in Western Mediterranean.

This subgenus is considered a Tyrrhenian element, pre-Quaternary, whose diffusion and speciation are correlated with the Messinian salinity crisis and with the Plio-Pleistocene events (Jannel 1941; Antoine 1955; Darnaud et al. 1981; Casale et al. 1982; La Greca 1984; Vigna Taglianti et al. 1993; Vigna Taglianti 1998; Turin et al. 2003). *Macrothorax* comprises also populations that seem to have originated in more recent times or, likely, from passive transport (see Casale et al. 1989; Turin et al. 2003). The larva is of the rostilabrous type, which brings this subgenus closer to the groups of more oriental origin.

Currently (see Löbl and Löbl 2017) the species listed in the subgenus *Macrothorax* are:

C. (*M.*) *morbillosus* Fabricius, 1792 (S-France, S-Spain, N-Morocco, N-Algeria, N-Tunisia, Corse, Sardinia, Tyrrhenian central Italy, Southern Calabria, Sicily, Sicilian islands and Malta);
C. (*M.*) *rugosus* Fabricius, 1792 (S-Spain, Portugal, N-Morocco);
C. (*M.*) *aumontii* Lucas, 1849 (NE-Morocco, NW-Algeria), type species;
C. (*M.*) *planatus* Chaudoir, 1843 (Sicily);
C. (*M.*) *meurguesianus* Ledoux, 1990 (Morocco) (Fig. 1).

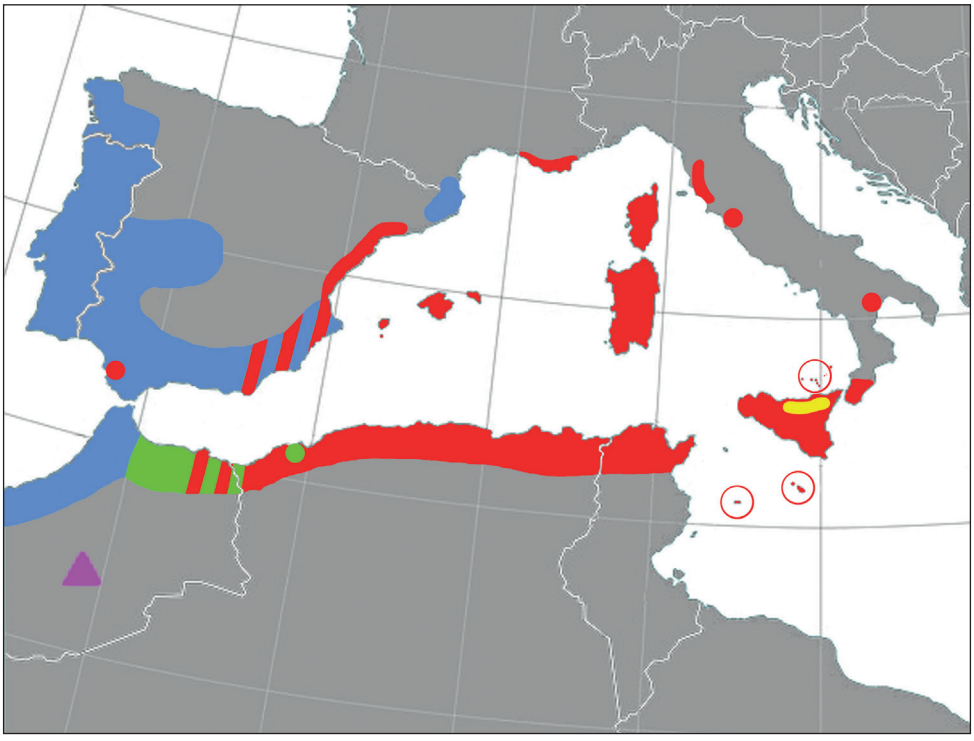

Figure 1. Distribution map of *Carabus* (*Macrothorax*) species in Mid Mediterranean areas. Red: *C.* (*M.*) *morbillosus*; yellow: *C.* (*M.*) *planatus*; blue: *C.* (*M.*) *rugosus*; green: *C.* (*M.*) *aumontii*; Purple triangle: *C.* (*M.*) *meurguesianus*.

These species live in varied habitats. *Carabus* (*M.*) *morbillosus* and *C.* (*M.*) *aumontii* mostly occur at low and medium altitudes in dense Mediterranean shrubland or palm forest soils with sufficient vegetation coverage, but also in areas with sparse vegetation or stony ground. *Carabus* (*M.*) *rugosus* and *C.* (*M.*) *planatus* are present in mountain and woodland environments.

With the exception of *C.* (*M.*) *planatus*, subspecies limited to well-defined geographic areas are ascribed to each of these species.

Considering only *C.* (*M.*) *morbillosus*, these subspecies include:

Carabus (*M.*) *m. morbillosus* Fabricius, 1792, locus typicus: "Mauretania" (Fabricius 1792).
Carabus (*M.*) *m. alternans* Palliardi, 1825, locus typicus: Sicilia (Palliardi 1825).
Carabus (*M.*) *m. macilentus* Lapouge, 1899, "sud de l'Espagne" (Lapouge 1899).
Carabus (*M.*) *m. cychrisans* Lapouge, 1899, NW-Algeria: Oran env. ? Maghnia (Lapouge 1899).
Carabus (*M.*) *m. galloprovincialis* Lapouge, 1910, locus typicus: Le Muy, Var, France (Lapouge 1910; Jannel 1941).
Carabus (*M.*) *m. constantinus* Lapouge, 1899, locus typicus: "Constantine [Algeria]" (Lapouge 1899).
Carabus (*M.*) *m. bruttianus* Born, 1906, locus typicus: "Calabria" (Born 1906).
Carabus (*M.*) *m. arborensis* Krausse, 1908, locus typicus: "Asuni [Sardinia, Italy]" (Krausse 1908).
Carabus (*M.*) *m. corsicanus* Lapouge, 1913, locus typicus: "Corsica" (Lapouge 1913).
Carabus (*M.*) *m. lampedusae* Born, 1925, locus typicus: "Lampedusa" (Born 1925).
Carabus (*M.*) *m. cheminorum* Deuve, 1988.

Many of these taxa are not accepted or have had different interpretations (Casale et al. 1982; Vigna Taglianti 1995; Březina 1999; Vigna Taglianti et al. 2002; Löbl and Smetana 2003; Turin et al. 2003; Deuve 2004; Vigna Taglianti 2009; Cavazzuti and Ghiretti 2020). The latest checklist of the Italian fauna reports *C.* (*M.*) *m. morbillosus* in Tuscany, Sardinia, and Sicily, *C.* (*M.*) *m. alternans* in Basilicata, Calabria, and Sicily, and *C.* (*M.*) *planatus* in Sicily (Casale et al. 2021).

The taxonomy and morphological characteristics of the main *morbillosus* subspecies accepted so far are briefly reported below.

Carabus (*M.*) *m. morbillosus*: N-Algeria SE-France (but the French populations were probably introduced from Kabylia: subsp. *cheminorum*). Pronotum widened anteriorly, sides arcuate, slightly narrowed anteriorly side, elytra elongate-ovate, subconvex, elytral sculpture with primary intervals catenulate, convex, 4th secondary interval evident, complete, tertiary intervals reduced, broken in rows of granulations, dorsal surface often darker and more polychromous, in some populations green to blue-violet.

Carabus (*M.*) *m. macilentus*: SE-Spain (Murcia, Catalonia), Algeciras (Cádiz), Balearic Islands. Pronotum narrowed anteriorly, the sides slightly arched, very short tertiary intervals, depressed elytra, cupreous dorsal surface normally dark, or greenish, the disc of the pronotum often blackish.

Carabus (*M.*) *m. constantinus*: NE-Algeria, Tunisia, Italy (Tuscany, Lazio: probably introduced), Sardinia, Corse, Lampedusa, SE-France (introduced probably from Corse). Elytra more convex; intervals less convex, 4th secondary interval fully reduced, tertiary intervals granulated but more evident than in the typical form, dorsal surface more constantly metallic bronze to reddish-cupreous.

Carabus (*M.*) *m. alternans*: Sicily, Calabria (Aspromonte), Basilicata, Malta. This population is differentiated from the other populations by a large shiny pronotum flattened posteriorly, with maximum width at middle and constricted forward; primary intervals elongated and slightly salient, secondary ribs depressed, tertiary intervals less raised than secondary ones, 1st elytral interstria deeply punctured with points sometimes juxtaposed; apex of aedeagus relatively short and wide, elytra elongate, rounded and dilated in the rear third, elytra apex short and sightly sinuate at sides.

A few years ago, Rapuzzi and Sparacio (2015) proposed the validity of *C.* (*M.*) *m. lampedusae* (Lampedusa) and *C.* (*M.*) *m. bruttianus* (S-Calabria, NE-Sicily: Messina and surrounding areas, Aeolian Islands).

Carabus (*M.*) *m. lampedusae* is similar to *C.* (*M.*) *m. constantinus* but shows a large and convex body shape and is less bright in color. Dark pronotum with basal sulci large and deep, side sinuate before hind angle, primary intervals wider, 1st elytral interstria with points on the surface, well separated from each other.

Carabus (*M.*) *m. bruttianus* is similar to *C.* (*M.*) *m. alternans* but is smaller and convex on elytron apex, less shiny, pronotum narrower and slightly rounded forward with maximum width in the fore half, elytra evidently shorter and oval, primary intervals in granules shorter and less raised, elytron apex stretched and clearly sinuate at side.

Likewise, Müller and Mifsud (2017) described *C.* (*M.*) *m. gozomaltensis* Müller & Mifsud, 2017 from Malta and Gozo Islands. These Maltese populations appear to be characterized by a smaller size and a darker coloration of the surface than Sicilian specimens, and a particular male genitalia structure.

To date interpretation of *C* (*M.*) *morbillosus* subspecies remains elusive. To contribute to this problem, we used both a morphometric analysis of four morphological characters (i.e., elytra length, elytra width, pronotum length, and pronotum width), and a genetic analysis of a fragment of the cytochrome oxidase subunit I (COI) gene to determine additional information on the basal relationships among representative populations of *C.* (*M.*) *morbillosus* in mid-Mediterranean areas. Our focus was on populations inhabiting central mainland Italy, Sardinia, Sicily, circum-Sicilian islands, Malta, Spain, the Balearic Islands, and Tunisia.

Materials and methods

Materials

A total of 128 *Carabus* (*M.*) *morbillosus* male specimens were studied in the morphometric analysis. Samples were collected in Italy (Lampedusa, Sardinia, Calabria,

Sicily, including four locations throughout the island, plus Messina province, which is interesting for its biogeographical connections with Calabria), Tunisia, and the Balearic Islands.

Morphometric analysis

For each specimen four characters were measured: length of elytra (**EL**), width of elytra (**EW**), length of pronotum (**PL**), width of pronotum (**PW**).

Morphometric characters were used in an exploratory cluster analysis (complete linkage, Euclidean distance) to determine if the combinations of biometric characters allow to delimit groups concordant with the subspecies. Afterwards, a discriminant analysis was performed to assess the usefulness of the recorded variables to identify groups. A principal component (**PC**) analysis was then performed using the same four morphometric factors. Since one character (PL) was not available for one specimen from Sardinia, 127 male specimens were used for the analyses. Moreover, analysis of mean differences of morphometric characters among groups was then performed with ANOVA, after data normalization by means of a Box-Cox transformation. All analyses were concluded with Tukey *post hoc* tests to compare the groups for each character ($p < 0.05$). Minitab software has been used throughout for all statistical analyses.

Molecular analysis

Molecular analysis was performed on 38 specimens of *C.* (*M.*) *morbillosus* from several localities: Malta [(collection site not available, (CMAL)]; Vizzini [Italy: Sicily (VIZ)]; Custonaci [Italy: Sicily (CUST)]; Corleone, Ficuzza [Italy: Sicily (FIC)]; Messina [Italy: Sicily (MES); Reggio Calabria [Italy: S-Calabria (RCAL)]; Lipari [Italy: Aeolian Islands (LIP)]; Olmedo Prepalzos [Italy: N-Sardinia (OLM)]; Capoterra and Is Cannoneris [Italy: S-Sardinia (SARD)]; Follonica [Italy: Tuscany (FOL)]; Castiglione della Pescaia [Italy: Tuscany (CAST)]; Lampedusa [Italy: Sicily, Pelagie Islands, (LAMP)]; Cap Gammarth (Tunisia (CGAM)]; Ses Mongetes, Citadella de Menorca [Spain: Balearic Islands, Menorca (MEN)]; and Lloc de Monges, [Spain: Balearic Islands, Menorca (MON)] (Fig. 2).

Samples were stored at –20 °C in test tubes. Total genomic DNA was isolated from a small piece of tissue taken from the ethanol-preserved specimens. The extractions were carried out using the Wizard Genomic DNA Purification Kit (Promega). All the DNA extractions were kept at 4 °C for short-time use. Undiluted or different dilutions (1:10–1:50, based on the DNA concentration) of each DNA extraction were used as templates for PCR amplification of a portion of the cytochrome oxidase subunit I (mt-COI) gene.

COI amplicons were obtained by the universal internal primers LCO1490 and HCO2198 as in Folmer et al. (1994) by the following PCR protocol: 95 °C for 5 min; 95 °C for 1 min, 50 °C for 1 min, 72 °C for 1 min (35 cycles); 72 °C for 10 min. To remove primers and unincorporated nucleotides, the amplified products were purified by the Wizard SV gel and PCR Clean-up Kit (Promega). Sequencing of the

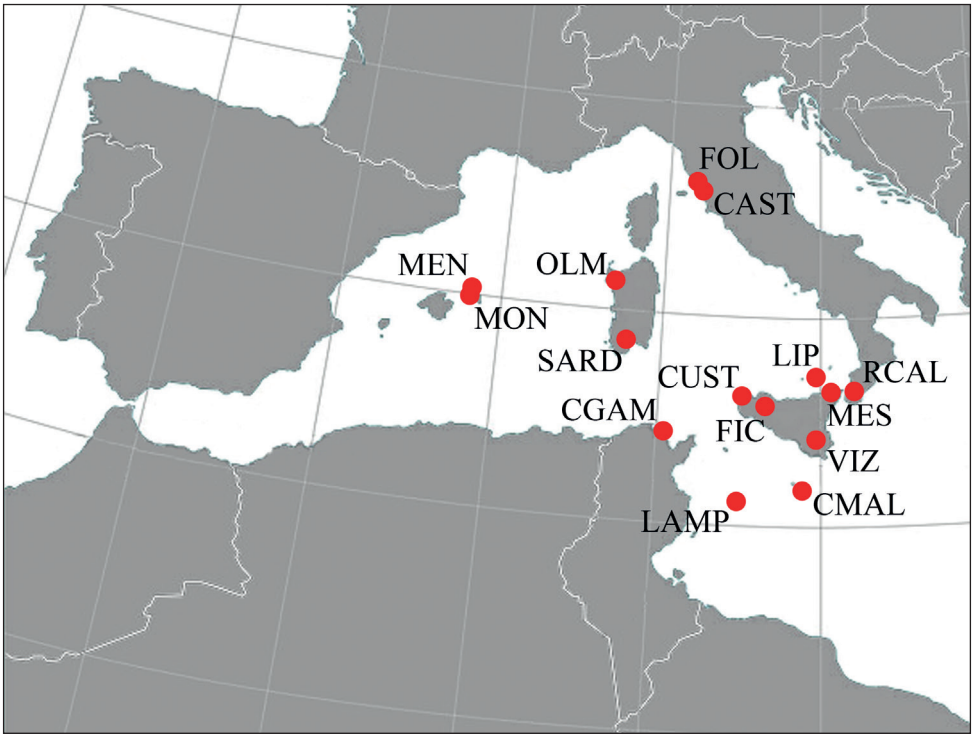

Figure 2. Collection sites of *C.* (*M.*) *morbillosus* specimens employed for molecular analyses are reported as red dots. Details and locality labels are described in the text.

purified PCR products was carried out using automated DNA sequencers at Eurofins MWG Operon (Germany). Sequence chromatograms of each amplified fragment were browsed visually. Sequences were visualized with BioEdit Sequence Alignment Editor 7 (Hall 1999), aligned with the ClustalW option included in this software and double checked by eye.

All sequences generated in the present study were deposited in NCBI GenBank (OM681023–OM681060).

Phylogenetic analyses were conducted in BEAST 1.6.1 (Drummond and Rambaut 2007) with 10×10^6 generations and 10% burnin. The best-fit evolution model of nucleotide substitution resulted in HKY+G (gamma = 0.128) with empirical base composition; the Yule Process tree prior for mitochondrial data with piecewise linear population size model was applied with a UPGMA-generated tree as the starting point. Trees were combined to produce an ultrametric consensus tree using TreeAnnotator 1.6.1. Support for nodes is expressed as posterior probabilities.

In addition, homologous sequences (retrieved from GenBank) of *Carabus rugosus* (JQ689882, JQ689892), *C. morbillosus alternans* (JQ646591), *C. morbillosus* (JQ689896-JQ689898, JQ689883, JX279622), *C. planatus* (JQ646589), *Calosoma sycophanta* (JQ693413), and *Cychrus semigranosus* (JQ689876) were included. *Campalita auropunctatum* (JQ689899) was used as outgroup (OG).

Results

Morphometric data

The dendrogram obtained from the cluster analysis (Fig. 3) highlights the localities which clearly group together. These are: (i) Messina/Calabria; (ii) Spain/Balearic Islands; and (iii) Tunisia/Lampedusa, corresponding respectively to the subspecies *C.* (*M.*) *m. bruttianus*, *C.* (*M.*) *m. macilentus*, and *C.* (*M.*) *m. constantinus*. The population from Sardinia, based on the morphometric characters used, would seem closer to the Sicilian population [*C.* (*M.*) *m. alternans*], although this requires further investigation, which certainly needs to consider other additional morphological characters. Moreover, despite the morphometric similarity between the populations from Tunisia and Lampedusa, we prefer to consider these two populations as separate groups in the following biometric analyses, thus analyzing separately all the populations which have been alternatively included in the *C.* (*M.*) *m. constantinus* group (Sardinia, Tunisia, and Lampedusa).

The results of the discriminant analysis, conducted on the groups from Sicily, Sardinia, Tunisia, Lampedusa, Messina/Calabria, and Spain/Balearic Islands, reveals that the proportion of correct attribution is 0.646 (Table 1). A higher correct classification of samples was found for Messina/Calabria and Spain/Balearic Islands (0.85 and 0.78, respectively), while the highest misclassification was found for Sardinia, with less than 50% correctly classified. For all the other populations, the proportion of correct classification ranged between 0.54 (Tunisia) and 0.61 (Lampedusa), thus confirming the need of a more comprehensive approach for a better characterization. The linear discriminant function shows that PL was the most relevant parameter in the group attribution, followed by EL and PW, while EW resulted the less discriminant parameter.

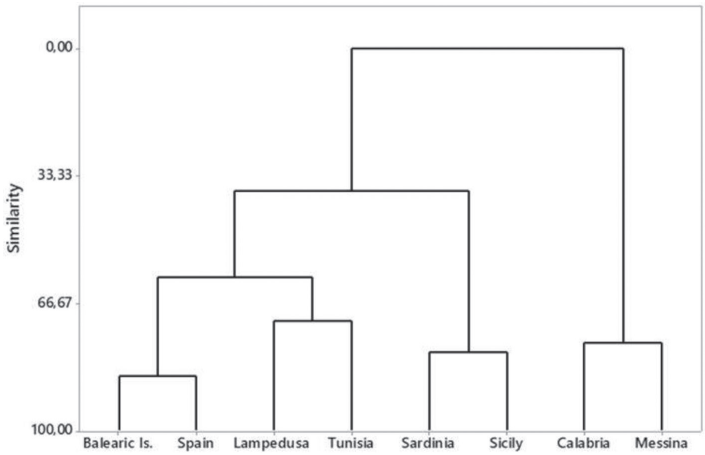

Figure 3. Similarity tree obtained from the cluster analysis based on the means of the four morphometric parameters. Morphological characters measured were as follows: elytra length, elytra width, pronotum length, pronotum width.

Table 1. Classification of *Carabus* (*Macrothorax*) *morbillosus* male specimens of the different groups determined by the discriminant analysis performed on all parameters. Coefficients of the discriminant function show the impact of each parameter in the correct attribution to the four groups.

	Lampedusa	Messina/Calabria	Sardinia	Sicily	Spain/Balearic Is.	Tunisia
Lampedusa	14	0	3	1	0	4
Messina/Calabria	0	28	2	4	3	0
Sardinia	1	1	8	2	0	1
Sicily	1	3	5	11	0	0
Spain/Balearic Is.	2	1	2	2	14	1
Tunisia	5	0	0	0	1	7
Total *N*	23	33	20	20	18	13
N correct	14	28	8	11	14	7
Proportion	0.61	0.85	0.4	0.55	0.78	0.54
N = 127		*N* correct = 82		Proportion correct = 0.646		
Linear Discriminant Function for groups						
	Lampedusa	Messina/Calabria	Sardinia	Sicily	Spain/Balearic Is.	Tunisia
Constant	−345.05	−274.38	−298.79	−303.67	−332.05	−366.62
Elytra width	−0.20	−0.16	−0.11	−0.08	−0.21	−0.20
Elytra length	2.20	1.73	1.84	1.86	2.01	2.27
Pronotum width	1.91	1.57	1.88	1.63	1.64	1.78
Pronotum length	2.24	2.84	2.43	2.71	2.97	2.56

Table 2. Biometrics (mean ± S.E.) of males of the different *Carabus* (*Macrothorax*) *morbillosus* groups. Different letters within the column indicate significant differences among group means (One-way ANOVA performed after Box-Cox transformation of data: EW $F_{5,122}$ = 11.52; EL $F_{5,122}$ = 46.58; PW $F_{5,122}$ = 22.94; PL $F_{5,121}$ = 10.84 followed by Tukey post-hoc test, $p < 0.05$).

Groups	No.	EW ± SE (min-max)	EL ± SE (min-max)	PW ± SE (min-max)	PL ± SE (min-max)
Calabria/Messina	33	103.94 ± 2.36 c (86–150)	166.45 ± 1.14 d (151–178)	71.55 ± 0.61 d (65–81)	58.36 ± 0.40 b (55–63)
Spain/Balearic Is.	18	108.28 ± 0.94 bc (100–114)	184.72 ± 1.79 b (170–200)	77.72 ± 1–16 bc (70–88)	63.33 ± 0.63 a (59–68)
Tunisia	13	116.62 ± 1.99 ab (105–130)	197.31 ± 2.97 a (180–220)	82.38 ± 1.06 a (77–90)	63.85 ± 0.96 a (59–70)
Lampedusa	23	113.43 ± 1.51 ab (100–133)	191.43 ± 1.70 ab (180–210)	81.61 ± 1.09 ab (74–90)	60.65 ± 0.96 b (54–70)
Sardinia	21 (20 for PL)	124.71 ± 5.28 ab (99–170)	175.57 ± 1.79 c (153–190)	77.60 ± 0.70 c (70–82)	58.57 ± 0.72 b (53–64)
Sicily	20	131.00 ± 5.48 a (98–180)	177.25 ± 1.44 c (166–192)	76.15 ± 0.85 c (70–82)	60.45 ± 0.34 ab (58–64)

Results of the statistical analysis for the examined morphometric parameters are reported in Table 2. Significant differences among groups were found for all considered parameters. The group of specimens from Calabria/Messina shows significantly lower values in three out of four parameters (EW, EL, and PW), confirming that *C.* (*M.*) *m. bruttianus* is clearly smaller than the other three groups. Sicily and Sardinia differed from Lampedusa and Tunisia for EL and PW. As expected, no significant differences were found between Sicily and Sardinia and between Tunisia and Lampedusa for all morphometric characters.

The PC analysis indicates that the four morphometric characters explained 83.2% of all variance, mainly related to PL, PW, and EL (PC1, 61.6%) (Fig. 4). Despite the overlapping of the different groups, the PC2 (mainly related to EW) seems to have a more relevant role in the two populations from Sicily and Sardinia compared to Lampedusa, Tunisia, and Spain/Balearic Islands.

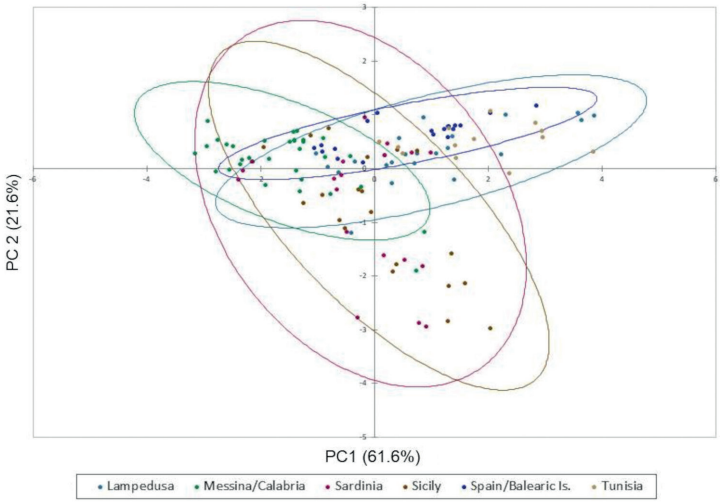

Figure 4. The principal component analysis applied to morphometric characters explained 83.2% of all variance. The first principal component (61.6%) is related to PL, PW and EL, whereas the second one (21.6%) is related to EW.

Molecular data

As shown in Fig. 5, the Bayesian analysis using COI partial sequences reveals several clearly distinct clusters. It is possible to distinguish the different genera included in the study, in particular, the genus *Calosoma* (represented by *Calosoma sycophanta*), the genus *Carabus* (represented by the species *C.* (*M.*) *rugosus*, *C.* (*M.*) *morbillosus* sspp., and *C.* (*M.*) *planatus*), the genus *Cychrus* (represented by *C. semigranosus*), and the genus *Campalita* (represented by *C. auropuctatum*, which in our analysis was chosen as the outgroup). Relationships between these genera are supported by a clear tree topology with high posterior probability values at the main nodes. Among *Carabus* species, posterior probability values are very high, and affinity relationships can be easily deduced from the tree topology. *Carabus* (*M.*) *rugosus* is sister of *C.* (*M.*) *morbillosus*, with *C.* (*M.*) *planatus* slightly more distant and sister of the clade *C.* (*M.*) *rugosus*/*C.* (*M.*) *morbillosus*. At the subspecific level, it is possible to clearly distinguish within *C.* (*M.*) *morbillosus* four clusters: the first contains the sequences of the specimens from Malta and Sicily together with a sequence retrieved from GenBank database (JQ646591) of a specimen sampled in "Italy" and reported as *C. morbillosus alternans*. According to our interpretation, this cluster contains specimens that can be ascribed with reasonable certainty to the subspecies

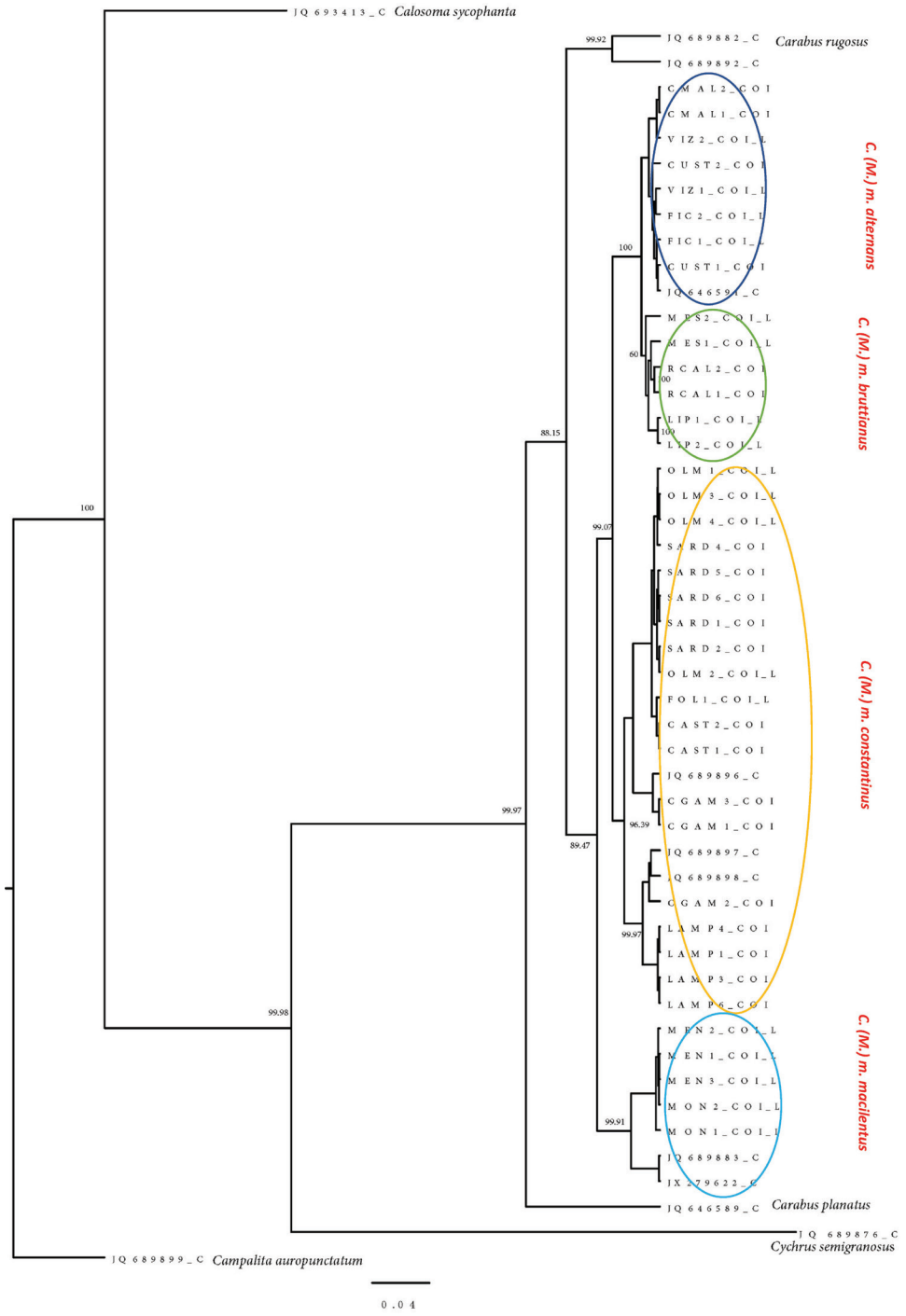

Figure 5. 50% majority rule Bayesian tree inferred from dataset including partial sequences of the mitochondrial COI genes available in the present paper along with homologous sequences retrieved from GenBank (see text for details). Nucleotide substitution model: HKY + G (gamma = 0.128). Numbers above branches represent Bayesian posterior probabilities. Scale bar represents units of length in expected substitutions per site.

C. (*M.*) *m. alternans*. The second group includes specimens from Messina (NE-Sicily), Reggio Calabria (S-Calabria), and Lipari (Aeolian Islands) and, in our opinion, these specimens belong to the subspecies *C.* (*M.*) *m. bruttianus*. The third group includes specimens from Sardinia, Tuscany, Tunisia, and Lampedusa plus three sequences (from Tunisia) from GenBank (JQ689896–JQ689898). This group, which is the biggest one, represents the subspecies *C.* (*M.*) *m. constantinus*. Finally, the fourth group includes specimens from the Balearics plus two sequences (JQ689883 and JX279622) from Spain reported as *C. morbillosus.* This group, in our interpretation, represents the subspecies *C.* (*M.*) *m. macilentus*. As regards the distances expressed in *p* distance (i.e., number of nucleotide substitutions), the subspecies *alternans* is 0.038 far from *constantinus*, and 0.045 from *macilentus*. A very small distance (0.014) separates *alternans* from *bruttianus*.

Discussion

The results of the morphometric and molecular analyses in this study show a significant agreement between hypothesized relationships of taxa. Combining information from the similarity tree and the phylogenetic tree, the validity of the subspecies *alternans*, *bruttianus*, *constantinus*, and *macilentus* is supported.

The subspecies *bruttianus* is only separated by a small genetic distance (ca 1%) from *alternans*, but the subspecific rank is supported by the tree topology. In addition, a comparison between the Calabria/Messina clustering obtained with morphometric analysis and the MES+RCAL+LIP cluster in the Bayesian tree clearly supports the validity of the subspecies *bruttianus*, as proposed by Rapuzzi and Sparacio (2015). As shown in Fig. 5, the posterior probability supporting the cluster is 60%. On closer examination, the RCAL and LIP sequences are very homogeneous (100%, each), so the overall posterior probability value drops to 60% due to the greater heterogeneity observed in the sequences of the Messina specimens. Given that it is probably necessary to analyze many more beetles from the hypothesized distribution area of *bruttianus*, these results may be explained by Messina specimens having undergone more rapid molecular change than morphological change. This could explain the difference in COI despite being rather morphologically similar to continental ones.

Within the large clade *constantinus*, out of three subgroups, two homogeneous geographic groupings were found in Sardinia (including also Tuscany) and Lampedusa, whereas the third one (Tunisia) appears to be more heterogeneous. Of the Sardinian specimens, all individuals cluster within the *constantinus* group, while the morphometric analysis shows them to be closer to *alternans*.

The molecular similarity between Sardinian and Tuscan populations is in agreement with their morphological similarity which, depending on different hypotheses, is considered the result of ancient passive transport (i.e., by anthropogenic transport, perhaps by the Phoenicians; Casale et al. 1989; Turin et al. 2003) or native (Vigna Taglianti 1998). If we wanted to distinguish at the subspecific level the populations of Sardinia and central Italy (Tuscany), *arborensis* could be used. However, we are fully

aware that the present data do not allow us to draw any definitive conclusions, which is worth exploring in a future study.

Although Lampedusa specimens are all included in a homogeneous geographical subgroup, the subspecific rank is only partially supported by the tree topology using COI data. However, such an outcome does not necessarily affect the validity of the subspecies which was diagnosed morphologically. Combining molecular with morphological monophylies, a subgenus is supported, but more in-depth study is needed by analyzing more morphological characters, more beetle specimens, and more genes (at least one nuclear) to obtain a clearer insight on the evolutionary paths followed by *morbillosus* in Italy and Tunisia. Of course, this larger study must also include beetles from Algeria, northern Morocco, and southeastern Spain.

In conclusion, our results provide new evidence supporting the validity of the *C.* (*M.*) *morbillosus* subspecies, *C.* (*M.*) *m. alternans*, C. (*M.*) *m. bruttianus*, *C.* (*M.*) *m. constantinus*, and *C.* (*M.*) *m. macilentus*, and we can redefine their distribution in mid-Mediterranean areas.

One latter consideration refers to *C.* (*M.*) *planatus* which was shown in the phylogenetic tree as the most distant *Macrothorax* species analysed. It is an endemic species that lives exclusively in the Nebrodi and Madonie woods of Sicily (Magistretti 1965; Bruno 1968; Rapuzzi 1992; Sparacio 1995; Busato and Casale 2004), at higher altitudes; externally, it looks like *C.* (*M.*) *rugosus* of Spain and Morocco. Darnaud et al. (1981) reported it as the most primitive species of the subgenus *Macrothorax*, in agreement with other authors (Prüser and Mossakowski 1998; Turin et al. 2003) who considered *C.* (*M.*) *planatus* as one of the most ancient species of the Mediterranean *Macrothorax*. This species was confused with *C.* (*M.*) *morbillosus* for many years (see Casale et al. 1982), despite that many authors, including Chaudoir (1843), noted that *C.* (*M.*) *morbillosus* and *C.* (*M.*) *planatus* are not the same species (see also Ragusa 1871, 1883, 1908, 1921; Vitale 1912), and this is worth further study.

Acknowledgements

We are grateful to all friends and colleagues who provided help and specimens used in the study. They are, in alphabetical order, Marcello Arnone, Marco Bastianini, Michele Bellavista, Giuseppe Maraventano, David Mifsud, Pietro Lo Cascio, Stefano Nappini, Roberto Pantaleoni, Elena Prazzi, Josep Quintana Cardona, Ivan Rapuzzi, and Marcello Romano. We also wish to thank José Serrano Marino for his comments and suggestions on the manuscript and Robert Forsyth for English revision.

References

Andújar C, Gómez-Zurita J, Rasplus J-Y, Serrano J (2012a) Molecular systematics and evolution of the subgenus *Mesocarabus* Thomson, 1875 (Coleoptera: Carabidae: *Carabus*), based

on mitochondrial and nuclear DNA. Zoological Journal of the Linnean Society 166(4): 787–804. https://doi.org/10.1111/j.1096-3642.2012.00866.x

Andújar C, Serrano J, Gómez-Zurita J (2012b) Winding up the molecular clock in the genus *Carabus* (Coleoptera: Carabidae): assessment of methodological decisions on rate and node age estimation. BMC Evolutionary Biology 12(1): e40. https://doi.org/10.1186/1471-2148-12-40

Andújar C, Arribas P, Ruiz C, Serrano J, Gomez-Zurita J (2014) Integration of conflict into integrative taxonomy: fitting hybridization in species delimitation of *Mesocarabus* (Coleoptera: Carabidae). Molecular Ecology 23(17): 4344–4361. https://doi.org/10.1111/mec.12793

Antoine M (1955) Coléoptères Carabiques du Maroc, I. Mémoire de la Société des Sciences Naturelles du Maroc 1: 1–177.

Born P (1906) Über einige *Carabus*. Formen aus Calabrien. Insekten-Börse 23: 1–6.

Born P (1925) *Carabus morbillosus lampedusae* nov. subspec. Societas Entomologica 7: 25–26.

Březina B (1999) World Catalogue of the Genus *Carabus* L. Pensoft, Sofia-Moscow, 170 pp.

Bruno S (1968) Distribuzione, morfologia ed ecologia del *Carabus* (*Macrothorax*) *planatus* Chaudoir, 1843 (Coleoptera, Carabidae, Carabinae). Bollettino Accademia Gioenia di Scienze Naturali (Serie 4) 9: 733–753.

Busato E, Casale A (2004) Note sul ciclo biologico e sulla morfologia pre-immaginale di *Carabus* (*Macrothorax*) *planatus* Chaudoir, 1843, specie endemica dell'Appennino siculo (Coleoptera, Carabidae). Studi Trentini di Scienze Naturali Acta Biologica 81: 177–187.

Casale A, Sturani M, Vigna Taglianti A (1982) Coleoptera Carabidae. I. Introduzione, Paussinae, Carabinae. Fauna d'Italia, XVIII. Edizioni Calderini, Bologna, 500 pp.

Casale A, Bastianini M, Minniti M (1989) Sulla presenza in Toscana di *Carabus* (*Macrothorax*) *morbillosus* Fabricius (Coleoptera, Carabidae, Carabini) e sul suo significato zoogeografico. Frustula Entomologica 10(1987): 67–72.

Casale A, Allegro G, Magrini P, Benelli A (2021) Insecta Coleoptera Carabidae. In: Bologna MA, Zapparoli M, Oliverio M, Minelli A, Bonato L, Cianferoni F, Stoch F (Eds) Checklist of the Italian Fauna. Version 1. https://www.lifewatchitaly.eu/en/initiatives/checklist-fauna-italia-en/checklist/ [Last update: 2021-05-31]

Cavazzuti P, Ghiretti D (2020) *Carabus* d'Italia. Natura Edizioni Scientifiche, Bologna, 380 pp.

Chaudoir M (1843) Carabique nouveaux. Bulletin de la Société Impériale des Naturalistes de Moscou 16: 671–795.

Darnaud J, Lecumberry M, Blanc R (1981) Coléoptères Carabidae, Genre *Macrothorax* Desmarest, 1850. Iconographie Entomologique, Coléoptères, planche 13: 8.

Desmarest ME (1850) In: Encyclopédie d'histoire naturelle ou traité complet de cette science d'après les travaux des naturalistes les plus éminents de tous les pays et de toutes les époques; Buffon, Daubenton, Lacépède, G. Cuvier, F. Cuvier, Geoffroy Saint-Hilaire, Latreille, de Jussieu, Brongniart, etc., etc. Ouvrage résumant les observations des auteurs anciens et comprenant toutes les découvertes modernes jusqu'à nos jours. Par le D^{r} Chenu. Coléoptères cicindelètes, carabiques, dytisciens, hydrophiliens, sylphales et nitidulaires, avec la collaboration de M.E. Desmarest, secrétaire de la Société Entomologique. Marescq et Compagnie, Paris, [2 +] 312 pp. [+ 28 pls.]

Deuve T (1998) Trois fossiles remarquablement conserves du Miocene de France, appartenant aux genres *Carabus* L. et *Ledouxnebria* nov. (Coleoptera, Carabidae et Nebriidae). Bulletin

de la Société Entomologique de France 103(3): 229–236. https://doi.org/10.3406/bsef.1998.17421

Deuve T (2004) Illustrated Catalogue of the Genus *Carabus* of the World (Coleoptera, Carabidae). Pensoft Publishers, Sofia–Moscow, 461 pp.

Deuve T, Cruaud A, Genson G, Rasplus JY (2012) Molecular systematics and evolutionary history of the genus *Carabus* (Col. Carabidae). Molecular Phylogenetics and Evolution 65(1): 259–275. https://doi.org/10.1016/j.ympev.2012.06.015

Drummond AJ, Rambaut A (2007) BEAST: Bayesian evolutionary analysis by sampling trees. BMC Evolutionary Biology 7(1): e214. https://doi.org/10.1186/1471-2148-7-214

Fabricius JC (1792) Entomologia systematica emendata et aucta. Secundum Classes, Ordines, Genera, Species adjectis Synonimis, Locis, Observationibus, Descriptionibus. Tom. 1. Proft, Christian Gottlob, Hafniae, 330 pp. https://doi.org/10.5962/bhl.title.125869

Folmer O, Black M, Hoeh W, Lutz R, Vrijenhoek R (1994) DNA primers for amplification of mitochondrial cytochrome c oxidase subunit I from diverse metazoan invertebrates. Molecular Marine Biology and Biotechnology 3: 294–299.

Hall TA (1999) BioEdit: A User-Friendly Biological Sequence Alignment Editor and Analysis Program for Windows 95/98/NT. Nucleic Acids Symposium Series 41: 95–98.

Jannel R (1941) Coléoptères Carabiques (Première partie). Faune de France, 39. Lechevalier, Paris, 571 pp.

Krausse AH (1908) I Carabi sardi e i loro parenti. Rivista Coleotterologica Italiana 6: 175–179.

La Greca M (1984) L'origine della fauna italiana. Le Scienze 187: 66–79.

Lapouge G, Vacher de (1899) Phylogénie des *Carabus* (suite) V—Le groupe du Parreyssi. Bulletin de la Société Scientifique et Médicale de l'Ouest 8: 97–113.

Lapouge G, Vacher de (1910) Phylogénie des *Carabus* (suite) 17. - Rectifications aux Memoirs 1–9. Bulletin de la Société Scientifique et Médicale de l'Ouest 17: 212–232.

Lapouge G, Vacher de (1913) *Carabus* nouveaux o mal connus. Miscellanea Entomologica 9: 9–10.

Löbl I, Löbl D [Eds] (2017) Catalogue of Palaearctic Coleoptera. Archostemata–Myxophaga–Adephaga. Vol. 1. Revised and updated edition. Brill, Leiden, Boston, [xxxiv +] 1443 pp.

Löbl I, Smetana A [Eds] (2003) Catalogue of Palaearctic Coleoptera. Volume 1. Archostemata–Myxophaga–Adephaga. Apollo Books, Stenstrup, 819 pp. https://doi.org/10.1163/9789004330290

Magistretti M (1965) Coleoptera Cicindelidae, Carabidae. Fauna d'Italia, VIII. Edizioni Calderini, Bologna, 512 pp.

Mossakowski D (2003) Morphological or molecular systematics? A case study of *Carabus*. European Carabidology 2003. Proceedings of the 11th European Carabidologist Meeting. DIAS Report 114: 231–241.

Müller A, Mifsud D (2017) Über die *Carabus*-Fauna der beiden Mittelmeerinseln Malta und Gozo (Coleoptera, Carabidae, Carabini). Lambillionea 117: 200–203.

Opgenoorth L, Hofmann S, Schmidt J (2021) Rewinding the molecular clock in the genus *Carabus* (Coleoptera: Carabidae) in light of fossil evidence and the Gondwana split: a reanalysis. PLoS ONE 16(9): e0256679. https://doi.org/10.1371/journal.pone.0256679

Osawa S, Su ZH, Imura Y (2004) Molecular Phylogeny and Evolution of Carabid Ground Beetles, Springer-Verlag, Tokyo, 197 pp. https://doi.org/10.1007/978-4-431-53965-0

Palliardi AA (1825) Dissertatio inauguralis physiographica sistens descriptiones decadum duarum Carabicorum novorum et minus cognitorum (Beschreibung zweyer Decaden neuer und wenig bekannter Carabicinen). Heubner, Wien, [x + 44 +] 2 pp. https://doi.org/10.5962/bhl.title.151802

Prüser F, Mossakowski D (1998) Low substitution rates in mitochondrial DNA in Mediterranean carabid beetles. Insect Molecular Biology 7(2): 121–128. https://doi.org/10.1046/j.1365-2583.1998.72056.x

Ragusa E (1871) Breve escursione entomologica fatta sulle Madonie e nei boschi di Caronia. Bollettino della Società Entomologica Italiana 3: 366–380.

Ragusa E (1883) Catalogo ragionato dei Coleotteri di Sicilia. Il Naturalista Siciliano 2: 193–199.

Ragusa E (1908) Due giorni di caccia sulle Madonie. Il Naturalista Siciliano 20: 129–134.

Ragusa E (1921) Coleotteri nuovi o poco conosciuti della Sicilia. Bollettino della Società Entomologica Italiana 51: 31–36.

Rapuzzi I (1992) Contributo alla conoscenza sulla distribuzione geografica di *C.* (*Macrothorax*) *planatus* Chaudoir, 1843 in Sicilia. Lambillionea 92: 167–177.

Rapuzzi I, Sparacio I (2015) New taxonomic data on some populations of *Carabus* (*Macrothorax*) *morbillosus* Fabricius, 1792 (Coleoptera Carabidae). Biodiversity Journal 6: 107–114.

Sota T, Ishikawa R (2004) Phylogeny and life-history evolution in *Carabus* (subtribe Carabina: Coleoptera, Carabidae) based on sequences of two nuclear genes. Biological Journal of the Linnean Society 81(1): 135–149. https://doi.org/10.1111/j.1095-8312.2004.00277.x

Sparacio I (1995) Coleotteri di Sicilia. I. L'Epos Editore, Palermo, 256 pp.

Turin H, Penev L, Casale A (2003) The Genus *Carabus* in Europe. A Synthesis. Pensoft Publishers, Sofia & European Invertebrate Survey, Sofia & Leiden, [xvi +] 512 pp.

Vigna Taglianti A (1995) Coleoptera Archostemata, Adephaga 1 (Carabidae). In: Minelli A, Ruffo S, La Posta S (Eds) Checklist delle specie della fauna italiana. 44. Calderini, Bologna, 500 pp.

Vigna Taglianti A (1998) I Carabidi nella faunistica e biogeografia. In: Vigna Taglianti A, Casale A (Eds) Giornata di Studio su: filogenesi e sistematica dei carabidi. Atti della Accademia Nazionale di Entomologia 46: 245–276.

Vigna Taglianti A (2009) An updated checklist of the ground beetles (Coleoptera: Carabidae) of Sardinia. In: Cerretti P, Mason F, Minelli A, Nardi G, Whitmore D (Eds) Research on the Terrestrial Arthropods of Sardinia (Italy). Zootaxa 2318: 169–196. https://doi.org/10.11646/zootaxa.2318.1.7

Vigna Taglianti A, Audisio PA, Belfiore C, Biondi M, Bologna MA, Carpaneto GM, De Biase A, De Felici S, Piattella E, Racheli T, Zapparoli M, Zoia S (1993) Riflessioni sui corotipi fondamentali della fauna W-Paleartica ed in particolare italiana. Biogeographia 16: 159–179. https://doi.org/10.21426/B616110375

Vigna Taglianti A, Casale A, Fattorini S (2002) I Carabidi di Sicilia ed il loro significato biogeografico (Coleoptera, Carabidae). Bollettino dell'Accademia Gioenia di scienze naturali 35 (361): 435–464.

Vitale F (1912) Catalogo dei Coleotteri di Sicilia. Rivista Coleotterologica Italiana 10: 41–50.

ZooKeys 1127: 135–154 (2022)
doi: 10.3897/zookeys.1127.86004
https://zookeys.pensoft.net

RESEARCH ARTICLE

A peer-reviewed open-access journal
ZooKeys
Launched to accelerate biodiversity research

Resurrection and redescription of *Clepsine pallida* Verrill, 1872 (Hirudinida, Glossiphoniidae) with a phylogeny of the genus *Alboglossiphonia*

William E. Moser[1], Dennis J. Richardson[2], Charlotte I. Hammond[2], Lourdes Rojas[3], Eric Lazo-Wasem[3], Anna J. Phillips[4]

1 *Smithsonian Institution, National Museum of Natural History, Department of Invertebrate Zoology, Museum Support Center MRC 534, 4210 Silver Hill Road, Suitland, MD 20746, USA* **2** *School of Biological Sciences, Quinnipiac University, 275 Mt. Carmel Avenue, Hamden, CT 06518, USA* **3** *Division of Invertebrate Zoology, Peabody Museum of Natural History, Yale University, P.O. Box 208118, New Haven, CT 06520, USA* **4** *Smithsonian Institution, National Museum of Natural History, Department of Invertebrate Zoology, 10th St and Constitution Ave, NW, Washington, DC 20560-0163, USA*

Corresponding author: William E. Moser (moserw@si.edu)

Academic editor: Fredric Govedich | Received 29 April 2022 | Accepted 7 September 2022 | Published 2 November 2022

https://zoobank.org/33659F1C-C631-4111-B85B-C0FA6D2787C4

Citation: Moser WE, Richardson DJ, Hammond CI, Rojas L, Lazo-Wasem E, Phillips AJ (2022) Resurrection and redescription of *Clepsine pallida* Verrill, 1872 (Hirudinida, Glossiphoniidae) with a phylogeny of the genus *Alboglossiphonia*. ZooKeys 1127: 135–154. https://doi.org/10.3897/zookeys.1127.86004

Abstract

Alboglossiphonia pallida (Verrill, 1872) **comb. nov.** is resurrected and redescribed based on morphological and molecular data from specimens of the type locality (New Haven County, Connecticut, USA) that demonstrate it is distinct from North American *Alboglossiphonia heteroclita*, European *Alboglossiphonia heteroclita*, and *Alboglossiphonia papillosa*. *Alboglossiphonia pallida* is characterized by having dark chromatophores on the dorsal surface arranged lateral to patrilaterally and medially as a thin line or interrupted thin line along with three pairs of eye spots (with the first pair closest together), six pairs of crop ceca, and a united gonopore. Additional sampling of specimens of the genus *Alboglossiphonia* is needed to understand its phylogeny especially as many species have not been collected since their description.

Keywords

Alboglossiphonia heteroclita, Clitellata, *Glossiphonia*, *Glossiphonia swampina*, Glossiphoniiformes, leech, Rhynchobdellida

Introduction

The species concept of *Alboglossiphonia heteroclita* (Linnaeus, 1761) has become very heterogenous over time through a combination of formal synonymy and informal accumulation of diagnostic morphological characters. Other species of the genus *Alboglossiphonia* exhibit similar taxonomic confusion, including *Alboglossiphonia hyalina* (O.F. Müller, 1774), *Alboglossiphonia inflexa* (Goddard, 1908), *Alboglossiphonia novaecaledoniae* (Johansson, 1918), *Alboglossiphonia papillosa* (Braun, 1805), and *Alboglossiphonia striata* (Apáthy, 1888) (Lukin 1976; Nesemann and Neubert 1999; Govedich 2001; Kaygorodova et al. 2014; Klass et al. 2018; Bolotov et al. 2019).

Hirudo heteroclita was originally described from Europe by Linnaeus (1761) and is characterized by the possession of six eye spots and a translucent body with black spots. Moquin-Tandon (1846) transferred *H. heteroclita* to the genus *Glossiphonia* Johnson, 1816. Carena (1820) and Blanchard (1894) stated that this species was very rare. Based upon pigmentation and the comparative distance between the first pair versus the second and third pair of eye spots, Lukin (1976) erected the subgenus *Alboglossiphonia* containing *Glossiphonia* (*Alboglossiphonia*) *heteroclita*. Klemm (1982) raised *Alboglossiphonia* to the genus rank, creating the combination *Alboglossiphonia heteroclita* as the type species.

In North America, Verrill (1872) described *Clepsine pallida* based on individuals from the West River of New Haven, Connecticut (Fig. 1). *Clepsine pallida* is characterized by the possession of six eyes and a pale body with scattered black specks and a median light line interrupted by a row of small black spots (Verrill 1872). Verrill (1874) updated the species concept by describing *C. pallida* Verrill, 1872 as *Clepsine pallida* var. a, and described *Clepsine pallida* var. b from New Haven, Connecticut and Colorado, respectively. As described by Verrill (1874), *Clepsine pallida* var. b is very similar to the North American *Glossiphonia elegans* (Verrill, 1872), a leech species resurrected by Siddall et al. (2005) and subsequently reaffirmed by Moser et al. (2012) and Mack and Kvist (2019).

In describing *Glossiphonia concolor* from Europe, Apáthy (1888) mentioned that the species was very similar to *C. pallida* in North America, but he did not indicate which of Verrill's varieties (var. a or var. b) was the most similar. In European studies, Blanchard (1894) considered *G. concolor* to be a simple variety of *Glossiphonia complanata* (Linnaeus, 1758), thus inferring similarity of *C. pallida* to *G. complanata* (including *Glossiphonia elegans* (Verrill, 1872) that was considered a synonym to *G. complanata* at that time). Castle (1900) synonymized *C. pallida* with *Glossiphonia elegans* (Verrill, 1872) while simultaneously recognizing *G. heteroclita* from the vicinity of Cambridge, Massachusetts. *Clepsine pallida* was subsequently ignored until Moore (1952) severed the association of *C. pallida* with *G. complanata* and determined *C. pallida* as a junior synonym of *Glossiphonia heteroclita* (Linnaeus, 1761) (Fig. 1). However, Soós (1969) caused further confusion by listing *Clepsine pallida* as a synonym of *Glossiphonia complanata* in his key and comprehensive list of all the species of the family Glossiphoniidae.

Hirudo swampina was described by Bosc (1802) as abundant in the swamps of "Carolina" and attached to turtles or frogs. As described, *H. swampina* has five eye

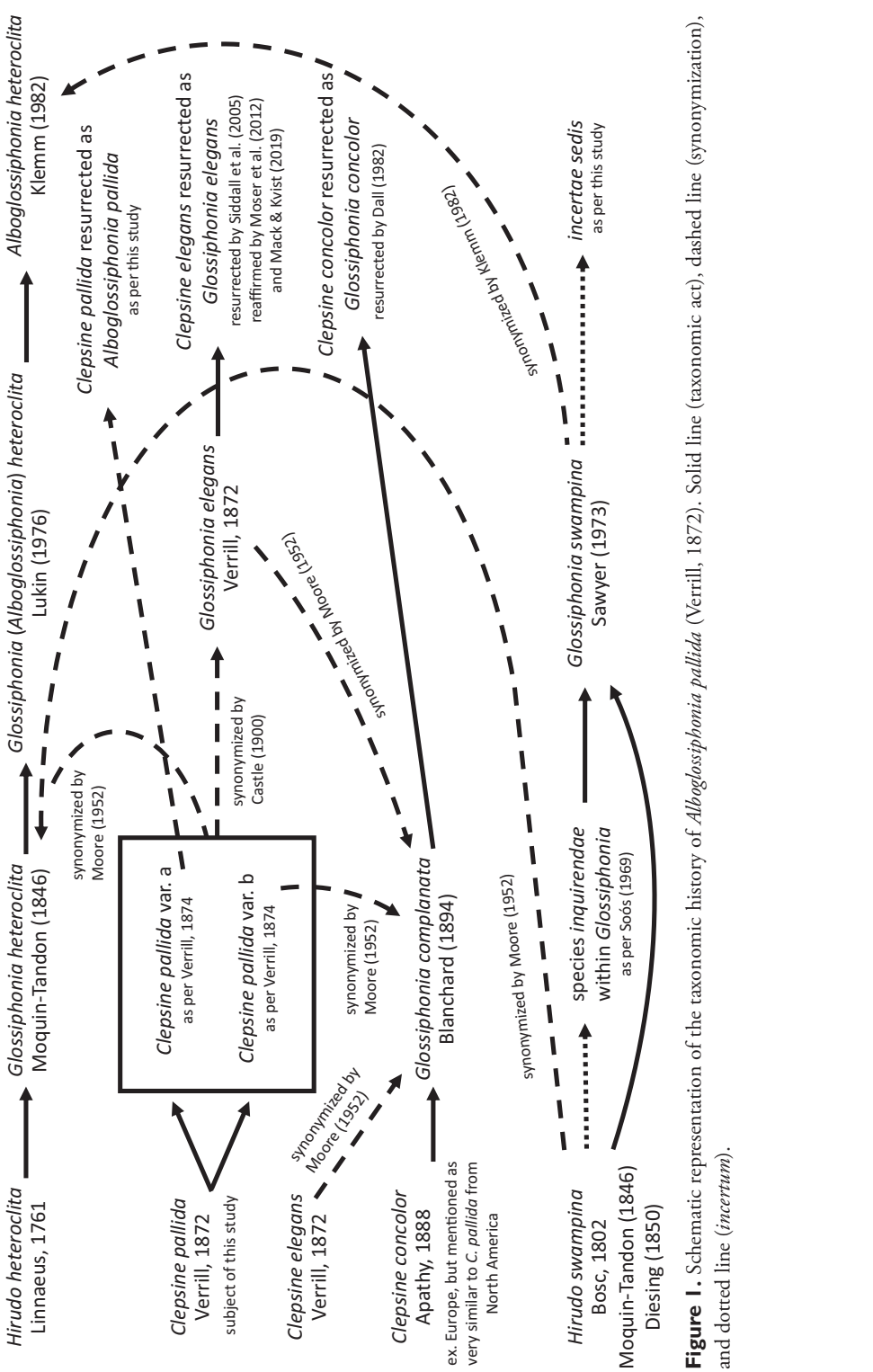

Figure 1. Schematic representation of the taxonomic history of *Alboglossiphonia pallida* (Verrill, 1872). Solid line (taxonomic act), dashed line (synonymization), and dotted line (*incertum*).

spots, a rough dorsum with green varied with brown, and the head, margins, and the posterior are spotted with white. The species description was updated by Moquin-Tandon (1846) and Diesing (1850). Although the species description indicated *H. swampina* possessed five eye spots, the redescriptions indicated that "five?" (Moquin-Tandon 1846) or six (Diesing 1850) eye spots were found, a character also present in several species of *Alboglossiphonia* and *Glossiphonia*. However, the rough dorsum, green/brown coloration, and attachment to turtles and frogs indicate that it is more similar to a species in the genus *Placobdella*, as species of *Alboglossiphonia* and *Glossiphonia* feed on invertebrates. *Placobdella hollensis* (Whitman, 1892) has up to five pairs of accessory "eyes" and has been found in North Carolina (Moser et al. 2017), and Sawyer (2021) stated that some adult individuals of *Placobdella multilineata* from North Carolina have pigment patterns that resemble multiple eye spots (accessory eyes). In comparison with the drawing and description of Bosc (1802), *H. swampina* could just as likely have represented an undesignated species of *Placobdella* as it could have represented *Glossiphonia* or *Alboglossiphonia*. It is likely that Bosc (1802) used the name *H. swampina* to describe a suite of species presently recognized as belonging to *Placobdella*. It is clear from Bosc (1802) that *H. swampina* referred to a leech parasitic on turtles and frogs. Additionally, it is assumed that the description of Bosc (1802) was based on specimens from the "Carolinas" of the United States. However, Moquin-Tandon (1846) indicated that *H. swampina* parasitized turtles and frogs in the marshes of South America. Adding credence to this understanding, there are references to "Carolina" in Argentina, Brazil, and Surinam. Soós (1969) listed *H. swampina* as a *species inquirenda* in the genus *Glossiphonia*.

Ignoring the similarities of *H. swampina* to the genus *Placobdella*, Moore (1952) declared *Clepsine swampina* as a junior synonym of *G. heteroclita* (= *A. heteroclita*). Later, Sawyer (1973) published a rediscovery of *Glossiphonia swampina* (Bosc, 1802) from two localities in the coastal plain of South Carolina and deposited a neotype in the National Museum of Natural History (USNM 47122), Smithsonian Institution. Sawyer (1973) stated that *G. swampina* is distinct from the unpigmented, translucent *G. heteroclita*, because *G. swampina* has four to seven mid-dorsal pigment bars. However, such a pigmentation pattern also occurs in *C. pallida* (Fig. 2). Additional specimens of *G. swampina* were found in the coastal plain of North Carolina by Sawyer and Shelley (1976). Klemm (1976) suggested that *G. swampina* is a color variant of *G. heteroclita*, and after examining specimens from Quebec and Maryland, Klemm (1982) declared *G. swampina* a junior synonym of *A. heteroclita*.

In recent phylogenetic studies, Trontelj et al. (1999) used *A. heteroclita* from Italy and Apakupakul et al. (1999), Light and Siddall (1999), and Siddall et al. (2005) used *A. heteroclita* from Michigan, Jueg (2008) used *A. heteroclita* from Germany and Michigan, and Bolotov et al. (2019) used *A. heteroclita* from Michigan and *A. papillosa* from Russia as a basis for molecular studies. However, *A. heteroclita* from Europe and *A. heteroclita* from North America have not been compared to *A. papillosa* nor to specimens of *C. pallida* in a molecular analysis.

The convoluted history of this assemblage is given in Fig. 1. In this study, we provide a molecular comparison of contemporary specimens that are morphologically consistent with the *C. pallida* of Verrill (1872) and *C. pallida* var. a of Verrill (1874) collected from the type locality of West River, Connecticut to specimens identified as *A. heteroclita* from Michigan, USA and from Germany, providing the basis for a redescription, resurrection, and molecular characterization of *C. pallida*.

Materials and methods

Collection of leeches and morphological analysis

During the course of a survey of the leech fauna of south-central Connecticut, individuals matching the description of *Clepsine pallida* Verrill, 1872 were collected by hand from submerged substrate in the West River, New Haven, New Haven County, the type locality of *C. pallida*. Specifically, collections were made from the West River at Konolds Pond (41°20'52.1"N, 72°58'41.6"W) and Whalley Avenue Bridge (41°19'30.13"N, 72°57'26.76"W) south to the "Duck Pond" (41°18'51.30"N, 72°57'21.75"W) as illustrated on page 12 of Shumway and Hegel (1990) and Clark's Pond (41°24'47.9"N, 72°53'46.8"W) between May 2008 and September 2009, and later in September 2020 and July 2021. A collection was also made from Sturges Pond (41°11'50"N, 73°18'2"W), Larsen Sanctuary, Fairfield County Connecticut on 27 July 2021. Specimens were relaxed, examined, and fixed as described by Moser et al. (2006). Several specimens were pressed, stained with Semichon's acetocarmine and mounted in Canada Balsam for examination by light microscopy according to techniques outlined by Richardson (2006), as modified by Richardson and Barger (2006). Specimens were examined using an Olympus SZX16 dissecting microscope and were photographed with a Zeiss Stemi 2000-CS macroscope fitted with a Q-Capture 5.0 RTV Micropublisher camera. Images were acquired at different focal levels and the resulting stacks rendered with Helicon Focus 7 Pro to make an extended focus image. Post-processing was done using Adobe Photoshop CC 2015. Terminology for plane shapes follows Clopton (2004). Specimens were deposited in the Peabody Museum of Natural History (**YPM**), Yale University, New Haven, Connecticut, USA and the National Museum of Natural History (**USNM**), Smithsonian Institution, Washington, District of Columbia, USA.

DNA and phylogenetic analysis

Molecular analyses were conducted on newly collected material according to Richardson et al. (2010) as follows: DNA was isolated from the caudal suckers of five individual leeches (YPM IZ 058354, YPM IZ 062698, YPM IZ 109351–109353) with

the DNeasy Blood & Tissue Kit from Qiagen (cat. no. 69504), following the protocol given for the purification of total DNA from animal tissues (spin-column). For the proteinase K treatment step, tissue samples were lysed overnight at 56 °C. DNA was eluted from the spin columns with 150 µl of buffer.

Polymerase chain reactions (PCR) were prepared using the Illustra PuRe Taq Ready-To-Go PCR beads from GE Health Care (cat. no. 27-9559-01). Primers were purchased from Invitrogen and were comprised of two primers each for cytochrome c oxidase subunit I (COI) as specified by Folmer et al. (1994) and Light and Siddall (1999). Specifically, the COI primers were LCO1490 (5'-GGTCAACAAATCATAAAGATATTGG-3') and HCO2198 (5'-TAAACTTCAGGGTGACCAAAAAATCA-3'). Final volume of PCR reactions was 25 µl with 2 µl of leech genomic DNA added per reaction. DNA was amplified under the following PCR conditions: 94 °C for 5 min; 35 cycles of (94 °C for 30 s, 50 °C for 30 s, 72 °C for 45 s); 72 °C for 7 min. Following PCR, samples were cleaned up using a QIAquick PCR purification kit from Qiagen (cat. no. 28104).

Purified PCR products were sequenced using the HCO2198 and LCO1490 primers for the COI products by the W.M. Keck Foundation Biotechnology Resource Laboratory at Yale University. DNA sequences were edited and assembled using Geneious Prime (v. 2020.1.2, Biomatters Ltd.). Novel sequences were deposited in GenBank (Benson et al. 2018; Table 1). Comparable sequence data for seven recognized *Alboglossiphonia* species (24 sequences), sequences identified as *Alboglossiphonia* sp. (three individuals), *Glossiphonia complanata* (two individuals), and *Glossiphonia elegans* (two individuals) were downloaded from GenBank (Table 1). Additionally, five sequences identified as *A. heteroclita* were downloaded from BOLD (Ratnasingham and Hebert 2013; Table 1). The COI sequences were aligned using the MAFFT multiple sequence alignment plug-in for Geneious Prime (Katoh and Standley 2013) with default settings, checked by eye for gaps, and the sequences were translated to amino acids to assess sequence quality. Uncorrected pairwise sequence distances were calculated using Geneious Prime.

The best partitioning scheme was tested using ModelFinder within IQ-TREE (Kalyaanamoorthy et al. 2017) using the *-m MF+MERGE* command, as well as estimation of substitution models by codon position, resulting in the following models as best fit by partition by the Bayesian information criterion: first codon position = F81+F, second codon position = TN+F+I, and third codon position = K3Pu+F+G4. A maximum likelihood (ML) analysis was performed with IQ-TREE v. 1.6.12 (Nguyen et al. 2015), using the models suggested for each unlinked partition, the *-spp* command to allow each partition to have its own evolutionary rate, and 1,000 ultrafast bootstrap (UFBOOT2) approximations (Hoang et al. 2018). *Glossiphonia complanata* (AY047321 and HM246608) and *Glossiphonia elegans* (JQ073858 and JQ73860) served as outgroups. FigTree v. 1.4.4 (Rambaut 2018) was used to visualize trees that were then edited with Adobe Illustrator Creative Cloud (https://www.adobe.com).

Table 1. Species, collection locality, museum catalog number, and Genbank accession information or BOLD for sequences included in this study.

Species	State/province	Country	Location	Catalog number /citation	GenBank or BOLD#
Alboglossiphonia iberica	Huelva	Spain		8789, Jueg 2008	N/A
Alboglossiphonia quadrata		Namibia		Siddall et al. 2005	AY962455
Alboglossiphonia heteroclita		Germany		9195, Jueg 2008	N/A
Alboglossiphonia heteroclita	Michigan	USA		Apakupakul et al. 1999	AF116016
Alboglossiphonia heteroclita	Michigan	USA		BSC-160.1, SUNY Buffalo State	ANNMO802-20
Alboglossiphonia heteroclita	Michigan	USA		BSC-160.2, SUNY Buffalo State	ANNMO803-20
Alboglossiphonia heteroclita	Michigan	USA		BSC-160.6, SUNY Buffalo State	ANNMO807-20
Alboglossiphonia heteroclita	Wisconsin	USA		BSC-160.3, SUNY Buffalo State	ANNMO804-20
Alboglossiphonia heteroclita	Wisconsin	USA		BSC-160.4, SUNY Buffalo State	ANNMO805-20
Alboglossiphonia pallida	Connecticut	USA	Konolds Pond, West River	YPM IZ 058354, this study	ON738431
Alboglossiphonia pallida	Connecticut	USA	Konolds Pond, West River	YPM IZ 109351, this study	ON738432
Alboglossiphonia pallida	Connecticut	USA	Konolds Pond, West River	YPM IZ 109352, this study	ON738433
Alboglossiphonia pallida	Connecticut	USA	Konolds Pond, West River	YPM IZ 109353, this study	ON738434
Alboglossiphonia pallida	Connecticut	USA	Clarks Pond	YPM 062698, this study	ON738435
Alboglossiphonia papillosa	Siberia	Russia	Lake Gusinoe	Kaygorodova et al. 2014	KM095100
Alboglossiphonia papillosa	Siberia	Russia	Lake Gusinoe	Kaygorodova et al. 2014	KM095101
Alboglossiphonia papillosa	Siberia	Russia	Lena River basin	RMBH Hir13/3, Klass et al. 2018	MH286269
Alboglossiphonia papillosa	Siberia	Russia	Lena River basin	RMBH Hir13/4, Klass et al. 2018	MH286270
Alboglossiphonia papillosa	Siberia	Russia	Lena River basin	RMBH Hir13/5, Klass et al. 2018	MH286271
Alboglossiphonia papillosa	Siberia	Russia	Lena River basin	RMBH Hir13/2, Klass et al. 2018	MH286268
Alboglossiphonia papillosa	Siberia	Russia	Lena River basin	RMBH Hir13/1, Klass et al. 2018	MH286267
Alboglossiphonia sp. 2		Myanmar		RMBH HIR58/2 Bolotov et al. 2019	MN295404
Alboglossiphonia sp.	Victoria	Australia	Melbourne	MRD16Gloss2, Carew et al. 2018	MG976199
Alboglossiphonia lata	Primorsky Krai	Russia		RMBH HIR58/1, Bolotov et al. 2019	MN295414
Alboglossiphonia lata		South Korea		RMBH HIR113/4, Bolotov et al. 2019	MN393286
Alboglossiphonia lata		South Korea		RMBH HIR103/5, Bolotov et al. 2019	MN393275
Alboglossiphonia lata		South Korea		RMBH HIR110/5, Bolotov et al. 2019	MN393279
Alboglossiphonia lata		South Korea		RMBH HIR113/3, Bolotov et al. 2019	MN393284
Alboglossiphonia lata		South Korea		RMBH HIR112/1, Bolotov et al. 2019	MN393281
Alboglossiphonia lata		South Korea		RMBH HIR114/12, Bolotov et al. 2019	MN393288
Alboglossiphonia lata		South Korea		RMBH HIR111/22, Bolotov et al. 2019	MN393280
Alboglossiphonia lata		South Korea		RMBH HIR114/1, Bolotov et al. 2019	MN393287
Alboglossiphonia lata		South Korea		RMBH HIR109/1, Bolotov et al. 2019	MN393276
Alboglossiphonia lata		South Korea		RMBH HIR110/32, Bolotov et al. 2019	MN393277
Alboglossiphonia lata		South Korea		RMBH HIR113/32, Bolotov et al. 2019	MN393285
Alboglossiphonia weberi	Hawaii	USA		Siddall et al. 2005	AY962453
Alboglossiphonia sp.		South Korea		HJK-2020, Kwak et al. 2021	MN503262
Glossiphonia complanata		United Kingdom		Light and Siddall 1999	AY047321
Glossiphonia complanata	Mecklenburg-Vorpommern	Germany		Trajanovski et al. 2010	HM246608
Glossiphonia elegans	Connecticut	USA	West River	Moser et al. 2012	JQ073858
Glossiphonia elegans	Connecticut	USA	West River	Moser et al. 2012	JQ073860

Results and discussion

Morphological analysis

Examination of the type series of *Clepsine pallida* (YPM IZ 00253) revealed a single specimen (Fig. 2). The more than 150-year-old holotype specimen is remarkably well preserved, but the pigmentation has faded and the eye spots are no longer discernible. The dorsal surface is smooth and there is a united gonopore. The original YPM Invertebrate Zoology Annelida ledger entry for YPM IZ 00253 indicates a single specimen of *Clepsine pallida* V. collected from West River, New Haven, Connecticut on 6 June 1871 and is labeled as type.

In further examination of the YPM Annelida Ledger, *Clepsine pallida* var. a and var. b of Verrill (1874) had not been assigned a catalog number. No specimens of *Clepsine pallida* var. a were found, and Verrill's (1874) account likely refers only to the holotype specimen, YPM IZ 00253. In Verrill (1874), *Clepsine pallida* var. b came from Colorado (US Geological and Geographic Survey of the Territories, i.e. Hayden's expedition) and again, Colorado (lake near Long's Peak, 9,000 feet elevation, Hayden's expedition, 1873). In the YPM uncataloged leech holdings, two lots were recently discovered that are likely the syntypes of *Clepsine pallida* var. b. One lot (now YPM IZ 106808) had an original label in Sidney Smith's handwriting that reads "Colorado Mts. & Plains, 1873" and another label in A.E. Verrill's handwriting as "*Clepsine pallida* var. b Colorado Mts. & Plains Haydens Exp. 1873." On the second label, *pallida* has been crossed out and "*elegans"* has been written in Verrill's handwriting, indicating an updated identification as *Clepsine elegans*. The single specimen (YPM IZ 106808) is in very good condition and morphologically consistent with *Glossiphonia elegans* (six eye spots; pair of dark paramedial lines; two pair of metameric white dots).

The second lot (now YPM IZ 106809) had a label in J. Percy Moore's handwriting as "*Clepsine pallida* Verrill, near Longs Peak, 9000 ft, Haydens Exp" with a reidentification as *Glossiphonia complanata* (Linnaeus) and a label written by former Yale Curator of Invertebrate Zoology Willard Hartman as "*Glossiphonia complanata* (Linn) Lake near Long's Peak, 9000 ft., Hayden's Expedition, 1873; Verrill's Ident: *Clepsine pallida*" – no Verrill-era label was found. This information matches Verrill (1874) of *Clepsine elegans* var. b. YPM IZ 106809 containing three specimens of average condition which have likely dried out and subsequently been rehydrated without benefit of a restorative surfactant. Two of the specimens are morphologically consistent with *Glossiphonia elegans* (six eye spots and pair of paramedial dark lines). The third specimen is smaller and difficult to discern.

Sawyer (1973) designated a neotype (USNM 47122) and an additional specimen (USNM 51436) of *Glossiphonia swampina* (Bosc, 1802) from French Quarter Creek, Clement's Ferry Road, Berkeley County, South Carolina at the National Museum of Natural History, Smithsonian Institution. The pigmentation has faded, but both specimens had small transverse bands (primarily in the medial region), six eye spots, and a united gonopore. In light of the findings in this study, *G. swampina* needs to be reassessed with molecular data. We conclude that *Hirudo swampina*, as described and illustrated by Bosc (1802) is *incertae sedis*.

The following redescription of the new combination *Alboglossiphonia pallida* (Verrill, 1872) is based upon the holotype of *Clepsine pallida* (YPM IZ 000253) and newly collected specimens (YPM IZ 043467–043468, YPM IZ 058354, YPM IZ 062698, YPM IZ 109351–109353, YPM IZ 106029–106030, and USNM 1662161 from New Haven County, Connecticut, USA and YPM IZ 107064 from Fairfield County, Connecticut, USA.

Family Glossiphoniidae

Alboglossiphonia pallida (Verrill, 1872), comb. nov.

Figs 2–5

Diagnosis. Dark chromatophores on the dorsal surface arranged lateral to patrilaterally and medially as a thin line or interrupted thin line along with three pair of eye spots (where the first pair are closest together), six pair of crop ceca, and a united gonopore.

External morphology. Body narrowly ovoid to narrowly pyriform. Rounded anterior region. Dorsum buff to translucent, smooth (without papillae), and with small, black chromatophores that form thin lines with scattered areas; thin, interrupted middorsal line with larger chromatophore patches (typically on sensory annuli); black chromatophores in a lateral pattern on the sensory annulus of the lateral to paralateral region (Figs 2, 3). Three pair of eye spots which are typically separate and arranged

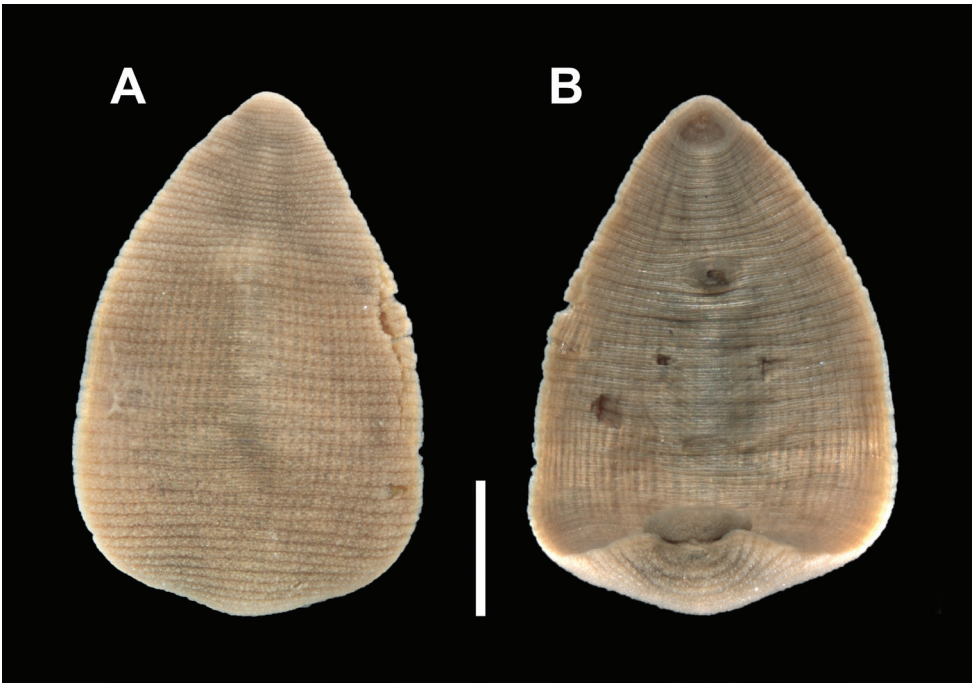

Figure 2. Holotype specimen of *Clepsine pallida* Verrill, 1872 (YPM IZ 000253) **A** dorsal surface **B** ventral surface. Scale bar: 1 mm.

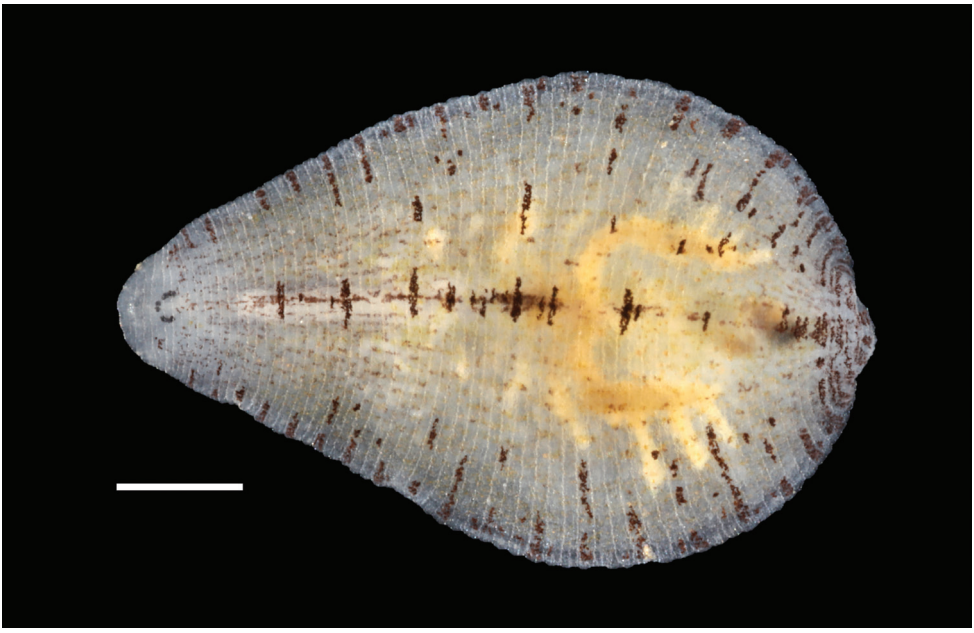

Figure 3. Living specimen of *Alboglossiphonia pallida* (Verrill, 1872) from the type locality of New Haven County, Connecticut, USA. YPM IZ 106029, dorsal surface Scale bar: 1 mm.

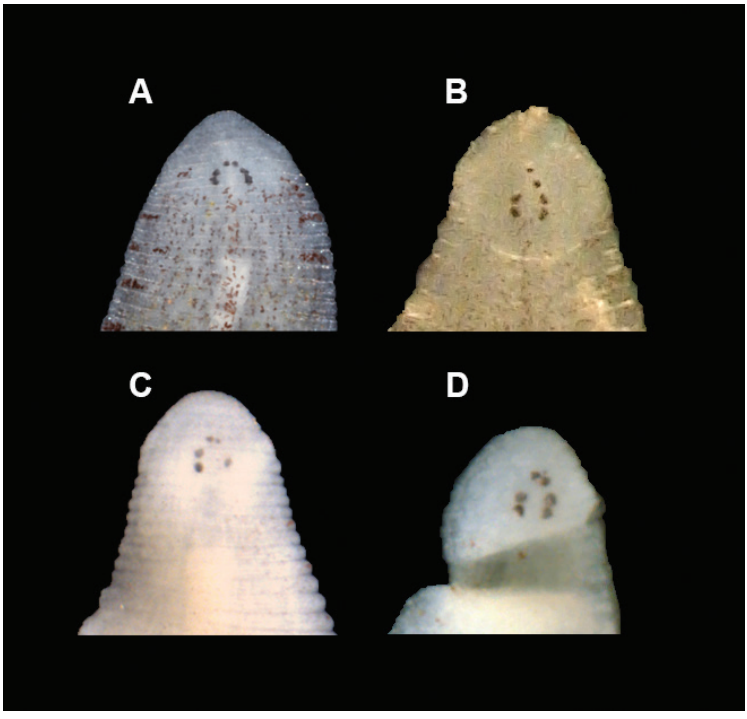

Figure 4. Images of the arrangement of eyespots of *Alboglossiphonia pallida* (Verrill, 1872) **A** YPM IZ 106029 **B** USNM 1662161 **C** YPM IZ 062698 **D** YPM IZ 107064.

linearly or with groupings of two and four eye spots in unpigmented cephalic area with the first pair of eye spots closest together (Figs 3, 4). Some individuals have five eye spots where the first pair is present and there are only three eye spots in the second and third pair. Caudal sucker of moderate size (half diameter of mid-body) without pigment or papillae. Ventrum without pigment or papillae and with united male and female gonopores (single opening) (Fig. 2).

Alimentary tract. Cylindrical, blunt-tipped protrusible proboscis (approximate length of 14 annuli), opening at the center of the oral sucker. Short esophagus and diffuse salivary glands that are distributed in the anterior third of the body (Fig. 5). Crop with six pair of ceca and last pair extend posteriad and diverticulated with four sections; four pair of simple, saccular intestinal ceca with hind gut saccate and rectum opening into anus, located one annulus anteriad of the caudal sucker (Fig. 5).

Reproductive anatomy. Male atrium opening into paired narrowly ovoid atrial cornua that extends laterally and narrows abruptly at junction with ejaculatory ducts and extends posteriad (Fig. 5). Six pair of testisacs between crop ceca. Pair of tubular ovisacs; length of ovisacs dependent on the reproductive state of the leech (Fig. 5). Male and female gonopores united.

Molecular analysis

Uncorrected *p*-distances between COI sequences of each species are given in Table 2. Pairwise distances of COI sequences among *A. pallida* specimens (*n* = 5) ranged 0.24–1.05%. Among *Alboglossiphonia* species, pairwise distances of COI between *A. pallida* and specimens of *A. heteroclita* from Michigan and Wisconsin ranged 5.78–8.35%, between *A. pallida* and *A. heteroclita* (9195) from Germany ranged 12.72–12.94%, between *A. pallida* and *A. papillosa* ranged 9.07–9.7%, between *A. pallida* and *A. lata+A. weberi* ranged 10.86–13.29%, between *A. pallida* and *Alboglossiphonia* sp. 2 (MN295404) from Myanmar ranged 11.17–11.55%, between *A. pallida* and *Alboglossiphonia* sp. (MG976199) from Australia ranged 12.72–13.14%, between *A. pallida* and *A. quadrata* (AY962455) from Namibia ranged 16.84–17.1%, and between *A. pallida* and *A. iberica* (8739) from Spain ranged 17.36–17.58%.

The molecular dataset included COI sequences of 41 specimens (37 members of *Alboglossiphonia* and two specimens each of *Glossiphonia complanata* and *Glossiphonia elegans* that served as outgroups; Table 1) and a total of 631 aligned characters. The log-likelihood of the topology was –3174.987 and the topology is shown in Fig. 6.

The genus *Alboglossiphonia* is well supported as monophyletic (bs = 100). *Alboglossiphonia pallida* and *A. papillosa* were represented by more than one individual in our analysis and each of these species was monophyletic with strong support (*A. pallida* bs = 100, *A. papillosa* bs = 98). The clade of *A. pallida* specimens (bs = 100) was adjacent to two sequences of *Alboglossiphonia* sp. from Wisconsin (bs = 54). Individuals of *A. heteroclita* were not each other's closest relatives. *Alboglossiphonia heteroclita* (GenBank: AF116016) from Michigan placed with three sequences of *A. heteroclita* from Michigan (BOLD:ANNMO802, BOLD:ANNMO803) and two sequences of *A. heteroclita* from Wisconsin (BOLD:ANNMO804, BOLD:ANNMO805) in a series of branches with

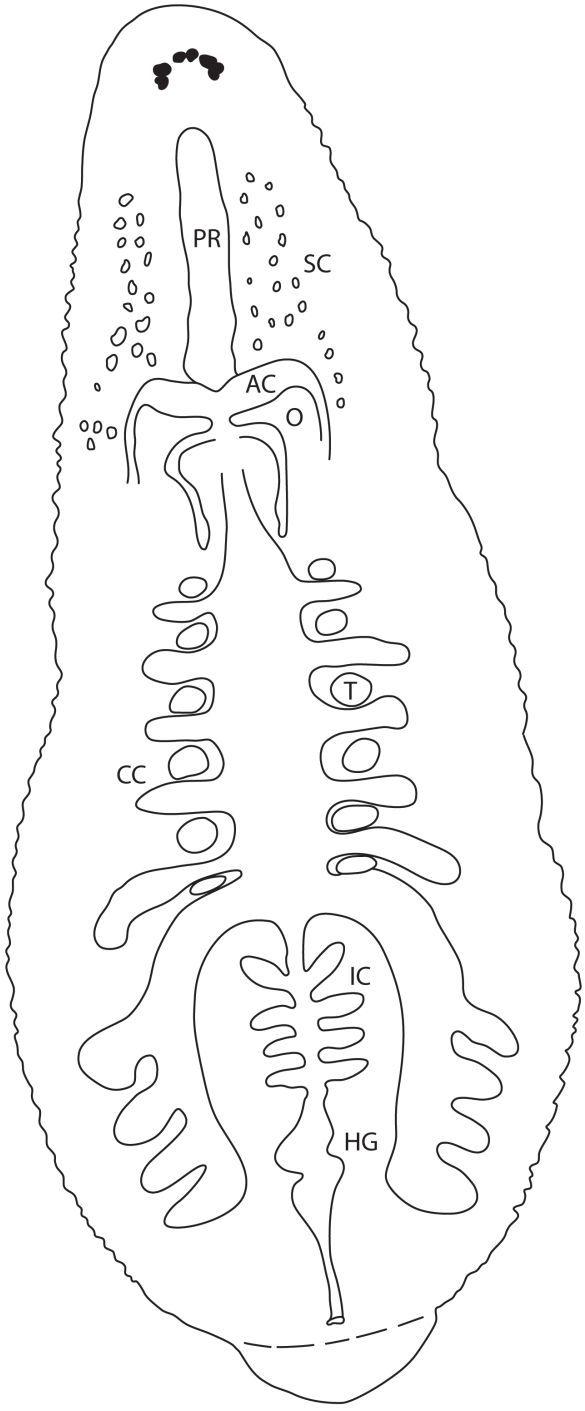

Figure 5. Schematic drawing of the internal morphology of *Alboglossiphonia pallida* (Verrill, 1872). Abbreviations: AC, atrial cornuae; CC, crop ceca; HG, hind gut; IC, intestinal ceca; O, ovisac; PR, proboscis; SC, salivary cells; T, testisac.

Table 2. COI uncorrected pairwise sequence differences among specimens of *Alboglossiphonia* included in this study. Values presented are range followed by average in parentheses ().

	1	2	3	4	5	6	7	8	9	10
A. iberica (1)	—	—	—	—	—	—	—	—	—	—
A. quadrata (2)	17.05	—	—	—	—	—	—	—	—	—
A. heteroclita Germany (3)	16.47	16.13	—	—	—	—	—	—	—	—
Alboglossiphonia sp. S. Korea HJK (4)	15.28	14.92	11.71	—	—	—	—	—	—	—
A. lata/*A. weberi* (5)	15.28–17.05 (16.26)	15.21–16.96 (16.03)	13.27–14.38 (13.68)	13.18–14.44 (13.43)	0–3.96 (2.23)	—	—	—	—	—
Alboglossiphonia sp. 2 Myanmar (6)	14.74	16.48	14.22	13.65	6.18–7.45 (6.84)	—	—	—	—	—
Alboglossiphonia sp. Australia (7)	16.16	14.9	14.54	13.65	7.45–9.19 (8.19)	7.92	—	—	—	—
A. papillosa (8)	15.10–15.95 (15.22)	16.64–17.56 (16.77)	12.16–12.87 (12.26)	13.97–14.83 (13.97)	9.83–12.05 (10.81)	10.3–11.12 (10.3)	11.89–12.40 (11.89)	0–0.86 (0.25)	—	—
A. heteroclita USA (9)	16.70–17.70 (17.08)	16.32–17.71 (16.92)	11.69–12.91 (12.16)	13.38–14.75 (13.40)	10.14–13.94 (11.61)	10.94–13.11 (11.81)	12.38–14.14 (13.18)	8.40–9.77 (9.04)	0.33–3.07 (1.89)	—
A. pallida (10)	17.36–17.58 (17.43)	16.84–17.10 (16.95)	12.72–12.94 (12.80)	15.16–15.54 (15.31)	10.86–13.29 (11.80)	11.17–11.55 (11.35)	12.72–13.14 (12.87)	9.07–9.70 (9.24)	5.78–8.35 (6.74)	0.24–1.05 (0.73)
	1	2	3	4	5	6	7	8	9	

short internodes and moderate support values (bs = 74–81). *Alboglossiphonia heteroclita* (9195) from Germany placed sister to a sequence of *Alboglossiphonia* from South Korea (GenBank: MN503262), albeit with low support (bs = 63), suggesting these are separate species, the latter not otherwise represented in GenBank. The clade of *A. heteroclita* from Germany + *Alboglossiphonia* sp. from South Korea (MN503262) placed adjacent to clades including *A. heteroclita* from Michigan and Wisconsin, *A. pallida*, *A. papillosa*, *A. lata*, *A. weberi*, *Alboglossophonia* sp. from Myanmar, and *Alboglossiphonia* sp. from Australia (bs = 98). *Alboglossiphonia pallida* + *A. heteroclita* from Michigan and Wisconsin was sister to *A. papillosa* (bs = 75). *Alboglossiphonia lata* specimens from South Korea and the specimen from Russia (MN295414) placed within a strongly supported clade (bs = 100) that included the specimen of *A. weberi* (GenBank: AY962453) from Hawaii, USA. Sequences of two unidentified specimens of *Alboglossiphonia* (MN295404 from Myanmar and MG976199 from Australia) placed sister to one another with strong support (bs = 100), within the *A. lata*/*weberi* clade, and sister to the *A. weberi* specimen from Hawaii (bs = 75). The sequences of *A. iberica* (8739) from Spain and *A. quadrata* (GenBank: AY962455) from Nambia were sister to one another (bs = 100), and that clade was well supported as sister to all other specimens of *Alboglossiphonia* in the tree (bs = 100).

Sawyer (1986) listed 14 species of the genus *Alboglossiphonia*: *A. heteroclita* (Linnaeus, 1761), *A. annandalei* Oka, 1922; *A. australiensis* (Goddard, 1908), *A. cheili* (Oosthuizen, 1978); *A. conjugata* (Oosthuizen, 1978); *A. disjuncta* (Moore, 1939); *A. intermedia* (Goddard, 1909), *A. lata* (Oka, 1910); *A. macrorhyncha* (Oosthuizen, 1978); *A. masoni* (Mason, 1974); *A. mesembrina* (Ringuelet, 1949); *A. multistriata*

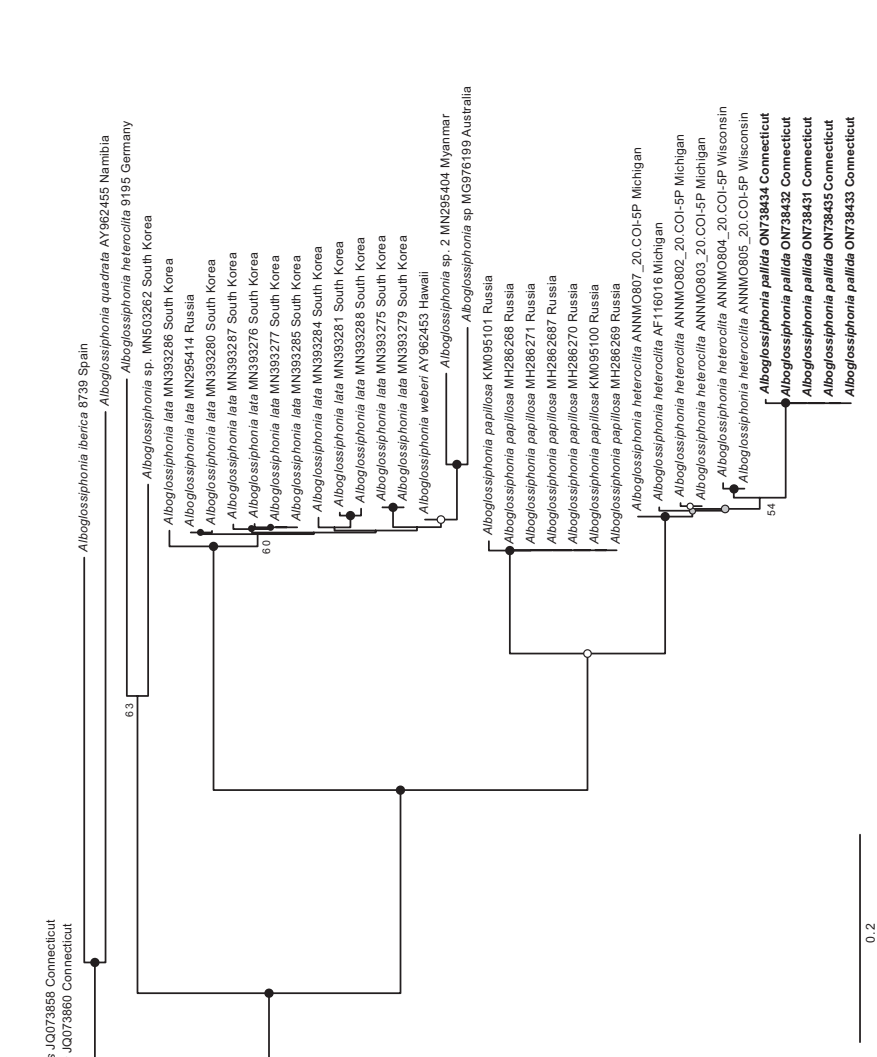

Figure 6. Maximum likelihood phylogeny (ln*L* = –2868.139) of *Alboglossiphonia pallida* and congeners based on mitochondrial COI sequence data partitioned by codon. Maximum likelihood bootstrap values above 70 are shown at the internodes. GenBank accession number and locality following each species name is provided for each terminal. Branches are drawn proportional to the amount of change.

(Mason, 1974), ?*A. quadrata* (Moore, 1939); *A. tasmaniensis* (Ingram, 1957); and *A. weberi* (Blanchard, 1897). Subsequently, Oosthuizen (1987) redescribed *A. quadrata* (Moore, 1939) and transferred the species to the genus *Hemiclepsis*. Additionally, six more species of the genus *Alboglossiphonia* have been described, *A. polypompholyx* Oosthuizen, Hussein, and El-Shimy, 1988; *A. disuqi* El-Shimy, 1990; *A. pahariensis* Nesemann & Sharma, 2007; *A. kashiensis* Nesemann, 2007; *A. iberica* Jueg, 2008; *A. levis* Gouda, 2010 and five additional species have been elevated or resurrected, *A. hyalina* (O.F. Müller, 1774); *A. inflexa* (Goddard, 1908); *A. papillosa* (Braun, 1805); *A. novaecaledoniae* (Johansson, 1918); *A. striata* (Apáthy, 1888). The species *Clepsine pallida* is herein resurrected in the new combination *Alboglossiphonia pallida* (Verrill, 1874), thus, making 25 recognized species of the genus *Alboglossiphonia*.

Alboglossiphonia pallida was strongly supported by morphological and molecular evidence as a species within the genus *Alboglossiphonia* and distinct from North American *A. heteroclita*, European *A. heteroclita*, *A. lata*, *A. weberi*, *A. iberica*, and *A. papillosa*. *Alboglossiphonia pallida* is characterized by having dark chromatophores on the dorsal surface arranged lateral to patrilaterally and medially as a thin line or interrupted thin line along with three pair of eye spots (where the first pair are closest together, the defining characteristic of the genus *Alboglossiphonia*), six pair of crop ceca, and a united gonopore. The non-monophyly of *A. heteroclita* continues to pose a challenge. The *A. heteroclita* specimens from North America were 11.69–12.91% different from *A. heteroclita* from Europe, indicating that the North American specimens are not *A. heteroclita* and most likely represent an undescribed species. The *A. heteroclita* specimens from North America were 0.33–3.07% different from one another. These specimens form a strongly supported clade with *A. pallida* (bs = 100), although the North American *A. heteroclita* specimens as a group were 5.78–8.35% different from the *A. pallida* specimens. North American specimens assigned to *A. heteroclita* are typically characterized by a lack of pigmentation on translucent bodies (Sawyer 1972, 1973; Klemm 1982; Moser et al. 2016). In North America, *A.* cf. *heteroclita* has been reported in the Great Lakes region and as far west as Nebraska in the USA and as far west as British Columbia in Canada (Klemm 1982; Moser 1991). Further collection is needed to elucidate the taxonomy and geographic distribution of the North American *Alboglossiphonia* specimens that were identified as *A. heteroclita* and its relationship with *A. pallida*.

In Europe, *A. heteroclita* had been a heterogenous concept and known more by the infraspecific varieties. These synonymies have since been elevated to the species rank with *A. hyalina* (O.F. Müller, 1774) having yellow chromatophores and no dark chromatophores and *A. striata* (Apáthy, 1888) with dark, transverse pigmentation (Lukin 1976; Nesemann and Neubert 1999; Jueg and Grosser per. comm.). As described and figured by Braun (1805), *A. papillosa* (Braun, 1805) has dark medial spots and some scattered dark chromatophores. This description is consistent with the description of *A. heteroclita* (Linnaeus, 1761) (Nesemann and Neubert 1999; Jueg and Grosser per. comm.). *Alboglossiphonia heteroclita* from Germany was 12.16–12.87% different than *A. papillosa* collected from Russia. As photographed by Klass et al. (2018), the specimen of *A. papillosa* has dark dorsal lines and is potentially a previously undescribed species.

Sequences of specimens from Asia, Australia, and Hawaii form a strongly supported clade, except for a single sequence from South Korea (MN503262). Sequences of *A. lata* form a clade with short internodes that were poorly supported for the most part. The clade predominantly consisted of sequences from South Korea, yet also included a single sequence from Primorsky Krai, Russia (MN295414) and the sequence of *A. weberi* from Hawaii, USA (AY962453). *Alboglossiphonia lata* is a widely distributed species that is considered invasive and spread via the aquatic plant trade. In particular, the specimen of *A. weberi* from Hawaii should be reexamined to determine if this might be an occurrence record of the invasive *A. lata*, which would be concerning for the Hawaiian island ecosystem. The sequences of *Alboglossiphonia* from Myanmar and Australia are supported as members of the genus and likely represent species distinct from one another and not otherwise represented in this analysis or publicly available databases (e.g., GenBank, BOLD), yet the specimens need to be examined to determine the species identification as there have been seven described species from Australasia and Oceania.

The sequence of *Alboglossiphonia quadrata* (AY962455) from Namibia has likely been assigned the incorrect name. Oosthuizen (1987) transferred the species name *quadrata* to the genus *Hemiclepsis*. This sequence is highly supported as a lineage within *Alboglossiphonia* and the specimen needs to be reexamined to determine if it belongs to one of the seven species of *Alboglossiphonia* described from Africa (Gouda 2010).

In this study, COI was largely successful at distinguishing congeners of *Alboglossiphonia*, but it had limited utility in resolving the relationships between species. Combining COI data with other loci, especially nuclear loci, is needed to determine relationships between glossiphonid species with confidence. The addition of sequences of more *Alboglossiphonia* species will improve our understanding of relationships within the genus. This study included all publicly available *Alboglossiphonia* sequences, although this represents only about one-third of the diversity of the genus.

Conclusion

Alboglossiphonia pallida (Verrill, 1872) is resurrected and redescribed based on morphological and molecular data that demonstrate it is distinct from the specimen assigned to *A. heteroclita* from Michigan and Wisconsin and *A. heteroclita* from Europe, as well as other species of *Alboglossiphonia*. Additional sampling of *Alboglossiphonia* is needed to understand its phylogeny especially as many species have not been collected since their original description.

Acknowledgements

Kristen E. Richardson and Krystal A. Lazos, Quinnipiac University assisted in field collection. Katie Ahlfeld, Department of Invertebrate Zoology, National Museum of Natural History, Smithsonian Institution, provided valuable assistance in specimen management. Harry Coyle, New Haven Parks and Recreation provided valuable

logistic insight. We are grateful to Dr Christian Albrecht, Justus-Liebig University, Giessen, Germany, and to Uwe Jueg, Ludwigslust, Germany, for providing the sequence data of *Alboglossiphonia heteroclita* from Germany and *A. iberica*. We thank Dr Milan Bull, Connecticut Audubon Society, for permission to collect at Sturges Pond, Larsen Sanctuary, Fairfield, Connecticut. We greatly appreciate Uwe Jueg and Clemens Grosser, Elstertrebnitz, Germany, for their insightful comments on the genus *Alboglossiphonia*. The State of Connecticut, Department of Environmental Protection provided permission to collect leeches. Funding for this project was provided in part by the Department of Biological Sciences and Schools of Arts and Sciences and Health Sciences at Quinnipiac University, Hamden, Connecticut.

References

Apakupakul K, Siddall ME, Burreson EM (1999) Higher level relationships of leeches (Annelida: Clitellata: Euhirudinea) based on morphology and gene sequences. Molecular Phylogenetics and Evolution 12(3): 350–359. https://doi.org/10.1006/mpev.1999.0639

Apáthy S (1888) Süsswasser-Hirudineen. Zoologische Jahrbucher 3(5): 725–794.

Benson DA, Cavanaugh M, Clark K, Karsch-Mizrachi I, Ostell J, Pruitt KD, Sayers EW (2018) GenBank. Nucleic Acids Research 46(D1): D41–D47. https://doi.org/10.1093/nar/gkx1094

Blanchard R (1894) Hirudinées de l'Italie continentale et insulaire. Bollettino dei Musei di Zoologia ed Anatomia Comparata dell R. Università di Torino 9(192): 1–84. https://doi.org/10.5962/bhl.part.8048

Bolotov IN, Klass AL, Kondakov AV, Vikhrev IV, Bespalaya YV, Gofaro MY, Filippov BY, Bogan AE, Lopes-Lima M, Lunn Z, Chan N, Aksenova OV, Dvoryankin GA, Chapurina YE, Kim SK, Kolosova YS, Konopleva ES, Lee JH, Makhrov AA, Palatov DM, Sayenko EM, Spitsyn VM, Sokolova SE, Tomilova AA, Win T, Zubrii NA, Vinarski MV (2019) Freshwater mussels house a diverse mussel-associated leech assemblage. Scientific Reports 9(1): e16449. https://doi.org/10.1038/s41598-019-52688-3

Bosc LAG (1802) Histoire naturelle des vers: contenant leur description et leurs moeurs, avec figures dessinées d'après nature. Guilleminet, Paris, 324 pp. https://doi.org/10.5962/bhl.title.64025

Braun JFP (1805) Systematische Beschreibung einiger Egelarten: sowohl nach ihren äussern Kennzeichen als nach ihrem innern Bau. Berlin, 74 pp.

Carena H (1820) Monographie du genre *Hirudo* ou description des espéces de sangsues qui se trouvent ou qui sont en usage en piémont, avec des observations sur la génération, et sur d'autres points de l'histoire naturelle de quelques unes de ces espéces. Memorie della Reale Accademia delle Scienze die Torino 25: 273–316.

Carew ME, Coleman RA, Hoffmann AA (2018) Can non-destructive DNA extraction of bulk invertebrate samples be used for metabarcoding? PeerJ 6: e4980. https://doi.org/10.7717/peerj.4980

Castle WE (1900) Some North American fresh-water Rhynchobdellidae, and their parasites. Bulletin of the Museum of Comparative Zoölogy at Harvard College 36: 17–64.

Clopton RE (2004) Standard nomenclature and metrics of plane shapes for use in gregarine taxonomy. Comparative Parasitology 71(2): 130–140. https://doi.org/10.1654/4151

Dall PC (1982) Diversity in reproduction and general morphology between two *Glossiphonia* species (Hirudinea) in Lake Esrom, Denmark. Zoologica Scripta 11(2): 127–133. https://doi.org/10.1111/j.1463-6409.1982.tb00525.x

Diesing CM (1850) Systema Helminthum. Vol. I. Sumptibus Academiae Caesareae Scientiarum. Apud Wilhelmum Braumüller, Vindobonae, 679 pp.

Folmer O, Black M, Hoeh W, Lutz R, Vrigenhoek R (1994) DNA primers for amplification of mitochondrial cytochrome c oxidase subunit I from diverse metazoan invertebrates. Molecular Marine Biology and Biotechnology 3(5): 294–299.

Gouda HA (2010) A new *Alboglossiphonia* species (Hirudinea: Glossiphoniidae) from Egypt: description and life history data. Zootaxa 2361(1): 46–56. https://doi.org/10.11646/zootaxa.2361.1.4

Govedich FR (2001) A Reference Guide to the Ecology and the Taxonomy of Freshwater and Terrestrial Leeches (Euhirudinea) of Australasia and Oceania. Cooperative Research Centre for Freshwater Ecology, Identification Guide 35. Cooperative Research Centre for Freshwater Ecology, Albury, 67 pp.

Hoang DT, Chernomor O, von Haeseler A, Minh BQ, Vinh LS (2018) UFBoot2: Improving the ultrafast bootstrap approximation. Molecular Biology and Evolution 35(2): 518–522. https://doi.org/10.1093/molbev/msx281

Jueg U (2008) *Alboglossiphonia iberica* nov. sp.—eine neue Egelart von der Iberischen Halbinsel (Hirudinea: Glossiphoniidae). Lauterbornia 65: 43–61.

Kalyaanamoorthy S, Minh BQ, Wong TKF, Von Haeseler A, Jermiin LS (2017) ModelFinder: Fast model selection for accurate phylogenetic estimates. Nature Methods 14(6): 577–589. https://doi.org/10.1038/nmeth.4285

Katoh K, Standley DM (2013) MAFFT Multiple Sequence Alignment Software version 7: Improvements in performance and usability. Molecular Biology and Evolution 30(4): 772–780. https://doi.org/10.1093/molbev/mst010

Kaygorodova IA, Mandzyak N, Petryaeva E, Pronin NM (2014) Genetic diversity of freshwater leeches in Lake Gusinoe (eastern Siberia, Russia). The Scientific World Journal 2014: e619127. [11 pp] https://doi.org/10.1155/2014/619127

Klass AL, Sokolova SS, Kondakov AV, Bespalaya YV, Gofarov MY, Tomilova AA, Vikhrev IV, Bolotov IN (2018) An example of a possible leech–bryozoan association in freshwater. ZooKeys 794: 23–30. https://doi.org/10.3897/zookeys.794.28088

Klemm DJ (1976) Leeches (Annelida: Hirudinea) found in North American mollusks. Malacological Review 9: 63–76.

Klemm DJ (1982) Leeches (Annelida: Hirudinea) of North America. EPA-600/3-82/025. United States Environmental Protection Agency, Environmental and Support Laboratory, Cincinnati, Ohio, 177 pp.

Kwak H-J, Kim J-H, Kim J-Y, Jeon D, Lee D-H, Yoo S, Kim J, Eyun S, Park PC, Cho S-J (2021) Behavioral variation according to feeding organ diversification in glossiphoniid leeches (phylum: Annelida). Scientific Reports 11(1): e10940. https://doi.org/10.1038/s41598-021-90421-1

Light JE, Siddall ME (1999) Phylogeny of the leech family Glossiphoniidae based on mitochondrial gene sequences and morphological data. The Journal of Parasitology 85(5): 815–823. https://doi.org/10.2307/3285816

Linnaeus C (1761) Fauna Svecica. Sistens Animalia Sveciae Regni: Mammalia, Aves, Amphibia, Pisces, Insecta, Vermes. Editio Altera, Auctior. Sumtu &Literis Direct. Laurentii Salvii, Stockholmiae, 578 pp. https://doi.org/10.5962/bhl.title.46380

Lukin E (1976) Leech of fresh and brackish waters. Fauna of the USSR no. 109. Science, Leningrad, 484 pp.

Mack J, Kvist S (2019) Improved geographic sampling provides further evidence for the separation of *Glossiphonida complanata* and *Glossiphonia elegans* (Annelida: Clitellata: Glossiphoniidae). Journal of Natural History 53(5–6): 335–350. https://doi.org/10.1080/00222933.2019.1590658

Moore JP (1952) Professor A. E. Verrill's fresh-water leeches—A tribute and a critique. Notulae Naturae of the Academy of Natural Sciences of Philadelphia 245: 1–15.

Moquin-Tandon A (1846) Monographie de la Famille des Hirudinées. J.B. Baillière, Paris, 448 pp. https://doi.org/10.5962/bhl.title.6598

Moser WE (1991) Leeches (Annelida: Hirudinea) in central and western Nebraska. Transactions of the Nebraska Academy of Sciences 28: 87–91.

Moser WE, Klemm DJ, Richardson DJ, Wheeler BA, Trauth SE, Daniels BA (2006) Leeches (Annelida: Hirudinida) of northern Arkansas. Journal of the Arkansas Academy of Science 60: 84–95.

Moser WE, Richardson DJ, Hammond CI, Lazo-Wasem EA (2012) Molecular characterization of *Glossiphoninia elegans* (Verrill, 1872) (Glossiphoniidae: Hirudinida) from its type locality, West River, New Haven County, Connecticut, USA. Zootaxa 3195(1): 57–60. https://doi.org/10.11646/zootaxa.3195.1.4

Moser WE, Govedich FR, Oceguera-Figueroa A, Richardson DJ, Phillips AJ (2016) Subclass Hirudinida. In: Thorp J, Rogers DC (Eds) Keys to Nearctic Fauna: Thorp and Covich's Freshwater Invertebrates, Academic Press, Boston, 244–259. https://doi.org/10.1016/C2010-0-65589-1

Moser WE, Richardson DJ, Hammond CI, Gotte SW, Lazo-Wasem EA (2017) Distribution of *Placobdella hollensis* (Whitman, 1892) (Hirudinida: Glossiphoniidae). Comparative Parasitology 84(2): 165–168. https://doi.org/10.1654/1525-2647-84.2.165

Nesemann H, Neubert E (1999) Clitellata, Branchiobdellada, Acanthobdellada, Hirudinea. In: Schwoebel J, Zwig P (Eds) Süsswasserfauna von Mitteleuropa. Spectrum Akademischer Verlag, Heidelberg, Berlin, 1–178.

Nguyen L-T, Schmidt HA, von Haeseler A, Minh BQ (2015) IQ-TREE: A fast and effective stochastic algorithm for estimating maximum likelihood phylogenies. Molecular Biology and Evolution 32(1): 268–274. https://doi.org/10.1093/molbev/msu300

Oosthuizen JH (1987) Redescription of *Hemiclepsis quadrata* (Moore, 1939) n. comb. (Hirudinea: Glossiphoniidae). Systematic Parasitology 10(1): 73–78. https://doi.org/10.1007/BF00009102

Rambaut A (2018) FigTree, version 1.4.4. https://github.com/rambaut/figtree/ [Accessed on 2018-11-25]

Ratnasingham S, Hebert PDN (2013) A DNA-based registry for all animal species: The barcode index number (BIN) system. PLoS ONE 8(8): e66213. https://doi.org/10.1371/journal.pone.0066213

Richardson DJ (2006) Life cycle of *Oligacanthorhynchus tortuosa* (Oligacanthorhynchidae), an acanthocephalan of the Virginia opossum (*Didelphis virginiana*). Comparative Parasitology 73(1): 1–6. https://doi.org/10.1654/4207.1

Richardson DJ, Barger MA (2006) Redescription of *Oligacanthorhynchus major* (Machado-Filho, 1963) Schmidt, 1972 (Acanthocephala: Oligacanthorhynchidae) from the white-lipped peccary (*Tayassu pecari*) in Bolivia. Comparative Parasitology 73(2): 157–160. https://doi.org/10.1654/4235.1

Richardson DJ, Moser WE, Hammond CI, Shevchenko AC, Lazo-Wasem EA (2010) New geographic distribution records and host specificity of *Placobdella ali* (Hirudinida: Glossiphoniidae). Comparative Parasitology 77(2): 202–206. https://doi.org/10.1654/4456.1

Sawyer RT (1972) North American freshwater leeches, exclusive of the Piscicolidae, with a key to all species. Illinois Biological Monographs 46: 1–154. https://doi.org/10.5962/bhl.title.53881

Sawyer RT (1973) The Rediscovery of *Glossiphonia swampina* (Bosc, 1802) in the Coastal Plain of South Carolina (Annelida: Hirudinea). Journal of the Elisha Mitchell Scientific Society 89: 4–5.

Sawyer RT (1986) Leech Biology and Behaviour, Volumes I–III. Clarendon Press, Oxford, 1065 pp.

Sawyer RT (2021) Description and taxonomic analysis of a tuberculated turtle leech, provisionally identified as *Placobdella multilineata*. Zootaxa 4991(1): 1–35. https://doi.org/10.11646/zootaxa.4991.1.1

Sawyer RT, Shelley RM (1976) New Records and Species of Leeches (Annelida: Hirudinea) from North and South Carolina. Journal of Natural History 10(1): 65–97. https://doi.org/10.1080/00222937600770061

Shumway FM, Hegel R [Eds] (1990) New Haven Outdoors: a Guide to the City's Parks. Citizens Park Council of Greater New Haven, New Haven, 81 pp.

Siddall ME, Budinoff RB, Borda E (2005) Phylogenetic evaluation of systematics and biogeography of the leech family Gossiphoniidae. Invertebrate Systematics 19(5): 105–102. https://doi.org/10.1071/IS04034

Soós Á (1969) Identification Key to the Leech (Hirudinoidea) Genera of the world, with a catalogue of the species. VI. Family Glossiphoniidae. Acta Zoologica Academiae Scientiarum Hungaricae 15(3–4): 397–454.

Trajanovski S, Albrecht C, Schreiber K, Schultheiß R, Stadler T, Benke M, Wilke T (2010) Testing the spatial and temporal framework of speciation in an ancient lake species flock: the leech genus *Dina* (Hirudinea: Erpobdellidae) in Lake Ohrid. Biogeosciences 7(11): 3387–3402. https://doi.org/10.5194/bg-7-3387-2010

Trontelj P, Sket B, Steinbrück G (1999) Molecular phylogeny of leeches: Congruence of nuclear and mitochondrial rDNA data sets and the origin of bloodsucking. Journal of Zoological Systematics and Evolutionary Research 37(3): 141–147. https://doi.org/10.1111/j.1439-0469.1999.tb00976.x

Verrill AE (1872) Descriptions of North American freshwater leeches. American Journal of Science 3(14): 126–139. https://doi.org/10.2475/ajs.s3-3.14.126

Verrill AE (1874) Synopsis of the North American fresh-water leeches. Report of U.S. Commissioner of Fish and Fisheries 1872–1873: 666–689.

ZooKeys 1127: 155–215 (2022)
doi: 10.3897/zookeys.1127.84628
https://zookeys.pensoft.net

RESEARCH ARTICLE

A peer-reviewed open-access journal
ZooKeys
Launched to accelerate biodiversity research

Exceptional larval morphology of nine species of the *Anastrepha mucronota* species group (Diptera, Tephritidae)

Erick J. Rodriguez[1], Gary J. Steck[2], Matthew R. Moore[2], Allen L. Norrbom[3], Jessica Diaz[1], Louis A. Somma[2], Raul Ruiz-Arce[4], Bruce D. Sutton[5], Norma Nolazco[6], Alies Muller[7], Marc A. Branham[1]

1 *Department of Entomology and Nematology, University of Florida, Gainesville, FL, USA* **2** *Florida Department of Agriculture and Consumer Services, Division of Plant Industry (FDACS/DPI), Gainesville, FL, USA* **3** *Systematic Entomology Laboratory, USDA, ARS, c/o Smithsonian Institution, Washington, DC, USA* **4** *USDA APHIS PPQ S and T Insect Management and Molecular Diagnostic Laboratory, 22675 N. Moorefield Road, Edinburg, TX 78541, USA* **5** *Research Associate, Department of Entomology, Smithsonian Institution, USNM, Gainesville, FL, USA* **6** *Centro de Diagnostico de Sanidad Vegetal, Servicio Nacional de Sanidad Agraria, Av. La Molina 1915, La Molina, Peru* **7** *(retired) Ministry of Agriculture, Animal Husbandry and Fisheries, Paramaribo, Suriname*

Corresponding author: Erick J. Rodriguez (erick.rodriguez@ufl.edu)

Academic editor: Teresa Vera | Received 31 March 2022 | Accepted 4 July 2022 | Published 3 November 2022

https://zoobank.org/8A484FF4-67F1-40E2-BB0B-BE756CF0883A

Citation: Rodriguez EJ, Steck GJ, Moore MR, Norrbom AL, Diaz J, Somma LA, Ruiz-Arce R, Sutton BD, Nolazco N, Muller A, Branham MA (2022) Exceptional larval morphology of nine species of the *Anastrepha mucronota* species group (Diptera, Tephritidae). ZooKeys 1127: 155–215. https://doi.org/10.3897/zookeys.1127.84628

Abstract

Anastrepha is the most diverse and economically important genus of Tephritidae in the American tropics and subtropics. The striking morphology of the third instars of *Anastrepha caballeroi* Norrbom, *Anastrepha crebra* Stone, *Anastrepha haplacantha* Norrbom & Korytkowski, *Anastrepha korytkowskii* Norrbom, *Anastrepha nolazcoae* Norrbom & Korytkowski, and three newly discovered and as yet formally unnamed species (*Anastrepha* sp. Peru-82, *Anastrepha* sp. nr. *protuberans*, and *Anastrepha* sp. Sur-16), and the more typical morphology of *Anastrepha aphelocentema* Stone, are described using light and scanning electron microscopy. To contribute to a better understanding of the interspecific and intraspecific variation among species in the *mucronota* species group and facilitate phylogenetic studies, we integrate molecular and morphological techniques to confirm the identity and describe third instars. Larva-adult associations and the identification of described larvae were confirmed using DNA barcodes. We provide diagnostic characters to distinguish larvae among these nine species of the *mucronota* group and separate them from those of the 29 other *Anastrepha* species previously described. We introduce the vertical comb-like processes on the oral

margin as a novel character, and the unusual character states, including position and shape of the preoral lobe, and dentate or fringed posterior margins of the oral ridges and accessory plates. Our comparative morphology concurs with most previously inferred phylogenetic relationships within the *mucronota* group.

Keywords
Biology, distribution, fruit fly, host plant, larvae, taxonomy

Introduction

Anastrepha Schiner is the most species-rich and economically important genus of fruit flies in the American tropics and subtropics, comprising 328 described species to date (Norrbom et al. 2012, 2015, 2018, 2021; Rodríguez Clavijo and Norrbom 2021), for which third instars of only 29 species (~ 9%) have been described (Rodriguez et al. 2021). Some *Anastrepha* species are well known major economic pests, including *Anastrepha fraterculus* (Wiedemann) sensu lato (South American fruit fly complex), *Anastrepha ludens* (Loew) (Mexican fruit fly), *Anastrepha obliqua* (Macquart) (West Indian fruit fly), *Anastrepha serpentina* (Wiedemann) (sapote fruit fly), *Anastrepha striata* Schiner (guava fruit fly), and *Anastrepha suspensa* (Loew) (Caribbean fruit fly). Approximately 40 other species are considered minor pests, most with more restricted ranges of edible host plants (Norrbom et al. 1999; Norrbom 2004; Steck et al. 2019). Despite the economic significance and high diversity of *Anastrepha*, there is limited information on the taxonomy of the immature stages.

Anastrepha is currently divided into 27 species groups (Norrbom et al. 1999; Mengual et al. 2017; Norrbom et al. 2018; Steck et al. 2019), of which the *mucronota* group (52 species) is the most diverse (Norrbom et al. 2012; Steck et al. 2019), although it may not be monophyletic (Mengual et al. 2017). The *mucronota* group contains several minor pest species, including *A. atrox* (Aldrich), *A. bezzii* Lima, *A. mucronota* Stone, and *A. nolazcoae* Norrbom & Korytkowski (Steyskal 1977; Norrbom and Kim 1988; White and Elson Harris 1992; Norrbom and Korytkowski 2011; Norrbom et al. 2015; Steck et al. 2019). Of these four species, a description of the larva has been published only for *A. mucronota* (as *A. nunezae*, Steyskal 1977), but it is brief and lacks measurement data and details of major morphological structures. *Anastrepha mucronota* has been reared from *Annona cherimola* Mill. (cherimoya) (Molineros et al. 1992), and *Quararibea cordata* (Bonpl.) Vischer (yellow zapote), and the latter plant is also a host of *A. nolazcoae* (Steyskal 1977; Yepes and Vélez 1989; Carrejo and González 1994, 1999; Norrbom and Korytkowski 2011). *Anastrepha atrox* has been reared from *Annona cherimola* and *Pouteria lucuma* (Ruiz and Pav.) Kuntze (lucumo, lucma, lucuma in Spanish) (Molineros et al. 1992; Peña and Bennett 1995; Tigrero 1998, 2009; Korytkowski 2001; Norrbom 2004). *Anastrepha bezzii* has been reported to attack fruits of *Sterculia apetala* (Jacq.) H. Karst. (Panama tree, camoruro, anacaguita) and *Sterculia curiosa* (Vell.) Taroda (Norrbom and Kim 1988; Norrbom 1991, 2004; White and Elson-Harris 1992; Hernández-Ortiz 2007; Zucchi and Moraes 2008). Of those five hosts, *Q. cordata*, *P. lucuma*, and *A. cherimola* have edible fruit. Pulp of *Q. cordata* is eaten fresh as dessert because of its

sweet flavor, and it is commonly grown on small farms and has the potential to become a more important commercial crop in native areas (Martin et al. 1987).

The host plant relationships of *Anastrepha* are poorly known and are reported for only 127 (39%) *Anastrepha* species, including 15 species in the *mucronota* group (Norrbom 2004; CoFFHI 2020). Host plant and geographic distribution data are important to regulate international trade, prevent introduction of invasive pests, and facilitate their control or eradication. Host plant information for both pest and non-pest *Anastrepha* species will also likely contribute to understanding the evolution of *Anastrepha* (Aluja 1994; Norrbom et al. 1999; Aluja and Mangan 2008; Mansell 2017). New host plant and distribution records for six species within the *mucronota* group are reported here.

Molecular data sets produced for the study of phylogenetic relationships within *Anastrepha*, as well as the development of identification tools, have included species in the *mucronota* group. Cytochrome oxidase c subunit I (COI) barcodes are available for 22 species (42%) of the 52 described species within the *mucronota* group (Barr et al. 2017; Mengual et al. 2017), including six species for which larvae are described in this study: *A. aphelocentema* Stone, *A. caballeroi* Norrbom, *A. crebra* Stone, *A. haplacantha* Norrbom & Korytkowski, *A. korytkowskii* Norrbom, and *A. nolazcoae*. Previously published and new COI sequence data from reared adult flies in this study proved valuable for confirming the identity of these larvae and thereby contributing to their accurate description. This work will contribute to a better understanding of the morphological variation among species in the *mucronota* group, facilitate future phylogenetic studies, and improve capabilities for the accurate identification of larvae.

The scope of this study is to describe and illustrate the third instars of *A. aphelocentema*, *A. caballeroi*, *A. crebra*, *A. haplacantha*, *A. korytkowskii*, *A. nolazcoae*, and three as yet unnamed species here identified by code names, including *Anastrepha* sp. Peru-82, *Anastrepha* sp. nr. *protuberans*, and *Anastrepha* sp. Sur-16, collected from naturally-infested fruits in Mexico, Ecuador, Peru, and Suriname. We provide diagnostic morphological characters that are useful for distinguishing larvae of these nine species of the *mucronota* group. These characters are effective for separating larvae of *A. nolazcoae* from all other *Anastrepha* species that also feed on yellow zapote (*Quararibea cordata*), including those in the *mucronota* group (*A. mucronota*), the *fraterculus* group (*A. fraterculus*, s. l.), and the *striata* group (*A. striata*). Finally, we discuss relationships within the *mucronota* species group based on a novel character and several unusual character states in the larvae including the position of the preoral organ and shape of the preoral lobe, the dentate or fringed posterior margins of the oral ridges and accessory plates, and the vertical comb-like processes on the oral margin.

Materials and methods

Collecting, rearing, and preservation

For Peruvian, Ecuadorian, and Surinamese samples, fallen fruits were collected and transported to a screened rearing room in 1- or 2-liter plastic containers. For each host plant

latitude, longitude, and elevation data at the collection site were recorded using a GPS, and two samples with leaves, flowers, and fruits as available were collected for identification and vouchering. Fruits were dissected to obtain larvae. Of the total third instars, 25–50% were preserved in 70% ethanol for morphological study and DNA extraction, and the other subset of 50–75% of larvae were saved for rearing to the adult stage. Living larvae were killed by immersion in boiling water for 2 min, allowed to cool at room temperature for 2–5 min, then preserved in 5 ml vials with 70% ethanol. Rearing was conducted by placing the third instars into 1-liter plastic containers with a layer of 2.5–5.0 cm of moist vermiculite as a substrate for pupation. The tops of the containers were covered with a thin mesh of polyester or nylon fabric. Rearing containers were kept at room temperature, inspected daily, and the substrate was moistened if necessary. Reared adults were kept alive for 24–48 h to allow full development of coloration, then killed and preserved in 95% ethanol. Before females hardened in alcohol, the aculeus was extruded for identification.

Identification of flies and host plants

Reared adults were identified by ALN and EJR. Vouchers are deposited at the Florida State Collection of Arthropods (**FSCA**), Gainesville, Florida, USA; U.S. National Museum of Natural History, Smithsonian Institution, Washington, DC (**USNM**); and Museo de Historia Natural Javier Padro, Universidad Nacional Mayor de San Marcos, Lima, Peru (**MHNJP**). Host plants were identified by Juan Celidonio Ruiz Herbarium Amazonense (**AMAZ**), Rufo Bustamante (Asociación para la Conservación de la Cuenca Amazónica - ACCA), Milton Zambrano (Pontificia Universidad Católica del Ecuador – PUCE, Estacion Cientifica Yasuni), and Sabitrie Jairam-Doerga (Nationaal Herbarium van Suriname – BBS). Plant vouchers are deposited at the U.S. National Museum of Natural History, Smithsonian Institution, Washington, D.C. (**USNM**); Universidad Nacional San Antonio Abad de Cusco, Perú (**UNSAAC**); Herbarium Amazonense (**AMAZ**) of the Universidad Nacional de la Amazonia Peruana, Iquitos, Perú (**UNAP**); and Nationaal Herbarium van Suriname (**BBS**).

Specimen preparation

Intact preserved larvae were submerged in 70% ethanol to photograph the habitus (dorsal and lateral views) at 10 × magnification, and anal lobe and oral ridges at 150 × magnification using a Zeiss Discovery V12 dissecting microscope, Zeiss AxioCam ICc 5 digital camera and ZEN 2 software (Blue edition 2011). For slide-mounted specimens, the cephaloskeleton was detached from the head, and the cuticle was incised following Steck et al. (1990).

Preparation and imaging of slide-mounted larval specimens

Internal tissues (gut and muscle tissue) were placed in 95–100% ethanol for molecular analysis. The cuticle of specimens to be slide-mounted was macerated overnight in 10%

cold sodium hydroxide solution (NaOH) and cleaned by washing with distilled water and squeezing out the undigested internal tissues with an insect pin. Then the cephaloskeleton and cuticle were separately slide mounted in glycerin for observation and imaging using a Zeiss Axio Imager M2 compound microscope, Zeiss AxioCam 503 color digital camera and ZEN 2 software. The cephaloskeleton was photographed and measured at 100 ×, and the prothoracic and posterior spiracles at 400 ×. Measurements were taken as described in Steck and Wharton (1988). Stacks of images were rendered with the Z-stack function of ZEN 2 and Zerene Stacker software. After imaging, specimens were returned to 70% ethanol for permanent preservation and stored at FSCA.

Preparation and imaging of larval specimens for SEM

The fifth abdominal segment was removed and placed in 95–100% ethanol for DNA extraction. The remaining anterior and posterior ends of the specimens were dehydrated by passing through an ethanol series of 70, 80, 95, and 100% (1 h each), followed by ethyl acetate (1 or 2 h), then air-dried, individually mounted on stubs with carbon tape, placed in a desiccator overnight, and sputter-coated with gold-palladium. Stub-mounted specimens were photographed and examined with a Phenon XL G1 and G2 Desktop SEM (Nanoscience Instruments, ThermoFischer Scientific, Phoenix, Arizona, USA) (Figs 28–32, 36, 39, 41–44, and 48–51) and JEOL JSM–5510LV SEM (JEOL USA, Inc., Peabody, Massachusetts, USA) (other SEM figures) at FDACS/DPI, Gainesville, FL. After imaging, specimens were stored at FSCA.

DNA barcodes for confirmation of larval identity

DNA was extracted from adult and larval specimens using Qiagen DNeasy Blood and Tissue kits. COI barcodes were amplified using the primers LCO1490/HCO2198 (Folmer et al. 1994) or LEPF1/LEPR1 (Hebert et al. 2004). Alternatively, the primers C1-J-1632 (Kambhampati and Smith 1995) and C1-N-2191 (Simon et al. 1994) were used in some samples. PCR products were purified and bidirectionally sequenced on an Applied Biosystems SeqStudio Platform with BigDye Terminator v. 3.1 chemistry. Sequence traces were trimmed and assembled in Sequencher 5.4.6. K2P sequence similarity (Kimura 1980) between adults and larvae was evaluated in MEGA7 (Kumar et al. 2016) and by GenBank BLAST searches. Larvae were identified with the consensus identity function in BarcodingR (Zhang et al. 2017) using a library of previously published and newly sequenced *Anastrepha* COI barcodes (Moore et al. in press). The consensus identity function in BarcodingR provides identifications of protein-coding sequences by three methods: fuzzy-set based, BP-based, and Bayesian methods (Munch et al. 2008; Zhang et al. 2008, 2012; Hao et al. 2011; Zhang et al. 2017). Consensus identifications are supported by numerical "votes", which is the total of the three analyses that provided the same identification. A support of two or three votes was the criterion of confidence used to make a molecular identification. Comparisons between larval and identified adult sequences yielding a single vote were considered ambiguous.

Terminology

We largely follow the terminology used in previous *Anastrepha* larva descriptions (e.g., Steck and Wharton 1988; White et al. 1999; Carroll et al. 2004; Rodriguez et al. 2021) and adopt current usage in other Diptera families and understanding of homologies following Courtney et al. (2000) and Borkent and Sinclair (2017). Terminology of the sensilla of the maxillary palp and dorsolateral group follows Chu-Wang and Axtell (1972). In the present study we introduce the term vertical comb-like process (Figs 53, 68, 111), which are elongate structures, connected laterally at the oral margin and projecting medially into the oral cavity, located adjacent to the labium and posterior to the oral ridges. We also introduce the term fringed and redefine the nomenclature of serrate, emarginate, and dentate to describe the posterior margins of the oral ridges and accessory plates. An emarginate margin is defined as having rounded (inverted U) or triangular (inverted V) notches, one quarter to one third the width of the basal part of the oral ridge, that are widely spaced (see White and Elson-Harris 1992: pls 5a, 6b; Carroll et al. 2004; Rodriguez et al. 2021: fig. 2). A serrate margin is defined as having small or minute teeth or projections less than one quarter the width of the basal part of the oral ridge, that are closely or moderately spaced (Figs 1, 2). A dentate margin is defined as having toothlike projections, one quarter to half the width of the basal part of the oral ridge, that are closely or moderately spaced, of even or uneven length, usually both sides of each tooth are equal, and the acute tips are above the middle of base (Figs 42, 109, and 110 for oral ridges; see Fig. 15 for accessory plates). A fringed margin is defined as having filaments or projections at least as long as the basal, non-incised part of the oral ridge (Figs 29, 67, 81, 82, 84, 95, 96), that are closely or moderately spaced, usually of even length, and tapering to a blunt tip.

Larval specimens of the outgroup for comparative morphology of the pseudocephalon

Larvae of 13 *Anastrepha* species classified in eight species group were photographed and examined with a JEOL JSM–5510LV SEM (JEOL USA, Inc., Peabody, Massachusetts, USA) at FDACS/DPI, and the descriptions and illustrations of 15 species in the literature were consulted (Table 1). After imaging, specimens were stored at FSCA. Characters of the pseudocephalon with relevant phylogenetic signal were evaluated to construct a character matrix including the ingroup (*mucronota* species group) and outgroup taxa.

Visualization of the phylogenetic relationships within the *mucronota* group

The novel larval morphological character states of the pseudocephalon were plotted on the phylogenetic tree for *Anastrepha* from Mengual et al. (2017: fig. 1) to aid our discussion of relationships within the *mucronota* group. We redrew a section of the phylogeny with the aid of FigTree v. 1.4.4 (Rambaut 2018), and the image (Fig. 123) was modified using Adobe Illustrator and Adobe Photoshop Elements.

Table 1. List of the examined outgroup taxa including literature for coding larval characters of the pseudocephalon.

Species group	Species	Collection site	Unique identifier	Additional specimens from literature
curvicauda	*A. curvicauda*	USA: Florida: Miami Dade Co., Homestead area, reared from fruit of *Carica papaya* L.	FF20170329.06–FF20170329.15	Frías et al. 2006
fraterculus	*A. amita*	–	–	Dutra et al. 2018a
	A. amplidentata	Peru: Madre de Dios: Puerto Maldonado, Centro de Investigación y Capacitación Rio Los Amigos, 12.5713°S, 70.0905°W, 277 m	AP20170713.09, AP20170713.12, AP20170713.15, AP20170713.17	Rodriguez et al. 2021
	A. bahiensis	Peru: Cusco: Pilcopata, Centro de Investigación Villa Carmen, 12.9020°S, 71.4113°W, 765 m.	AP20171024.08–AP20171024.10	Dutra et al. 2012
	A. coronilli	Panama: Cocle: Villa Carmen Village, 8.7973°S, 80.5470°W, 76 m.	AP20171115.01–AP20171115.03	Dutra et al. 2012
	A. durantae	Peru: Cusco: Echarate, Manto Real, 12.6552°S, 72.5766°W, 770 m.	AP20190827.16–AP20190827.18	Rodriguez et al. 2021
	A. ludens	Panama: Cocle: Barreta, 8.5892°S, 80.7139°W, 546 m. USA: Texas: USDA, ARS Lab. colony.	AP20180703.06–AP20180703.15	Carroll and Wharton 1989
	A. sororcula	–	–	Dutra et al. 2018a
	A. suspensa	–	–	White and Elson-Harris 1992
	A. zenildae	–	–	Dutra et al. 2018a
grandis	*A. grandis*	Austria: Viena: Seibersdorf, IAEA colony. USA: Florida: infested commodity from Peru intercepted at Miami International Airport	AP20180109.04–AP20180109.13	–
leptozona	*A. leptozona*	Peru: Cusco: Pilcopata, Centro de Investigación Villa Carmen, 12.8946°S, 71.4112°W, 619 m.	AL-01–AL-13	Frías et al. 2009
pseudoparalella	*A. limae*	Panama: Cocle: Villa Carmen Village, 8.7988°S, 80.5509°W, 77 m.	AP20180524.10–AP20180524.19	–
serpentina	*A. pulchra*	Peru: Madre de Dios: Puerto Maldonado, Centro de Investigación y Capacitación Rio Los Amigos, 12.5554°S, 70.1091°W, 281 m.	APU-01–APU-09	Dutra et al. 2018b
	A. serpentina	Peru: Lima: SENASA Lab. UCPMF/DM, colony	ASR-01–ASR-08	White and Elson-Harris 1992
spatulata	*A. pickeli*	Panama: Cocle: Barreta, 8.5812°S, 80.7414°W, 735 m. Peru: Cusco: Pilcopata, Centro de Investigación Villa Carmen, 12.5342°S, 71.2410°W, 534 m	API-01–API-12	Dutra et al. 2018b
striata	*A. striata*	Peru: Cusco: Pilcopata, Centro de Investigación Villa Carmen, 12.8936°S, 71.4054°W, 536 m.	AP20160223.01–AP20160223.02, AP20160223.06–AP20160223.07, AP20160223.09, AP20160223.11	White and Elson-Harris 1992

Results

Descriptions of third instars

***Anastrepha aphelocentema* Stone, 1942**
Figs 1–13

Material examined. Mexico • 4 larvae; Veracruz, Xalapa, Papantla; 20.3992°N, 97.3469°W; 72 m a.s.l.; Jul.1998; M. Aluja leg.; reared from fruit of *Pouteria glomerata* (Miq.) Radlk. (Sapotaceae); FSCA (AP20171024.07, AP20190827.04, AP20180726.01–AP20180726.02).

Diagnosis. *Anastrepha aphelocentema* runs to *A. leptozona* Hendel in the key of Steck et al. (1990), and to two species (*A. leptozona* and *A. serpentina*) in that of Carroll et al. (2004). It differs from all species within the *mucronota* group in having the posterior margins of the oral ridges and accessory plates finely serrate or entire. In addition, *A. aphelocentema* can be separated from *A. curvicauda* (Gerstaecker) by the position of the preoral organ (lateral vs. anterior to the mouthhook), and from *A. curitis* Stone in having a higher number of oral ridges (12–14 vs. 8–11). It can be also distinguished from most other species for which larvae have been described by the number of tubules of the prothoracic spiracle (24–27). This includes larvae of *A. pallens* Coquillett of the *daciformis* group (17–22 tubules), various species of the *fraterculus* group (9–22; see Rodriguez et al. 2021), *A. grandis* (Macquart) of the *grandis* group (31–37), *A. leptozona* of the *leptozona* group (15–21), two species of the *pseudoparallela* group (*A. limae* Stone with 18–21, and *A. consobrina* (Loew) with 12–15), two species of the *spatulata* group (*A. pickeli* Lima with 16–23, and *A. interrupta* Stone 10–13), two species of the *serpentina* group (*A. pulchra* Stone with 18–23, and *A. serpentina* (Wiedemann) with 13–19), and two species of the *striata* group (*A. bistrigata* Bezzi with 13–20, and *A. striata* Schiner with 11–18). The larva of *Anastrepha sagittata* Stone (*dentata* group), reared from seeds of the related species *Pouteria campechiana* (Kunth) Baehni, was described with limited data (Baker et al. 1944) but can be morphologically separated from *A. aphelocentema* by the longer and narrower posterior spiracle openings.

Description. ***Habitus.*** Third instar elongate, cylindrical, tapered anteriorly and truncate posteriorly; color creamy; amphipneustic. Length 11.00−11.77 mm and width 2.03−2.12 mm at the sixth abdominal segment.

Pseudocephalon (Figs 1–4). Antenna and maxillary palp on moderately developed lobe. Antenna with cylindrical base and apical knob. Maxillary palp bearing three papilla sensilla, two knob sensilla; dorsolateral group of sensilla bearing two well-developed papilla sensilla, aligned perpendicular to palp and surrounded by collar. Facial mask globular in lateral view. Preoral organ bearing three unbranched peg sensilla, located apically on simple elongate preoral lobe or on separate small cylindrical lobe (asymmetrical in Fig. 1) lateral to the mouthhook; three or four petal-like secondary lobes adjacent to preoral organ. Oral ridges in 12–14 rows, posterior margin finely

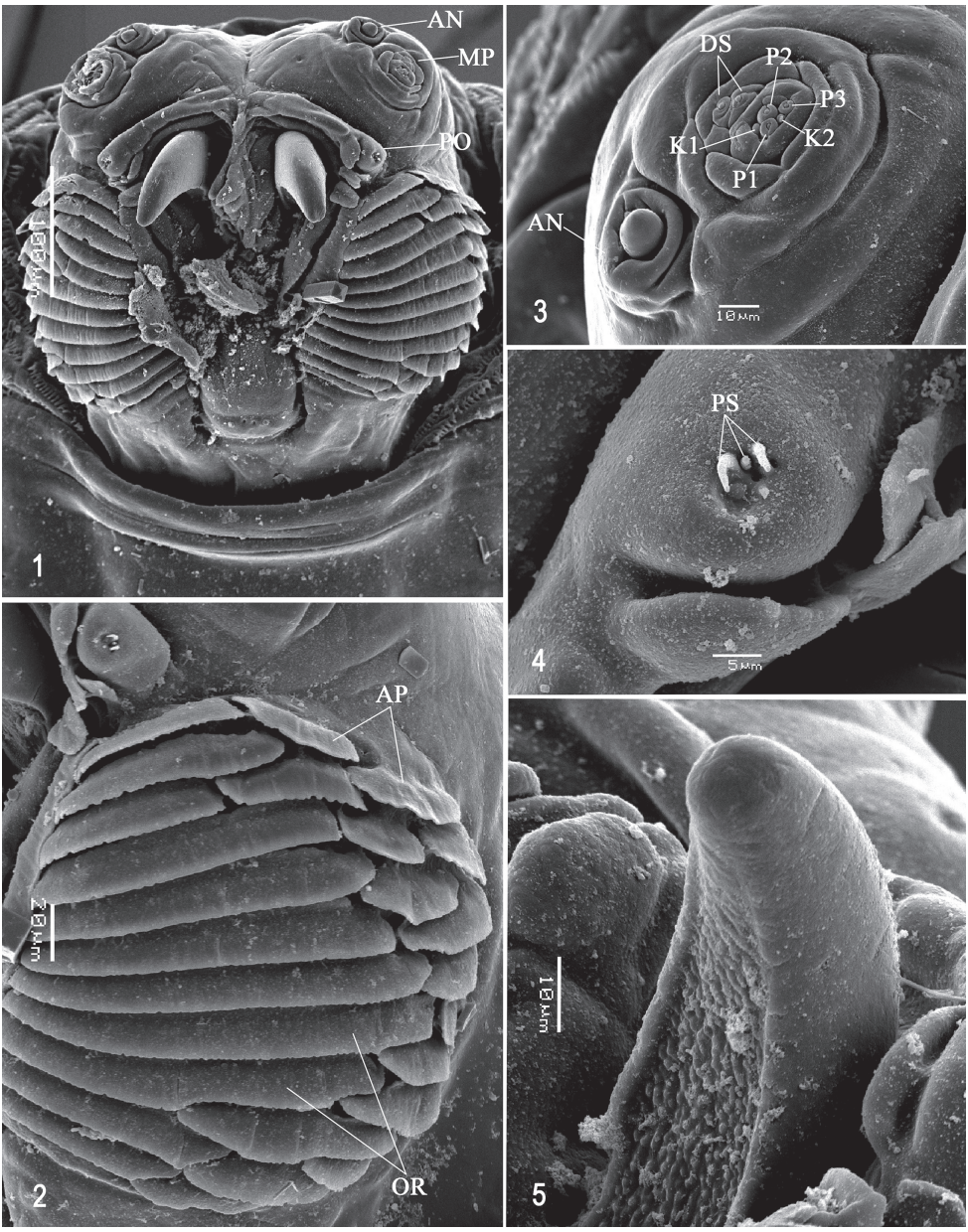

Figures 1–5. Scanning electron photomicrographs of third instar of *Anastrepha aphelocentema* **1** pseudocephalon **2** oral ridges **3** antenna and maxillary palp **4** preoral organ **5** ventral surface of mouthhook. Abbreviations: AN, antenna; MP, maxillary palp; PO, preoral organ; AP, accessory plates; OR, oral ridges; P1–P3, papilla sensilla; K1, K2, knob sensilla; DS, dorsolateral papilla sensilla; PS, peg sensilla. Scale bars: 5 µm (**4**); 10 µm (**3, 5**); 20 µm (**2**); 100 µm (**1**).

serrate or entire; 15–17 accessory plates, posterior margin usually serrate, most oral ridges bordered with single accessory plate laterally, except anterior 2–5 plates in two series, plates much narrower than ridges. Labium triangular, anterior surface knobby (not clearly visible in Fig. 1), ventrally with two visible sensilla and tubercles.

Cephaloskeleton (Figs 5–7). Total length from tip of mouthhook to end of ventral cornu 1.31 mm. Mouthhook well sclerotized, black apically and basally; length a 0.28 mm; length b 0.22 mm; height c 0.20 mm; ratio a:b 1.29; ratio a:c 1.4. Tooth long, sharp, deeply concave ventrally, strongly curved, concave ventrally, ventral surface rough. Intermediate sclerite 0.22–0.23 mm long, 0.16 mm wide at ventral bridge. Epipharyngeal sclerite visible only in dorsal view, with medial lobe directed anteriorly. Labial sclerite robust, sclerotized in dorsal view. Parastomal bar extending for almost entire length of intermediate sclerite. Dorsal arch 0.35 mm high. Dorsal cornu with well-defined sclerotized area adjacent to notch, 0.50 mm long. Dorsal bridge prominently projecting anteriorly from dorsal cornu and slightly sclerotized. Anterior sclerite irregularly shaped and sclerotized. Cornu notch (N) 0.33 mm long and cornu notch index (N/DC) 0.7. Ventral cornu with poorly defined sclerotized area along edge of notch. Pharyngeal filter with weakly sclerotized anterior bar and eight ridges forming a series of grooves along length of ventral cornu. Ventral cornu 0.81 mm long from pharyngeal bar to posterior end of grooves. Ventral cornu 1.63 × as long as sclerotized area of dorsal cornu.

Thoracic and abdominal segments. Thoracic segments with dorsal spinules conical, symmetrical to slightly posteriorly curved; dorsal spinule pattern, as follows: T1 with 5−7 rows, forming scalloped plates; T2 with four or five rows; T3 lacking spinules; ventral spinule pattern as follows: T1 with 5−7 rows; T2 with 0−2 rows; T3 with two rows. Abdominal segments (A1–A8) lacking dorsal spinules; ventral creeping welts present on all abdominal segments; ventral spinule pattern as follows: A1 with six or seven rows; A2 with 10–12 rows; A3–A6 with 14–18 rows; A8 with 12–16 rows. Additional four or five discontinuous rows of spinules surrounding anal lobes, spinules all equally small, basally broad, distally sharply pointed, pointing away from anal lobes.

Prothoracic spiracle (Figs 8, 9). Bilobed, bearing 24–27 tubules, distally rounded and arranged in a single, sinuous row laterally and double row medially. Spiracle distal width 0.35–0.36 mm; basal width 0.19 mm at junction with trachea.

Caudal segment (Figs 10, 11). Dorsal tubercles and sensilla weakly developed, D1 distinctly anterior to D2. Intermediate tubercles (I1 and I2) moderately developed, I1 lateral and sometimes slightly dorsal to I2, associated sensilla weakly developed. Lateral (L1) tubercles, and associated sensilla weakly developed. Ventral (V1 and V2) tubercles and sensilla weakly developed, V1 distinctly posterior to V2. Anal lobe entire or grooved and moderately protuberant.

Posterior spiracle (Figs 10, 12, 13). Located above horizontal midline. Posterior spiracle openings with thick rimae and numerous trabeculae; 94–101 μm long; 35−37 μm wide; ratio length/width 2.68−2.72. Ecdysial scar apparent. Felt chamber oval, 190−191 μm in diameter at junction with trachea. Spiracular process SP-I comprising 4−9 trunks and 12−21 tips; ratio tips/trunks 2.3−3.0; basal width 9−12 μm; ratio basal width/length of spiracular opening 0.09−0.12. SP-II comprising three or

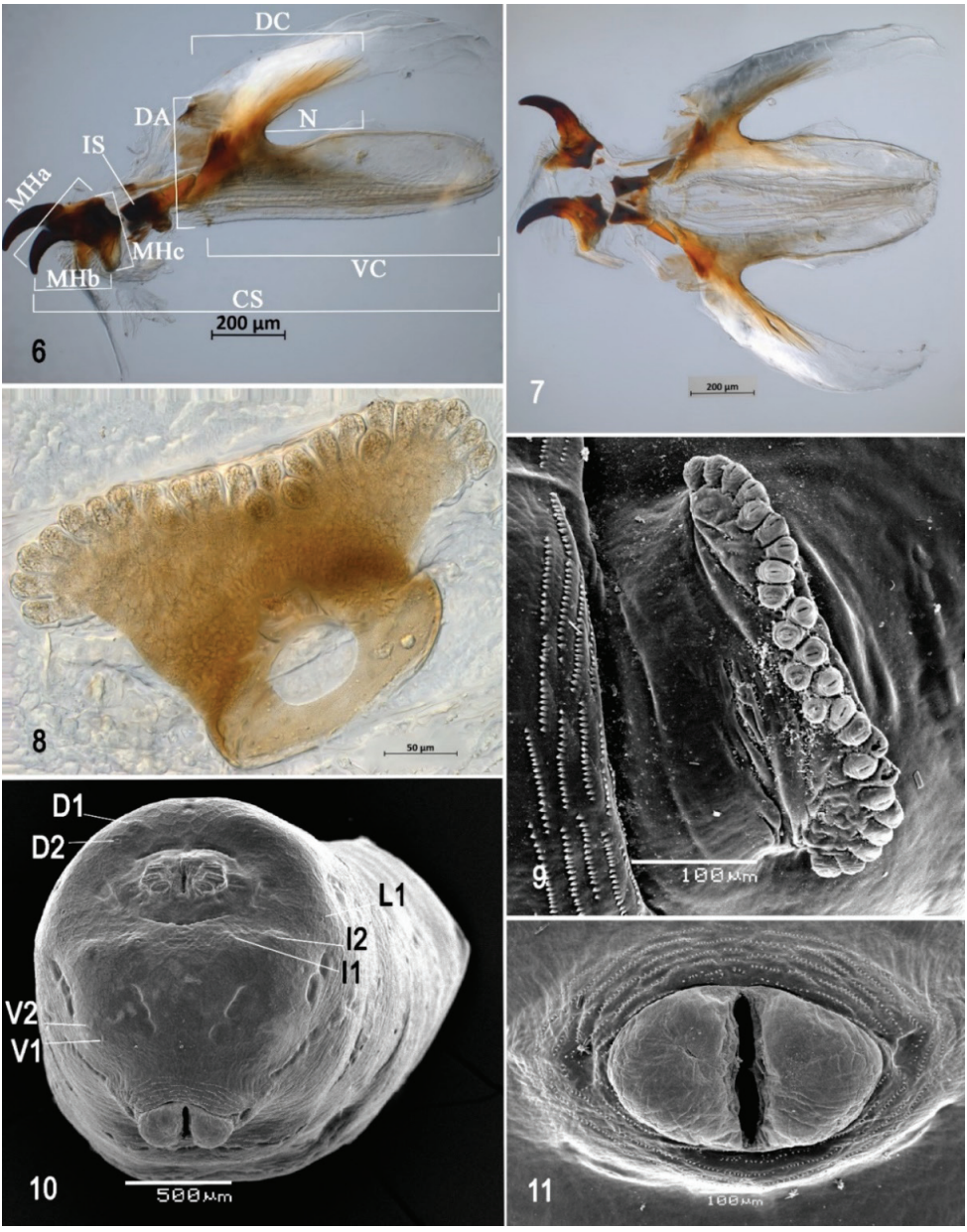

Figures 6–11. Optical photomicrographs and scanning electron photomicrographs of third instar of *Anastrepha aphelocentema* **6** cephaloskeleton, lateral view **7** cephaloskeleton, dorsal view **8** prothoracic spiracle, lateral view **9** prothoracic spiracle, dorslateral view **10** caudal segment **11** anal lobe. Abbreviations: CS, total length of cephaloskeleton; MHa, mouthhook length a; MHb, mouthhook length b; MHc, mouthhook height c; IS, intermediate sclerite; DA, dorsal arch; DC, length of sclerotized area of dorsal cornu; N, notch; VC, length of ventral cornu; D1, D2, dorsal tubercles and sensilla; I1, I2, intermediate tubercles and sensilla; L1, lateral tubercle and sensillum; V1, V2, ventral tubercles and sensilla. Scale bars: 50 µm (**8**); 100 µm (**9, 11**); 200 µm (**6, 7**); 500 µm (**10**).

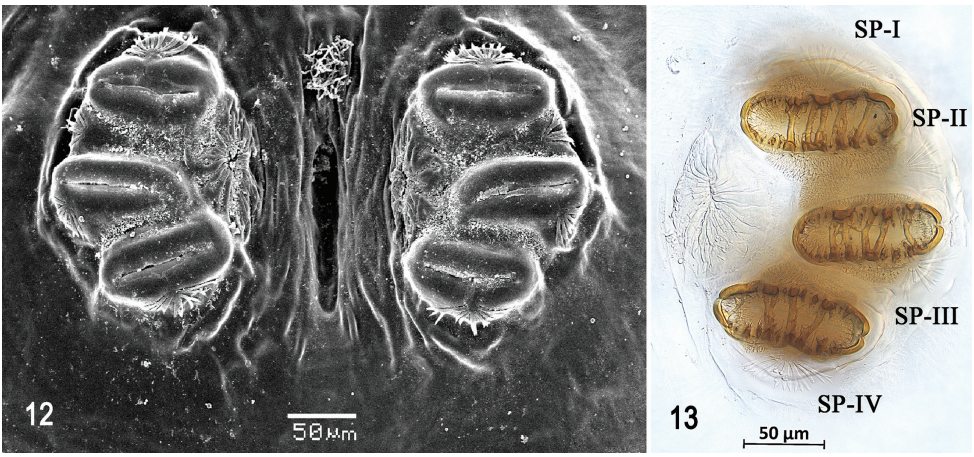

Figures 12, 13. Scanning electron photomicrograph and optical photomicrograph of posterior spiracles of third instar of *Anastrepha aphelocentema*. Abbreviations: SP-I to SP-IV, spiracular processes. Scale bars: 50 µm (**12, 13**).

four trunks and seven or eight tips. SP-III comprising 3–7 trunks and 6–12 tips. SP-IV comprising 3–7 trunks and 10–15 tips; ratio tips/trunks 2.14–3.33; basal width 9–10 µm; ratio basal width/length of spiracular opening 0.09–0.11.

Distribution. *Anastrepha aphelocentema* is known only from Mexico (northern Veracruz and San Luis Potosí) (Aluja et al. 2000; Norrbom 2004; Hernández-Ortiz 2007; CoFFHI 2020).

Biology. This species was reared from fruit of *Pouteria glomerata*. It has been previously reared from fruits of *Casimiroa edulis* La Llave and Lex. (Rutaceae) (Hernández-Ortiz 1992) and *Pouteria glomerata* (Sapotaceae) (Stone 1942; Baker et al. 1944; Norrbom and Kim 1988; Aluja et al. 2000; Hernández-Ortiz 2007).

Molecular identification. COI barcodes were generated from four larvae and submitted to GenBank (MT644043, MT654963–MT654965). These data further confirm the identity of the described larvae. K2P distances between *A. aphelocentema* larvae and the available adult sequence (KY428328) were less than one percent. BLAST searches were consistent with our new data, yielding only one good match: *A. aphelocentema* (99.84% sequence identity; KY428328). Additionally, all four barcodes returned consensus identifications of *A. aphelocentema* with three votes using the identity function in BarcodingR (Moore et al. in press).

Anastrepha caballeroi Norrbom, 2015

Figs 14–27

Material examined. Peru • 13 larvae; Madre de Dios, Puerto Maldonado, Centro de Investigación y Capacitación Río Los Amigos (CICRA), trail 2; 12.5612°S, 70.1085°W;

287 m a.s.l.; 28 Jan. 2014; E. J. Rodriguez and J. Caballero leg.; reared from fruit of *Quararibea malacocalyx* (A. Robyns and S. Nilsson) W.S. Alverson (Malvaceae); FSCA (AP20180321.05–AP20180321.14, AP20190827.07–AP20190827.09).

Diagnosis. *Anastrepha caballeroi* can be distinguished from all other species of *Anastrepha* by the dentate posterior margins of its accessory plates; in other species of the *mucronota* group the margins of the oral ridges are serrate or mostly or entirely fringed (see Tables 2–4). It also differs from all other *Anastrepha* species in having 27−36 accessory plates mostly in two series and covering a much larger area than the oral ridges.

Description. ***Habitus.*** Third instar elongate, cylindrical, tapered anteriorly and caudal end truncate; color creamy; amphipneustic. Length 10.24−10.61 mm and width 1.66−1.69 mm at the sixth abdominal segment.

Pseudocephalon (Figs 14–18). Antenna and maxillary palp on moderately developed lobe. Antenna with cylindrical base and apical knob. Maxillary palp bearing three papilla sensilla, two knob sensilla; dorsolateral group of sensilla bearing two well-developed papilla sensilla, aligned perpendicular to palp and surrounded by collar. Facial mask partly globular in lateral view, upper right section lacking ridges and accessory plates and forming almost a right angle. Preoral organ bearing 1–3 unbranched peg sensilla, located apically on small cylindrical lobe anterolateral to mouthhook, with or without one or two adjacent finger-like lobes; preoral lobe elongate, split apically, extending posterior to preoral organ. Oral ridges in 14 or 15 short rows, posterior margin entire or undulant (occasionally 1–3 posterior ridges emarginate); 27–36 accessory plates, posterior margin deeply dentate with sharply pointed teeth, anterior and posterior plates in one series, medial plates in two series, plates covering much larger area than oral ridges. Labium triangular, anterior surface knobby (not clearly visible in Fig. 14), ventrally with two visible sensilla on small tubercles.

Cephaloskeleton (Figs 19–21). Total length from tip of mouthhook to end of ventral cornu 1.26–1.31 mm. Mouthhook well sclerotized, black apically and basally; length a 0.28–0.29 mm; length b 0.21–0.23 mm; height c 0.18–0.20 mm; ratio a:b 1.28–1.37; ratio a:c 1.45–1.63. Tooth long, sharp, strongly curved, concave ventrally, ventral surface eroded. Intermediate sclerite 0.21–0.23 mm long, 0.13–0.15 mm wide at ventral bridge. Epipharyngeal sclerite visible only in dorsal view, with medial lobe directed anteriorly. Labial sclerite short, robust, sclerotized in dorsal view. Parastomal bar extending for almost entire length of intermediate sclerite. Dorsal arch 0.27–0.29 mm high. Dorsal cornu with well-defined sclerotized area adjacent to notch, 0.51–0.54 mm long. Dorsal bridge prominently projecting anteriorly from dorsal cornu and slightly sclerotized. Anterior sclerite irregularly shaped and sclerotized. Cornu notch (N) 0.30–0.34 mm long and cornu notch index (N/DC) 0.59–0.63. Ventral cornu with poorly defined sclerotized area. Pharyngeal filter with weakly sclerotized anterior bar and seven ridges forming a series of grooves along length of ventral cornu. Ventral cornu 0.79–0.83 mm long from pharyngeal bar to posterior end of grooves. Ventral cornu 1.54–1.56 × as long as sclerotized area of dorsal cornu.

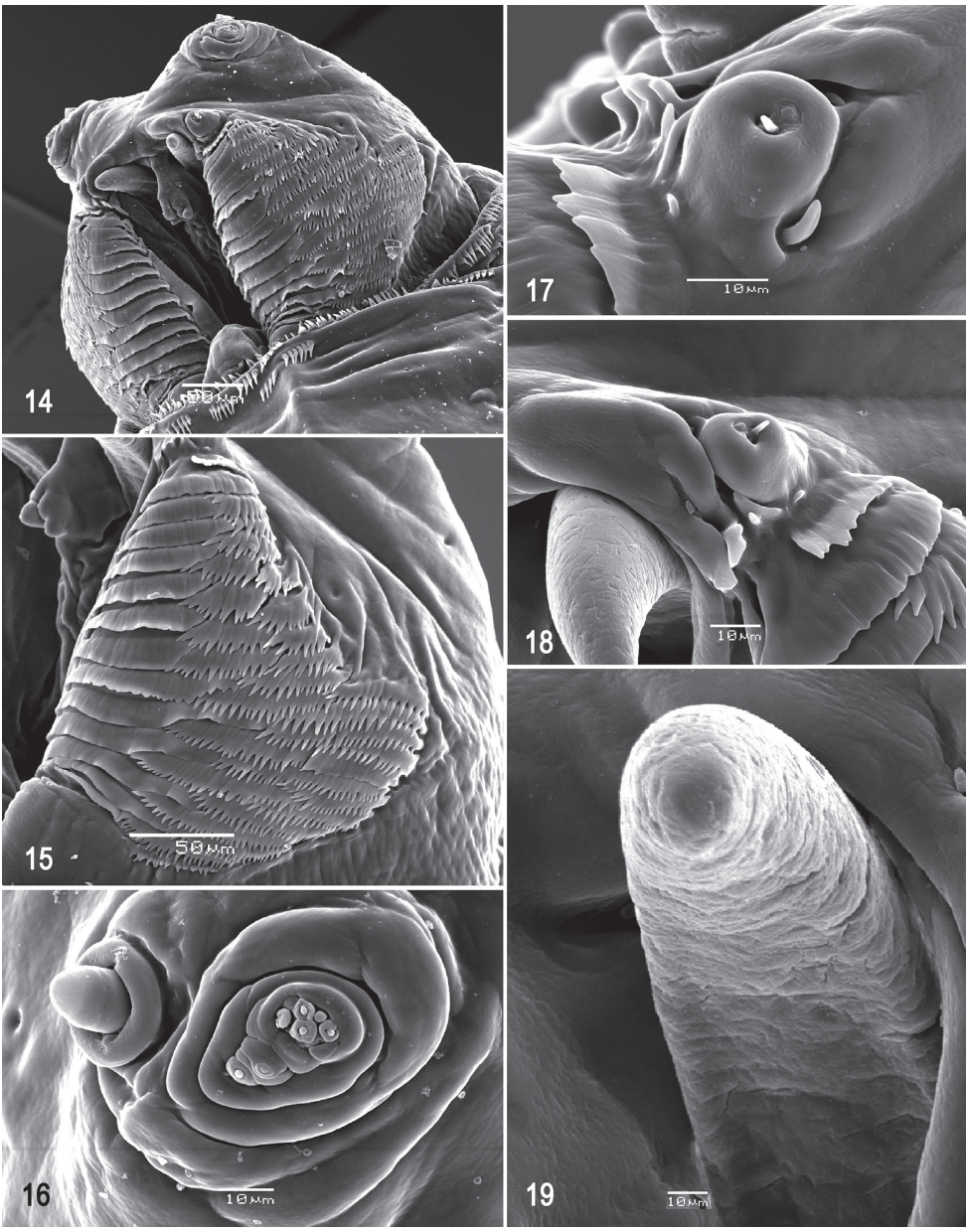

Figures 14–19. Scanning electron photomicrographs of third instar of *Anastrepha caballeroi* **14** pseudocephalon **15** oral ridges **16** antenna and maxillary palp **17** preoral organ, dorsal view **18** preoral organ, dorsolateral view **19** ventral surface of mouthhook. Scale bars: 10 µm (**16–19**); 50 µm (**14, 15**).

Thoracic and abdominal segments. Thoracic segments with dorsal spinules conical, symmetrical to slightly curved posteriorly; dorsal spinule pattern in rows as follows: T1 with three rows, forming scalloped plates; T2 with three rows; T3 lacking

spinules; ventral spinule pattern as follows: T1 with seven or eight rows; T2 with three rows; T3 with 0–2 rows. Abdominal segments (A1–A8) lacking dorsal spinules; ventral creeping welts present on all abdominal segments; ventral spinule pattern as follows: A1 with two or three rows; A2 with six or seven rows; A3 with seven or eight rows; A4–A5 with 7–9 rows; A6 with seven or eight rows, A7–A8 with six or seven rows. Additional three or four anterior and posterior discontinuous rows of spinules, and one or two lateral rows around anal lobes, spinules large, conical, distally sharp, pointing away from anal lobes.

Prothoracic spiracle (Figs 22, 23). Bilobed, bearing 17–21 tubules, distally rounded and arranged in a single sinuous row. Spiracle distal width 0.28–0.33 mm; basal width 0.13−0.16 mm at junction with trachea.

Caudal segment (Figs 24, 25). Dorsal tubercles and sensilla well developed, D1 distinctly anterior to D2. Intermediate tubercles (I1 and I2) moderately developed, I1 lateral and sometimes slightly ventral to I2, associated sensilla weakly developed. Lateral (L1) and ventral (V1 and V2) tubercles, and associated sensilla weakly developed. Anal lobe entire and moderately protuberant.

Posterior spiracle (Figs 24, 26, 27). Located above horizontal midline. Posterior spiracle openings with thick rimae and numerous trabeculae; 76–89 μm long; 31−37 μm wide; ratio length/width 2.4−2.5. Ecdysial scar apparent. Felt chamber oval, 143−184 μm in diameter at junction with trachea. Spiracular process SP-I comprising 5−8 trunks and 10−18 tips; ratio tips/trunks 2.0−2.3; basal width 7−13 μm; ratio basal width/length of spiracular opening 0.08−0.15. SP-II comprising 3−5 trunks and 3−10 tips. SP-III comprising 4−7 trunks and 4−12 tips. SP-IV comprising 4−7 trunks and 7−17 tips; ratio tips/trunks 1.8−2.4; basal width 5−7 μm; ratio basal width/length of spiracular opening 0.06−0.08.

Distribution. *Anastrepha caballeroi* is known only from southeastern Peru (Cusco and Madre de Dios).

Biology. We reared this species from fruit of *Quararibea malacocalyx*, the only known host plant (Norrbom et al. 2015). The larvae feed only on the pulp of the fruit.

Molecular identification. COI barcodes were generated from 13 larvae and nine adults of *A. caballeroi* and submitted to GenBank (MH070125, MT644046–MT644048, MT654994–MT655010, MT763935). One additional adult sequence was available for analysis (KY428405). These data further confirm the identity of the described larvae. K2P distances between *A. caballeroi* individuals ranged from 0.0–1.6%. In our larger COI dataset for *Anastrepha*, *A. caballeroi* is nearest-neighbor to the undescribed *Anastrepha* sp. Yasuni 01 from Ecuador. One of the *A. caballeroi* barcodes (MH070125) is more similar to A. sp. Yasuni 01 than other *A. caballeroi*. However, all barcoded larval specimens of *A. caballeroi* are best matches to adult *A. caballeroi* sequences. BLAST searches were consistent with our new data, yielding only two good matches, both to *A. caballeroi* (98.07%–100% sequence identity; KY428405 and MH070125). Additionally, all thirteen larval barcodes returned consensus identifications of *A. caballeroi* with three votes (Moore et al. in press).

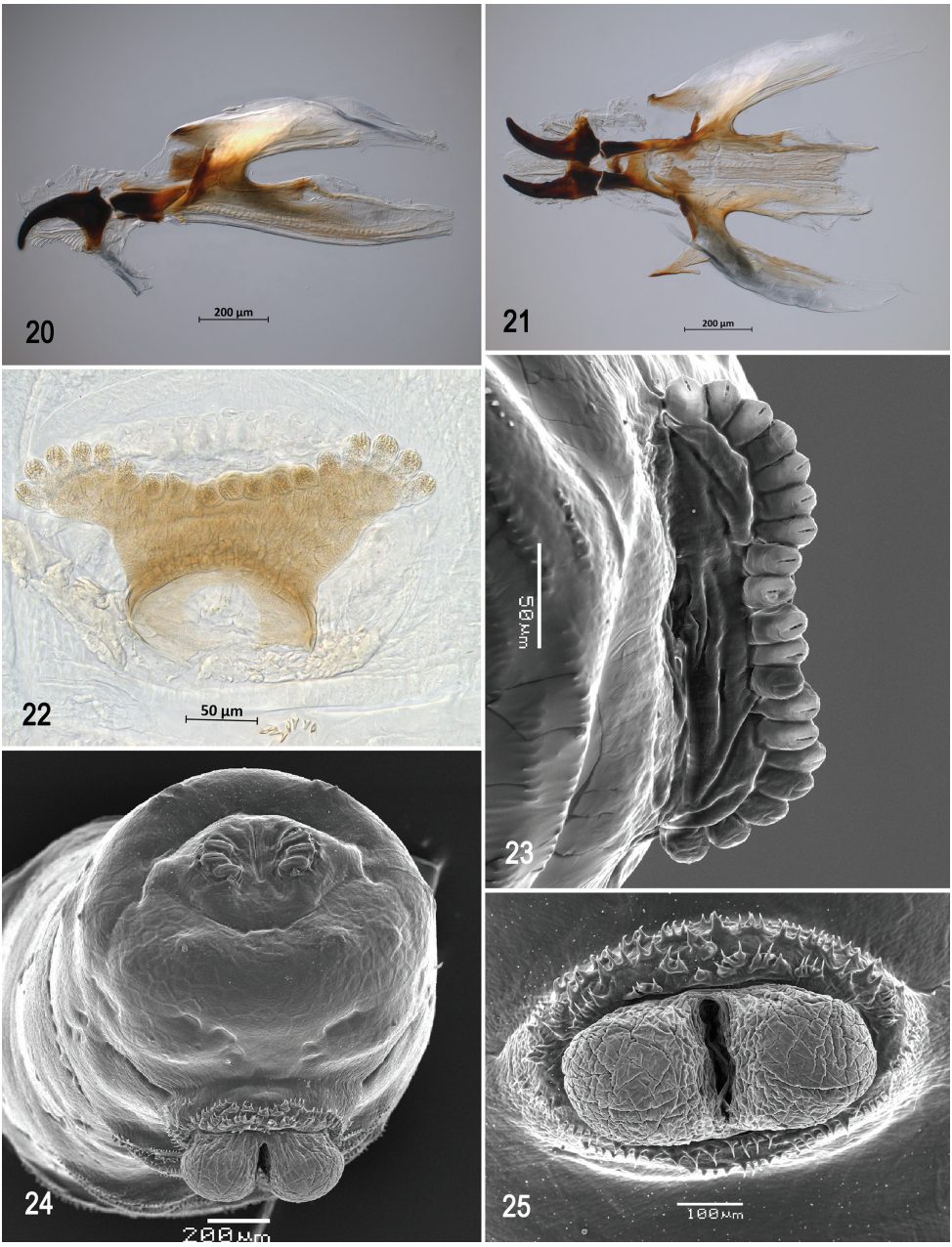

Figures 20–25. Optical photomicrographs and scanning electron photomicrographs of third instar of *Anastrepha caballeroi* **20** cephaloskeleton, lateral view **21** cephaloskeleton, dorsal view **22** prothoracic spiracle, lateral view **23** prothoracic spiracle, dorsolateral view **24** caudal segment **25** anal lobe. Scale bars: 50 µm (**22, 23**); 100 µm (**25**); 200 µm (**20, 21, 24**).

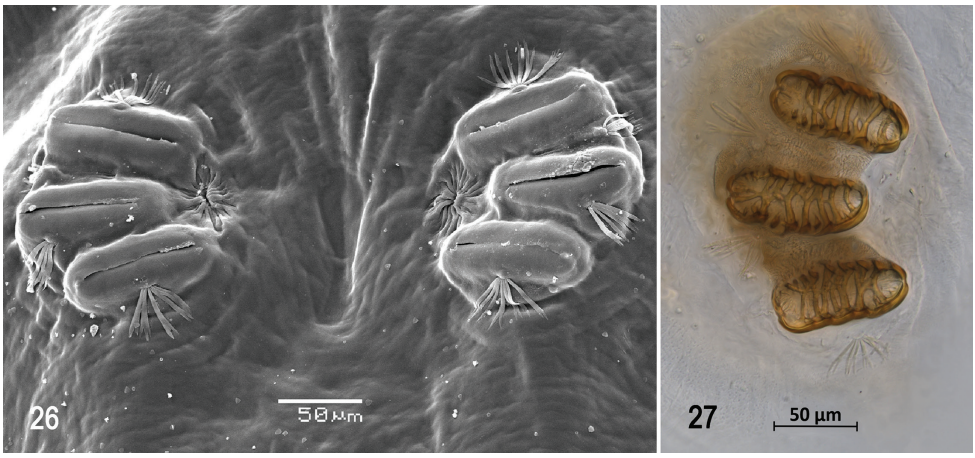

Figures 26, 27. Scanning electron photomicrograph and optical photomicrograph of posterior spiracles of third instar of *Anastrepha caballeroi*. Scale bars: 50 µm (**26, 27**).

Anastrepha crebra Stone, 1942

Figs 28–40

Material examined. Peru • 4 larvae; Madre de Dios, Puerto Maldonado, Centro de Investigación y Capacitación Río Los Amigos (CICRA), trail 21; 12.5721°S, 70.0889°W; 232 m a.s.l.; 22 Mar. 2016; N. Zenteno leg.; reared from fruit of *Quararibea wittii* K. Schumann and O. Ulbrich (Malvaceae); FSCA (AP20180315.6–AP20180315.10, AP20180329.08, AP20210415.01).

Diagnosis. *Anastrepha crebra* can be distinguished from other species of *Anastrepha*, except *A. nolazcoae*, *Anastrepha* sp. Peru-82, and *Anastrepha* sp. nr. *protuberans*, by the fringed posterior margin of its oral ridges. *Anastrepha crebra* differs from the latter three species in having fewer oral ridges, a higher number of trunks and tips of the posterior spiracular processes, and shorter spiracular opening length on the posterior spiracle (see Tables 2–4).

Description. ***Habitus.*** Third instar elongate, cylindrical, tapered anteriorly and caudal end truncate; color creamy; amphipneustic. Length 6.83−7.36 mm and width 1.10−1.21 mm at the sixth abdominal segment.

Pseudocephalon (Figs 28–31). Antenna and maxillary palp on moderately developed lobe. Antenna with cylindrical base and apical knob. Maxillary palp bearing three papilla sensilla, two knob sensilla; dorsolateral group of sensilla bearing two well-developed papilla sensilla, aligned at oblique angle to palp and surrounded by collar. Facial mask globular in lateral view. Preoral organ bearing one peg sensillum, located apically on small cylindrical lobe anterolateral to the mouthhook, with two or three adjacent irregular secondary lobes; preoral lobe elongate, broad, extending slightly posterior to preoral organ. Oral ridges in 13–15 rows, posterior margins fringed; accessory plates

apparently in one series lateral to oral ridges covering a much smaller area than oral ridges, with fringed posterior margins. Labium narrow, surface channeled medially, ventrally with two visible sensilla on small tubercles.

Cephaloskeleton (Figs 32–34). Total length from tip of mouthhook to end of ventral cornu 1.08–1.13 mm. Mouthhook well sclerotized, black apically and basally; length a 0.23–0.29 mm; length b 0.16–0.17 mm; height c 0.16–0.20 mm; ratio a:b 1.44–1.71; ratio a:c 1.44–1.45. Tooth long, sharp, strongly curved, concave ventrally with medial carina, ventral surface smooth. Intermediate sclerite 0.18–0.20 mm long, 0.14 mm wide at ventral bridge. Epipharyngeal sclerite visible only in dorsal view, with medial lobe directed anteriorly. Labial sclerite robust, sclerotized, and triangular in dorsal view. Parastomal bar extending three-fourths length of intermediate sclerite. Dorsal arch 0.23–0.24 mm high. Dorsal cornu with well-defined sclerotized area adjacent to notch, 0.42–0.48 mm long. Dorsal bridge projecting anteriorly from dorsal cornu and sclerotized. Anterior sclerite irregularly shaped and sclerotized. Cornu notch (N) 0.36 mm long and cornu notch index (N/DC) 0.75–0.85. Ventral cornu with weakly defined sclerotized area. Pharyngeal filter with weakly sclerotized anterior bar and ridges forming a series of grooves along length of ventral cornu. Ventral cornu 0.62–0.65 mm long from pharyngeal bar to posterior end of grooves. Ventral cornu 1.4–1.5 × as long as sclerotized area of dorsal cornu.

Thoracic and abdominal segments. Thoracic segments with dorsal spinules conical, symmetrical to slightly curved posteriorly; dorsal spinules pattern in rows as follows: T1 with 9−11 rows, forming scalloped plates; T2 with 3−5 rows; T3 with one or two rows; ventral spinule pattern as follows: T1 with 11–15 rows; T2 and T3 lacking spinules. Abdominal segments (A1–A8) lacking dorsal spinules; ventral creeping welts present on all abdominal segments; ventral spinule pattern as follows: A1 with four rows; A2 with 8–10 rows; A3 with 10–13 rows; A4 with 12 rows; A5 with 11–13 rows; A6 with 11 or 12 rows, A7 with 9–11 rows; A8 with nine or ten rows. Additional three anterior and posterior and two lateral irregular rows of spinules surrounding anal lobes, spinules large, conical, distally sharp, pointing away from anal lobes.

Prothoracic spiracle (Figs 35, 36). Bilobed, bearing 16–21 tubules, distally rounded and arranged in a single sinuous row. Spiracle distal width 0.22–0.24 mm; basal width 0.09−0.10 mm at junction with trachea.

Caudal segment (Figs 37, 38). Dorsal (D1 and D2) tubercles and sensilla moderately developed; D1 distinctly anterior to D2. Intermediate tubercles I1 and I2 and associated sensilla moderately developed; I1 ventral to I2. L1, V1, and V2 tubercles and associated sensilla weakly developed. Anal lobe entire and protuberant.

Posterior spiracle (Figs 37, 39, 40). Located above horizontal midline. Posterior spiracle openings with thick rimae and numerous trabeculae; 58–73 μm long; 21−25 μm wide; ratio length/width 2.8−2.9. Ecdysial scar apparent. Felt chamber oval, 127−135 μm in diameter at junction with trachea. Spiracular process SP-I comprising 14−18 trunks and 33−51 tips; ratio tips/trunks 2.4− 2.8; basal width 20−30 μm; ratio basal width/length of spiracular opening 0.33−0.41. SP-II comprising 5−7 trunks and 11−23 tips. SP-III comprising 8−13 trunks and 21−32 tips. SP-IV comprising 14−20

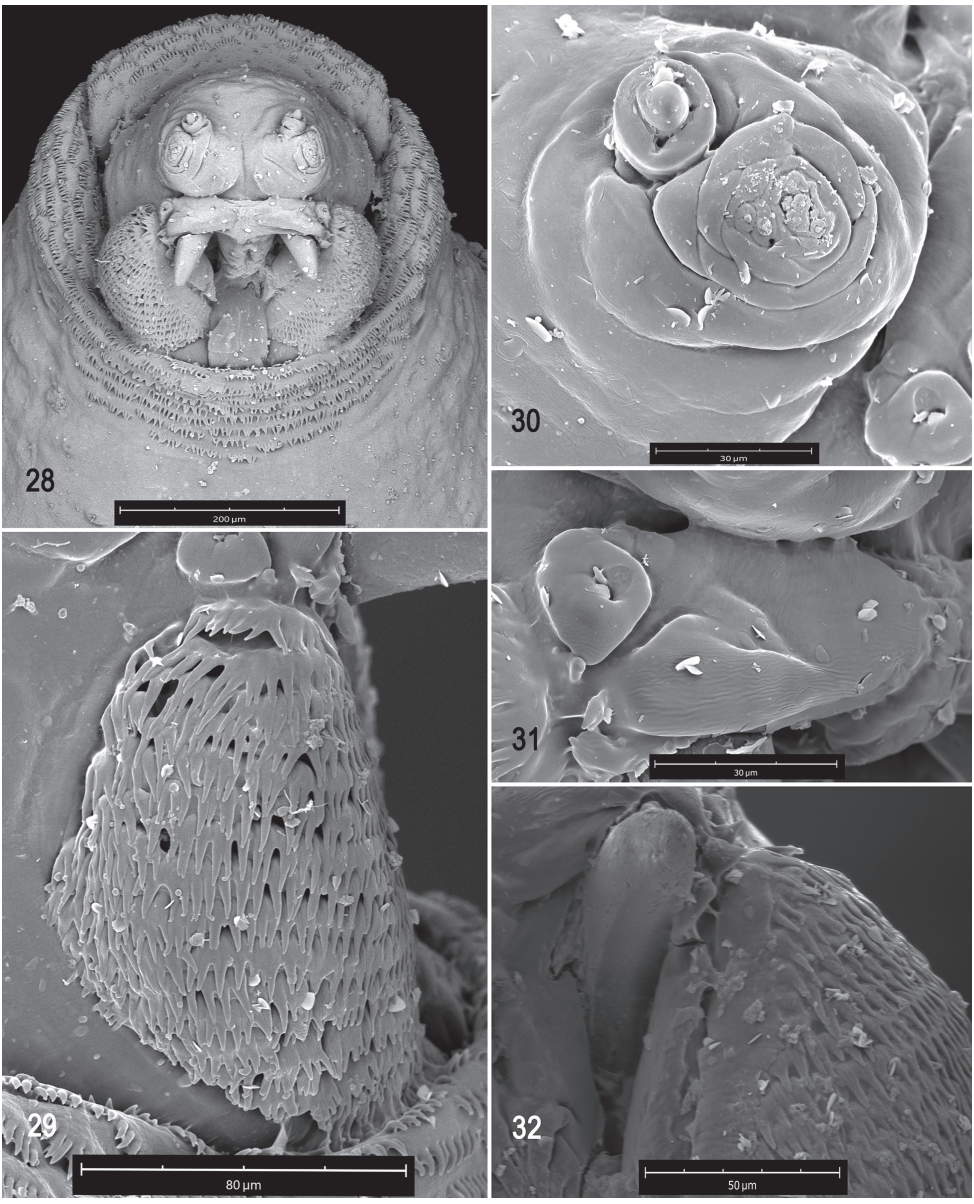

Figures 28–32. Scanning electron photomicrographs of third instar of *Anastrepha crebra* **28** pseudocephalon **29** oral ridges **30** antenna and maxillary palp **31** preoral organ **32** ventral surface of mouthhook. Scale bars: 30 µm (**30, 31**); 50 µm (**32**); 80 µm (**29**); 200 µm (**28**).

trunks and 31–39 tips; ratio tips/trunks 2.0–2.2; basal width 16–28 µm; ratio basal width/length of spiracular opening 0.28–0.39.

Distribution. *Anastrepha crebra* is known from Mexico, Guatemala, Nicaragua, Costa Rica, Panama, Ecuador (Norrbom 2004; CoFFHI 2020), and Colombia (Rodríguez Clavijo et al. 2018). It is recorded for the first time from Peru.

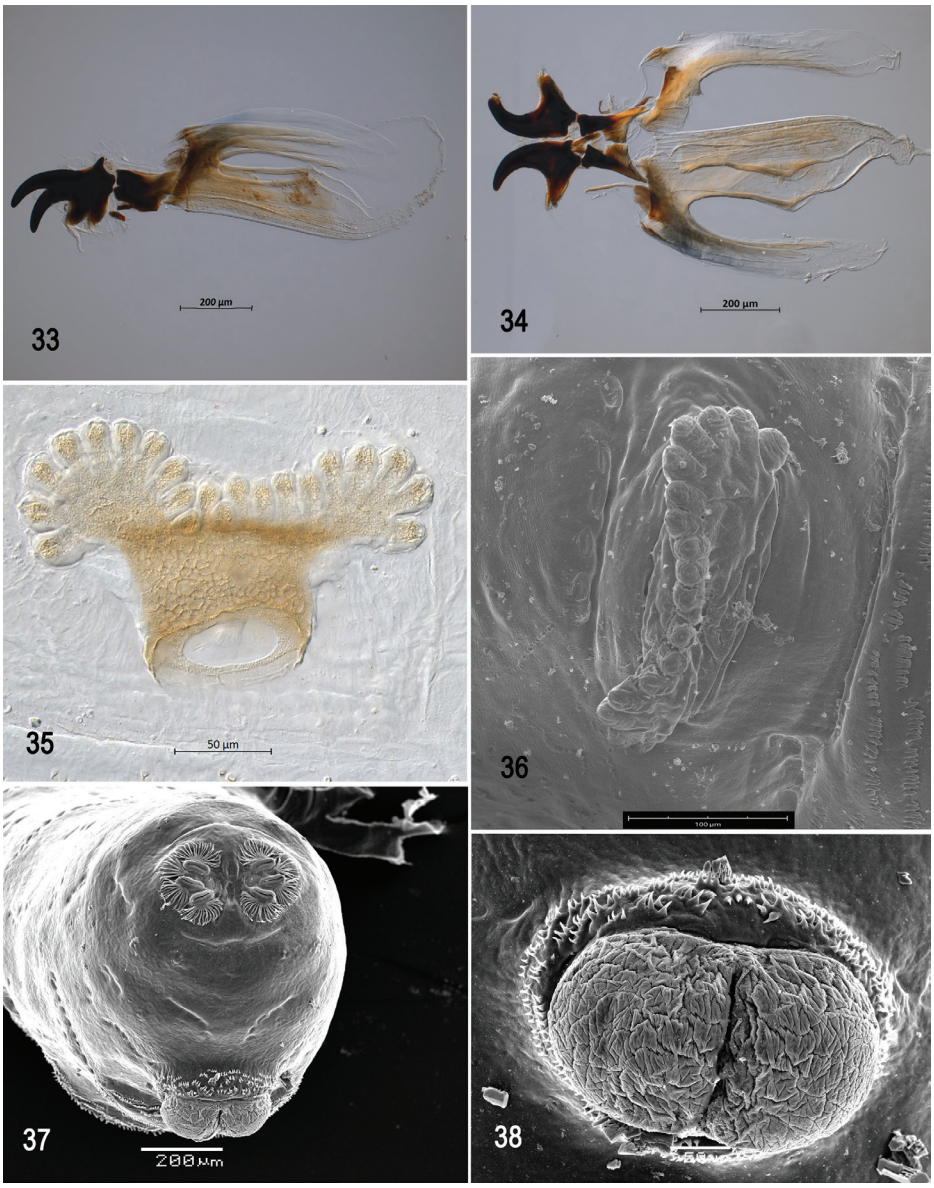

Figures 33–38. Optical photomicrographs and scanning electron photomicrographs of third instar of *Anastrepha crebra* **33** cephaloskeleton, lateral view **34** cephaloskeleton, dorsal view **35** prothoracic spiracle, lateral view **36** prothoracic spiracle, dorsolateral view **37** caudal segment **38** anal lobe. Scale bars: 50 µm (**35, 38**); 100 µm (**36**); 200 µm (**33, 34, 37**).

Biology. This species was reared from fruit of *Quararibea wittii*, a new host plant record for *A. crebra*. It has been previously reared from fruits of *Quararibea asterolepis* Pittier (Malvaceae) (Stone 1942), *Quararibea funebris* (La Llave) Vischer (Malvaceae) (Hernández-Ortiz and Pérez-Alonso 1993; Aluja et al. 2000), and *Quararibea yunckeri* Standl. (Malvaceae) (Aluja et al. 2003).

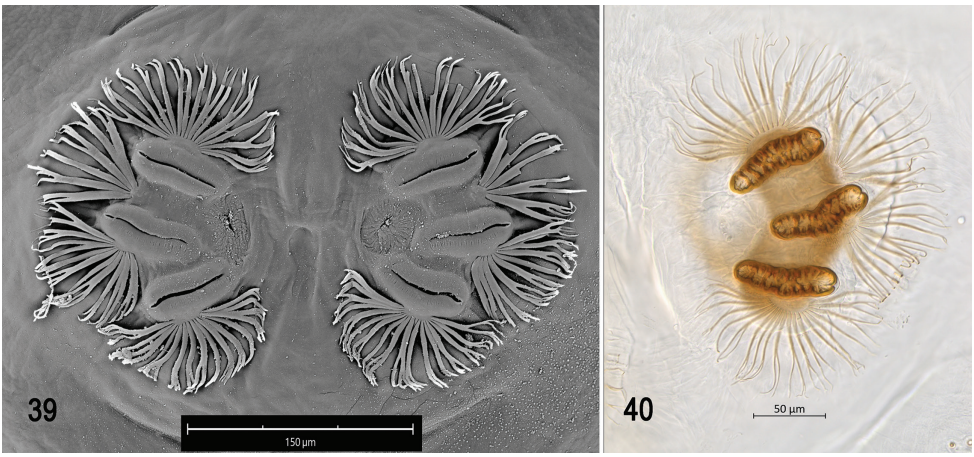

Figures 39–40. Scanning electron photomicrograph and optical photomicrograph of posterior spiracles of third instar of *Anastrepha crebra*. Scale bars: 50 µm (**40**); 150 µm (**39**).

Molecular identification. COI barcodes were generated from three larvae and three adults submitted to GenBank (MT655069–MT655074). These data further confirm the identity of the described larvae. K2P distances among *A. crebra* larvae and the 14 available adult sequences (KY428335, MK758576, MK758598, MK759164, MK759601, MK767247, MK767700, MK768011, MK768248, MK768483, MK769383, MK770033, MT655069–MT655071) ranged from 0.0–3.0%. BLAST searches were consistent with our new data, yielding good matches only to *A. crebra* (97.00–100.00% sequence identity). Additionally, all three larval barcodes returned consensus identifications of *A. crebra* with three votes (Moore et al. in press).

Anastrepha haplacantha Norrbom & Korytkowski, 2012

Figs 41–52

Material examined. Ecuador • 4 larvae; Orellana, Estacion Cientifica Yasuní, trail 5; 0.6692°S, 76.4018°W; 235 m a.s.l.; 9 Mar. 2018; E. J. Rodriguez leg.; reared from fruit of *Quararibea malacocalyx*; FSCA (AP20200622.01–AP20200622.04).

Diagnosis. *Anastrepha haplacantha* can be distinguished from other species of *Anastrepha*, except *A. korytkowskii* and *Anastrepha* sp. Sur-16, by the dentate posterior margin of its oral ridges. *Anastrepha haplacantha* differs from the latter two species in having more oral ridges, lacking comb-like processes, and by other morphological characters, such as number of trunks and tips of the posterior spiracular processes and basal width of the posterior spiracle (see Tables 2–4).

Description. ***Habitus.*** Third instar elongate, cylindrical, tapered anteriorly and caudal end truncate; color creamy; amphipneustic. Length 7.58−8.31 mm and width 1.04−1.42 mm at the sixth abdominal segment.

Pseudocephalon (Figs 41–44). Antenna and maxillary palp on moderately developed lobe. Antenna with cylindrical base and apical knob. Maxillary palp bearing three papilla sensilla, two knob sensilla; dorsolateral group of sensilla bearing two well-developed papilla sensilla, aligned at an oblique angle to palp and surrounded by collar. Facial mask globular in lateral view. Preoral organ bearing 2–4 peg sensilla, located apically on simple elongate preoral lobe lateral to mouthhook, 3–5 short elongate single or bifid secondary lobes adjacent to preoral organ. Oral ridges in 19 or 20 rows, posterior margins dentate with long moderately spaced projections; numerous accessory plates lateral to oral ridges, some elongate and interleaved with oral ridges, covering a much smaller area than oral ridges, with fringed posterior margins. Labium triangular, anterior surface with reclinate spines, ventrally with visible sensilla on small tubercles.

Cephaloskeleton (Figs 45, 46). Total length from tip of mouthhook to end of ventral cornu 1.3 mm. Mouthhook well sclerotized, reddish orange; length a 0.31–0.32 mm; length b 0.21–0.22 mm; height c 0.22–0.24 mm; ratio a:b 1.45–1.46; ratio a:c 1.33–1.42. Tooth long, sharp, strongly curved, concave ventrally, ventral surface apparently smooth. Intermediate sclerite 0.20–0.23 mm long, 0.14 mm wide at ventral bridge. Epipharyngeal sclerite visible only in dorsal view, with medial lobe directed anteriorly. Labial sclerite robust, weakly sclerotized, and triangular in dorsal view. Parastomal bar extending three-fourths length of intermediate sclerite. Dorsal arch 0.25–0.26 mm high. Dorsal cornu weakly sclerotized, 0.49 mm long. Dorsal bridge prominently projecting anteriorly from dorsal cornu and sclerotized. Anterior sclerite absent. Cornu notch (N) 0.35 mm long and cornu notch index (N/DC) 0.7. Ventral cornu weakly sclerotized. Pharyngeal filter with weakly sclerotized anterior bar and 7–9 ridges forming a series of grooves along length of ventral cornu. Ventral cornu 0.85 mm long from pharyngeal bar to posterior end of grooves. Ventral cornu 1.7 × as long as sclerotized area of dorsal cornu.

Thoracic and abdominal segments. Thoracic segments with dorsal spinules conical, symmetrical to slightly curved posteriorly; dorsal spinules pattern in rows as follows: T1 with 5−7 rows, forming scalloped plates; T2 with three or four rows; T3 with one row; ventral spinule pattern as follows: T1 with seven rows; T2 with four rows; T3 with two rows. Abdominal segments (A1–A8) lacking dorsal spinules; ventral creeping welts present on all abdominal segments; ventral spinule pattern as follows: A1 with two or three rows; A2 with six rows; A3 with eight rows; A4 with eight or nine; A5 with eight or nine rows; A6 with seven or eight rows; A7 with eight rows; A8 with eight rows. Additional three rows of irregular spinules anterior and posterior to anal lobes, lateral rows apparently absent, spinules large, conical, distally sharp, pointing away from anal lobes.

Prothoracic spiracle (Figs 47, 48). Bilobed, bearing 20–24 tubules, distally rounded and arranged in a single sinuous row. Spiracle distal width 0.32–0.35 mm; basal width 0.12−0.13 mm at junction with trachea.

Caudal segment (Figs 49, 50). Dorsal (D1 and D2), intermediate (I1 and I2), lateral (L1), and ventral (V1 and V2) tubercles and sensilla weakly developed; D1 distinctly anterior to D2. Intermediate tubercles I1 and I2 and associated sensilla weakly

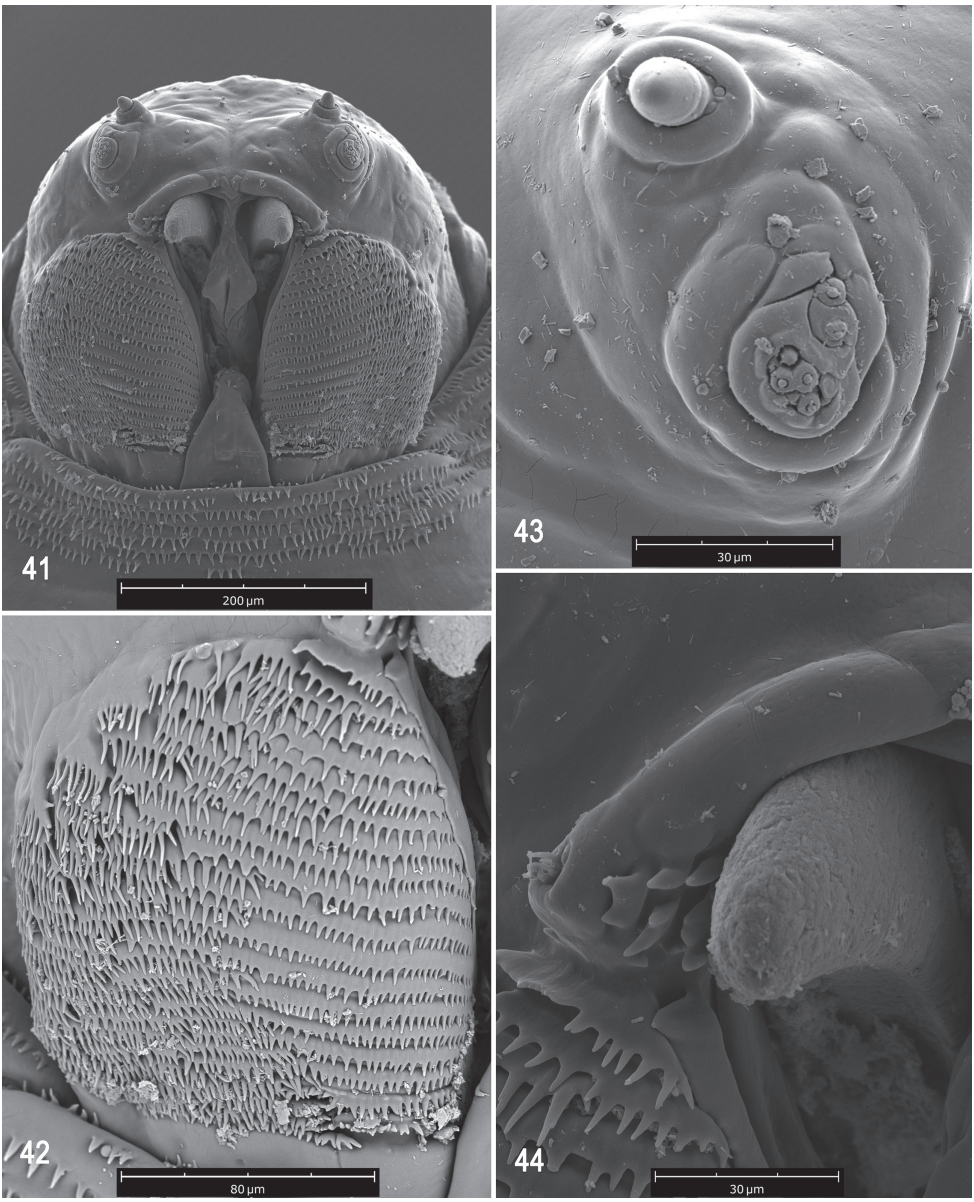

Figures 41–44. Scanning electron photomicrographs of third instar of *Anastrepha haplacantha* **41** pseudocephalon **42** oral ridges **43** antenna and maxillary palp **44** preoral organ and ventral surface of mouthhook. Scale bars: 30 µm (**43, 44**); 80 µm (**42**); 200 µm (**41**).

developed; I1 dorsal to I2. L1, V1 and V2 tubercles, and associated sensilla weakly developed. Anal lobe entire and protuberant.

Posterior spiracle (Figs 49, 51, 52). Located above horizontal midline. Posterior spiracle openings with thick rimae and numerous trabeculae; 69–80 µm long;

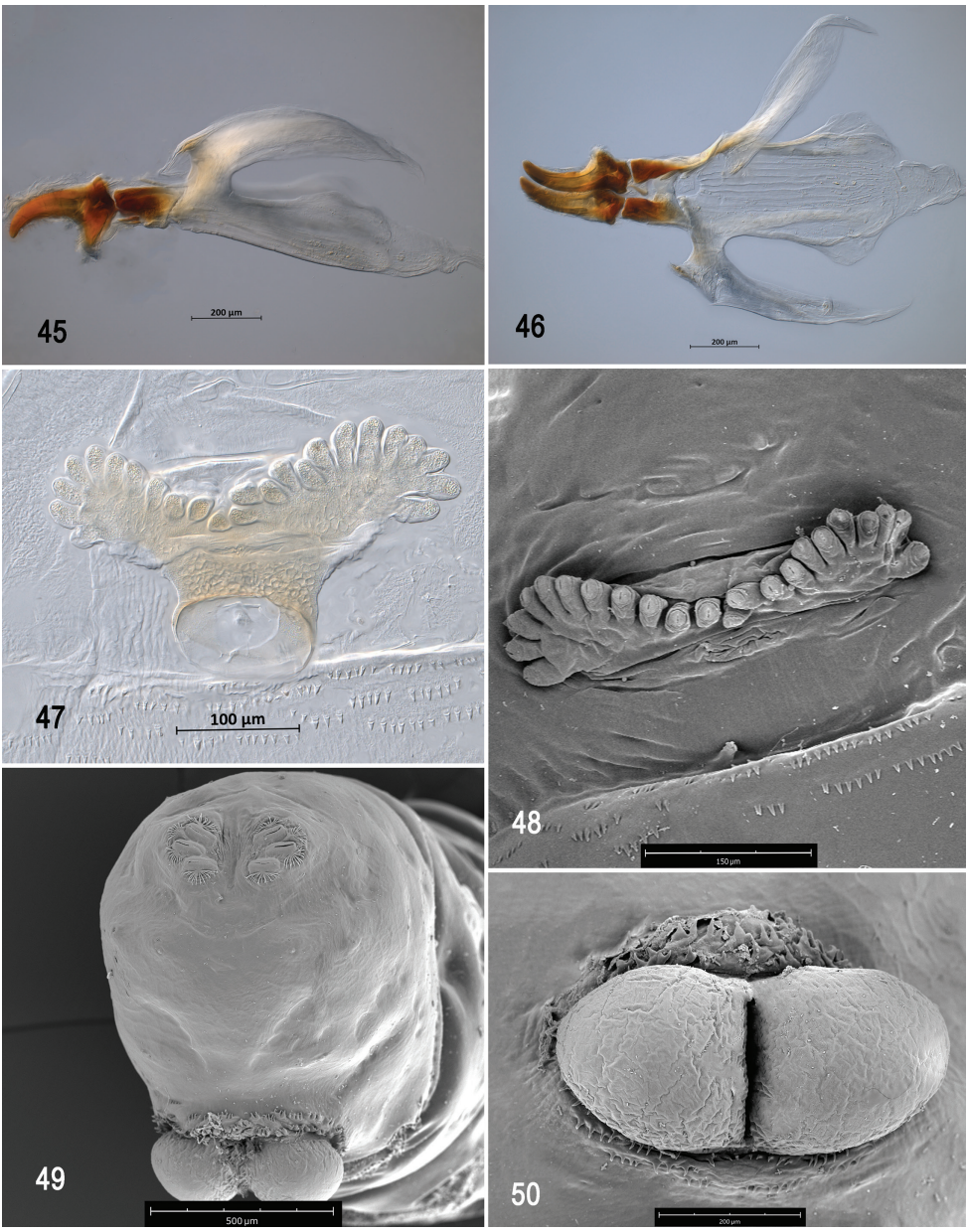

Figures 45–50. Optical photomicrographs and scanning electron photomicrographs of third instar of *Anastrepha haplacantha* **45** cephaloskeleton, lateral view **46** cephaloskeleton, dorsal view **47** prothoracic spiracle, lateral view **48** prothoracic spiracle, dorsolateral view **49** caudal segment **50** anal lobe. Scale bars: 100 µm (**47**); 150 µm (**48**); 200 µm (**45, 46, 50**); 500 µm (**49**).

27–33 µm wide; ratio length/width 2.2–2.8. Ecdysial scar apparent. Felt chamber oval, 158–180 µm in diameter at junction with trachea. Spiracular process SP-I comprising 9–12 trunks and 13–27 tips; ratio tips/trunks 1.4– 2.3; basal width 12–18 µm; ratio

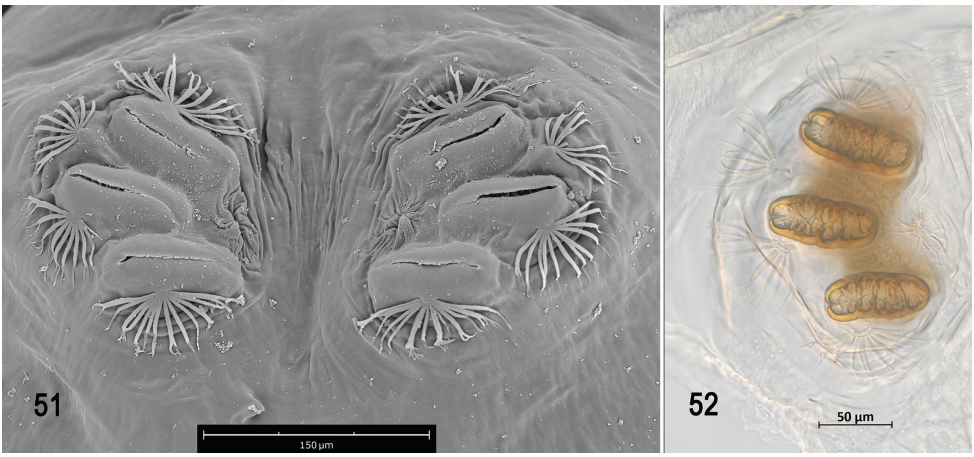

Figures 51–52. Scanning electron photomicrograph and optical photomicrograph of posterior spiracles of third instar of *Anastrepha haplacantha*. Scale bars: 50 µm (**52**); 150 µm (**51**).

basal width/length of spiracular opening 0.16–0.23. SP-II comprising 6–9 trunks and 8–19 tips. SP-III comprising 6–11 trunks and 12–24 tips. SP-IV comprising 9–12 trunks and 16–23 tips; ratio tips/trunks 1.8–1.9; basal width 14–15 µm; ratio basal width/length of spiracular opening 0.19–0.21.

Distribution. *Anastrepha haplacantha* is known only from Ecuador (Orellana) (Norrbom and Korytkowski 2012).

Biology. We reared this species from fruit of *Quararibea malacocalyx*, the first host plant record for *A. haplacantha*. The larvae feed only on the endocarp (developing seed) of the fruit.

Molecular identification. COI barcodes were generated from three larvae and four adults and submitted to GenBank (MT654690, MT763901–MT763904, MT763941, MT763944). These data further confirm the identity of the described larvae. K2P distances among *A. haplacantha* ranged from 0.0–2.7%. BLAST searches were consistent with our new data, yielding only one good match: *A. haplacantha* (97% sequence identity; KY428381). Additionally, all three larval barcodes returned consensus identifications of *A. haplacantha* with three votes (Moore et al. in press).

Anastrepha korytkowskii Norrbom, 2015

Figs 53–65

Material examined. Peru • 2 larvae; Madre de Dios, Puerto Maldonado, Centro de Investigación y Capacitación Río Los Amigos (CICRA), trail 21; 12.5721°S, 70.0889°W; 232 m a.s.l.; 17 Apr. 2016; N. Zenteno leg.; reared from fruit of *Quararibea wittii*; FSCA (AP20180315.02– AP20180315.03) • 7 larvae; same, trail 11; 12.5636°S, 70.0847°W; 250 m a.s.l.; 4 Dec. 2015; R. Bustamante leg.; reared from fruit of *Quararibea wittii*; FSCA (AP20180315.01, AP20180315.04, AP20180315.05, AP20180321.03,

Table 2. Diagnostic characters of the pseudocephalon of species within the *mucronota* group.

Species	Location of preroal organ	Shape of preoral lobe	Oral ridges		Accessory plates		Mouthhook		No. of comb-like processes
			Number	Posterior margins	Number	Posterior margins	Ventral surface	Length b (mm)	
A. aphelocentema	Lateral to MH	Long, narrow, with 3–4 petal-like lobes adjacent to preoral organ	12–14	Finely serrate or entire	15–17; mostly in one series	Finely serrate or entire	Concave, Rough	0.22	Absent
A. caballeroi	Anterolateral to MH	Long, narrow, split apically, extending posterior to preoral organ	14–15	Entire or undulant	27–36, covering a much larger area than oral ridges	Dentate	Concave, eroded	0.21–0.23	Absent
A. crebra	Anterolateral to MH	Long, broad, extending posterior to preoral organ	13–15	Fringed	Present; apparently in one series	Fringed	Concave, medial carina, smooth	0.16–0.17	Absent
A. haplacantha	Lateral to MH	Long, narrow, with 3–5 single or bifid secondary lobes adjacent to preoral organ	19–20	Dentate with long moderately spaced projections	Numerous plates	Fringed	Concave, apparently smooth	0.21–0.22	Absent
A. korytkowskii	Anterior to MH	Short, irregular-rounded lobe, smaller than preoral organ	12–14	Irregularly dentate and entire	14–20; plates in one series	Fringed	Concave, eroded	0.10–0.13	3–5
A. mucronota	?	?	13–15	?	?	?	?	?	?
A. nolazcoae	Anterior to MH	Short, narrow, extends to posterior middle of preoral organ	16–19	Fringed, 3–4 posterior ridges entire	~ 36; medial and posterior plates in two series	Fringed	Concave, Smooth	0.12–0.15	6–8
Anastrepha sp. Peru-82	Anterior to MH	Short, broad, irregular shape, larger than preoral organ	22–23	Densely fringed, posterior ridges dentate	Numerous plates, overlapping with oral ridges	Fringed	Concave, medial carina, smooth	0.18–0.20	Absent
Anastrepha sp. nr. *protuberans*	Lateral to MH	Long, narrow	18–23	Fringed	Present; apparently in one series	Fringed	Concave, smooth	0.24–0.25	Absent
Anastrepha sp. Sur-16	Anterior to MH	Short-elongate, narrow, extends partially posterior to preoral organ	13–16	Dentate with long closely spaced projections, 2–3 posterior ridges entire	Numerous plates; plates in two or more series	Fringed	Concave, eroded	0.16–0.17	7–9

(?) Unknown data from previous studies.

Table 3. Diagnostic characters of the thoracic and abdominal segments of species within the *mucronota* group.

Species	Prothoracic spiracle		Dorsal spinule pattern	
	No. of tubules	Apical width (mm)	Thoracic segment No. of rows	Abdominal segment No. of rows
A. aphelocentema	24–27	0.35–0.36	T1 5–7; T2 4–5; T3 absent	Absent on A1–A8
A. caballeroi	17–21	0.28–0.33	T1 3; T2 3; T3 absent	Absent on A1–A8
A. crebra	16–21	0.22–0.24	T1 9–11; T2 3–5; T3 1–2	Absent on A1–A8
A. haplacantha	20–24	0.32–0.35	T1 5–7; T2 3–4; T3 1	Absent on A1–A8
A. korytkowskii	12–18	0.19–0.24	T1 6–7; T2 2–5; T3 absent	Absent on A1–A8
A. mucronota	20–22	?	Present on T2–T3 with minute spinules	?
A. nolazcoae	18–21	0.26–0.34	T1 3–5; T2 3–5; T3 1–2	Absent on A1–A8
Anastrepha sp. Peru-82	23–29	0.28–0.35	T1 2; T2 5–6; T3 2–3	A1 3; absent on A2–A8
Anastrepha sp. nr. *protuberans*	22–30	0.41–0.44	T1 3; T2 4–5; T3 4	A1 2; absent on A2–A8
Anastrepha sp. Sur-16	12–17	0.23–0.28	T1 5; T2 3; T3 absent	Absent on A1–A8

(?) Unknown data from previous studies.

Table 4. Diagnostic characters of the caudal segment of species within the *mucronota* group.

Species	Posterior spiracle (SP-I and SP-IV)				Anal lobe
	Length of spiracular opening (µm)	No. of trunks	No. of tips	Basal width (µm)	
A. aphelocentema	94–101	SP-I 4–9; SP-IV 3–7	SP-I 12–21; SP-IV 10–15	SP-I 9–12; SP-IV 9–10	Grooved, entire
A. caballeroi	76–89	SP-I 5–8; SP IV 4–7	SP I 10–18; SP IV 7–17	SP I 7–13; SP IV 5–7	Entire
A. crebra	58–73	SP-I 14–18; SP IV 14–20	SP I 33–51; SP IV 31–39	SP I 20–30; SP IV 16–28	Entire
A. haplacantha	69–80	SP-I 9–12; SP IV 9–12	SP I 13–27; SP IV 16–23	SP I 12–18; SP IV 14–15	Entire
A. korytkowskii	56–77	SP-I 9–15; SP-IV 8–15	SP-I 21–33; SP-IV 17–31	SP-I 14–28; SP-IV 12–21	Entire
A. mucronota	~100	SPI ~8–9; SP IV ~7–8	SPI 12; SP IV 11	?	?
A. nolazcoae	83–108	SP-I 8–11; SP IV 4–12	SP I 9–26; SP IV 8–24	SP I 9–15; SP IV 7–12	Entire
Anastrepha sp. Peru-82	84–97	SP- I 9–11; SP-IV 7–11	SP-I 12–20; SP-IV 13–16	SPI 12–15; SP IV 9–19	Entire
Anastrepha sp. nr. *protuberans*	122–145	SP- I 5–11; SP-IV 7–10	SP-I 9–20; SP-IV 14–21	SPI 8–11; SP IV 9–12	Entire
Anastrepha sp. Sur-16	69–80	SP- I 13–18; SP-IV 13–17	SP-I 19–34; SP-IV 25–40	SPI 29–36; SP IV 23–34	Entire

(?) Unknown data from previous studies.

AP20180321.04, AP20180329.01, AP20180329.05) • 2 larvae; same, trail 21; 12.5708°S, 70.0847°W; 224 m a.s.l.; 2 Dec. 2015; R. Bustamante leg.; reared from fruit of *Quararibea wittii*; FSCA (AP20180315.07, AP20180516.13) • 8 larvae; same, trail 21; 12.5721°S, 70.0889°W; 232 m a.s.l.; 14–21 Mar. 2016; N. Zenteno leg.; reared from fruit of *Quararibea wittii*; FSCA (AP20180315.08, AP20180315.09, AP20180329.06, AP20180329.07, AP20180329.09–AP20180329.12).

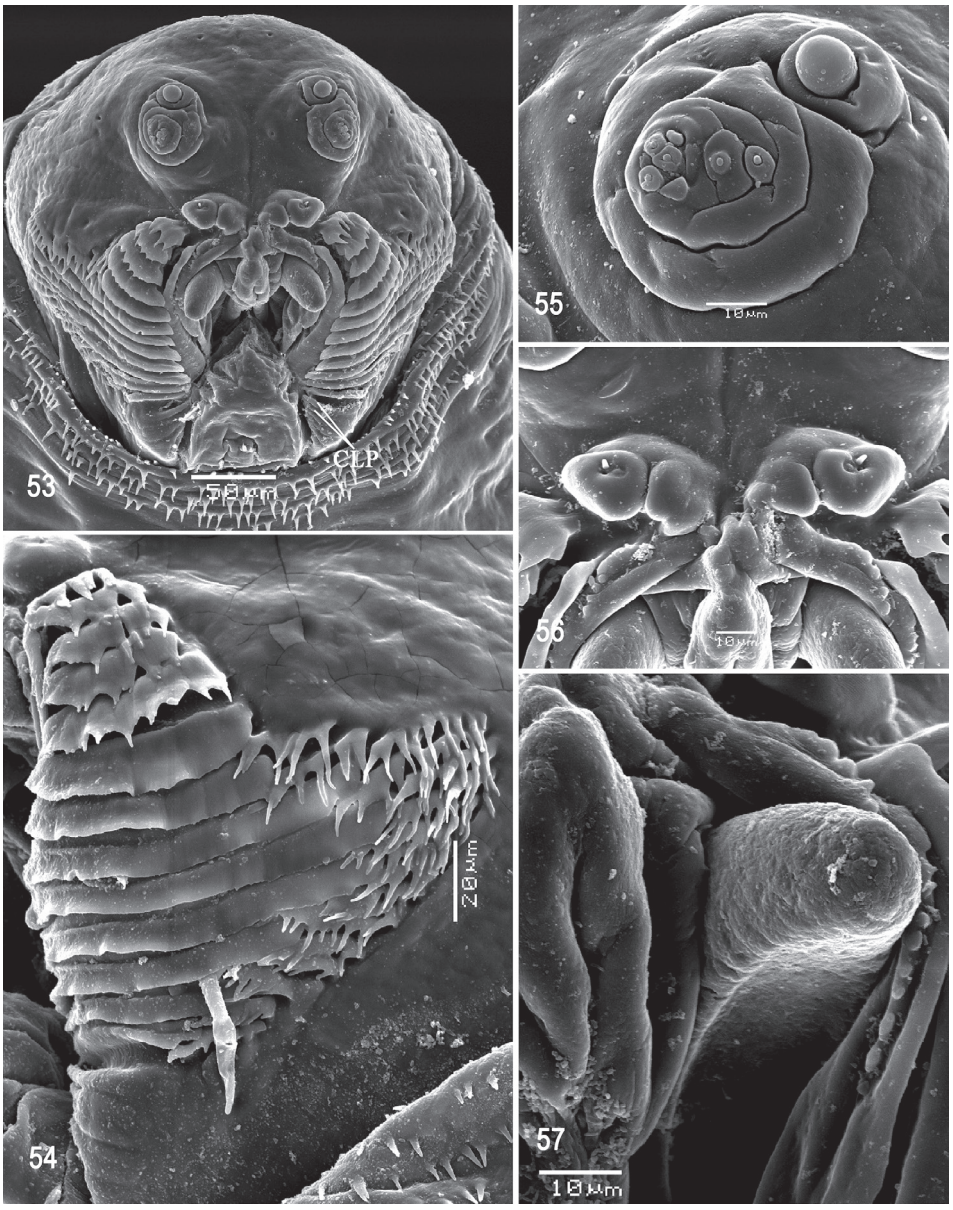

Figures 53–57. Scanning electron photomicrographs of third instar of *Anastrepha korytkowskii* **53** pseudocephalon **54** oral ridges **55** antenna and maxillary palp **56** preoral organ **57** ventral surface of mouthhook. Abbreviations: CLP, comb-like processes. Scale bars: 10 µm (**55–57**); 20 µm (**54**); 50 µm (**53**).

Diagnosis. The larvae of *A. korytkowskii* can be distinguished from those of other species of *Anastrepha* by its peculiar short preoral lobe medial to the lobe bearing the preoral organ, fringed posterior margins of the accessory plates, posterior margins of the oral ridges (2–5 anterior ridges dentate, medial and posterior ridges entire), and 3–5 comb-like processes adjacent to the labium and posterior to the oral ridges. The posterior

margins of the accessory plates resemble those of *A. crebra*, *A. haplacantha*, *A. nolazcoae*, *Anastrepha* sp. Peru-82, *Anastrepha* sp. nr. *protuberans*, and *Anastrepha* sp. Sur-16, although in *A. korytkowskii* the posterior margins of the oral ridges are distinct (as shown above). *Anastrepha korytkowskii* further differs from the latter six species by the number of oral ridges, ventral surface of mouthhook, number of tubules and distal width of the prothoracic spiracle, and basal width of the posterior spiracle (see Tables 2–4).

Description. ***Habitus.*** Third instar elongate, cylindrical, tapered anteriorly and caudal end truncate; color creamy; amphipneustic. Length 6.10−8.54 mm and width 0.93−1.57 mm at the sixth abdominal segment.

Pseudocephalon (Figs 53–56). Antenna and maxillary palp on moderately developed lobe. Antenna with cylindrical base and apical knob. Maxillary palp bearing three papilla sensilla, two knob sensilla; dorsolateral group of sensilla bearing two well-developed papilla sensilla, aligned perpendicular to palp and surrounded by a collar. Facial mask partly globular in lateral view, upper right section lacking ridges and accessory plates and forming almost a right angle. Preoral organ bearing one unbranched peg sensillum, located apically on small, elongate-rounded lobe directly anterior to mouthhook; adjacent medial preoral lobe separate, slightly smaller and irregularly rounded. Oral ridges in 12–14 rows, margins of anterior 2–5 ridges irregularly dentate, margins of medial and posterior ridges entire (some sparsely notched); 3–5 comb-like processes adjacent to labium and posterior to oral ridges; 14–20 accessory plates in one series, but absent adjacent to the anterior five or six oral ridges, covering a much smaller area than oral ridges, with fringed posterior margins. Labium triangular, anterior surface knobby, ventrally with two visible sensilla.

Cephaloskeleton (Figs 57–59). Total length from tip of mouthhook to end of ventral cornu 0.76–0.86 mm. Mouthhook well sclerotized, black apically and basally; length a 0.16–0.18 mm; length b 0.10–0.13 mm; height c 0.11–0.13 mm; ratio a:b 1.4–1.6; ratio a:c 1.4–1.5. Tooth long, sharp, strongly curved, concave ventrally, ventral surface eroded. Intermediate sclerite 0.15–0.17 mm long, 0.13–0.14 mm wide at ventral bridge. Epipharyngeal sclerite visible only in dorsal view, with medial lobe directed anteriorly. Labial sclerite robust, sclerotized, and triangular in dorsal view. Parastomal bar extending for almost entire length of intermediate sclerite. Dorsal arch 0.19–0.21 mm high. Dorsal cornu with well-defined sclerotized area adjacent to notch, 0.36–0.46 mm long. Dorsal bridge prominently projecting anteriorly from dorsal cornu and slightly sclerotized. Anterior sclerite irregularly shaped and sclerotized. Cornu notch (N) 0.24–0.29 mm long and cornu notch index (N/DC) 0.6–0.7. Ventral cornu sclerotized between notch and pharyngeal bar and grooves. Pharyngeal filter with weakly sclerotized anterior bar and 7–9 ridges forming a series of grooves along length of ventral cornu. Ventral cornu 0.39–0.55 mm long from pharyngeal bar to posterior end of grooves. Ventral cornu 1.2–1.4 × as long as sclerotized area of dorsal cornu.

Thoracic and abdominal segments. Thoracic segments with dorsal spinules conical, symmetrical to slightly curved posteriorly; dorsal spinule pattern as follows: T1 with six or seven rows, forming scalloped plates; T2 with 2−5 rows; T3 lacking spinules; ventral spinule pattern as follows: T1 with 8–12 rows; T2 with three rows; T3 lacking spinules. Abdominal segments (A1–A8) lacking dorsal spinules; ventral creeping welts present on all abdominal segments (A1–A8); ventral spinule pattern as follows: A1

with one or two rows; A2 with six or seven rows; A3 with seven or eight rows; A4 with seven or eight rows; A5 with 6–8 rows; A6 with eight rows; A7 with 6–8 rows; A8 with 6–8 rows. Additional 2–4 irregular rows of spinules anteriorly and posteriorly to anal lobes, spinules large, conical, pointing away from anal lobes.

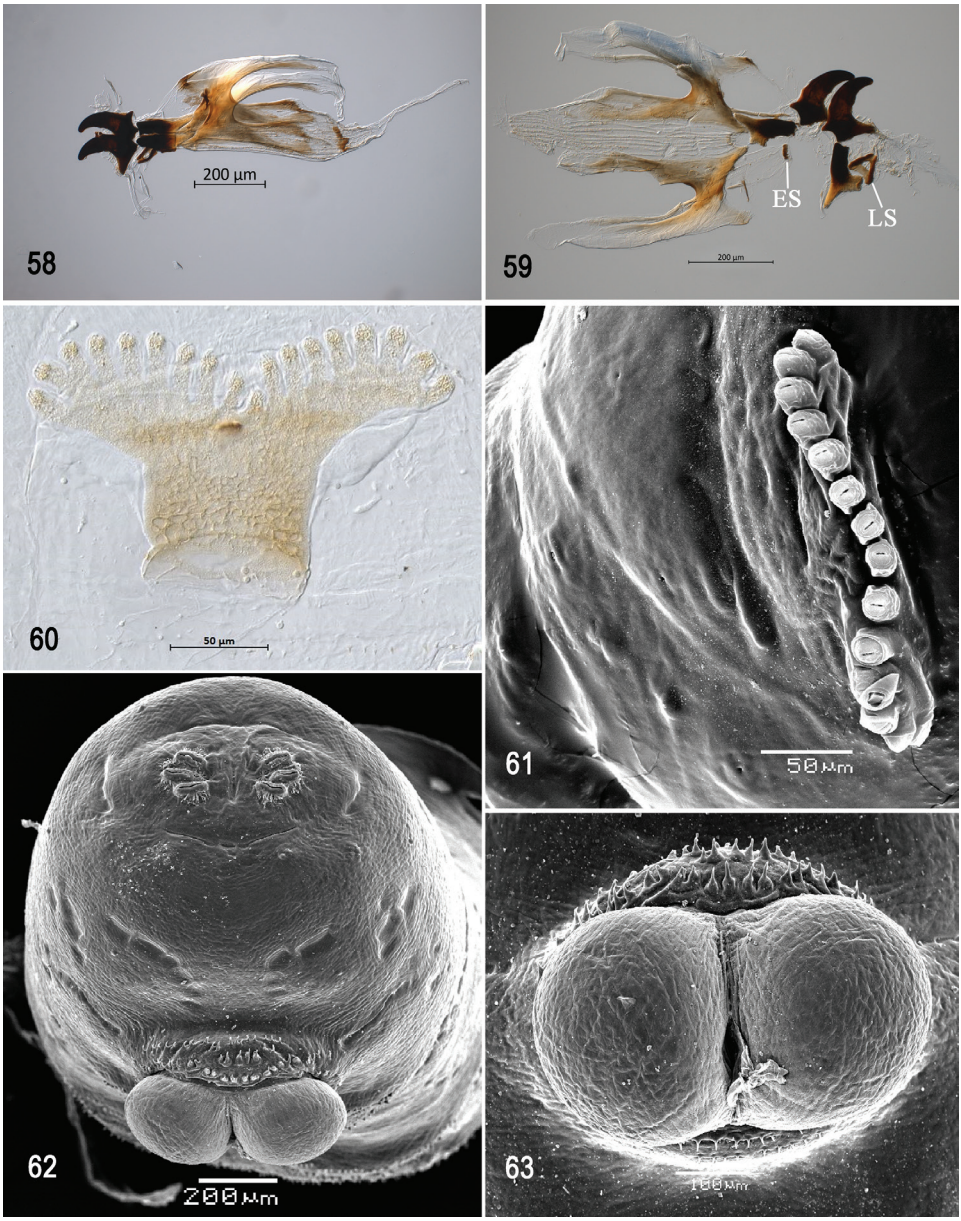

Figures 58–63. Optical photomicrographs and scanning electron photomicrographs of third instar of *Anastrepha korytkowskii* **58** cephaloskeleton, lateral view **59** cephaloskeleton, dorsal view **60** prothoracic spiracle, lateral view **61** prothoracic spiracle, dorsolateral view **62** caudal segment **63** anal lobe. Abbreviations: ES, epipharyngeal sclerite; LS, labial sclerite. Scale bars: 50 µm (**60, 61**); 100 µm (**63**); 200 µm (**58, 59, 62**).

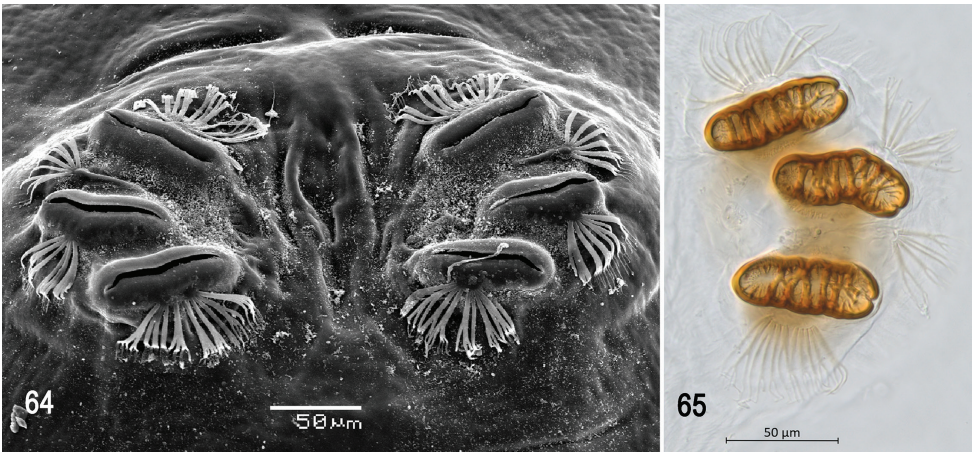

Figures 64, 65. Scanning electron photomicrograph and optical photomicrograph of posterior spiracles of third instar of *Anastrepha korytkowskii*. Scale bars: 50 µm (**64, 65**).

Prothoracic spiracle (Figs 60, 61). Bilobed, bearing 12–18 tubules, distally rounded and arranged in a single sinuous row. Spiracle distal width 0.19–0.24 mm; basal width 0.07−0.10 mm at junction with trachea.

Caudal segment (Figs 62, 63). Dorsal (D1 and D2), intermediate (I1 and I2), lateral (L1), and ventral (V1 and V2) tubercles and sensilla weakly developed; D1 distinctly anterior to D2. Intermediate tubercles I1 and I2 more strongly developed, but associated sensilla weakly developed; I1 lateral and sometimes slightly ventral to I2. Lateral (L1) and ventral (V1 and V2) tubercles and associated sensilla weakly developed. Anal lobe entire and very protuberant.

Posterior spiracle (Figs 62, 64, 65). Located above horizontal midline. Posterior spiracle openings with thick rimae and numerous trabeculae; 56–77 µm long; 20−24 µm wide; ratio length/width 2.8−3.2. Ecdysial scar apparent. Felt chamber oval, 124−148 µm in diameter at junction with trachea. Spiracular process SP-I comprising 9−15 trunks and 21−33 tips; ratio tips/trunks 2.2− 2.3; basal width 14−28 µm; ratio basal width/length of spiracular opening 0.24−0.47. SP-II comprising 4−7 trunks and 9−17 tips. SP-III comprising 5−10 trunks and 12−19 tips. SP-IV comprising 8−15 trunks and 17−31 tips; ratio tips/trunks 2.0−2.1; basal width 12−21 µm; ratio basal width/length of spiracular opening 0.21−0.30.

Distribution. *Anastrepha korytkowskii* is known only from Bolivia (La Paz and Santa Cruz) and eastern Peru (Cusco, Huánuco, Junín, and Madre de Dios).

Biology. We reared this species from fruit of *Quararibea wittii*, the only known host plant (Norrbom et al. 2015). The larvae feed only on the pulp of the fruit.

Molecular identification. COI barcodes were generated from 19 larvae and two adults and submitted to GenBank (MT654705–MT654725). These data further confirm the identity of the described larvae. K2P distances between *A. korytkowskii* larvae and the three adult sequences (MT654712, MT654722, KY428387) ranged from 0.0–2.1%. BLAST searches were consistent with our new data, yielding only one good

match: *A. korytkowskii* (97.77–99.04% sequence identity; KY428387). Additionally, all 19 larval barcodes returned consensus identifications of *A. korytkowskii* with three votes (Moore et al. in press).

Anastrepha nolazcoae Norrbom & Korytkowski, 2011

Figs 66–80

Material examined. Peru • 20 larvae; Madre de Dios, Puerto Maldonado, Centro de Investigación y Capacitación Río Los Amigos (CICRA), trail 21; 12.5722°S, 70.0885°W; 233 m a.s.l.; 1–5 Feb. 2014; E. J. Rodriguez and J. Caballero leg.; reared from fruit of *Quararibea cordata*; FSCA (AP20180222.01–AP20180222.10, AP20180206.01–AP20180206.10).

Diagnosis. The larva of *A. nolazcoae* differs from those of all other species of *Anastrepha* that have been adequately described by the combination of having fringed posterior margins of the oral ridges and accessory plates, and the presence of 6–8 comb-like processes adjacent to the labium. The posterior margins of the oral ridges and accessory plates resemble those of *A. crebra*, *A. haplacantha*, *Anastrepha* sp. Peru-82, and *Anastrepha* sp. nr. *protuberans*, but those species lack the comb-like processes. In addition, *A. nolazcoae* resembles *A. korytkowskii* and *Anastrepha* sp. Sur-16 in the presence of comb-like processes, but *A. nolazcoae* can be distinguished from them by the fringed posterior margins of its oral ridges. Other characters such as the ventral surface of the mouthhook, number of tubules and apical width of the prothoracic spiracle, and dorsal spinules on thoracic segments further differentiate *A. nolazcoae* (see Tables 2–4).

Anastrepha nolazcoae shares the same host plant, *Quararibea cordata*, with species within the *fraterculus* group (*A. fraterculus* complex), *mucronota* group (*A. mucronota*), and *striata* group (*A. striata*). The larva of *A. mucronota* was described with limited data (Steyskal 1977) but can be morphologically separated from *A. nolazcoae* by the lower number of oral ridges (13–15 vs. 16–19) and dorsal irregularly light brown plaques on the abdominal segments (present vs. absent). The description of *A. mucronota* lacks information for most of the characters of the pseudocepalon (Table 2) and most of the available data overlap with those of *A. nolazcoae* (Table 3, 4). *Anastrepha nolazcoae* differs from five morphotypes within the *A. fraterculus* complex (Canal et al. 2015, 2018) and *A. striata* as follows: 1) greater number of oral ridges (16–19; see the dichotomous key in Steck et al. 1990), except unknown for Andean and Peruvian morphotypes of *A. fraterculus* complex; 2) posterior margin of oral ridges fringed in *A. nolazcoae*, irregularly serrate in *A. fraterculus* (Brazil-1 and Ecuadorian morphotypes), scalloped or emarginate in *A. fraterculus* (Mexican morphotype), entire or serrate in *A. striata*; and 3) approximately 36 accessory plates with fringed posterior margins in *A. nolazcoae*, apparently seven plates and serrate in *A. fraterculus* (Ecuadorian morphotypes; see plate 4b in White and Elson-Harris 1992), eight plates and serrate in *A. fraterculus* (Mexican morphotype), 8–9 plates and entire in *A. striata*. *Anastrepha nolazcoae* differs further from the *A. fraterculus* complex in having a greater number of tubules on the prothoracic spiracle (18–21 vs. 9–18 in *fraterculus* complex, see Rodriguez et al. 2021), although in this character it overlaps with *A. striata*.

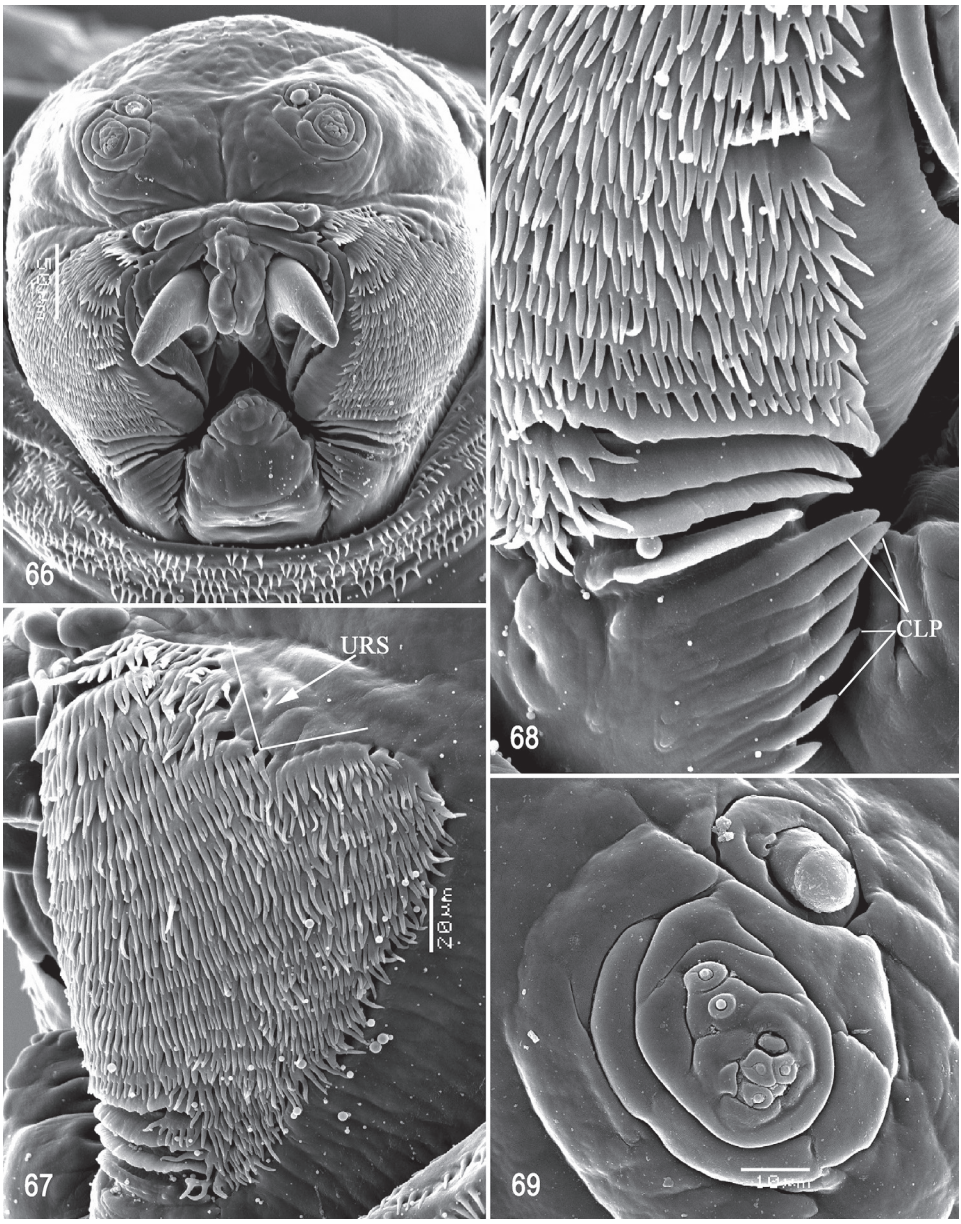

Figures 66–69. Scanning electron photomicrographs of third instar of *Anastrepha nolazcoae* **66** pseudocephalon **67** oral ridges **68** comb-like processes **69** antenna and maxillary palp. Abbreviations: CLP, comb-like processes; URS, upper right section with right angle shape. Scale bars: 10 μm (**69**); 20 μm (**67**); 50 μm (**66**).

Description. ***Habitus.*** Third instar elongate, cylindrical, tapered anteriorly and caudal end truncate; color creamy; amphipneustic. Length 5.33−11.76 mm and width 0.93−1.92 mm at the sixth abdominal segment.

Pseudocephalon (Figs 66–70). Antenna and maxillary palp on moderately developed lobe. Antenna with cylindrical base and apical knob. Maxillary palp bearing

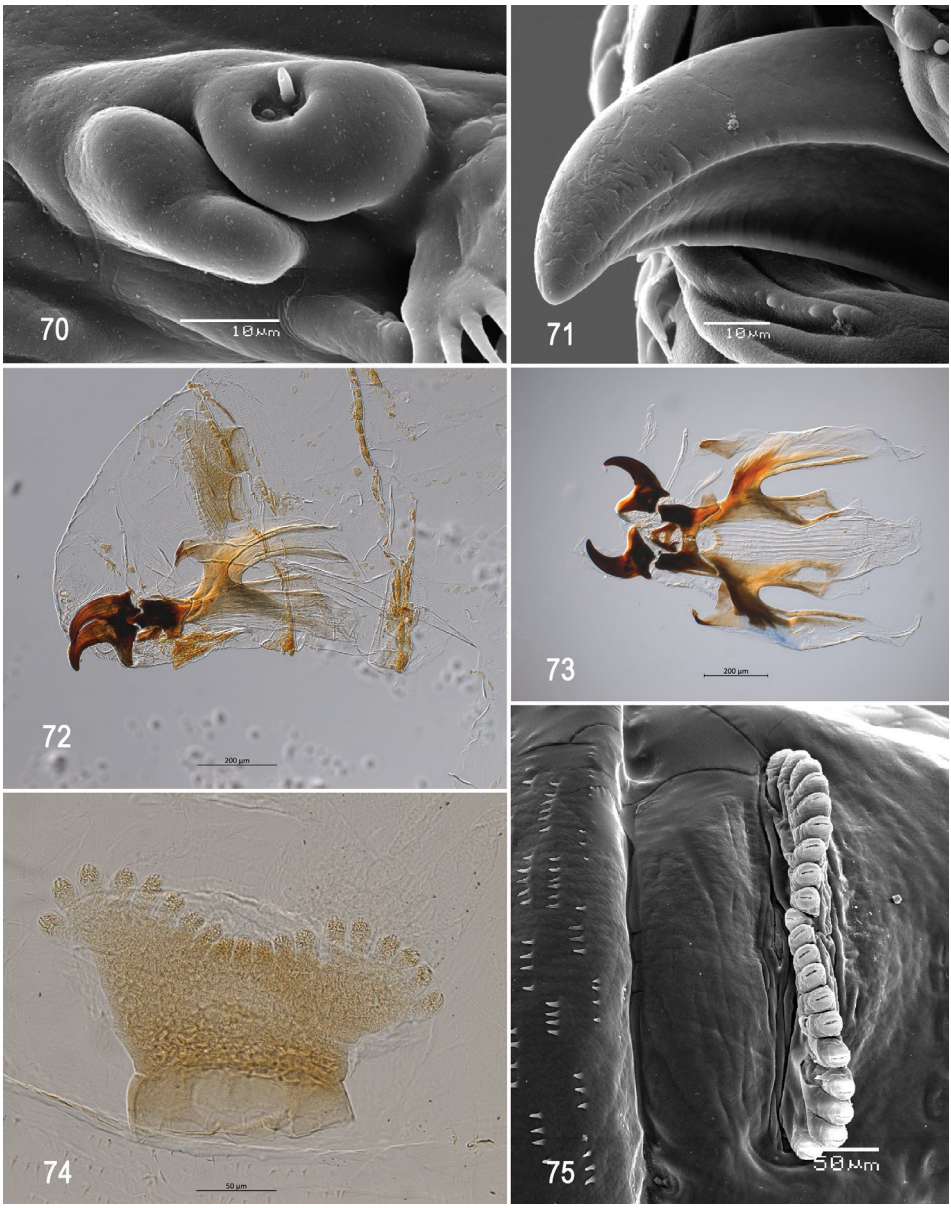

Figures 70–75. Optical photomicrographs and scanning electron photomicrographs of third instar of *Anastrepha nolazcoae* **70** preoral organ **71** ventral surface of mouthhook **72** cephaloskeleton, lateral view **73** cephaloskeleton, dorsal view **74** prothoracic spiracle, lateral view **75** prothoracic spiracle, dorsolateral view. Scale bars: 10 µm (**70, 71**); 50 µm (**74, 75**); 200 µm (**72, 73**).

three papilla sensilla, two knob sensilla; dorsolateral group of sensilla bearing two well-developed papilla sensilla, aligned perpendicular to palp and surrounded by collar. Facial mask partly globular in lateral view, upper right section lacking ridges and accessory plates and forming almost a right angle. Preoral organ bearing one unbranched

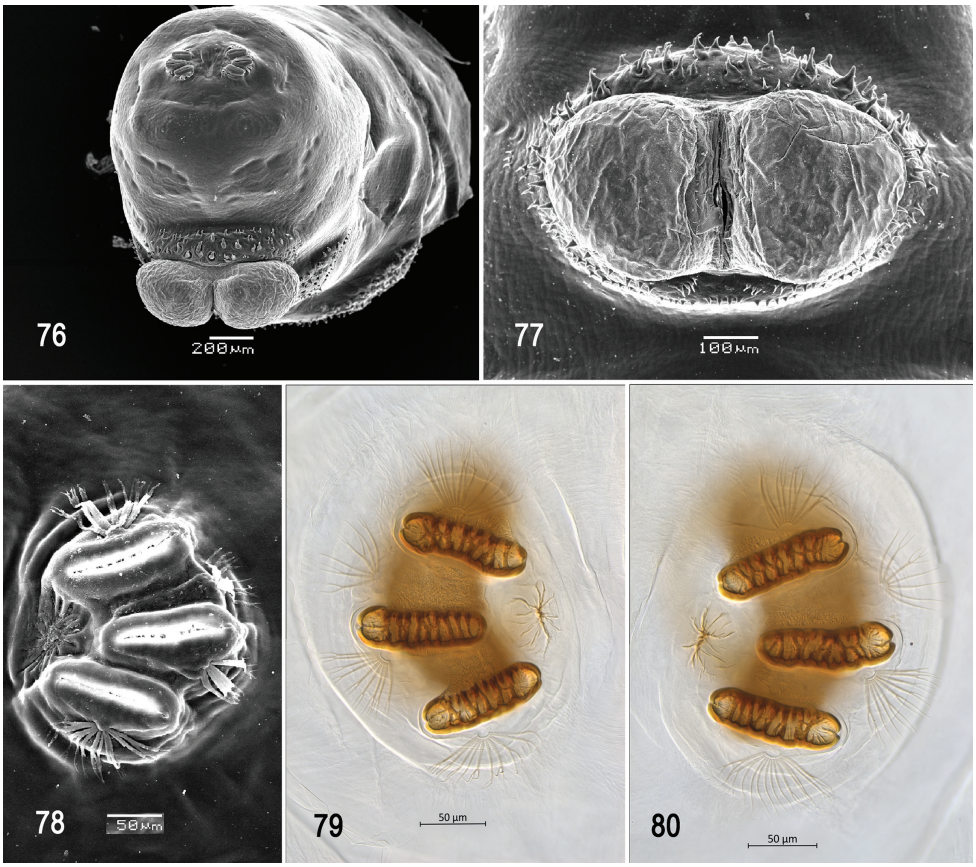

Figures 76–80. Scanning electron photomicrographs and optical photomicrographs of third instar of *Anastrepha nolazcoae* **76** caudal segment **77** anal lobe **78–80** posterior spiracles. Scale bars: 50 µm (**78–80**); 100 µm (**77**); 200 µm (**76**).

peg sensillum, located apically on a small, elongate-rounded lobe directly anterior to mouthhook; adjacent medial preoral lobe separate, short-elongate, extending partially posterior to lobe bearing preoral organ. Oral ridges in 16–19 rows, 13–15 anterior ridges with fringed posterior margins, three or four posterior ridges entire, undulant; 6–8 comb-like processes adjacent to labium and posterior to oral ridges; approximately 36 accessory plates lateral to oral ridges covering a much smaller area than oral ridges, with fringed posterior margins as on oral ridges, in two series. Labium triangular, anterior surface knobby, ventrally with two visible sensilla.

Cephaloskeleton (Figs 71–73). Total length from tip of mouthhook to end of ventral cornu 0.69–1.10 mm. Mouthhook well sclerotized, black apically and basally; length a 0.20–0.23 mm; length b 0.12–0.15 mm; height c 0.14–0.17 mm; ratio a:b 1.5–1.7; ratio a:c 1.3–1.4. Tooth long, sharp, strongly curved, concave ventrally with weak medial carina, ventral surface smooth. Intermediate sclerite 0.16–0.20 mm long, 0.18–0.21 mm wide at ventral bridge. Epipharyngeal sclerite visible only in dorsal view, with medial lobe directed anteriorly. Labial sclerite robust, sclerotized, and triangular

in dorsal view. Parastomal bar extending three-fourths length of intermediate sclerite. Dorsal arch 0.23–0.29 mm high. Dorsal cornu with well-defined sclerotized area adjacent to notch, 0.38–0.53 mm long. Dorsal bridge prominently projecting anteriorly from dorsal cornu and slightly sclerotized. Anterior sclerite irregularly shaped and sclerotized. Cornu notch (N) 0.25–0.34 mm long and cornu notch index (N/DC) 0.6–0.7. Ventral cornu with well-defined sclerotized area between notch and pharyngeal bar and grooves. Pharyngeal filter with weakly sclerotized anterior bar and seven ridges forming a series of grooves along length of ventral cornu. Ventral cornu 0.44–0.71 mm long from pharyngeal bar to posterior end of grooves. Ventral cornu 1.18–1.34 × as long as sclerotized area of dorsal cornu.

Thoracic and abdominal segments. Thoracic segments with dorsal spinules conical, symmetrical to slightly curved posteriorly; dorsal spinule pattern as follows: T1 with 3−5 rows; T2 with 3−5 rows; T3 with one or two rows; ventral spinule pattern as follows: T1 with 8−11 rows; T2 with four or five rows; T3 with three or four rows. Abdominal segments (A1–A8) lacking dorsal spinules; ventral creeping welts present on all abdominal segments (A1–A8); ventral spinule pattern as follows: A1 with three or four rows; A2 with six or seven rows; A3–A6 with 6–8 rows; A7 with six or seven rows; A8 with 6–9 rows. Additional two or three irregular rows of spinules anteriorly and posteriorly to anal lobes, two rows laterally, spinules large, conical, pointing away from anal lobes.

Prothoracic spiracle (Figs 74, 75). Bilobed, bearing 18–21 tubules, distally rounded and arranged in a single sinuous row. Spiracle distal width 0.26–0.34 mm; basal width 0.12−0.17 mm at junction with trachea.

Caudal segment (Figs 76, 77). Dorsal (D1 and D2), intermediate (I1 and I2), lateral (L1), and ventral (V1 and V2) tubercles and sensilla weakly developed; D1 distinctly anterior to D2. Intermediate tubercles I1 and I2 more strongly developed, but associated sensilla weakly developed; I1 lateral and sometimes slightly ventral to I2. L1, V1, and V2 tubercles and associated sensilla weakly developed. Anal lobe entire and very protuberant.

Posterior spiracle (Figs 76, 78–80). Located above horizontal midline. Posterior spiracle openings with thick rimae and numerous trabeculae; 83–108 μm long; 27−32 μm wide; ratio length/width 3.0−3.4. Ecdysial scar apparent. Felt chamber oval, 187−210 μm in diameter at junction with trachea. Spiracular process SP-I comprising 8−11 trunks and 9−26 tips; ratio tips/trunks 1.1− 2.4; basal width 9−15 μm; ratio basal width/length of spiracular opening 0.09−0.17. SP-II comprising 3−7 trunks and 6−14 tips. SP-III comprising 3−9 trunks and 5−20 tips. SP-IV comprising 4−12 trunks and 8−24 tips; ratio tips/trunks 2.0; basal width 7−12 μm; ratio basal width/length of spiracular opening 0.08−0.12.

Distribution. *Anastrepha nolazcoae* is known only from Peru (Amazonas, Cajamarca, Huánuco, San Martín) (Norrbom and Korytkowski 2011; Barr et al. 2017; Bartolini et al. 2020).

Biology. We reared this species from fruit of *Quararibea cordata*, the only known host. It was previously reared from the same fruit in Peru: Huánuco: Tingo Maria (Norrbom and Korytkowski 2011). The larvae feed only on the pulp of the fruit.

Molecular identification. COI barcodes were generated for 29 larvae and five adults and submitted to GenBank (MH070234, MT643950–MT643954, MT654802–MT654827, MT884299, MT884396). These data further confirm the identity of the described larvae. K2P distances between *A. nolazcoae* larvae and the nine available adult sequences ranged from 0.0–1.1%. BLAST searches were consistent with our new data, yielding only four good matches: *A. nolazcoae* (99.21–100% sequence identity; KY428297, MN454445, MN454488, MF695205 [identified as *A. kuhlmanni* in GenBank, reported as *A. nolazcoae* in Barr et al. 2017]). Additionally, 27 larval barcodes returned consensus identifications of *A. nolazcoae* with either three or two votes, and two samples returned ambiguous identifications (Moore et al. in press).

Anastrepha sp. Peru-82

Figs 81–94

Material examined. Peru • 6 larvae; Loreto, Iquitos, ExplorNapo, main trail; 3.2547°S, 72.9133°W; 132 m a.s.l.; 11 Feb. 2015; E. J. Rodriguez and J. Caballero leg.; reared from fruit of *Scleronema praecox*; FSCA (AP20180109.02, AP20180124.03, AP20180124.04, AP20190827.10– AP20190827.12).

Diagnosis. The larva of *Anastrepha* sp. Peru-82 differs from those of other species of *Anastrepha*, except *A. crebra*, *A. haplacantha*, *A. korytkowskii*, *A. nolazcoae*, *Anastrepha* sp. nr. *protuberans*, and *Anastrepha* sp. Sur-16, in having the posterior margins of the accessory plates fringed. It differs from all other species except *A. korytkowskii*, *A. nolazcoae*, and *Anastrepha* sp. Sur-16 by the position of its preoral organ anterior to the mouthhook, and short preoral lobe. *Anastrepha* sp. Peru-82 can be further distinguished from *A. crebra* in having a higher number of oral ridges, and it further differs from *A. korytkowskii*, *A. nolazcoae*, and *Anastrepha* sp. Sur-16 in lacking comb-like processes adjacent to the labium. The number of tubules on the prothoracic spiracle and the dorsal spinule pattern on the thoracic segments are useful to further distinguish *Anastrepha* sp. Peru-82 from other species in the *mucronota* group (see Table 3).

Description. ***Habitus.*** Third instar elongate, cylindrical, tapered anteriorly and caudal end truncate; color creamy; amphipneustic. Length 8.71−10.94 mm and width 1.40−1.72 mm at the sixth abdominal segment.

Pseudocephalon (Figs 81–84). Antenna and maxillary palp on moderately developed lobe. Antenna with cylindrical base and apical knob. Maxillary palp bearing three papilla sensilla, two knob sensilla; dorsolateral group of sensilla bearing two well-developed papilla sensilla, aligned perpendicular to palp and surrounded by collar. Facial mask partly globular in lateral view, upper right section lacking ridges and accessory plates and forming almost a right angle. Preoral organ bearing one unbranched peg sensillum, located apically on a small, rounded lobe directly anterior to mouthhook; adjacent medial preoral lobe of broad, irregular shape, approximately double size of lobe bearing preoral organ and extending partially posterior to it. Oral ridges in 22 or 23 rows, all densely fringed with very long, thin, tapering, pointed projections, but

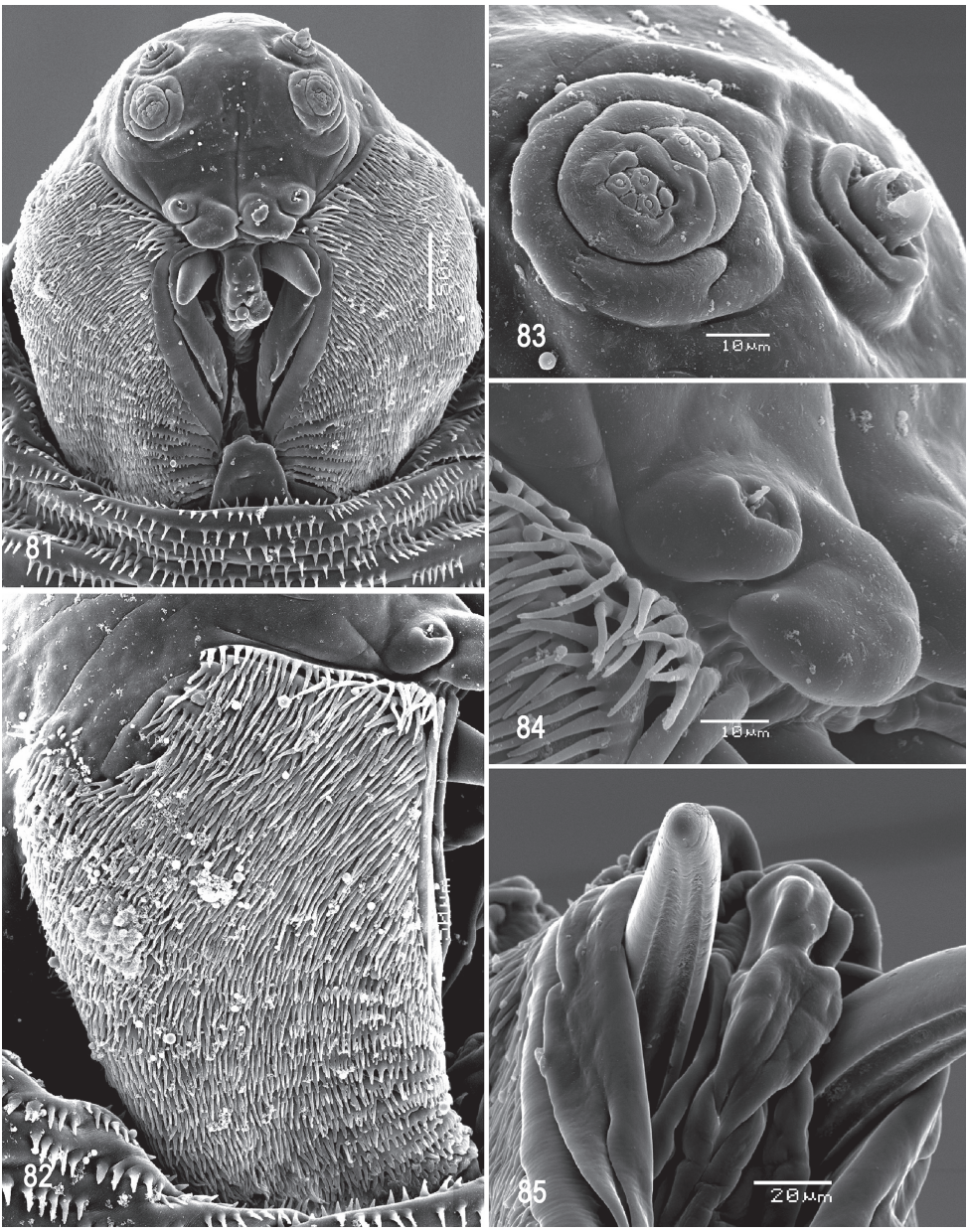

Figures 81–85. Scanning electron photomicrographs of third instar of *Anastrepha* sp. Peru-82 **81** pseudocephalon **82** oral ridges **83** antenna and maxillary palp **84** preoral organ **85** ventral surface of mouthhook. Scale bars: 10 µm (**83, 84**); 20 µm (**85**); 50 µm (**81, 82**).

8–12 posterior ridges with short weakly dentate section medially; numerous accessory plates present, with fringed posterior margins, in one or more series and overlapping with oral ridges (unable to distinguish end points). Labium triangular, anterior surface knobby (not clearly visible in Fig. 81), ventrally with visible sensilla.

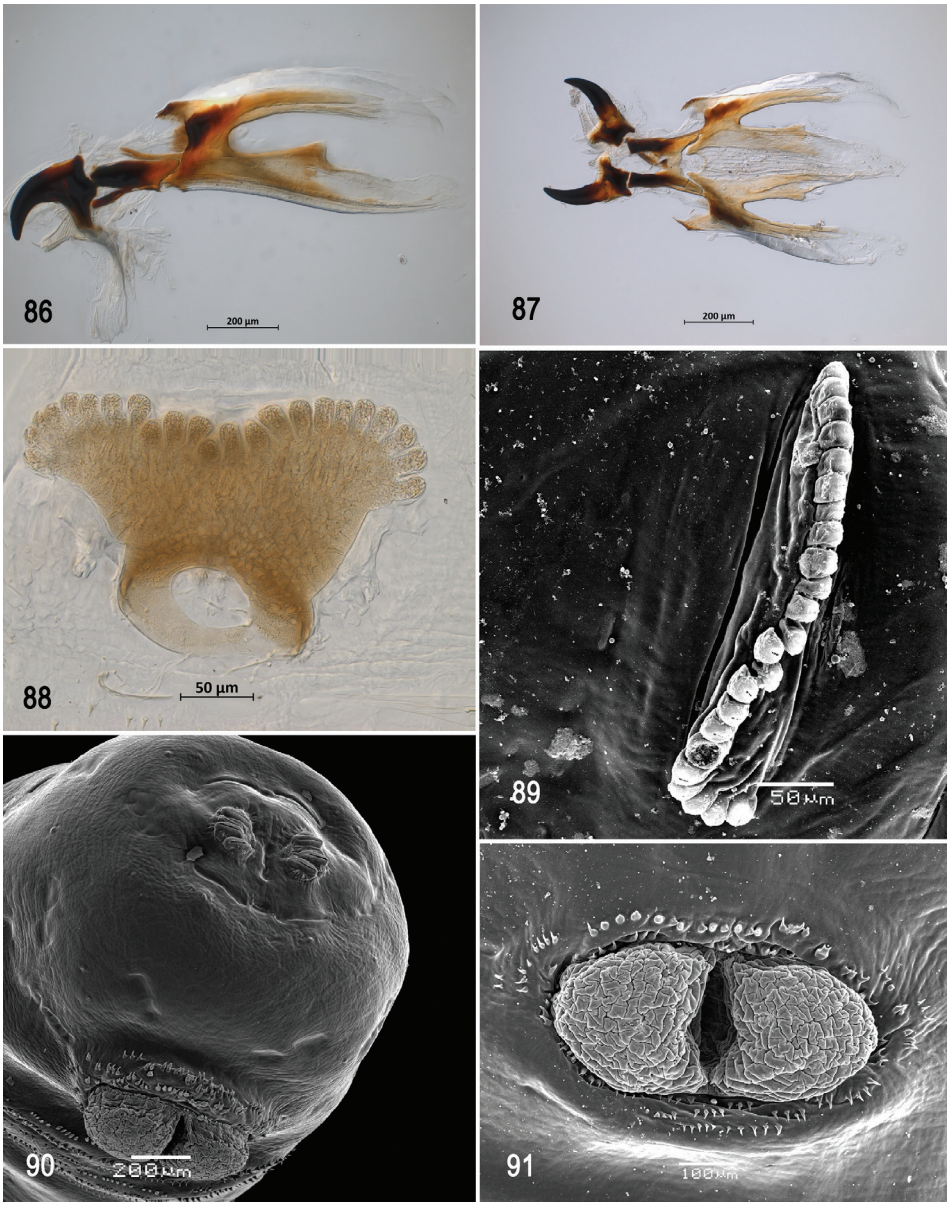

Figures 86–91. Optical photomicrographs and scanning electron photomicrographs of third instar of *Anastrepha* sp. Peru-82 **86** cephaloskeleton, lateral view **87** cephaloskeleton, dorsal view **88** prothoracic spiracle, lateral **89** prothoracic spiracle, dorsolateral **90** caudal segment **91** anal lobe. Scale bars: 50 µm (**88, 89**); 100 µm (**91**); 200 µm (**86, 87, 90**).

Cephaloskeleton (Figs 85–87). Total length from tip of mouthhook to end of ventral cornu 1.0–1.28 mm. Mouthhook well sclerotized, black apically and basally; length a 0.25–0.28 mm; length b 0.18–0.20 mm; height c 0.17–0.20 mm; ratio a:b 1.31–1.41; ratio a:c 1.39–1.50. Tooth long, sharp, strongly curved, concave ventrally with medial

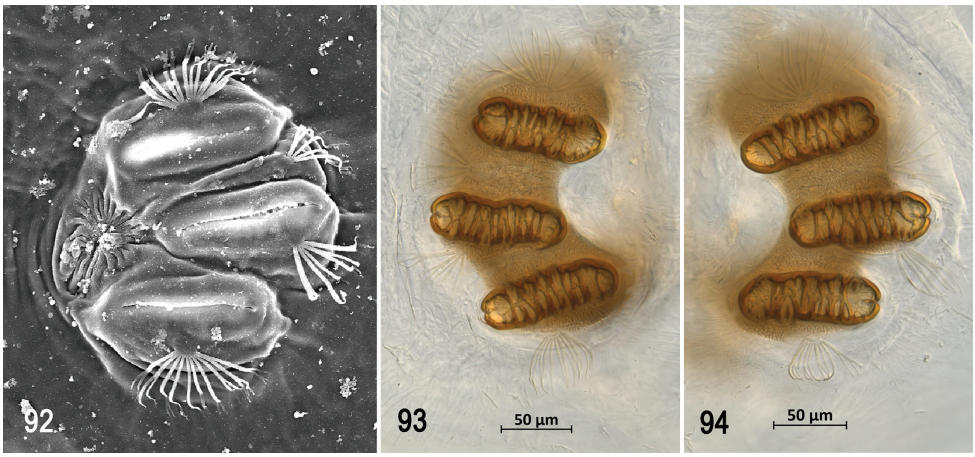

Figures 92–94. Scanning electron photomicrograph and optical photomicrographs of posterior spiracles of third instar of *Anastrepha* sp. Peru-82. Scale bars: 50 µm (**93, 94**).

carina and smooth surface. Intermediate sclerite 0.23–0.26 mm long, 0.14 mm wide at ventral bridge. Epipharyngeal sclerite visible only in dorsal view, with medial lobe directed anteriorly. Labial sclerite robust, sclerotized, and triangular in dorsal view. Parastomal bar extending three-fourths length of intermediate sclerite. Dorsal arch 0.22–0.24 mm high. Dorsal cornu with well-defined sclerotized area adjacent to notch, 0.48–0.64 mm long. Dorsal bridge prominently projecting anteriorly from dorsal cornu and strongly sclerotized. Anterior sclerite irregularly shaped and sclerotized. Cornu notch (N) 0.30–0.43 mm long and cornu notch index (N/DC) 0.63–0.67. Ventral cornu with well-defined sclerotized area from notch to pharyngeal bar and grooves. Pharyngeal filter with weakly sclerotized anterior bar and seven ridges forming a series of grooves along length of ventral cornu. Ventral cornu 0.58–0.81 mm long from pharyngeal bar to posterior end of grooves. Ventral cornu 1.20–1.45 × as long as sclerotized area of dorsal cornu.

Thoracic and abdominal segments. Thoracic segments with dorsal spinules conical, symmetrical to slightly curved posteriorly; dorsal spinule pattern as follows: T1 with two rows; T2 with five or six rows; T3 with two or three rows; ventral spinules as follows: T1 with 7−10 rows; T2 with 3–5 rows; T3 with two or three rows. Abdominal segments (A1–A8) lacking dorsal spinules, except A1 with three rows; ventral creeping welts present on all abdominal segments; ventral spinule pattern as follows: A1 with three or four rows; A2 with 7–9 rows; A3 with eight or nine rows; A4 with nine or ten rows; A5 with ten rows; A6 with 8–10 rows; A7 with 9–11 rows; A8 with 6–9 rows. Additional three irregular rows of spinules anteriorly and posteriorly to anal lobes, two rows laterally; spinules large, conical, pointing away from anal lobes.

Prothoracic spiracle (Figs 88, 89). Bilobed, bearing 23–29 tubules, distally rounded and arranged in a single sinuous row. Spiracle distal width 0.28–0.35 mm; basal width 0.12−0.16 mm at junction with trachea.

Caudal segment (Figs 90, 91). Dorsal (D1 and D2), intermediate (I1 and I2), lateral (L1), and ventral (V1 and V2) tubercles and sensilla weakly developed; D1

distinctly anterior to D2. Intermediate tubercles I1 and I2 more strongly developed, but associated sensilla weakly developed; I1 lateral and sometimes slightly ventral to I2. L1, V1 and V2 most very weakly developed. Anal lobe entire and moderately protuberant.

Posterior spiracle (Figs 90, 92–94). Located above horizontal midline. Posterior spiracle openings with thick rimae and numerous trabeculae; 84–97 μm long; 29–34 μm wide; ratio length/width 2.6–3.0. Ecdysial scar apparent. Felt chamber oval, 185–212 μm in diameter at junction with trachea. Spiracular process SP-I comprising 9–11 trunks and 12–20 tips; ratio tips/trunks 1.3– 1.8; basal width 12–15 μm; ratio basal width/length of spiracular opening 0.14–0.16. SP-II comprising 4–5 trunks and 5–12 tips. SP-III comprising 4–8 trunks and 5–13 tips. SP-IV comprising 7–11 trunks and 13–16 tips; ratio tips/trunks 1.45–1.85; basal width 9–19 μm; ratio basal width/length of spiracular opening 0.11–0.19.

Distribution. *Anastrepha* sp. Peru-82 is only known from Peru (Loreto).

Biology. We reared this species from fruit of *Scleronema praecox*, the first host plant record. The larvae feed only on the pulp of the fruit.

Molecular identification. COI barcodes were generated from six larvae and two adults and submitted to GenBank (MT644049–MT644051, MT763894–MT763898). These data further confirm the identity of the described larvae. K2P distances between *Anastrepha* sp. Peru-82 larvae and the adult sequences ranged from 0.0–1.1%. BLAST searches yielded no close matches to sequences from other *Anastrepha* species. Six larval barcodes returned consensus identifications of *Anastrepha* sp. Peru 82 with either three or two votes (Moore et al. in press).

Anastrepha sp. near *protuberans*

Figs 95–108

Material examined. Ecuador • 5 larvae; Orellana, Estacion Cientifica Yasuní, trail 6, near tower; 0.6805°S, 76.3851°W; 247 m a.s.l.; 6 Jan. 2018; M. R. Steck, G. J. Steck, E. J. Rodriguez and A. Padilla leg.; reared from fruit of *Sterculia frondosa* Rich. (Malvaceae); FSCA (AP20180321.01, AP20180321.02, AP20200622.09–AP20200622.11).

Diagnosis. The larva of *Anastrepha* sp. near *protuberans* differs from those of other species of *Anastrepha* except *A. crebra*, *A. haplacantha*, A. korytkowskii, *A. nolazcoae*, *Anastrepha* sp. Peru-82, and *Anastrepha* sp. Sur-16 by the fringed posterior margins of their oral ridges and accessory plates. *Anastrepha* sp. near *protuberans* can be distinguished from the latter six species in having a greater apical width of the prothoracic spiracle and slit length of the posterior spiracle. The number of oral ridges, number of tubules on the prothoracic spiracle, and dorsal spinule pattern on the thoracic segments further distinguish *Anastrepha* sp. near *protuberans* from species in the *mucronota* group (see Tables 2, 3).

Description. *Habitus*. Third instar elongate, cylindrical, tapered anteriorly and caudal end truncate; color creamy; amphipneustic. Length 14.43–17.15 mm and width 2.52–2.68 mm at the sixth abdominal segment.

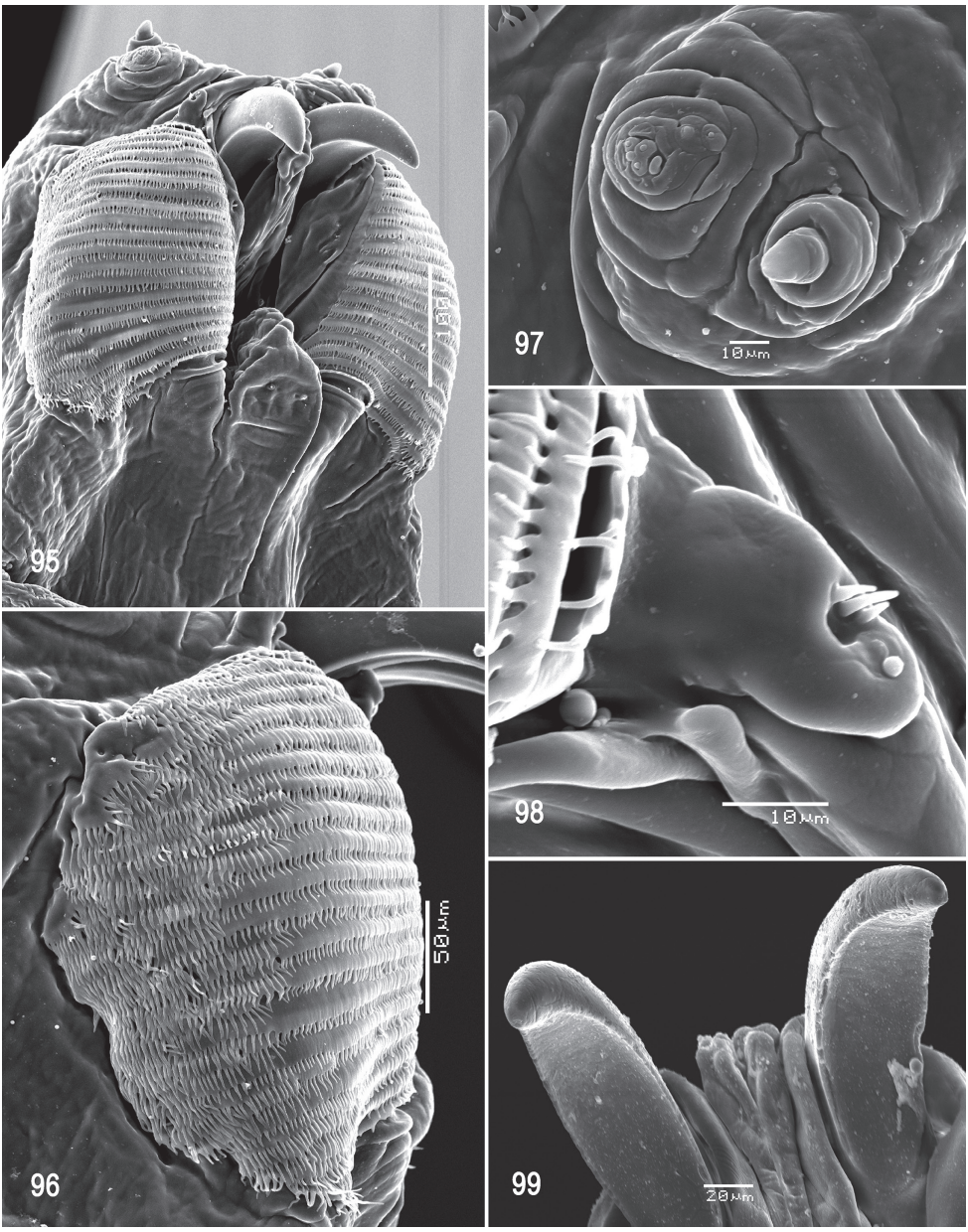

Figures 95–99. Scanning electron photomicrographs of third instar of *Anastrepha* sp. nr. *protuberans* **95** pseudocephalon **96** oral ridges **97** antenna and maxillary palp **98** preoral organ **99** ventral surface of mouthhook. Scale bars: 10 μm (**97, 98**); 20 μm (**99**); 50 μm (**96**); 50 μm (**95**).

Pseudocephalon (Figs 95–98). Antenna and maxillary palp on moderately developed lobe. Antenna with cylindrical base and apical knob. Maxillary palp bearing three papilla sensilla, two knob sensilla; dorsolateral group of sensilla bearing two well-developed papilla sensilla, aligned at strongly oblique angle to palp and surrounded by a

collar. Facial mask globular in lateral view. Preoral organ bearing three unbranched peg sensilla, located apically on simple elongate preoral lobe lateral to mouthhook. Oral ridges in 18–23 rows, posterior margins densely and evenly fringed; accessory plates present covering a much smaller area than oral ridges, with fringed posterior margins longer than oral ridges, apparently in one series. Labium triangular, anterior surface knobby, ventrally with two visible sensilla and tubercles.

Cephaloskeleton (Figs 99–101). Total length from tip of mouthhook to end of ventral cornu 1.48–1.51 mm. Mouthhook well sclerotized, black apically and basally; length a 0.34–0.35 mm; length b 0.24–0.25 mm; height c 0.26–0.28 mm; ratio a:b 1.41–1.46; ratio a:c 1.25–1.30. Tooth long, sharp, strongly curved, concave ventrally with smooth surface. Intermediate sclerite 0.24–0.26 mm long, 0.15 mm wide at ventral bridge. Epipharyngeal sclerite visible only in dorsal view, with medial lobe directed anteriorly. Labial sclerite robust, sclerotized, and triangular in dorsal view. Parastomal bar extending three-fourths length of intermediate sclerite. Dorsal arch 0.33–0.35 mm high. Dorsal cornu with well–defined sclerotized area adjacent to notch, 0.64–0.74 mm long. Dorsal bridge prominently projecting anteriorly from dorsal cornu and sclerotized. Anterior sclerite irregularly shaped and sclerotized. Cornu notch (N) 0.37–0.52 mm long and cornu notch index (N/DC) 0.57–0.69. Ventral cornu with well-defined sclerotized area from notch to pharyngeal bar and grooves. Pharyngeal filter with weakly sclerotized anterior bar and eight or nine ridges forming a series of grooves along length of ventral cornu. Ventral cornu 0.93–1.01 mm long from pharyngeal bar to posterior end of grooves. Ventral cornu 1.26–1.57 × as long as sclerotized area of dorsal cornu.

Thoracic and abdominal segments. Thoracic segments with dorsal spinules conical, symmetrical to slightly curved posteriorly; dorsal spinule pattern as follows: T1 with three rows; T2 with four or five rows; T3 with four rows; ventral spinule pattern as follows: T1 with 13 or 14 rows; T2 with 4–6 rows; T3 with 3–5 rows. Abdominal segments with dorsal spinules as follows: A1 with two rows; A2–A8 lacking spinules; ventral creeping welts present on all abdominal segments; ventral spinule pattern as follows: A1 with 5–8 rows; A2 with 6–9 rows; A3 with eight or nine rows; A4 with 9–12 rows; A5 with 8–12 rows; A6 with 9–11 rows; A7 with seven or eight rows; A8 with 6–9 rows. Additional three irregular rows of spinules anterior and posterior to anal lobes, lateral rows apparently absent, spinules large, conical, pointing away from anal lobes.

Prothoracic spiracle (Figs 102, 103). Bilobed, bearing 22–30 tubules, distally rounded and arranged in a single, sinuous row except medially when spacing is irregular. Spiracle distal width 0.41–0.44 mm; basal width 0.18−0.20 mm at junction with trachea.

Caudal segment (Figs 104, 105). Dorsal (D1 and D2) tubercles and sensilla weakly developed; D1 distinctly anterior to D2. Intermediate tubercles I1 and I2 more strongly developed, but associated sensilla moderately developed; I1 distinctly anterior to I2. L1, V1, and V2 tubercles and associated sensilla weakly developed. Anal lobe entire and protuberant.

Posterior spiracle (Figs 104, 106–108). Located above horizontal midline. Posterior spiracle openings with thick rimae and numerous trabeculae; 122–145 μm long; 40−48 μm wide; ratio length/width 2.8−3.4. Ecdysial scar apparent. Felt chamber oval, 271−305 μm in diameter at junction with trachea. Spiracular process SP-I comprising

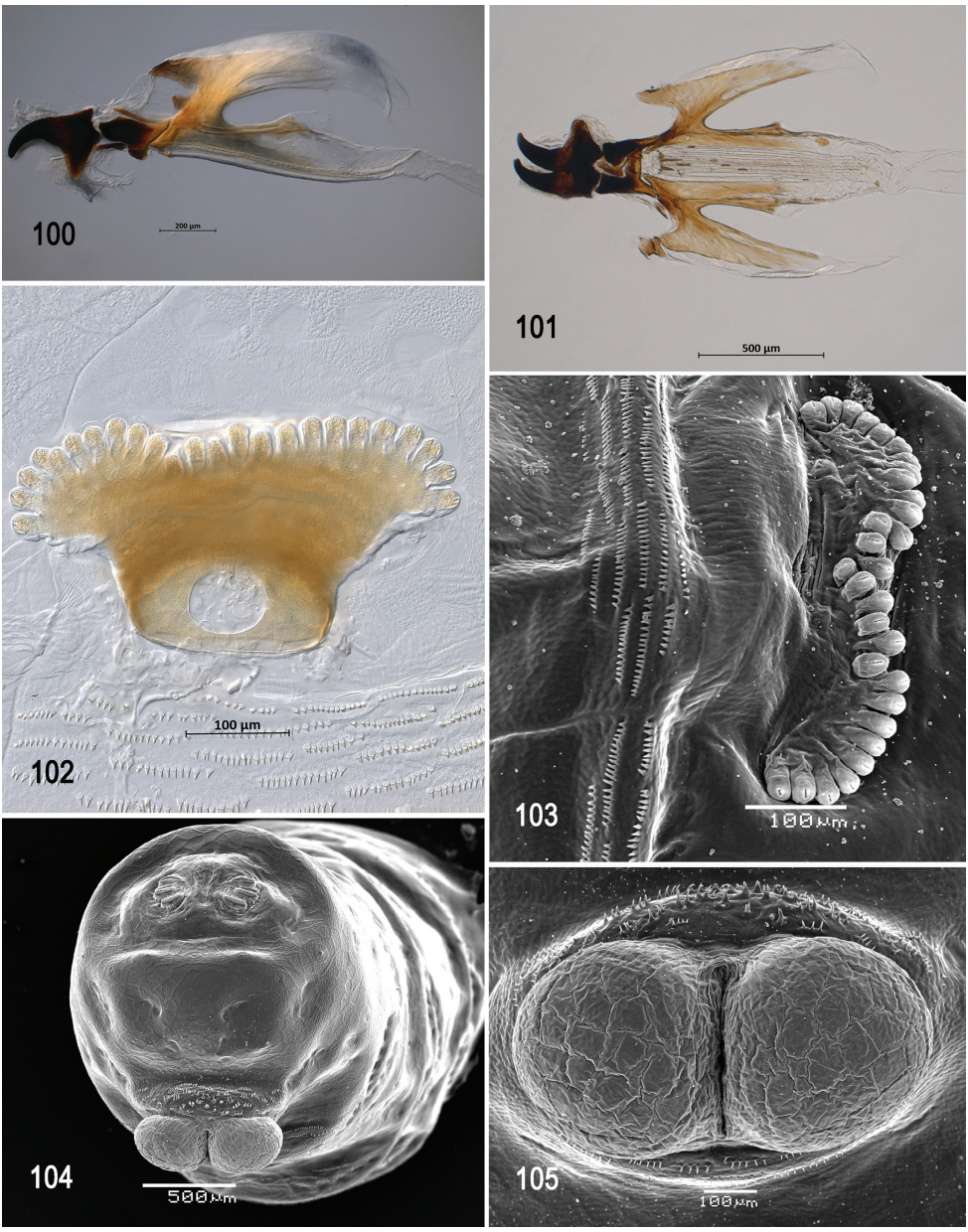

Figures 100–105. Optical photomicrographs and scanning electron photomicrographs of third instar of *Anastrepha* sp. nr. *protuberans* **100** cephaloskeleton, lateral view **101** cephaloskeleton, dorsal view **102** prothoracic spiracle, lateral view **103** prothoracic spiracle, dorsolateral view **104** caudal segment **105** anal lobe. Scale bars: 100 µm (**102, 103, 105**); 200 µm (**100**); 500 µm (**101, 104**).

Figures 106–108. Scanning electron photomicrograph and optical photomicrographs of posterior spiracles of third instar of *Anastrepha* sp. nr. *protuberans*. Scale bars: 100 µm.

5–11 trunks and 9–20 tips; ratio tips/trunks 1.4– 2.5; basal width 8–11 µm; ratio basal width/length of spiracular opening 0.06–0.08. SP-II comprising 4–9 trunks and 11–19 tips. SP-III comprising 4–8 trunks and 7–16 tips. SP-IV comprising 7–10 trunks and 14–21 tips; ratio tips/trunks 1.55–2.6; basal width 9–12 µm; ratio basal width/length of spiracular opening 0.07–0.09.

Distribution. *Anastrepha* sp. near *protuberans* is known only from Ecuador and Peru.

Biology. We collected larvae of this species from fruit of *Sterculia frondosa*, the first host plant record. The larvae feed only on the seeds of the fruit.

Molecular identification. COI barcodes were generated from five larvae from Ecuador and two adults from Peru and submitted to GenBank (MT672163–MT672165, MT763909–MT763911, MT763914). The identity of the described larvae is only based on these data. K2P distances between *Anastrepha* sp. nr. *protuberans* larvae and the adult sequences ranged from 0.0–1.2%. BLAST searches yielded no close matches to sequences from other *Anastrepha* species. The five larval barcodes returned consensus identifications of *Anastrepha* sp. nr. *protuberans* with either three or two votes (Moore et al. in press).

Anastrepha sp. Sur-16

Figs 109–122

Material examined. Suriname • 8 larvae; Brokopondo, Bergendal Amazonia Wellness Resort; 5.1506°N, 55.0690°W; 16 m a.s.l.; 10 May 2018; A. Muller leg.; reared from fruit of *Quararibea guianensis* Aubl. (Malvaceae); FSCA (AP20191024.03–AP20191024.07, AP20201117.01–AP20201117.03).

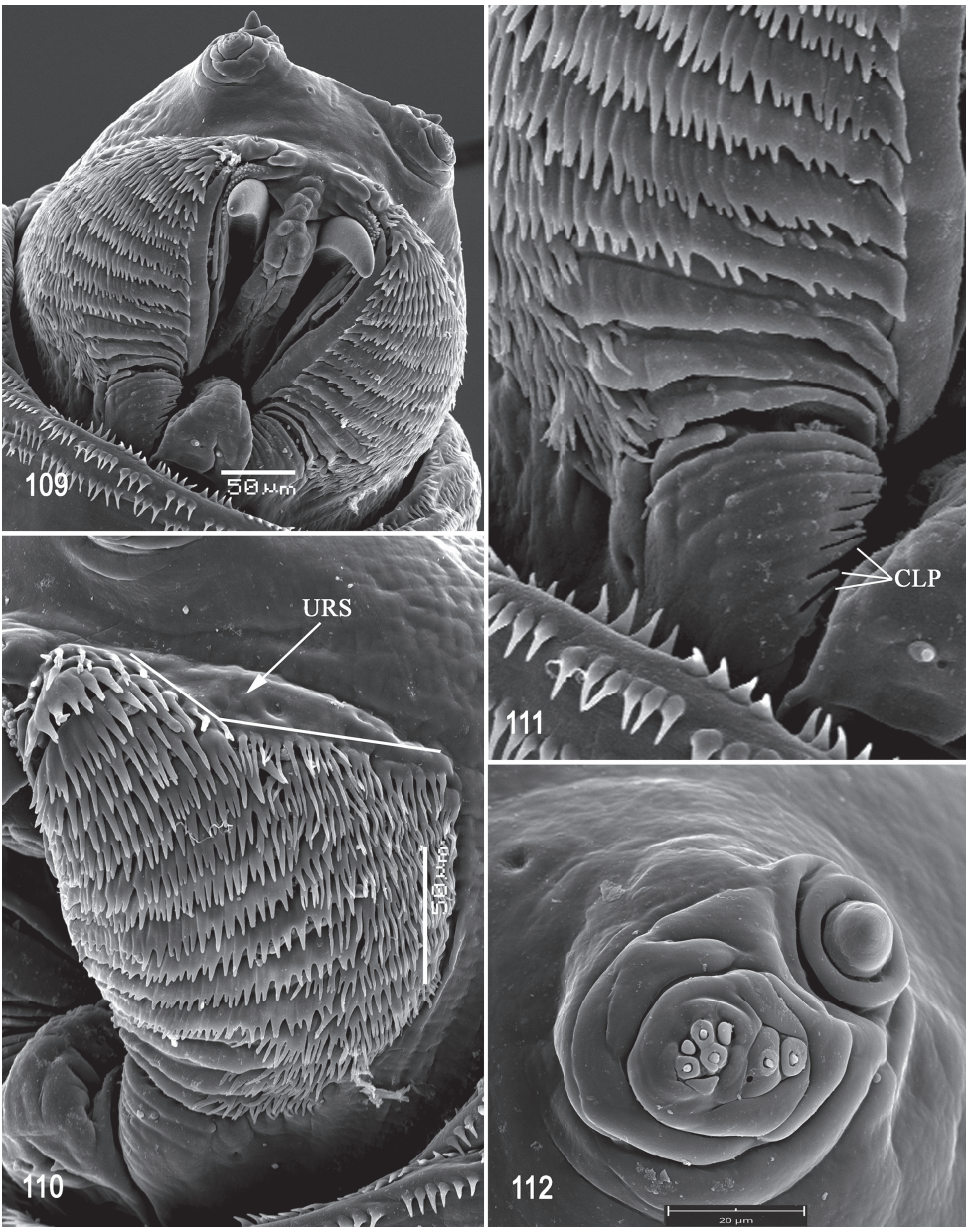

Figures 109–112. Scanning electron photomicrographs of third instar of *Anastrepha* sp. Sur-16 **109** pseudocephalon **110** oral ridges **111** comb-like processes **112** antenna and maxillary palp. Abbreviations: CLP, comb-like processes; URS, upper right section with an obtuse angle shape. Scale bars: 20 µm (**112**); 50 µm (**109, 110**).

Diagnosis. The larvae of *Anastrepha* sp. Sur-16 differs from other species of *Anastrepha* in having deeply dentate posterior margin of the oral ridges and group of small cuticular processes located adjacent to the mouthhook and posterior to the

preoral organ. The posterior margins of the oral ridges resemble those of *A. haplacantha*, but that species lacks the comb-like processes. It can be further distinguished from *A. haplacantha*, in having fewer oral ridges, fewer tubules on the prothoracic spiracle, and greater basal width of the posterior spiracle.

Description. ***Habitus.*** Third instar elongate, cylindrical, tapered anteriorly and caudal end truncate; color creamy; amphipneustic. Length 8.10−8.60 mm and width 1.52−1.62 mm at the sixth abdominal segment.

Pseudocephalon (Figs 109–113). Antenna and maxillary palp on moderately developed lobe. Antenna with cylindrical base and apical knob. Maxillary palp bearing three papilla sensilla, two knob sensilla; dorsolateral group of sensilla bearing two well-developed papilla sensilla, aligned perpendicular to palp and surrounded by a collar. Facial mask partly globular in lateral view, upper right section lacking ridges and accessory plates and forming almost an obtuse angle. Preoral organ bearing 1–3 peg sensilla, located apically on a large, elongated-rounded lobe directly anterior to mouthhook; adjacent medial preoral lobe separate, short-elongate, narrow, extending partially posterior to lobe bearing preoral organ. A group of small cuticular processes arranged in at least two rows arising distally from the medial preoral lobe, located adjacent to the mouthhook and posterior to the preoral organ. Oral ridges in 13–16 rows, 10–13 anterior ridges with deeply dentate margins, projections closely spaced, two or three posterior ridges with entire margins; numerous accessory plates present covering a much smaller area than oral ridges, with fringed posterior margins, medial and posterior plates in two or more series; 7–9 comb-like processes adjacent to labium. Labium triangular, anterior surface knobby, ventrally with two visible sensilla.

Cephaloskeleton (Figs 114–116). Total length from tip of mouthhook to end of ventral cornu 1.13–1.18 mm. Mouthhook well sclerotized, black apically and basally; length a 0.22–0.23 mm; length b 0.16–0.17 mm; height c 0.16–0.17 mm; ratio a:b 1.30–1.41; ratio a:c 1.34–1.40. Tooth long, sharp, strongly curved, concave ventrally with eroded surface. Intermediate sclerite 0.20–0.21 mm long, 0.13–0.14 mm wide at ventral bridge. Epipharyngeal sclerite visible only in dorsal view, with medial lobe directed anteriorly. Labial sclerite robust, sclerotized, and triangular in dorsal view. Parastomal bar extending three-fourths length of intermediate sclerite. Dorsal arch 0.25–0.26 mm high. Dorsal cornu with well-defined sclerotized area adjacent to notch, 0.50–0.54 mm long. Dorsal bridge prominently projecting anteriorly from dorsal cornu and slightly sclerotized. Anterior sclerite irregularly shaped and sclerotized. Cornu notch (N) 0.30–0.35 mm and cornu notch index (N/DC) 0.61–0.66. Ventral cornu with well-defined sclerotized area from notch to pharyngeal bar and grooves. Pharyngeal filter with weakly sclerotized anterior bar and eight ridges forming a series of grooves along length of ventral cornu. Ventral cornu 0.73–0.73 mm long from pharyngeal bar to posterior end of grooves. Ventral cornu 1.40–1.49 × as long as sclerotized area of dorsal cornu.

Thoracic and abdominal segments. Thoracic segments with dorsal spinules conical, symmetrical to slightly curved posteriorly; dorsal spinule pattern as follows: T1 with five rows, forming scalloped plates; T2 with three rows; T3 lacking spinules; ventral spinule pattern as follows: T1 with ten rows; T2 with three or four rows; T3 with one or two rows. Abdominal segments all lacking dorsal spinules; ventral creeping

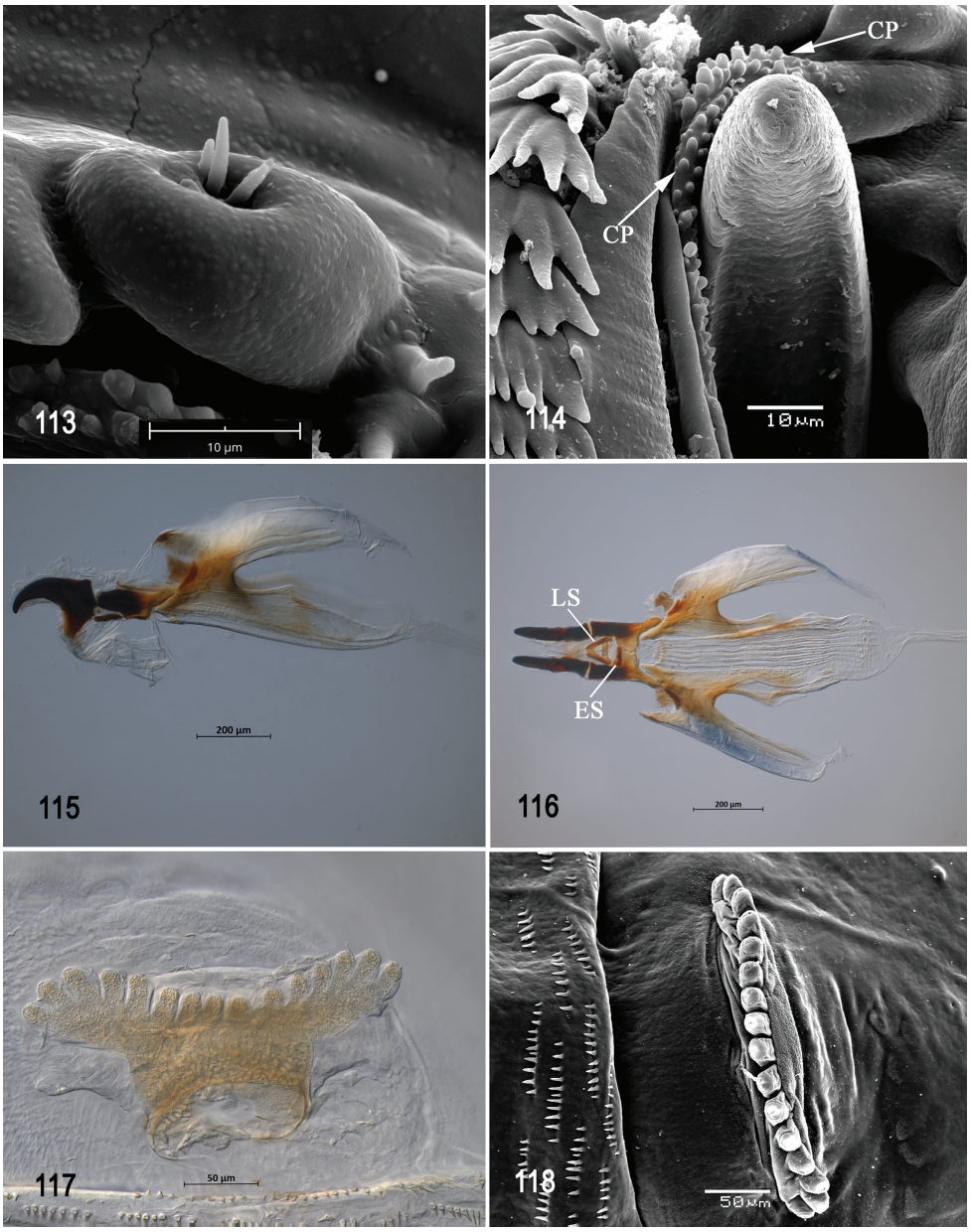

Figures 113–118. Optical photomicrographs and scanning electron photomicrographs of third instar of *Anastrepha* sp. Sur-16 **113** preoral organ **114** ventral surface of mouthhook **115** cephaloskeleton, lateral view **116** cephaloskeleton, dorsal view **117** prothoracic spiracle, lateral view **118** prothoracic spiracle, dorsolateral view. Abbreviations: CP, cuticular processes; ES, epipharyngeal sclerite; LS, labial sclerite. Scale bars: 10 µm (**113, 114**); 50 µm (**117, 118**); 200 µm (**115, 116**).

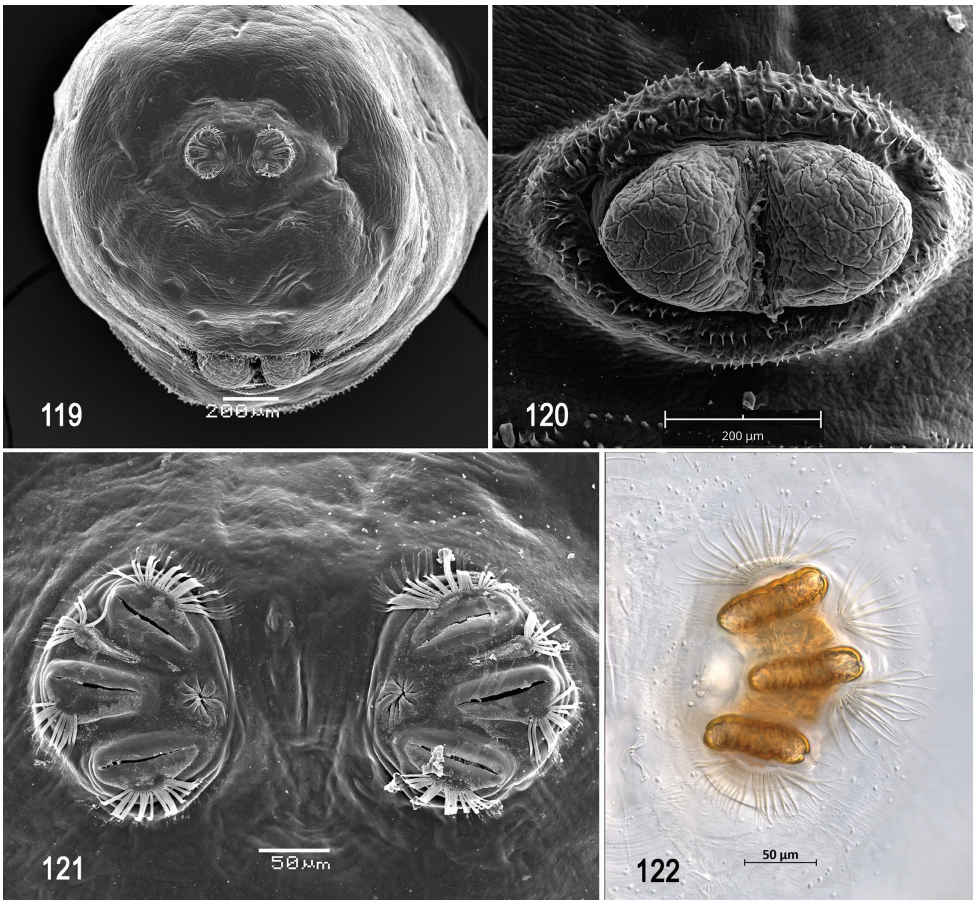

Figures 119–122. Scanning electron photomicrographs and optical photomicrograph of third instar of *Anastrepha* sp. Sur-16 **119** caudal segment **120** anal lobe **121, 122** posterior spiracle. Scale bars: 50 µm (**121, 122**); 200 µm (**119, 120**).

welts present on all abdominal segments; ventral spinule pattern as follows: A1 with three rows, A2 with six or seven rows; A3 with 6–10 rows, A4 with eight or nine rows; A5 to A7 with seven or eight rows; A8 with 6–9 rows. Additional three irregular rows of spinules anteriorly and posteriorly to anal lobes, one or two rows laterally, spinules large, conical, pointing away from anal lobes.

Prothoracic spiracle (Figs 117, 118). Bilobed, bearing 12–17 tubules, distally rounded and arranged in a single sinuous row. Spiracle distal width 0.23–0.28 mm; basal width 0.09−0.11 mm at junction with trachea.

Caudal segment (Figs 119, 120). Dorsal (D1) tubercles moderately developed, D2 tubercles and associated sensilla weakly developed; D1 distinctly anterior to D2. Intermediate tubercles I1 and I2 more strongly developed, but associated sensilla moderately developed; I1 distinctly ventral to I2. L1, V1 and V2 tubercles and associated sensilla weakly developed. Anal lobe entire and protuberant.

Posterior spiracle (Figs 119, 121, 122). Located above horizontal midline. Posterior spiracle openings with thick rimae and numerous trabeculae; 69–80 μm long; 24–27 μm wide; ratio length/width 2.9–3.0. Ecdysial scar apparent. Felt chamber oval, 129–168 μm in diameter at junction with trachea. Spiracular process SP-I comprising 13–18 trunks and 19–34 tips; ratio tips/trunks 1.5–1.8; basal width 29–36 μm; ratio basal width/length of spiracular opening 0.39–0.44. SP-II comprising 5–8 trunks and 7–18 tips. SP-III comprising 8–13 trunks and 14–24 tips. SP-IV comprising 13–17 trunks and 25–40 tips; ratio tips/trunks 1.92–2.35; basal width 23–34 μm; ratio basal width/length of spiracular opening 0.33–0.45.

Distribution. *Anastrepha* sp. Sur-16 is known only from Suriname (Brokopondo).

Biology. We reared this species from fruit of *Quararibea guianensis*, the first host plant record. Larvae feed on the pulp.

Molecular identification. COI barcodes were generated from five larvae and two adults and submitted to GenBank (MT644074–MT644078, MT672219–MT672220). These data further confirm the identity of the described larvae. K2P distances between *Anastrepha* sp. Sur-16 larvae and the adult sequences ranged from 0.02–1.2%. BLAST searches yielded no close matches to sequences of other *Anastrepha* species. The five larval barcodes returned consensus identifications of *Anastrepha* sp. Sur-16 with either three or two votes (Moore et al. in press).

Discussion

The extraordinary morphology of the pseudocephalon of third instars of the species of the *mucronota* group treated in this study includes characters that appear to be relevant to analysis of the phylogenetic relationships of this species group. Norrbom et al. (1999) recognized the *mucronota* group for 31 species but indicated that it could be paraphyletic. It included species without a strong crease in the proctiger (a plesiomorphic state) but lacking synapomorphies of other species groups with this character state. Two wing characters common within the group (C- and S-bands separated; vein R_{2+3} sinuous) were mentioned as possibly of phylogenetic significance, but they are not consistent nor unique to the group. Additional species have subsequently been described or transferred to the *mucronota* group such that it currently includes 54 described and a number of as yet undescribed species (Norrbom et al. 2012; Moore et al. in press). Mengual et al. (2017) included 19 described and four undescribed species (sp. 4 and sp. nr. *submunda* are now believed to be the same species) that are currently placed in the *mucronota* group. In their maximum likelihood tree (Fig. 3), these species were placed in four clades comprising, respectively, 14 species, four species (with species of the *raveni* group), two clades with two species each, and one species grouped with a species of the *schausi* group. The *mucronota* group thus may indeed not be monophyletic, but support for some of the intermediate branches was low enough that the relationships of some species remain unclear.

Of the nine species for which larvae are described in this paper, six were included by Mengual et al. (2017): *A. aphelocentema* was clustered with *A. galbina* Stone rather

distant from the other species; *A. caballeroi* and *A. haplacantha* were placed in the clade with the species of the *raveni* group; and *A. crebra*, *A. korytkowskii*, and *A. nolazcoae* were in the largest cluster of 14 species. Because the number of species for which larvae are known is still very limited and the number of larval morphological characters that appear useful for phylogenetic analysis is also small, we consider it premature to undertake a rigorous analysis at this time. However, to explore the potential of the

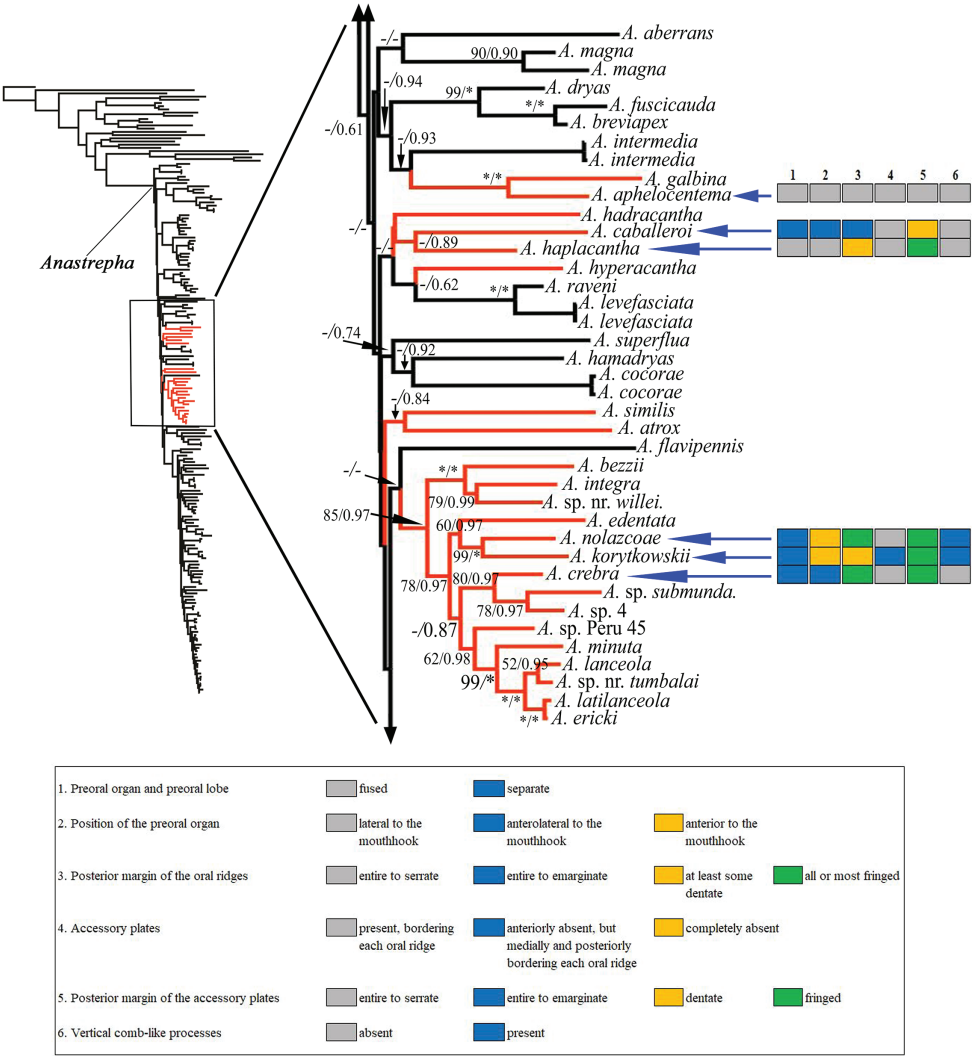

Figure 123. Tree visualization of the novel characters of the pseudocephalon. *Anastrepha* phylogeny and relationships of species within the *mucronota* group (clades and branches in orange) were taken from Mengual et al. (2017). The larval characters are indicated for the six selected traits: (1) Preoral organ and preoral lobe; (2) Position of the preoral organ; (3) Posterior margin of the oral ridges; (4) Accessory plates; (5) Posterior margin of the accessory plates; (6) Vertical comb-like processes.

novel larval characters for this purpose, we plotted these characters onto the Mengual et al. (2017: fig. 1, partially redrawn here as Fig. 123) tree. We discuss each character, indicate the species in which the apomorphic states occur and where these species are placed on the tree, and speculate regarding the significance of these character states.

The characters with new character states are the size and shape of the preoral lobe bearing the preoral organ, the position of the preoral organ, and the posterior margins of the oral ridges and accessory plates (see Tables 5, 6). The position of the preoral organ anterior to the mouthhook in *A. korytkowskii*, *A. nolazcoae*, *Anastrepha* sp. Peru-82, and *Anastrepha* sp. Sur-16, and anterolateral to the mouthhook in *A. caballeroi* and *A. crebra* are unique character states within *Anastrepha* and found only in these six species and *A. curvicauda* (anterior to mouthhook) (Figs 18, 31, 53, 66, 81, 109; character 2). The separation of the preoral organ from the preoral lobe is only found in the six species of the *mucronota* group above, *A. grandis*, *A. leptozona*, *and A. pickeli* (Table 6), although in *A. grandis*, *A. leptozona*, and *A. pickeli* the preoral organ is lateral to the mouthhook (see Frías et al. 2009: fig. 4 and Dutra et al. 2018a: fig. 2A). In most *Anastrepha* species, the preoral organ is lateral to the mouthhook, on the end of a long simple preoral lobe, not on a separate cylindrical lobe (e.g., as in *A. aphelocentema*, *A. haplacantha*, and *Anastrepha* sp. nr. *protuberans* (Figs 1, 41, 44, 95). The position of the preoral organ anterior to the mouthhook has not been observed in other genera of Tephritidae, however, the presence of a separate cylindrical lobe bearing the preoral organ does occur in many genera of Dacinae, such as *Bactrocera*, *Dacus*, and *Zeugodacus* of the Dacini, *Ceratitis* of the Ceratitidini, and *Acroceratitis* and *Ichneumonopsis* of the Gastrozonini (White and Elson-Harris 1992; Carroll et al. 2004; Kovac et al. 2013; Schneider et al. 2018). The position of the preoral organ anterolateral or anterior to the mouthhook (apomorphic states) in most species of the *mucronota* group that we examined suggests that this character has phylogenetic signal, although the plesiomorphic state in *A. haplacantha* and *A.* sp. nr. *protuberans*, as well as *A. aphelocentema*, suggests that these species may be less closely related than the other species or that there is some homoplasy in this character.

In all previously described larvae of *Anastrepha*, the posterior margins of the oral ridges (character 3) and accessory plates are variously entire, serrate, occasionally

Table 5. Larval characters and character states used for comparative morphology of the pseudocephalon.

Character	State
1. Preoral organ and preoral lobe	0, fused; 1, separate
2. Position of the preoral organ	0, lateral to the mouthhook; 1, anterolateral to the mouthhook; 2, anterior to the mouthhook
3. Posterior margin of the oral ridges	0, entire to serrate; 1, entire to emarginate; 2, at least some dentate; 3, all or most fringed
4. Accessory plates	0, present, bordering each oral ridge; 1, anteriorly absent, but medially and posteriorly bordering each oral ridge; 2, completely absent
5. Posterior margin of the accessory plates	0, entire to serrate; 1, entire to emarginate; 2, dentate; 3, fringed
6. Vertical comb-like processes	0, absent; 1, present

Table 6. Character matrix of the outgroup and ingroup taxa used for comparative morphology of the pseudocephalon.

Species group	Species	Characters					
		1	2	3	4	5	6
	Outgroup						
curvicauda	*A. curvicauda*	0	2	0	0	0	0
fraterculus	*A. amita*	0	0	1	0	?	0
	A. amplidentata	0	0	1	0	0	0
	A. bahiensis	0	0	1	0	1	0
	A. coronilli	0	0	1	2	–	0
	A. durantae	0	0	1	0	1	0
	A. ludens	0	0	1	0	1	0
	A. sororcula	0	0	1	0	1	0
	A. suspensa	0	0	1	0	1	0
	A. zenildae	0	0	1	0	1	0
grandis	*A. grandis*	1	0	1	0	1	0
leptozona	*A. leptozona*	1	0	0	0	0	0
pseudoparalella	*A. limae*	0	0	1	0	1	0
serpentina	*A. pulchra*	0	0	1	0	1	0
	A. serpentina	0	0	1	0	1	0
spatulata	*A. pickeli*	1	0	1	0	1	0
striata	*A. striata*	0	0	1	0	1	0
	Ingroup						
mucronota	*A. aphelocentema*	0	0	0	0	0	0
	A. caballeroi	1	1	1	0	2	0
	A. crebra	1	1	3	0	3	0
	A. haplacantha	0	0	2	0	3	0
	A. korytkowskii	1	2	2	1	3	1
	A. nolazcoae	1	2	3	0	3	1
	Anastrepha sp. Peru-82	1	2	3	1	3	0
	Anastrepha sp. nr. *protuberans*	0	0	3	0	3	0
	Anastrepha sp. Sur-16	1	2	2	0	3	1

(?) Unknown data from previous studies.
(–) Inapplicable data because the accessory plates are absent in *A. coronilli*.

incised, sparsely emarginate, or scalloped; in none of these species are the margins dentate or fringed (Steck et al. 1990; Carroll et al. 2004; Dutra et al. 2018b; Rodriguez et al. 2021). Although there is some variation in this character in other, rather distantly related genera (e.g., *Rioxoptilona dunlopi* (Wulp), *Rioxoptilona ochropleura* (Hering), and *Rioxoptilona vaga* (Wiedemann) of the subfamily Phytalmiinae, tribe Acanthonevrini, *Bactrocera bryoniae* (Tryon), *Bactrocera carambolae* Dew and Hancock, *Bactrocera frauenfeldi* (Schiner), *Bactrocera jarvisi* (Tryon), *Bactrocera latifrons* (Hendel), *Bactrocera musae* (Tryon) of the subfamily Dacinae, tribe Dacini, *Anoplomus rufipes* Hardy, *Chaetellipsis alternata* (Zia), *Chaetellipsis* sp., *Cyrtostola limbata* (Hendel), and *Paraxarnura anephelobasis* Hardy of the subfamily Dacinae, tribe Gastrozonini) (see Elson-Harris 1992: pls 3, 8, 14, 93, 314; White and Elson-Harris 1992: pls 9a, 14a, 17b, 18c, 20b: Schneider et al. 2017: figs 1E, 4E, 7D, 7E, 12D, 12E), the dentate and fringed

margins of the accessory plates appear to be apomorphic character states (see Table 6), and one or both states are present in species of the *mucronota* group, except for *A. aphelocentema*, in which they are finely serrate or entire. That and the dentate or fringed (i.e., more deeply incised) margins of the oral ridges could be synapomorphies for a large portion of the species within the *mucronota* group (with some homoplasy involving states 2 and 3 of these characters) or alternatively could have arisen independently in the clade including *A. crebra*, *A. korytkowskii*, and *A. nolazcoae* and that containing *A. caballeroi* and *A. haplacantha* (perhaps with reversal in character 3 in *A. caballeroi*) if the relationships among these species in the tree of Mengual et al. (2017) are correct (Fig. 123). *Anastrepha* sp. Peru-82, *A.* sp. nr. *protuberans*, and *A.* sp. Sur-16 also share these apomorphic character states (Table 6), supporting their inclusion in the *mucronota* group. The accessory plates (Figs 14, 15) covering a much larger area than the oral ridges appear to be an autapomorphy of *A. caballeroi*.

Another remarkable feature reported for the first time in *Anastrepha* is the vertical comb-like processes on the margin of the oral cavity found only in *A. korytkowskii*, *A. nolazcoae*, and *Anastrepha* sp. Sur-16 (Figs 53, 68, 111). These processes are exceptional and absent in other tephritid larvae described to date. This morphological feature appears to be a synapomorphy of *A. korytkowskii* and *A. nolazcoae*, which are sister taxa in the Mengual et al. (2017) tree (Fig. 123, Table 6), and perhaps some other closely related taxa (but not *A. crebra*). We hypothesize that *Anastrepha* sp. Sur-16, which also has the apomorphic state, is also very closely related to these two species based on this character and those previously discussed (fringed margins of the accessory plates and preoral organ located anterior to mouthhook).

Our results support the hypothesis of Mengual et al. (2017) that *A. aphelocentema* is an outlier from the *mucronota* group, as it possesses no apomorphic larval character states. In particular, the posterior margins of the oral ridges and accessory plates are entire to finely serrate (plesiomorphy) (Figs 2, 123, Table 6), whereas in the other species the margins of the accessory plates are dentate (*A. caballeroi*, Figs 15, 123, Table 6) or fringed (the other four species, *A. crebra*, *A. haplacantha*, *A. korytkowskii*, *A. nolazcoae*, Figs 29, 42, 54, 67, 123, Table 6). The fringed margins of the accessory plates, and the at least sometimes dentate and fringed margins of the oral ridges of those other four species are distributed across the *mucronota* group in two distant clades (Fig. 123). Within the well-supported clade with 14 taxa, the location of the preoral organ (anterior to mouthhook) and the preoral lobe and preoral organ (separate) supports the relationship of *A. korytkowskii* + *A. nolazcoae* and may indicate that *Anastrepha* sp. Peru-82 + *Anastrepha* sp. Sur-16 belong to this clade (Table 6). Of these four species, *A. korytkowskii*, *A. nolazcoae*, and *Anastrepha* sp. Sur-16 appear to be more closely related due to the presence of the vertical comb-like processes (Table 6). The comparative morphology of the pseudocephalon concurs with the molecular phylogeny of Mengual et al. (2017), with the exception of *A. caballeroi* and *A. haplacantha* not sharing derived larval morphological character states (although presence of states 5.2 or 5.3, i.e., more incised accessory plates, could be considered a synapomorphy if these

states are interpreted as part of a transformation series). It also suggests that *Anastrepha* sp. Peru-82, *Anastrepha* sp. nr. *protuberans*, and *Anastrepha* sp. Sur-16 may belong to the largest and well-supported clade (Table 6, Fig. 123). However, the relationships of these and all of the species of the *mucronota* group should be further evaluated and confirmed from additional molecular and morphological phylogenetic analysis as samples of larvae and adults become available.

Acknowledgements

We thank Able Chow of the University of Florida - Department of Entomology and Nematology (UF Ent/Nem) for his support with specimen preparation and photographs. We also sincerely thank Martin Aluja for providing larvae from Mexico, and Jorge Caballero, Nilver Zenteno, M. R. Steck, and the late Rufo Bustamante who helped to collect larvae. Collection of most of this material was made possible by a Cooperative Agreement (3.0342 (2012), 13-8131-0291-CA (2013), 3.0295.01 (2014), 3.0281 (2015), 3.0520.03 (2017), 3.0542.04 (2018), 3.0439.04 (2019), 3.0577.04 (2020), and 3.1122.04 (2021) from the United States Department of Agriculture's Animal and Plant Health Inspection Service (APHIS). Results and conclusions of this publication may not necessarily express APHIS' views. We are grateful to Megan MacDowell, Valerie Peterson, and Eileen Rosin of the Amazon Conservation Association (ACA), Laura Samaniego of the Asociación para la Conservación de la Cuenca Amazónica (ACCA), Pam Bucur and Marisol Rivera of the Amazon Explorama Lodges (EXPLORAMA), Erick Yábar of the Universidad Nacional de San Antonio Abad de Cusco (UNSAAC), Erika Paliza and Frank Azorsa of the Centro de Ecología y Biodiversidad (CEBIO), and Cliff Keil of Pontificia Universidad Católica del Ecuador (PUCE), whose collaboration was essential to the success of the project. Juan Celidonio Ruiz of the Herbarium Amazonense (AMAZ) – Universidad Nacional de la Amazonia Peruana (UNAP), Iquitos, Peru, Rufo Bustamante (ACCA), Milton Zambrano (PUCE – Estacion Cientifica Yasuní), and Sabitrie Jairam-Doerga (Nationaal Herbarium van Suriname) kindly identified the host plants. Specimens from Peru were collected under permission of Dirección General Forestal y de Fauna Silvestre (Resolución Directoral No. 209–2013–MINAGRI–DGFFS/DGEFFS, No. 022–2015–SERFOR–DGGSPFFS), specimens from Ecuador under permission of Ministerio del Ambiente y Agua (permiso de investigacion cientifica No. 011-2018-IC-FAU-DNB/MA), and in Suriname with permission of the Suriname Forest Service, Nature Conservation Division (2016, 2017–2018, 2019–2020). We thank the Florida Department of Agriculture and Consumer Services – Division of Plant Industry for its support of this work. Mention of the trade names or commercial products in this publication is solely for the purpose of providing specific information and does not imply recommendation or endorsement. USDA is an equal opportunity provider and employer.

References

Aluja M (1994) Bionomics and management of *Anastrepha*. Annual Review of Entomology 39(1): 155–178. https://doi.org/10.1146/annurev.en.39.010194.001103

Aluja M, Mangan RL (2008) Fruit fly (Diptera: Tephritidae) host status determination: Critical conceptual, methodological, and regulatory considerations. Annual Review of Entomology 53(1): 473–502. https://doi.org/10.1146/annurev.ento.53.103106.093350

Aluja M, Piñero J, López M, Ruíz C, Zúñiga A, Piedra E, Díaz-Fleischer F, Sivinski J (2000) New host plant and distribution records in Mexico for *Anastrepha* spp., *Toxotrypana curvicauda* Gerstacker, *Rhagoletis zoqui* Bush, Rhagoletis sp., and *Hexachaeta* sp. (Diptera: Tephritidae). Proceedings of the Entomological Society of Washington 102: 802–815.

Aluja M, Rull J, Sivinski J, Norrbom AL, Wharton RA, Macias-Ordoñez R, Diaz-Fleischer F, Lopez M (2003) Fruit flies of the genus *Anastrepha* (Diptera: Tephritidae) and associated native parasitoids (Hymenoptera) in the tropical rainforest biosphere reserve of Montes Azules, Chiapas, Mexico. Environmental Entomology 32(6): 1377–1385. https://doi.org/10.1603/0046-225X-32.6.1377

Baker AC, Stone WC, Plummer CC, McPhail M (1944) A review of studies on the Mexican-fruit fly and related Mexican species. U. S. Department of Agriculture. Miscellaneous Publication 531.

Barr NB, Ruiz-Arce R, Farris RE, Silva JG, Lima KM, Dutra VS, Ronchi-Teles B, Kerr PH, Norrbom AL, Nolazco N, Thomas DB (2017) Identifying *Anastrepha* (Diptera; Tephritidae) species using DNA barcodes. Journal of Economic Entomology 111(1): 405–421. https://doi.org/10.1093/jee/tox300

Bartolini I, Rivera J, Nolazco N, Olórtegui A (2020) Towards the implementation of a DNA barcode library for the identification of Peruvian species of *Anastrepha* (Diptera: Tephritidae). PLoS ONE 15(1): 1–12. https://doi.org/10.1371/journal.pone.0228136

Borkent A, Sinclair BJ (2017) Key to Diptera families – Larvae. In: Kirk-Spriggs AH, Sinclair BJ (Eds) Manual of Afrotropical Diptera. Volume I. Introductory chapters and keys to Diptera families. Suricata 4. South African National Biodiversity Institute, Pretoria, South Africa, 357–411.

Canal NA, Hernández-Ortiz V, Tigrero Salas JO, Selivon D (2015) Morphometric study of third-instar larvae from five morphotypes of the *Anastrepha fraterculus* cryptic species complex (Diptera, Tephritidae). In: De Meyer MM, Clarke AR, Vera TM, Hendrichs J (Eds) Resolution of cryptic species complexes of tephritid pests to enhance SIT application and facilitate international trade. ZooKeys 540: 41–59. https://doi.org/10.3897/zookeys.540.6012

Canal NA, Galeano-Olaya PE, Castañeda MR (2018) Phenotypic structure of Colombian populations of *Anastrepha fraterculus* Complex (Diptera: Tephritidae). The Florida Entomologist 101(3): 486–497. https://doi.org/10.1653/024.101.0307

Carrejo NS, González OR (1994) Lista preliminar de las moscas de la fruta del genero *Anastrepha* (Diptera: Tephritidae) en departamento del Valle del Cauca Cali, Colombia. Boletin del Museo de Entomologia de la Universidad del Valle 2(1–2): 85–93. http://hdl.handle.net/10893/4564

Carrejo NS, González OR (1999) Parasitoids reared from species of *Anastrepha* (Diptera: Tephritidae) in Valle del Cauca, Colombia. The Florida Entomologist 82(1): 113–118. https://doi.org/10.2307/3495842

Carroll LE, Wharton RA (1989) Morphology of the immature stages of *Anastrepha ludens* (Diptera: Tephritidae). Annals of the Entomological Society of America 82(2): 201–214. https://doi.org/10.1093/aesa/82.2.201

Carroll LE, Norrbom AL, Dallwitz MJ, Thompson FC (2004) Pest fruit flies of the world – larvae. Version: 9. April 2019. http://delta–intkey.com

Chu-Wang IW, Axtell RC (1972) Fine structure of the terminal organ of the house fly larva, *Musca domestica* L. Zeitschrift Zelforschung 127(3): 287–305. https://doi.org/10.1007/BF00306874

CoFFHI [Compendium of Fruit Fly Host Information] (2020) edn. 5.0. https://coffhi.cphst.org/ [accessed on 4 August 2020]

Courtney GW, Sinclair BJ, Meier R (2000) 1.4. Morphology and terminology of Diptera larvae. In: Papp L, Darvas B (Eds) Contribution to a manual of Paleartic Diptera (with special reference to flies of economic importance), Volume I. General and applied dipterology. Science Herald, Budapest, 85–161.

Dutra VS, Ronchi-Teles B, Steck GJ, Silva JG (2012) Description of larvae of *Anastrepha* spp. (Diptera: Tephritidae) in the *fraterculus* group. Annals of the Entomological Society of America 105(4): 529–538. https://doi.org/10.1603/AN11180

Dutra VS, Ronchi-Teles B, Steck GJ, Araujo EL, Souza-Filho MF, Raga A, Silva JG (2018a) Description of larvae of three *Anastrepha* species in the *fraterculus* group (Diptera: Tephritidae). Proceedings of the Entomological Society of Washington 120(4): 708–724. https://doi.org/10.4289/0013-8797.120.4.708

Dutra VS, Ronchi-Teles B, Steck GJ, Rodriguez EJ, Norrbom AL, Sutton BD, Silva JG (2018b) Description of third instar larvae of *Anastrepha curitis*, *Anastrepha pickeli*, and *Anastrepha pulchra* (Diptera: Tephritidae). Proceedings of the Entomological Society of Washington 120(1): 9–24. https://doi.org/10.4289/0013-8797.120.1.9

Elson-Harris MM (1992) A systematic study of the Tephritidae (Diptera) based on the comparative morphology of larvae. PhD Thesis, University of Queensland, Australia.

Folmer O, Black M, Hoeh W, Lutz R, Vrijenhoek R (1994) DNA primers for amplification of mitochondrial cytochrome c oxidase subunit I from diverse metazoan invertebrates. Molecular Marine Biology and Biotechnology 3: 294–299.

Frías D, Hernández-Ortiz V, Vaccaro NC, Bartolucci AF, Salles LA (2006) Comparative morphology of immature stages of some frugivorous species of fruit flies (Diptera: Tephritidae). Israel Journal of Entomology 35–36: 423–457.

Frías D, Hernández-Ortiz V, Muñoz LL (2009) Description of the third-instar of *Anastrepha leptozona* Hendel (Diptera: Tephritidae). Neotropical Entomology 38(4): 491–496. https://doi.org/10.1590/S1519-566X2009000400008

Hao X, Jiang R, Chen T (2011) Clustering 16S rRNA for OTU prediction: A method of unsupervised Bayesian clustering. Bioinformatics 27(5): 611–618. https://doi.org/10.1093/bioinformatics/btq725

Hebert PDN, Penton EH, Burns JM, Janzen DH, Hallwachs W (2004) Ten species in one: DNA barcoding reveals cryptic species in the neotropical skipper butterfly *Astrapes fulgerator.* Proceedings of the National Academy of Sciences of the United States of America 101(41): 14812–14817. https://doi.org/10.1073/pnas.0406166101

Hernández-Ortiz V (1992) El genero *Anastrepha* Schiner en Mexico (Diptera: Tephritidae). Taxonomia, distribucion y sus plantas huespedes. Instituto de Ecología and Sociedad Mexicana de Entomología, Xalapa, Veracruz, Mexico, 162 pp.

Hernández-Ortiz V (2007) Diversidad y biogegrafia del genero *Anastrepha* en México. In: Hernández-Ortiz V (Ed.) Mosca de la fruta en Latinoamerica (Diptera: Tephritidae): diversidad, biología y manejo. S y G Editores, México, D. F., 53–76.

Hernández-Ortiz V, Pérez-Alonso R (1993) The natural host plants of *Anastrepha* (Diptera: Tephritidae) in a tropical rain forest of Mexico. The Florida Entomologist 76(3): 447–460. https://doi.org/10.2307/3495645

Kambhampati S, Smith PT (1995) PCR primers for the amplification of four insect mitochondrial gene fragments. Insect Molecular Biology 4(4): 233–236. https://doi.org/10.1111/j.1365-2583.1995.tb00028.x

Kimura M (1980) A simple method for estimating evolutionary rate of base substitutions through comparative studies of nucleotide sequences. Journal of Molecular Evolution 16(2): 111–120. https://doi.org/10.1007/BF01731581

Korytkowski GCA (2001) Situación actual del género *Anastrepha* Schiner, 1868 (Diptera: Tephritidae) en el Perú. Revista Peruana de Entomología 42: 97–158. https://revperuentomol.com.pe/index.php/rev-peru-entomol/article/view/145

Kovac D, Freidberg A, Steck GJ (2013) Biology and description of the third instar larva and puparium of *Ichneumonopsis burmensis* Hardy (Diptera: Tephritidae: Dacinae: Gastrozonini), a bamboo-breeding fruit fly from the Oriental Region. The Raffles Bulletin of Zoology 61(1): 117–132.

Kumar S, Stecher G, Tamura K (2016) MEGA7: Molecular Evolutionary Genetics Analysis version 7.0 for bigger datasets. Molecular Biology and Evolution 33(7): 1870–1874. https://doi.org/10.1093/molbev/msw054

Mansell MW (2017) Phytosanitary significance of Diptera. In: Kirk-Spriggs AH, Sinclair BJ (Eds) Manual of Afrotropical Diptera. Volume I. Introductory chapters and keys to Diptera families. Suricata 4. South African National Biodiversity Institute, Pretoria, South Africa, 195–202.

Martin FW, Campbell CW, Ruberté RM (1987) Perennial edible fruits of the tropics: An inventory. U.S. Department of Agriculture. Agriculture Handbook, Washington, DC, 642 pp.

Mengual X, Kerr P, Norrbom AL, Barr NB, Lewis ML, Stapelfeldt AM, Scheffer SJ, Woods P, Islam M-S, Korytkowski CA, Uramoto K, Rodriguez EJ, Sutton BD, Nolazco N, Steck GJ, Gaimari S (2017) Phylogenetic relationships of the tribe Toxotrypanini (Diptera: Tephritidae) based on molecular characters. Molecular Phylogenetics and Evolution 113: 84–112. https://doi.org/10.1016/j.ympev.2017.05.011

Molineros J, Tigrero JO, Sandoval D (1992) Diagnostico de la situacion actual del problema de las moscas de la fruta en el Ecuador. Comision Ecuatoriana de Energia Atomica, Direccion de Investigaciones. Quito, Ecuador, 53 pp.

Moore MR, Steck GJ, Rodriguez EJ, Norrbom AL, Ruiz-Arce R, Tood TN, Roberts CG, Troya H, Vilatuña JE, Donoso DA, Wiegmann BM, Cassel BK, Soghigian J, Xuan J, Muller A, Gangadin A, Nolazco N, Rodriguez Clavijo PA, Arevalo Peñaranda E, Srivastava P, Drovetski SV, Quisberth Ramos E, Lagrava Sánchez JJ, Colque F, Savaris M, Lampert S, Martinez J, Canal NA, Keil C, Padilla A, Tigrero JO, Rodriguez P, Peñaloza Barria Y, Gripenberg S, Rivera M, Branham M (in press) A COI DNA barcode library for *Anastrepha* Schiner (Diptera: Tephritidae). PLoS ONE.

Munch K, Boomsma W, Huelsenbeck JP, Willerslev E, Nielsen R (2008) Statistical assignment of DNA sequences using Bayesian phylogenetics. Systematic Biology 57(5): 750–757. https://doi.org/10.1080/10635150802422316

Norrbom AL (1991) The species of *Anastrepha* (Diptera: Tephritidae) with a *grandis*-type wing pattern. Proceedings of the Entomological Society of Washington 93: 101–124.

Norrbom AL (2004) Host plant database for *Anastrepha* and *Toxotrypana* (Diptera: Tephritidae: Toxotrypanini). Diptera Data Dissemination Disk (CD-ROM) 2.

Norrbom AL, Kim KC (1988) A list of the reported host plants of the species of *Anastrepha* (Diptera: Tephritidae). U. S. Department of Agriculture. APHIS Miscellaneous Publication 81–52.

Norrbom AL, Korytkowski CA (2011) New species of and taxonomic notes on *Anastrepha* (Diptera: Tephritidae). Zootaxa 2740(1): 1–23. https://doi.org/10.11646/zootaxa.2740.1.1

Norrbom AL, Korytkowski CA (2012) New species of *Anastrepha* (Diptera: Tephritidae), with key for the species of the *megacantha* clade. Zootaxa 3478: 510–552. https://doi.org/10.11646/zootaxa.3478.1.43

Norrbom AL, Zucchi RA, Hernández-Ortiz V (1999) Phylogeny of the genera *Anastrepha* and Toxotrypana (Trypetinae: Toxotrypanini) based on morphology. In: Aluja M, Norrbom AL (Eds) Fruit flies (Tephritidae): Phylogeny and evolution of behavior. CRC Press, Boca Raton, 299–342. https://doi.org/10.1201/9781420074468.ch12

Norrbom AL, Korytkowski CA, Zucchi RA, Uramoto K, Venable GL, McCormick J, Dallwitz MJ (2012) *Anastrepha* and *Toxotrypana*: descriptions, illustrations, and interactive keys. Version: 9th April 2019. delta-intkey.com

Norrbom AL, Rodriguez EJ, Steck GJ, Sutton BD, Nolazco N (2015) New species and host plants of *Anastrepha* (Diptera: Tephritidae) primarily from Peru and Bolivia. Zootaxa 4041(1): 1–94. https://doi.org/10.11646/zootaxa.4041.1.1

Norrbom AL, Barr NB, Kerr P, Mengual X, Nolazco N, Rodriguez EJ, Steck GJ, Sutton BD, Uramoto K, Zucchi RA (2018) Synonymy of *Toxotrypana* Gerstaecker with *Anastrepha* Schiner (Diptera: Tephritidae). Proceedings of the Entomological Society of Washington 120(4): 834–841. https://doi.org/10.4289/0013-8797.120.4.834

Norrbom AL, Muller A, Gangadin A, Sutton BD, Rodriguez EJ, Savaris M, Lampert S, Rodriguez Clavijo PA, Steck GJ, Moore MR, Nolazco N, Troya H, Keil CB, Padilla A, Wiegmann BM, Cassel B, Branham M, Ruiz-Arce R (2021) New species and host plants of *Anastrepha* (Diptera: Tephritidae) primarily from Suriname and Pará, Brazil. Zootaxa 5044(1): 1–74. https://doi.org/10.11646/zootaxa.5044.1.1

Peña EJ, Bennett FD (1995) Arthropods associated with *Annona* spp. in the Neotropics. The Florida Entomologist 78(2): 329–349. https://doi.org/10.2307/3495906

Rambaut A (2018) FigTree v. 1.4.1: Tree Figure Drawing Tool. https://github.com/rambaut/figtree/releases

Rodriguez EJ, Steck GJ, Moore MR, Norrbom AL, Sutton BD, Branham MA (2021) Description of larvae of *Anastrepha amplidentata* and *Anastrepha durantae* with review of larval morphology of the *fraterculus* group (Diptera: Tephritidae). Proceedings of the Entomological Society of Washington 123(1): 169–189. https://doi.org/10.4289/0013-8797.123.1.169

Rodríguez Clavijo PA, Norrbom AL (2021) New species and new records of *Anastrepha* (Diptera: Tephritidae) from Colombia. Zootaxa 5004(1): 107–130. https://doi.org/10.11646/zootaxa.5004.1.4

Rodríguez Clavijo PA, Norrbom AL, Arévalo Peñaranda E, Balseiro Tehran F, Díaz PA, Benitez MC, Gallego J, Cruz MI, Montes JM, Rodriguez EJ, Steck GJ, Sutton BD, Quisberth Ramos E, Lagrava Sánchez JJ, Colque F (2018) New records of *Anastrepha* (Diptera: Tephritidae) primarily from Colombia. Zootaxa 4390(1): 1–63. https://doi.org/10.11646/zootaxa.4390.1.1

Schneider A, Kovac D, Steck GJ, Freidberg A (2017) Larval descriptions and biology of Oriental bamboo-shoot fruit flies belonging to the genera *Anoplomus*, *Chaetellipsis*, *Cyrtostola*, *Gastrozona*, and *Paraxarnuta* (Diptera: Tephritidae: Dacinae: Gastrozonini). Studia Dipterologica 24(1): 15–47.

Schneider A, Kovac D, Steck GJ, Freidberg A (2018) Larval descriptions of five Oriental bamboo-inhabiting *Acroceratitis* species (Diptera: Tephritidae: Dacinae) with notes on their biology. European Journal of Entomology 115: 535–561. https://doi.org/10.14411/eje.2018.053

Simon C, Frati F, Beckenbach A, Crespi B, Liu H, Flook P (1994) Evolution, weighting, and phylogenetic utility of mitochondrial gene sequences and a compilation of conserved polymerase chain reaction primers. Annals of the Entomological Society of America 87(6): 651–701. https://doi.org/10.1093/aesa/87.6.651

Steck GJ, Wharton RA (1988) Description of immature stages of *Anastrepha interrupta*, *A. limae*, and *A. grandis* (Diptera: Tephritidae). Annals of the Entomological Society of America 81(6): 994–1003. https://doi.org/10.1093/aesa/81.6.994

Steck GJ, Carroll LE, Celedonio-Hurtado H, Guillen-Aguilar J (1990) Methods for identification of *Anastrepha* larvae (Diptera: Tephritidae), and key to 13 species. Proceedings of the Entomological Society of Washington 92: 333–346.

Steck GJ, Rodriguez EJ, Norrbom AL, Dutra VS, Ronchi-Teles B, Silva JG (2019) Review of *Anastrepha* (Diptera: Tephritidae) immature stage taxonomy. In: Pérez-Staples D, Díaz-Fleischer F, Montoya P, Vera MT (Eds) Area-wide management of fruit fly pests. CRC Press, Boca Raton, 57–85. https://doi.org/10.1201/9780429355738-7

Steyskal GC (1977) Two new neotropical fruitflies of the genus *Anastrepha*, with notes on generic synonymy (Diptera: Tephritidae). Proceedings of the Entomological Society of Washington 79: 75–81.

Stone A (1942) The fruitflies of the genus *Anastrepha*. U. S. Department of Agriculture. Miscellaneous Publication 439. Washington, DC, 112 pp.

Tigrero JO (1998) Revisión de especies de moscas de la fruta presentes en el Ecuador. Published by the author. Sangolquí, Ecuador, 55 pp.

Tigrero JO (2009) Lista anotada de hospederos de moscas de la fruta presentes en Ecuador. Boletín Técnico. Serie Zoológica 8(4–5): 111–120.

White IM, Elson-Harris MM (1992) Fruit flies of economic significance: their identification and bionomics. CAB International, Wallingford, 601 pp.

White IM, Headrick DH, Norrbom AL, Carroll LE (1999) Glossary. In: Aluja M, Norrbom AL (Eds) Fruit flies (Tephritidae): Phylogeny and evolution of behavior. CRC Press, Boca Raton, 881–924. https://doi.org/10.1201/9781420074468.sec8

Yepes RF, Vélez AR (1989) Contribucion al conocimiento de las moscas de las frutas (Tephritidae) y sus parasitoides en el departamento de Antioquia. Revista Facultad Nacional de Agronomía 42: 73–98.

Zhang AB, Sikes DS, Muster C, Li SQ (2008) Inferring species membership using DNA sequences with back-propagation neural networks. Systematic Biology 57(2): 202–215. https://doi.org/10.1080/10635150802032982

Zhang AB, Muster C, Liang HB, Zhu CD, Crozier R, Wan P, Feng J, Ward RD (2012) A fuzzy-set-theory-based approach to analyse species membership in DNA barcoding. Molecular Ecology 21(8): 1848–1863. https://doi.org/10.1111/j.1365-294X.2011.05235.x

Zhang AB, Hao MD, Yang CQ, Shi ZY (2017) BarcodingR: An integrated R package for species identification using DNA barcodes. Methods in Ecology and Evolution 8(5): 627–634. https://doi.org/10.1111/2041-210X.12682

Zucchi RA, Moraes RCB (2008) Fruit flies in Brazil - *Anastrepha* species their host plants and parasitoids. [Available in:] www.lea.esalq.usp.br/Anastrepha/ [updated on 8 July 2020] [accessed on 17 August 2020]